ASSIMILATION OF TRACE GAS RETRIEVALS OBTAINED FROM SATELLITE (SCIAMACHY), AIRCRAFT AND GROUND OBSERVATIONS INTO A REGIONAL SCALE AIR QUALITY MODEL (CMAQ-DDM/3D)

A Dissertation
Presented to
The Academic Faculty

by

Burcak Kaynak

In Partial Fulfillment
of the Requirements for the Degree
Doctor of Philosophy in the
School of Civil and Environmental Engineering

Georgia Institute of Technology
December 2009

ASSIMILATION OF TRACE GAS RETRIEVALS OBTAINED FROM SATELLITE (SCIAMACHY), AIRCRAFT AND GROUND OBSERVATIONS INTO A REGIONAL SCALE AIR QUALITY MODEL (CMAQ-DDM/3D)

Approved by:

Dr. Armistead G. Russell, Advisor
School of Civil and Environmental Engineering
Georgia Institute of Technology

Dr. Irina N. Sokolik
School of Earth and Atmospheric Sciences
Georgia Institute of Technology

Dr. Michael H. Bergin
School of Civil and Environmental Engineering
Georgia Institute of Technology

Dr. Yuhang Wang
School of Earth and Atmospheric Sciences
Georgia Institute of Technology

Dr. M. Talat Odman
School of Civil and Environmental Engineering
Georgia Institute of Technology

Date Approved: August 18, 2009

To all wandering minds,

ACKNOWLEDGEMENTS

I would like to start with thanking my academic advisor, Dr. Ted Russell, for his guidance, patience, and encouragement. His guidance made the time I spent in his group a valuable learning experience and gave me a strong background in not only my research but also a wide range of other air pollution issues. I feel lucky that I had the chance to work with him and his research group.

I would also like to express my gratitude to my committee members, Drs. Michael Bergin, Talat Odman, Irina Sokolik and Yuhang Wang for their valuable time and suggestions throughout my research. In addition, I like to thank Muthukumar Subrahmanyam for his help in ArcGIS.

I would like to thank all the faculty and staff within the Environmental Engineering Program at the Georgia Institute of Technology. In particular, all the past and present members of Dr. Russell's research group whom I had the chance to work with during my time. I would like to give my special thanks to Dr. Yongtao Hu for his mentorship and patience.

I would like to thank all my friends here and at home that made my life easier. In particular, Sinem Gökgöz Kılıç for welcoming me in Atlanta and making me feel that I am at home whenever I am with her.

I am grateful to my family; Müzeyyen, Musa and Burak Kaynak for all their love, support and encouragement. I never felt they are far away even though they are. Last but not least, I want to thank Ulaş Tezel for walking with me in this road called life and becoming an inspiration with his passion in science and excellence in his work.

This research is supported by NASA and EPA projects. Finally, the Higher Education Council of Turkey is acknowledged for the partial financial support of my Ph.D. studies.

TABLE OF CONTENTS

LIST OF TABLES

LIST OF FIGURES

SUMMARY

A major opportunity for using satellite observations of tropospheric chemical concentrations is to improve our scientific understanding of atmospheric processes by integrated analysis of satellite, aircraft, and ground-based observations with global and regional scale models. One endpoint of such efforts is to reduce modeling biases and uncertainties. The idea of coupling these observations with a regional scale air quality model was the starting point of this research. The overall objective of this research was to improve the NO_x emission inventories by integrating observations from different platforms and regional air quality modeling. Specific objectives were: 1) Comparison of satellite NO_2 retrievals (SCIAMACHY) with simulated NO_2 by the regional air quality model (MM5-SMOKE-CMAQ); 2) Comparison of simulated tropospheric gas concentrations simulated by the regional air quality model, with aircraft (ICARTT INTEX-NA) and ground-based observations; 3) Assessment of the uncertainties in comparing satellite NO_2 retrievals with NO_x emissions estimates and model simulations; 4) Identification of biases in emission inventories by data assimilation of satellite NO_2 retrievals, and ground-based NO, NO_2 and O_3 observations with an iterative inverse method using the regional air quality model coupled with sensitivity calculations; 5) Improvement of our understanding of NO_x emissions, and the interaction between regional and global air pollution by an integrated analysis of satellite NO_2 retrievals with the regional air quality model.

Along with these objectives, a lightning NO_x emission inventory was prepared for two months of summer 2004 to account for a significant upper level NO_x source.

Spatially-resolved weekly NO_2 variations from satellite retrievals were compared with estimated NO_x emissions for different region types indicating higher reductions during the weekends from satellite retrievals in urban areas than model simulations. Comparison of satellite NO_2 retrievals with NO_2 simulations indicated model simulations show more NO_2 in urban centers, but less NO_2 in surroundings of these urban centers and in rural areas than satellite retrievals. NO, NO_2, O_3, NO_x, NO_y and PAN simulations were also evaluated with ground-based and aircraft observations. Data assimilation of satellite NO_2 retrievals, and ground-based NO, NO_2 and O_3 observations were performed to evaluate the NO_x emission inventory. Both datasets suggested increases in western United States mobile NO_x emissions and reductions in all other NO_x emissions.

This research contributes to a better understanding of the use of satellite NO_2 retrievals in air quality modeling, and improvements in the NO_x emission inventories by correcting some of the inconsistencies that were found in the inventories. Therefore, it may provide groups that develop emissions estimates guidance on areas for improvement. In addition, this research indicates the weaknesses and the strengths of the satellite NO_2 retrievals and offers suggestions to improve the quality of the retrievals for further use in the tropospheric air pollution research.

CHAPTER 1

INTRODUCTION

1.1. Background

Along with the industrial development, air pollution became a significant environmental issue around highly populated and industrialized areas. The health effects associated with exposure to air pollution showed themselves with extreme cases (e.g. Great London smog) which raised public awareness and it became obvious that air pollutants have numerous effects on human health, including pulmonary, cardiac, vascular, and neurological impairments. Although pollutants can affect the skin, eyes and other body systems, they affect primarily the respiratory system.

The Clean Air Act (CAA) defines Environmental Protection Agency's (EPA) responsibilities for protecting and improving the nation's air quality and the stratospheric ozone layer. There are six priority air pollutants that are regulated in United States (US) along with hazardous air pollutants according to CAA. These six priority air pollutants are ozone (O_3), sulfur dioxide (SO_2), particulate matter that are 10 micrometers in diameter or smaller (PM_{10}, $PM_{2.5}$), nitrogen dioxide (NO_2), carbon monoxide (CO), and lead (Pb). Priority air pollutants are regulated according to National Ambient Air Quality Standards (NAAQS) by the EPA strictly on a public health basis, with an adequate margin of safety to protect the population and special attention given to protection of vulnerable populations [*EPA*, 2009]. Nitrogen oxides (NO_x: $NO+NO_2$) play a significant role in tropospheric chemistry. NO_2 itself is among the six priority air pollutants. NO_x combined with volatile organic compounds (VOCs) produce O_3 and also form nitric acid

(HNO_3) and aerosol nitrate (NO_3^-) which can be a significant part of the ambient PM. Both O_3 and PM are also among the six priority air pollutants.

Particularly compliance with the NAAQS for O_3 and PM requires future reductions in NO_x emissions and decision making to determine the implementation plans to be in attainment with the NAAQS. Research on future pollutant emission reductions requires a tool that connects the changes in pollutant emissions to their ambient concentrations especially when this relationship is not linear. Air quality modeling is a useful tool to predict the fate of pollutants emitted from different sources and for different meteorological conditions, understanding atmospheric dynamics, effects of pollutants on different ecosystems for future scenarios and for regions where measurements are not available. If the current air quality can not reach the desired goals with current level of emissions, candidate control strategies can be identified and tested with air quality modeling which often involves many model calculations, simulating the effects of many different emissions changes, to decide on the appropriate management strategy [*Russell,* 1997].

Air quality models can either simulate changes in a chemical composition of a given air parcel as it is advected to the atmosphere (Lagrangian) or concentrations in an array of fixed cells (Eulerian) [*Seinfeld and Pandis,* 1997]. Some of the earliest modeling of long-range transport was conducted using Lagrangian trajectory models, in part because of the more limited computational requirements but most of the current regional air quality models are Eulerian. The main components of an Eulerian air quality model are emissions, transport and physicochemical transformation which require temporally and spatially resolved fields of emissions, meteorology, topographic features, initial and

background pollutant concentrations, and domain definition information to simulate the evolution of pollutant concentrations throughout the modeling domain [*Russell*, 1997]. These models simulate the pollutant concentrations according to current scientific knowledge of the atmosphere and inputs mentioned above, thus improvement of the scientific knowledge and the inputs will greatly help to improve their performances and show possible improvements.

With the significant impact on O_3 and PM formation, NO_x emissions are one of the most significant inputs to the regional air quality models for policy purposes. NO_x sources are mainly anthropogenic, particularly due to fossil fuel combustion (e.g. mobile sources, electricity generation), but they can also come from natural sources (e.g., lightning, biomass burning) to a lesser extent. Currently, NO_x emission inventories which are the inputs to the air quality models are developed by a bottom-up approach which based on the current knowledge of emission factors and process activities including factory process rates and vehicle-miles traveled. This information is subject to uncertainties. Also, the ground observations of NO_x are limited to mainly urban areas and the evaluations of the air quality models with these observations show lower correlations because of their nature as being primary pollutants, short lifetime and the representability of the observation station locations.

Recent developments in the remote sensing allow to acquire vertical column information of NO_2 in the atmosphere with the use of electromagnetic radiation [*Martin*, 2008]. The availability of these retrievals as tropospheric NO_2 column amounts with comparable spatial resolutions with regional air quality models and global coverage within days including remote areas where other means of measurements are not available

is a well-needed addition to the sparse ground-based observations. Improvement of the bottom-up NO_x inventories can be achieved by combining the regional air quality model with a top-down approach called inverse modeling where the minimization of uncertainties in simulations via the optimal combination of observations from ground-based and satellite and *a priori* emissions [*Tarantola*, 2005].

This research contributes to a better understanding of the further use of satellite NO_2 retrievals in air quality modeling, and improvements in the NO_x emission inventories by correcting some of the inconsistencies that were found in the inventories. Therefore, it may provide groups that develop emissions estimates guidance on areas for improvement. In addition, this research indicates the weaknesses and the strengths of the satellite NO_2 retrievals and offers suggestions to improve the quality of the retrievals for further use in the tropospheric air pollution research.

1.2. Scope of This Work

Using satellite observations of tropospheric chemical concentrations in order to improve our scientific understanding of atmospheric processes by integrated analysis of satellite, aircraft, and ground-based observations with regional air quality models was the starting point of this research. One endpoint of integrating available observations with air quality modeling was to reduce modeling biases and uncertainties.

Summer of 2004 (July-August) serves as a perfect opportunity with all available observations from different platforms. Traditional ground-based observations supply continuous and accurate monitoring. However, they have incomplete spatial coverage because of the limited number of stations and representativeness issues may arise because these are point measurements and may be significantly impacted by local influences.

Further, they only provide information at the ground. Aircraft measurements, on the other hand, provide information on the vertical structure of the pollutant concentrations. They also typically include additional species which are not available from conventional ground-based observations. However, they are also very limited both temporally and spatially. Satellite retrievals supply on-going global coverage, including remote areas and upper troposphere where few other observations are available. On the other hand, they have higher uncertainties than other observations, but have potential to be improved. Availability of these observations gives us the chance to extensively evaluate the air quality model and to assess model and observation strengths and limitations and to use these observations in order to improve emission inventories.

This research required both an extensive comparison of measurements from multiple platforms and model simulations, and entailed assimilation of the observations in the model by an iterative, inverse method. The overall objective of the research presented here was to improve the NO_x emission inventories by integrating observations from different platforms and regional air quality modeling. The specific objectives in this research were:

(1) Comparison of satellite NO_2 retrievals with simulated tropospheric NO_2 concentrations by the regional air quality model;

(2) Comparison of simulated tropospheric gas concentrations simulated by the regional air quality model, with aircraft and ground-based measurements of tropospheric species to identify reasons for discrepancies;

(3) Assessment of the uncertainties in comparing satellite NO_2 retrievals with NO_x emissions estimates and model results;

(4) Identification of biases in emission inventories by data assimilation of satellite NO_2 retrievals, and ground-based NO, NO_2 and O_3 observations with an iterative inverse method using the regional air quality model coupled with sensitivity calculation;

(5) Improvement of our understanding of NO_x emissions, and the interaction between regional and global air pollution by an integrated analysis of satellite NO_2 retrievals with the regional air quality model.

Along with the framework of these specific objectives, this thesis was organized in six research chapters as follows:

- **Chapter 2: The Effect of Lightning NO_x Production on Surface Ozone in the Continental United States.**

  Lightning NO_x emission inventory was prepared for two months of summer (July-August) 2004. Impacts of lightning NO_x emissions on surface ozone and contribution to Policy Related Background (PRB) were investigated using the MM5-SMOKE-CMAQ system.

- **Chapter 3: Comparison of Weekly Cycle of NO_2 Satellite Retrievals and NO_x Emission Inventories for the Continental US.**

  Spatially-resolved weekly NO_2 variations were obtained from 2003-2005 SCIAMACHY for 3 different types of regions: urban, rural and rural-point, and were compared with estimated mobile and stationary nitrogen oxides NO_x emissions from the year 2004 for magnitudes and weekly profiles.

- **Chapter 4: Comparison of NO_2 from a Regional Scale Air Quality Model with Satellite Retrievals over the Continental U.S.: Emission Inventory Assessment Implications.**

  One-to-one comparison of modeled and satellite-observed NO_2 was performed for two months of summer (July-August) 2004 in order to help to identify reasons for discrepancies between retrievals and model predictions. Additional comparisons for 3 different types of regions: urban, rural and rural-point and for states were performed.

- **Chapter 5: Analysis of NO, NO_2 and O_3 between Model Simulations and Ground-Based, Aircraft and Satellite Platforms.**

  The model simulations of NO, NO_2, O_3 were compared with ground-based, aircraft and satellite observations for two months of summer (July-August) 2004 in order to evaluate the model and understand model and observation limitations. Additional comparisons of NO_x, NO_y and PAN were also performed where available.

- **Chapter 6: Inverse Modeling with Four Dimensional Data Assimilation (FDDA) Using Satellite and Ground-Based Observations**

  Data assimilation of satellite NO_2 retrievals, and ground-based NO, NO_2 and O_3 observations with FDDA were performed to evaluate the NO_x emissions. The scaling factors were obtained to update *a priori* NO_x emissions for different categories. The model results with *a posteriori* NO_x inventories were also compared with available aircraft observations as an independent evaluation.

- **Chapter 7: Determining the Source Strength of an Unknown NO_x Source from NO_2 Satellite Retrievals and Related Uncertainties: A Case Study for Point Sources**

  The NO_x emissions from selected significant point sources were estimated using satellite NO_2 retrievals and a simple box model approximation. The results were compared with NO_x emissions prepared according to EPA Continuous Emission Monitoring Database (CEM).

CHAPTER 2

THE EFFECT OF LIGHTNING NO_x PRODUCTION ON SURFACE OZONE IN THE CONTINENTAL UNITED STATES*

Abstract

Lightning NO_x emissions calculated using the United States National Lightning Detection Network (US NLDN) data were found to account for 30% of the total NO_x emissions for July-August 2004, a period chosen both for having higher lightning NO_x production and high ozone levels, thus maximizing the likelihood that such emissions could impact peak ozone levels. Including such emissions led to modest, but sometimes significant increases in simulated surface ozone when using the Community Multi-scale Air Quality Model (CMAQ). Three model simulations were performed, two with the addition of lightning NO_x emissions, and one without. Domain-wide daily maximum 8-h ozone changes due to lightning NO_x were less than 2 ppbV in 71% of the cases with a maximum of 10 ppbV; whereas the difference in 1-h ozone was less than 2 ppbV in 77% of the cases with a maximum of 6 ppbV. Daily maximum 1-h and 8-h ozone for grids containing O_3 monitoring stations changed slightly, with more than 43% of the cases differing less than 2 ppbV. The greatest differences were 42 ppbV for both 1-h and 8-h O_3, though these tended to be on days of lower ozone. Lightning impacts on the season-wide maximum 1-h and 8-h averaged ozone decreased starting from the 1^{st} to 4^{th} highest values (an average of 4^{th} highest, 8-h values is used for attainment demonstration in the

---

* This chapter is published in the Atmospheric Chemistry and Physics, 8(17), 5151-5159, 2008. Co-authors are Yongtao Hu, Randall V. Martin, Yunsoo Choi, Yuhang Wang and Armistead G. Russell.

US). Background ozone values from the y-intercept of O_3 versus NO_z curve were 42.2 and 43.9 ppbV for simulations without and with lightning emissions, respectively. Results from both simulations with lightning NO_x suggest that while North American lightning production of NO_x can lead to significant local impacts on a few occasions, they will have a relatively small impact on typical maximum levels and determination of Policy Relevant Background levels.

2.1. Introduction

Nitrogen oxides (NO_x=NO+NO_2) play a key role in tropospheric chemistry and impact the tropospheric ozone (O_3) budget. Sources of NO_x include fossil fuel combustion, biomass burning, soil release, oxidation of atmospheric ammonia, lightning, and stratospheric NO_x. Recent global estimates of NO_x production from lightning vary from 1 to 20 Tg N/year [*Boersma et al.*, 2005; *Labrador et al.*, 2005; *Martin et al.*, 2007], though 5±3 Tg N/year is applied in most global modeling [*Ridley et al.*, 2005; *Schumann and Huntrieser*, 2007].

Lightning can lead to significant increases in NO_x in the middle and upper troposphere and contribute significantly to columnar abundance of NO_2 [*Beirle et al.*, 2006; *Bond et al.*, 2001; *Choi et al.*, 2005; *Delmas et al.*, 1997; *Martin et al.*, 2006; *Pickering et al.*, 1998; *Ridley et al.*, 1996; *Tie et al.*, 2002; *Zhang et al.*, 2000; *Zhang et al.*, 2003]. This source is particularly important in the southeastern US during the summertime [*Biazar and McNider*, 1995; *Bond et al.*, 2001; *Hudman et al.*, 2007]. However, such emissions often are not included in regional modeling, unlike global modeling [*Allen and Pickering*, 2002; *Choi et al.*, 2005; *Egorova et al.*, 1999; *Stockwell et al.*, 1999; *Tie et al.*, 2002]. With further opportunities for evaluating our models using

satellite measurements which indicate the importance of lightning NO_x enhancements [*Boersma et al.*, 2005; *Choi et al.*, 2005; *Christian et al.*, 2003], including such emission in regional models should be considered.

Variability in background surface level ozone over the United States is a critical issue strongly related to air quality policy and a recent ozone criteria document [*EPA*, 2006] investigated such levels in terms of the Policy Related Background (PRB). PRB is defined as the distribution of O_3 concentrations that would be observed in the US in the absence of anthropogenic (man-made) emissions of O_3 precursors in the US, Canada, and Mexico. Estimates of background ozone range between 15-45 ppbV [*Altshuller and Lefohn*, 1996; *Fiore et al.*, 2002; *Hirsch et al.*, 1996; *Liang et al.*, 1998; *Lin et al.*, 2000; *Trainer et al.*, 1993], though some studies suggest that natural background ozone is higher than the 25-45 ppbV range recently used as the PRB. A higher PRB impacts how readily one can achieve the National Ambient Air Quality Standard (NAAQS) for ozone [*Lefohn et al.*, 2001]. The current NAAQS is 0.08 ppmV, calculated as the 3-year average of the fourth-highest daily maximum 8-h average ozone concentration measured at each monitor within an area over each year. Recently EPA has proposed tightening the standard to 0.075 ppmV further increasing the possible importance of how ozone production from lightning might impact levels. Fiore et al. [2003] suggested the O_3 background is generally 15-35 ppbV, with occasional incidences of 40-50 ppbV at high-altitude western sites in spring. Here, impacts of lightning NO_x emissions on surface ozone and contribution to PRB are investigated using the MM5-SMOKE-CMAQ system [*Byun and J.K.S.*, 1999; *Houyoux and Vukovich*, 1999; *Seaman*, 2000] applied to July-August 2004. CMAQ simulations can give additional information because the effect of

lightning might lead to high ozone at finer scales which can not be captured using current global models. July-August 2004 is chosen for a variety of reasons. First, pollutant data are available not only from the routine, ground based monitors, but from satellites and airborne platforms as well (ICARTT-International Consortium for Atmospheric Research on Transport and Transformation, NASA INTEX-NA -Intercontinental Chemical Transport Experiment-North America, Mission 2004), allowing for more detailed evaluation and investigation. Second, this period had a number of ozone exceedances across the US [*EPA*, 2008b]. Third, this period has frequent convective events and lightning NO_x formation. As such, July-August is a top candidate for identifying the potential impact of lightning NO_x formation on high ozone levels and non-attainment.

2.2. Methods

2.2.1. Model Description

The Community Multi-scale Air Quality Model (CMAQ) [*Byun and Schere*, 2006] with the SAPRC99 Chemical Mechanism [*Carter*, 2000] is used in this study. CMAQ is an advanced, atmospheric chemical transport model widely used for both research and regulatory applications. The modeling domain has a 36km × 36km horizontal grid resolution covering the continental United States, Southern Canada and Northern Mexico including 13 vertical layers reaching up to approximately 15 km. The Fifth-Generation NCAR/Penn State Mesoscale Model (MM5) [*Seaman*, 2000] is used to develop the meteorological fields, and the Sparse Matrix Operator Kernel Emissions (SMOKE) [*Houyoux and Vukovich*, 1999] is used to prepare input emissions for CMAQ. The emission inventory used for the year 2004 is projected from the emissions inventory for the year 2002 (VISTAS2002) prepared as part of Visibility Improvement State &

Tribal Association of the Southeast (VISTAS) [*MACTEC*, 2005]. Emission projection use growth factors from the Economic Growth Analysis System (EGAS) Version 4.0, and control efficiency data obtained from EPA for the existing federal control strategies which were in place in 2004. Additionally, actual NO_x emissions in 2004 from US power plants (i.e. electricity generating units, or EGUs) which are obtained from the continuous emissions monitoring (CEM) database from EPA website [*EPA*, 2008a] are integrated into the emission inventory.

MM5 is run with 34 vertical levels to produce highly resolved meteorological information. The Grell scheme [*Grell et al.*, 1995] is used to simulate cumulus (cloud) dynamics. The Four-Dimensional Data Assimilation (FDDA) [*Dudhia et al.*, 2005] with the Pleim-Chang planetary boundary layer (PBL) scheme [*Pleim and Chang*, 1992] and Pleim-Xiu Land Surface Model [*Xiu and Pleim*, 2001] are also used. Simulated ozone is compared with ground observations for performance evaluation (Figure 2.1).

2.2.2. Lightning NO_x Emissions

Typical emission inventories, e.g. US EPA's 1999 and 2002 National Emission Inventories (NEI) do not account for lightning NO_x emissions. Here, observed lightning strikes (US NLDN) are correlated to MM5 results, and used to enhance the traditional emission inventory. Three simulations were performed, one without lightning emissions, one with lightning emissions distributed using a vertical distribution based on Pickering [2007] for July-August 2004 and another for sensitivity purposes using an older profile where more NO_x is emitted near the ground (for August). Detailed analysis shows how including those emissions impacts simulated ozone, particularly with respect to whether this more complete treatment impacts regulatory applications of air quality models.

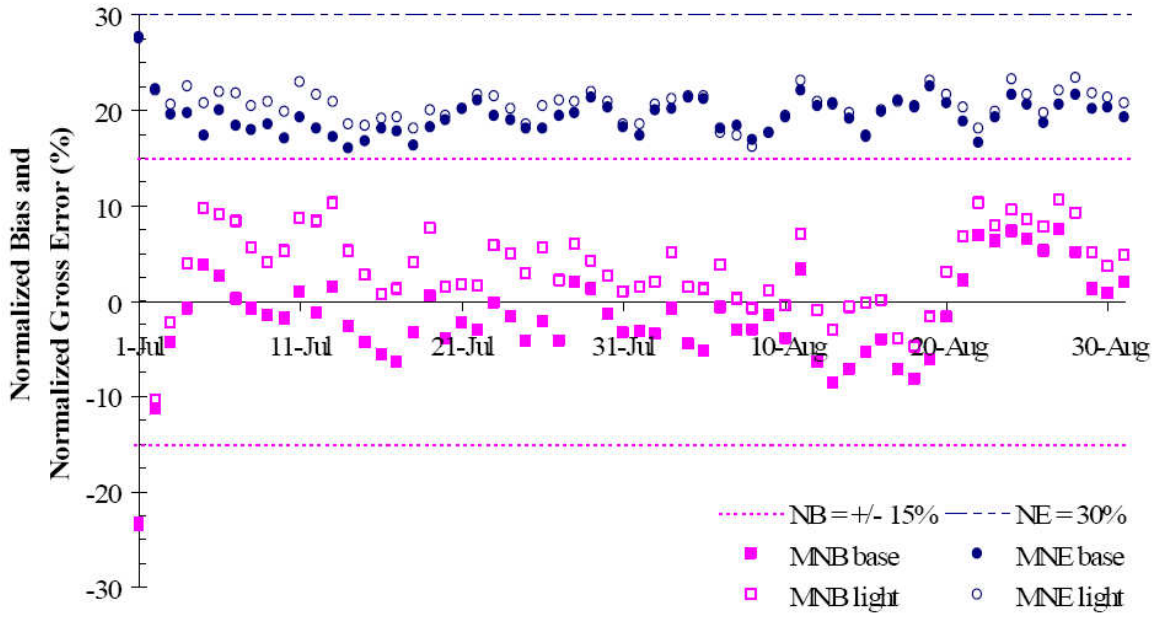

Figure 2.1. Domain-wide daily normalized bias and error for 8-h O_3 in CMAQ when compared with AIRS, CASTNET and SEARCH O_3 measurements (for all pairs of O_3 >40 ppbV)

Lightning NO_x emissions are estimated by using US NLDN lightning flash data. NLDN coverage includes the continental US and extends 200-300 km off the coastline, though includes only the cloud-to-ground (CG) lightning flashes. The detection efficiency for those data ranges from 80% to 90% for events with peak currents above 5 kA varying slightly by region over US and decreases gradually away from the coast (Cummins et al., 1998). As such, the actual number of flashes is either the same or more than the reported values. Previous studies [*Bond et al.*, 2001; *Price and Rind*, 1993; *Schumann and Huntrieser*, 2007] suggested that the number of intra-cloud (IC) flashes is about 3 times that of CG flashes, and we adopt this ratio in this study. This value is also consistent with the results that are derived from satellite lightning measurements from the Optical Transient Detector (OTD) for 1995-1999 over the contiguous US [*Boccippio et al.*, 2001]. Even though this ratio might be in the upper range for some regions, we chose

to use it to conservatively estimate the maximum likely impact on ozone. The vertical profile used for allocation of NO_x emissions is a modified form of a widely used vertical profile for mid-latitudes [*Pickering et al.*, 1998]. The "older" vertical profile is based on the assumption that IC flashes produce approximately 10 times less NO than CG flashes [*Price et al.*, 1997]. More recent studies suggest that the production of NO by an IC flash is approximately equal to that of a CG flash [*DeCaria et al.*, 2000; *DeCaria et al.*, 2005; *Fehr et al.*, 2004; *Ott et al.*, 2007]. The new scheme puts much less NO_x in boundary layers versus the previous profile [*Pickering*, 2007]. The difference in the amount of NO produced per flash for IC and CG flashes increases NO from IC flashes in the upper troposphere. As mentioned above, the original vertical distribution is modified by removing a fraction of lightning produced NO_x from the surface layers (0-1 km) and re-distributing this amount evenly to the layers between 5 and 12 km (Figure 2.2) [*Pickering*, 2007].

Using results from DeCaria, et al. (2005) led to an average of around 500 moles on NO per flash for both IC and CG flashes [*DeCaria et al.*, 2005; *Pickering*, 2007]. This value is also used for FLEXPART [*Cooper et al.*, 2006] and GEOS-Chem [*Hudman et al.*, 2007] simulations over North America during summer 2004 and good comparisons with aircraft data have been obtained. Even though this value is in the upper range for the literature [*Schumann and Huntrieser*, 2007], results obtained from this assumption will likely give us an upper limit for the effects, so we can be more certain about the potential effects of lightning NO_x on surface O_3.

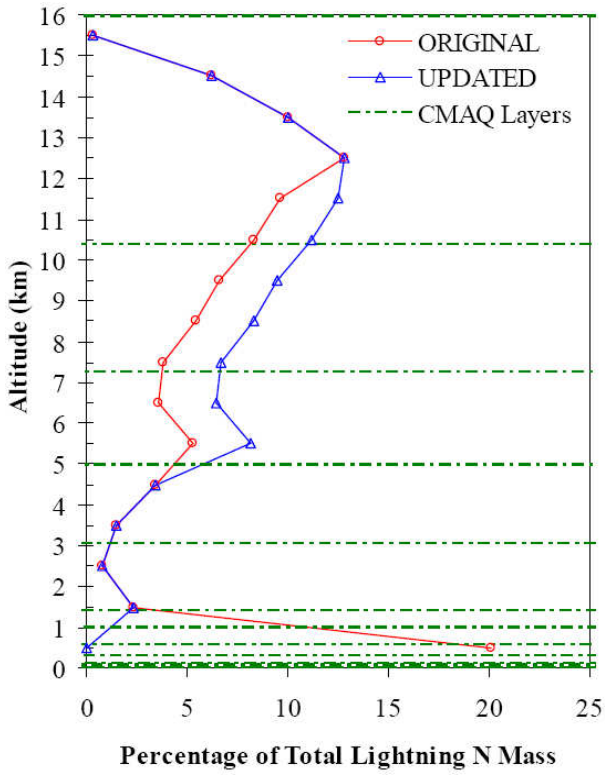

Figure 2.2. Original and updated vertical profiles used for allocating lightning NO_x emissions into model layers

To develop a spatially and temporally detailed NO_x inventory, the emissions estimates, along with lightning events were processed to obtain hourly and gridded lightning emissions. NO emissions from lightning were located into model layers according to the modified vertical profile scaled to the cloud top of the particular clouds at each CMAQ grid cell. Cloud occurrence (cloud cover) and cloud top are obtained from MM5 predictions at each CMAQ grid cell. Cloud occurrences are compared with locations of lightning events. Predicted cloud information and actual lightning data from NLDN are combined to allocate the lightning NO_x emissions. Allocation uses either (1) the actual grid's cloud information if its cloud cover is not zero or (2) averaged non-zero neighbor grids' cloud information if cloud cover is zero in the location of an observed

flash. Occurrence of lightning where no cloud is predicted was very rare: 0.18% of the time on average, with a 1.37% maximum on a specific day for the episode.

2.3. Results and Discussion

Lightning production is a significant fraction of the total NO_x emissions (Figure 2.3), accounting for 30% of the total for July-August 2004. This amount is higher than what would be found for an annual average because summer months are the most lightning active times of the year. The assumed NO_x production rate per flash and the IC to CG ratio also have a significant effect on this fraction and are still rather uncertain. The spatial distribution of the lightning NO_x emissions shows high intensity in three regions; the Southeast, Texas and its surrounding, and the Midwest (Figure 2.4).

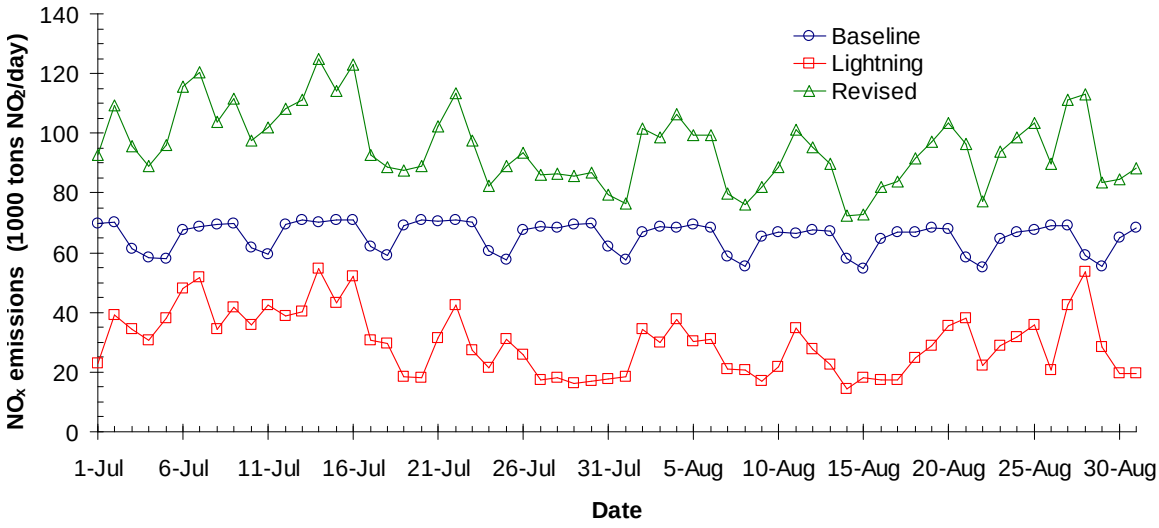

Figure 2.3. Domain-wide baseline, lightning, and revised NO_x emissions (as tons NO_2/day) for July-August 2004

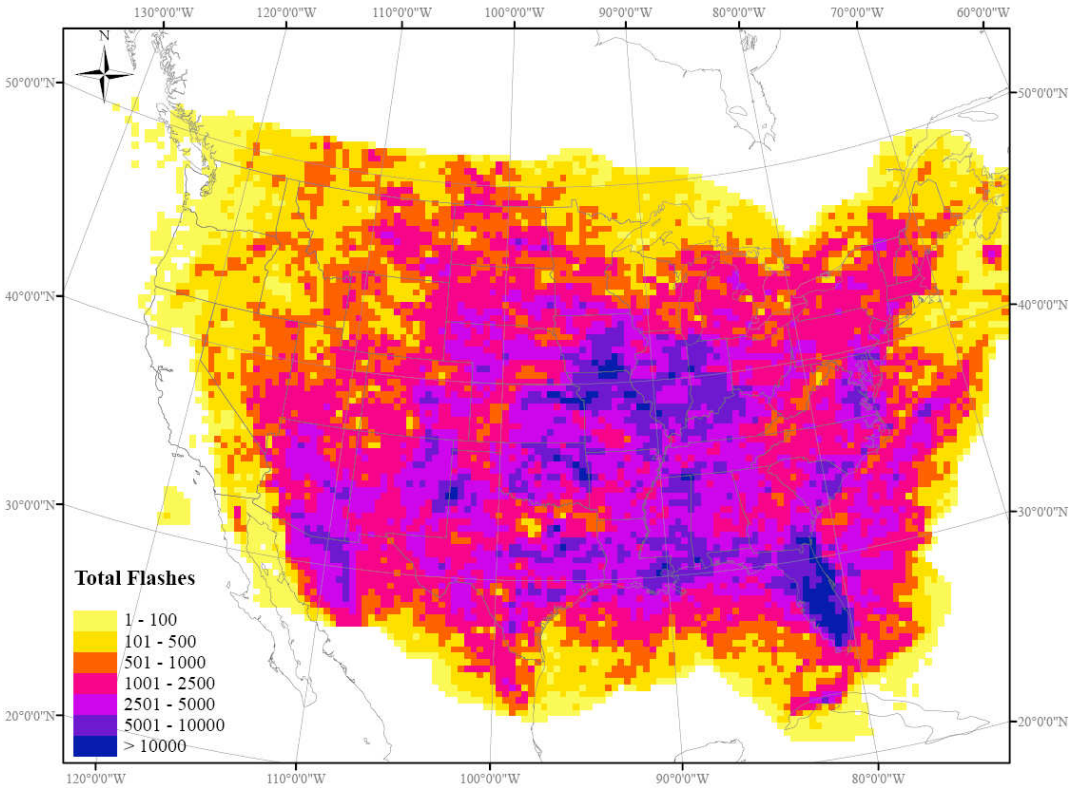

Figure 2.4. Domain-wide lightning intensity map for July-August 2004

Model results using the baseline and lightning enhanced inventories found that including lightning NO_x typically had a small impact on domain-wide, maximum 8-h O_3, with more than 71% of the daily peak concentrations being affected by less than 2 ppbV (Figure 2.5). There are only 2 days with a significant difference (~10 ppbV maximum). Impacts on 1-h O_3 are similar, with more than 77% of the domain-wide daily maximum ozone concentrations being within 2 ppbV (Figure 2.5). The largest impact is 6.4 ppbV. On average, the difference in domain-wide peak was 1.1 ppbV and 1.7 ppbV for 1-h and 8-h averages, respectively.

Further investigations into how lightning might impact ozone attainment in the US were carried out with the model results at the 692 grid cells where one or more routine ozone monitoring stations are located. Daily maximum 1-h and 8-h O_3 with

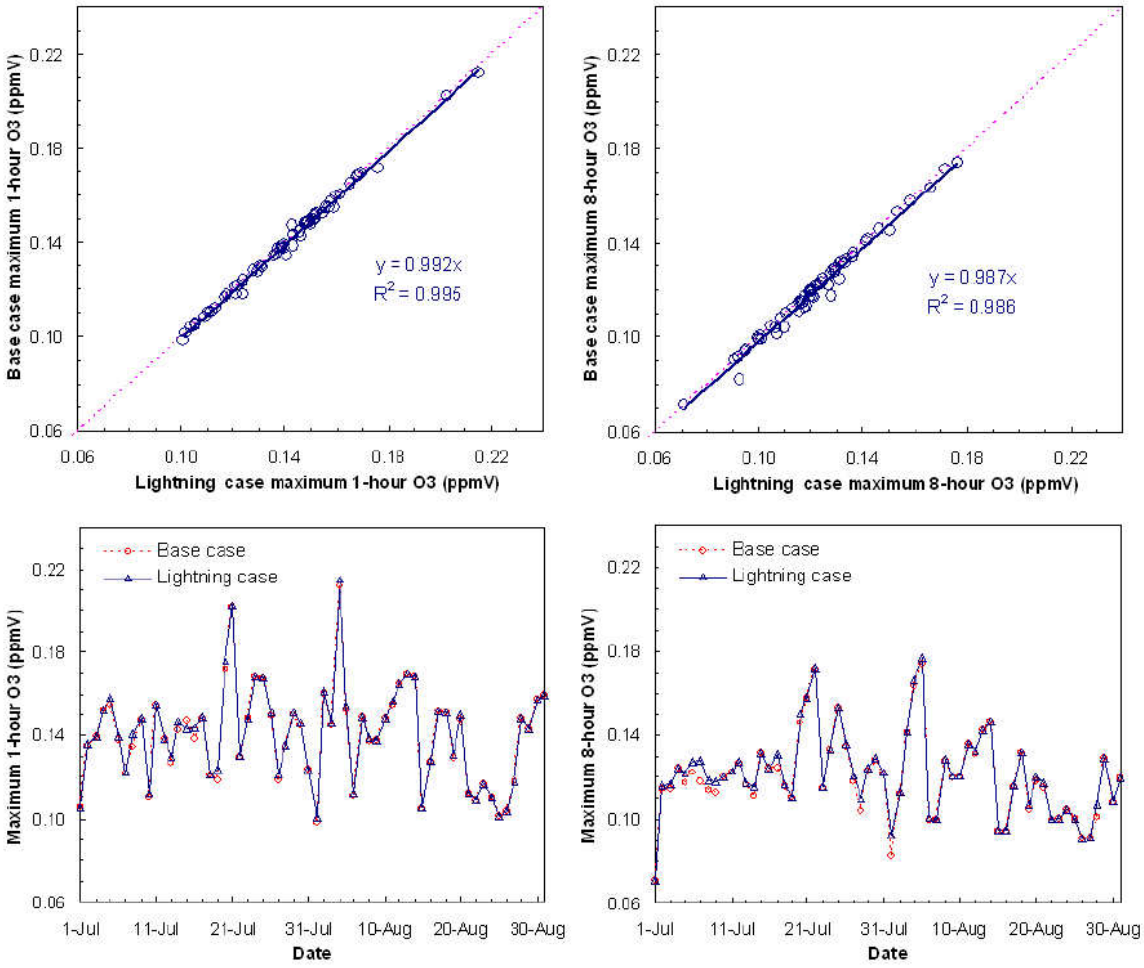

Figure 2.5. Temporal evolution of domain-wide daily maximum 1-h (left panel) and 8-h (right panel) O_3 values with versus without lightning for July-August, 2004 (One grid with the maximum 1-h and 8-h O_3 is selected throughout the whole domain for each day)

lightning emissions are generally, but not always, higher than the base case (Figure 2.6). For grids with monitors, differences due to lightning ranged from –16.7 to 41.5 ppbV for 1-h O_3 and –6.4 to 42.4 ppbV for 8-h O_3. When the base model O_3 is either quite high (more than 100 ppbV) or low (less than 40 ppbV) the differences are smaller (Figure 2.7). This shows that the maximum impacts do not occur when ozone is the maximum in the domain in cities where the anthropogenic emissions dominate. The distribution of the differences between two scenarios shows that for more than 43% of both 1- and 8-h O_3, the difference is less than 2 ppbV (Figure 2.6), though there are some extreme cases of more than 20 ppbV. This suggests that not including lightning NO_x emissions will typically, but not always, have little impact.

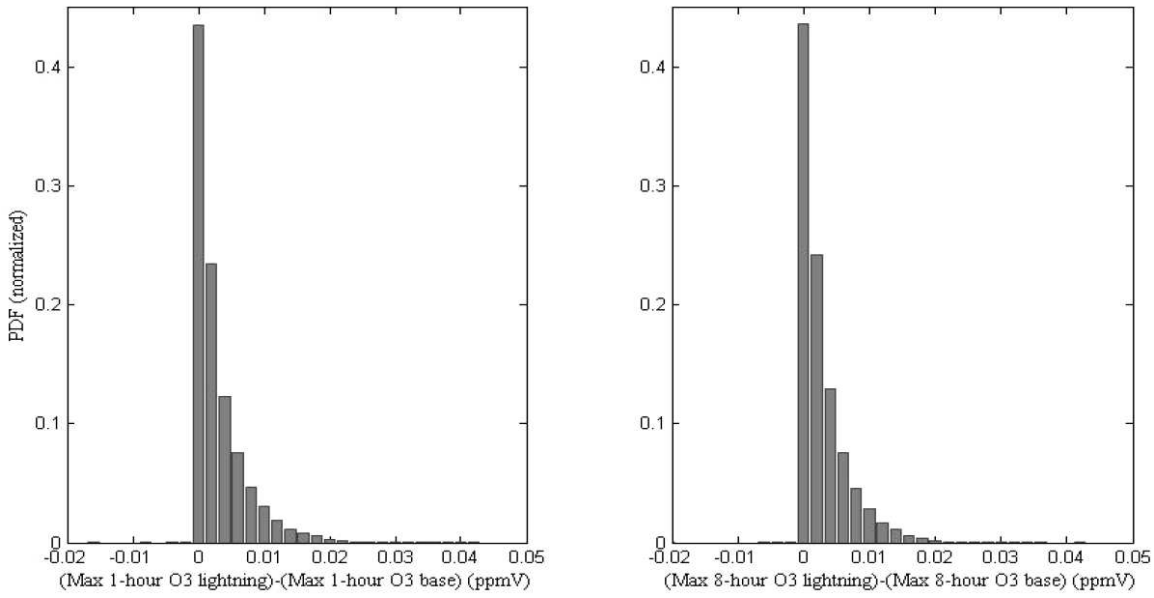

Figure 2.6. Distribution of the difference (Lightning case-Base case) in daily 1-h and 8-h maximum O_3 values for grids with AIRS ozone monitoring stations for July-August 2004

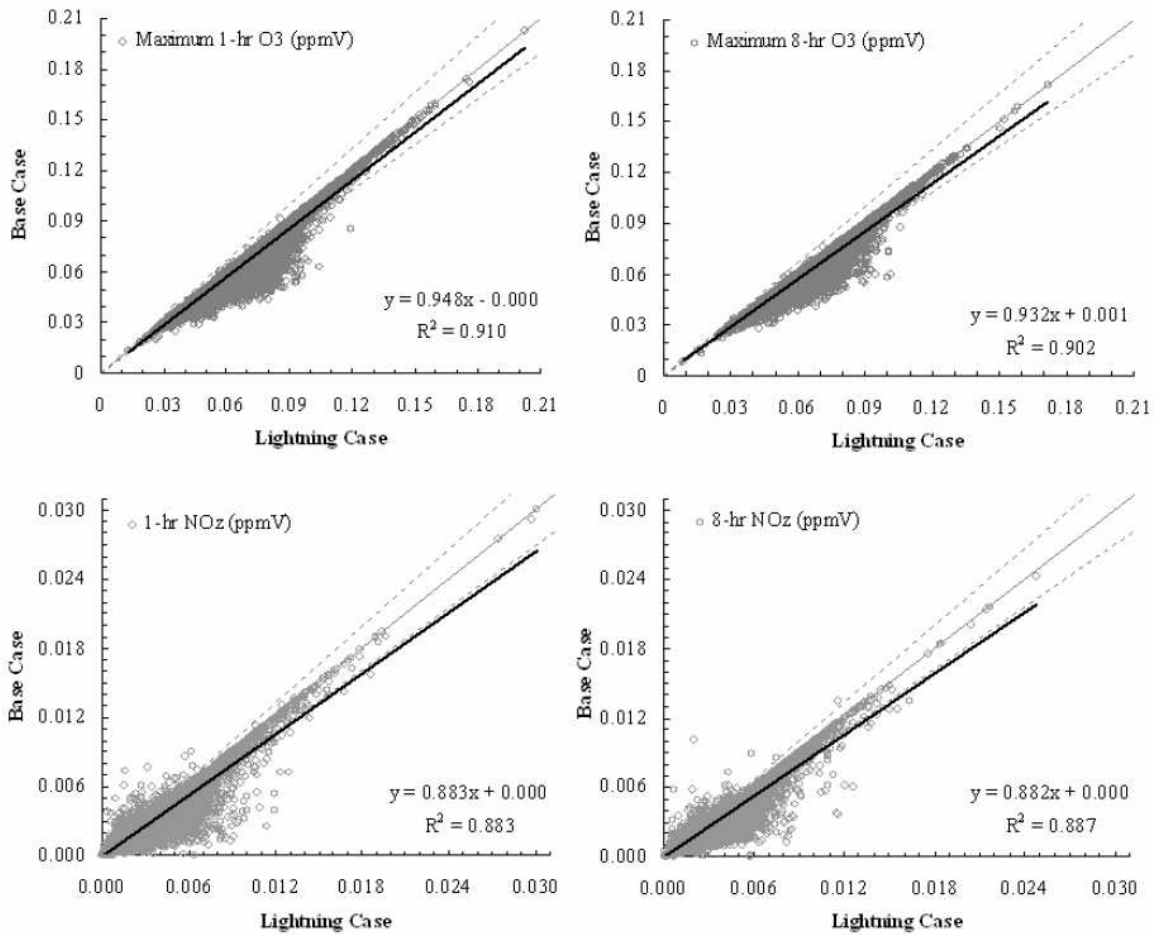

Figure 2.7. Daily 1-h (left panel) and 8-h (right panel) maximum O_3 values and corresponding 8-h NO_z values for model grids with AIRS Ozone monitoring stations for July-August 2004 (692×31 points, red lines indicate 1:1 line and ± %10 lines)

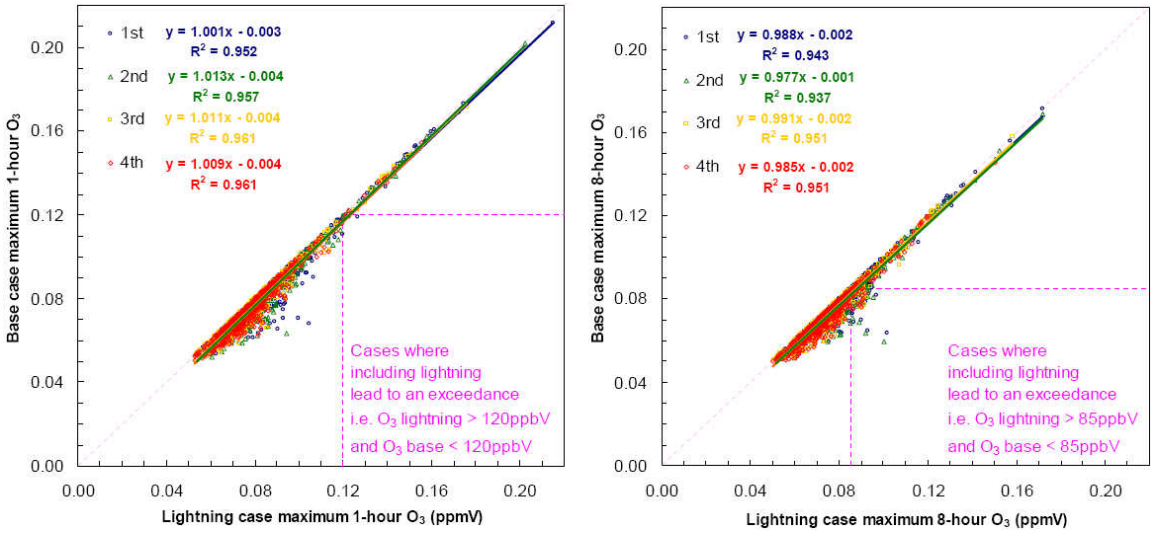

Figure 2.8. The 1st, 2nd, 3rd and 4th highest 1-h (left panel) and 8-h (right panel) maximum O_3 values for model grids with AIRS ozone monitoring stations for July-August 2004. (2768 (692×4) points)

The simulated first, second, third, and fourth highest daily O_3 values for the simulation period are also compared at each of these 692 grid cells (Figure 2.8). The impact of lightning on the 4th highest values of 8-h O_3 is smaller than for daily maximum values. The number of outliers where additional ozone coming from lightning is very high decreases and the correlation between the base case and lightning case ozone increases going from the 1st to 4th highest values (Figure 2.8). Out of the 2768 (4×692) cases, a total of 219 (77 for 1st, 73 for 2nd, 36 for 3rd and 33 for 4th highest values) occurred where including lightning NO_x led to an exceedance of the NAAQS that was not simulated otherwise (Table 2.1). With the recent strengthening of the NAAQS to 75 ppbV (effective May 27, 2008), additional exceedences increased to a total of 572 (~10%). Differences between the two cases narrows from the 1st to 4th highest values (Figure 2.9) suggesting the effect of lightning on 4th highest values is less than on the highest values, and that significant impacts of lightning on peak ozone levels are

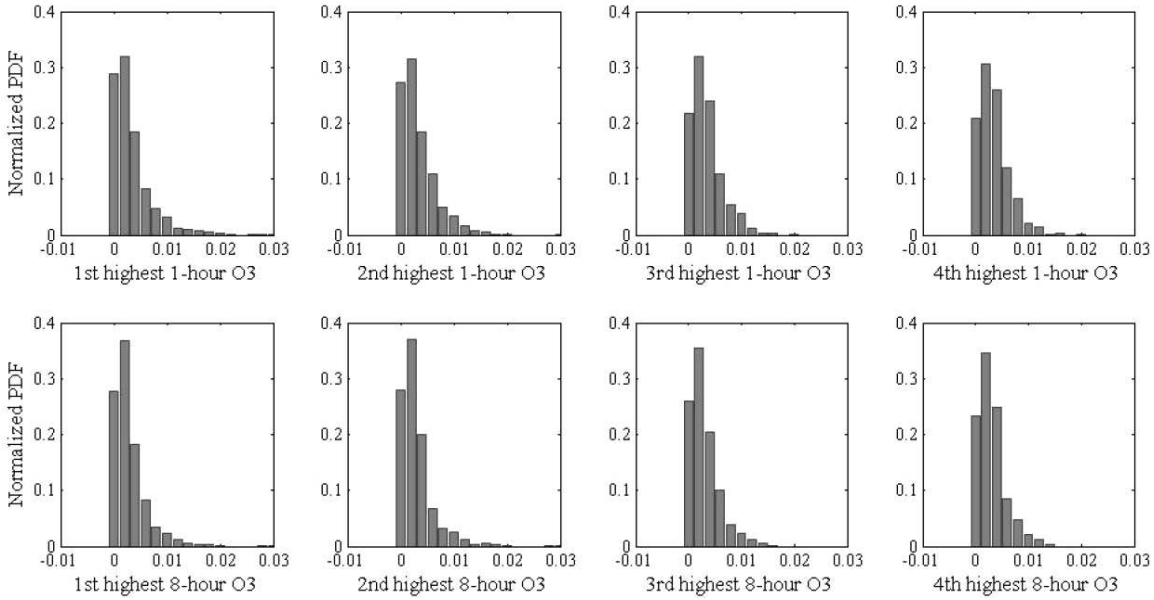

Figure 2.9. Distribution of the difference (Lightning case-Base case) in the 1st, 2nd, 3rd and 4th highest 1-h (top) and 8-h (bottom) maximum O_3 values for grids with AIRS Ozone monitoring stations (PDF's are normalized and differences in units of ppmV)

infrequent. The maximum difference in the 4th highest values is around 14 ppbV whereas it is around 38 ppbV for the 1st highest value. 1-h O_3 follows a similar pattern as 8-h O_3 (Figure 2.9) and the maximum difference in the 4th highest values is around 19 ppbV whereas it is around 36 ppbV for 1st highest value. While this work does find cases where including lightning NO_x leads to additional simulated exceedances of the NAAQS, the approach now used for demonstrating future attainment using a "Relative Reduction Factor" (RRF) will minimize the impact of lightning NO_x in such effects. RRF is the ratio between the modeled future year and basecase 8-h daily maximum O_3 concentrations at a given monitor averaged over the simulation period used for calculating the future design value by multiplying it with the current design value [*EPA*, 2005] The spatial distribution of the lightning effects in the 1st highest daily 1-h and 8-h O_3 shows that the most highly affected regions are high intensity lightning regions where biogenic VOC's are relatively

Table 2.1. The number and percentage of exceedances of 1st, 2nd, 3rd and 4th highest 1-h and 8-h maximum O_3 values for model grids with AIRS ozone monitoring stations for July-August 2004 with and without lightning. (prior O_3 NAAQS 1-h: 0.12 ppmV, 8-h: 0.085 ppmV)

Ozone		**Base case exceedances**		**Lightning case exceedances**		**Increase/ decrease due to lightning**	
		Number	**%**	**Number**	**%**	**Number**	**%**
1-h	1st	37	2.67	41	2.96	4	0.29
	2nd	25	1.81	28	2.02	3	0.22
	3rd	22	1.59	23	1.66	1	0.07
	4th	18	1.30	20	1.45	2	0.14
	Total	102	1.84	112	2.02	10	0.18
8-h	1st	210	15.17	287	20.74	77	5.56
	2nd	150	10.84	223	16.11	73	5.27
	3rd	100	7.23	136	9.83	36	2.60
	4th	77	5.56	110	7.95	33	2.38
	Total	537	9.70	756	13.66	219	3.96

abundant and O_3 production is limited by NO_x (Figure 2.10). The greatest differences in 8-h O_3 are in Ocala and Panama City, FL (more than 20 ppbV), Salt Lake City, UT (up to 14 ppbV) and Denver, CO (up to 16 ppbV). Florida, being the region with the most intense lightning during this period, is expected to have high impacts. Even though the other two cities do not have high biogenic emissions, the sensitivity of ozone to NO_x emissions from our simulations is positive, indicating an increase in ozone with additional NO_x emissions. The high altitude of those two cities, which results in high photolysis rates, increases radical production and allows more effective use of additional NO_x.

A sensitivity simulation for August 2004 using the older vertical profile showed less surface-layer O_3 than the updated profile even though it allocates more NO_x near the surface. Reasons for the depressed O_3 come from the timing of those emissions and the

level of NO_x production. Much of the lightning-derived NO_x is due to strong convective activity and found later in the afternoon into the evening and night. Such periods have decreased photolysis from cloud cover or high solar zenith angles, and large amounts of fresh NO_x emissions do not immediately contribute to photochemical ozone production and can lead to ozone decreases by both direct titration and nighttime chemistry that further reduces ozone as well as depletes much of the NO_x produced [*Russell et al.*, 1986]. Accordingly, the sensitivity simulation resulted in higher daily maximum domain-wide O_3 values for some days, and lower on others depending upon the timing and extent of NO_x production. The destruction effect is more obvious if AIRS monitoring stations are investigated. These results from AIRS monitors are focused on urban areas, and as such have higher NO_x levels. Including lightning emissions in the sensitivity case results in somewhat greater decreases with few increases in the first, second, third and fourth highest values compared to the updated profile. The maximum difference in the 4^{th} highest 8-h O_3 values is 23 ppbV whereas it is 35 ppbV for the 1^{st} highest. 1-h O_3 follows a similar pattern as 8-h O_3 and the maximum difference in the 4^{th} highest values is 33 ppbV versus 46 ppbV for 1^{st} highest value. There are also significant decreases in ozone with the addition of lightning by up to -20 ppbV. Overall, the net additional exceedance from lightning with the older lightning NO_x distribution profile is -1.8% for 8-h. The highest 8-hr ozone level also had the highest reduction with -3.6%, showing a negative sensitivity.

The effect of North American lightning NO_x emissions on average background ozone can also be investigated by finding the y-intercept of O_3 versus NO_z [*Hirsch et al.*, 1996; *Trainer et al.*, 1993] which gives the background ozone as 42.2 and 43.9 ppbV

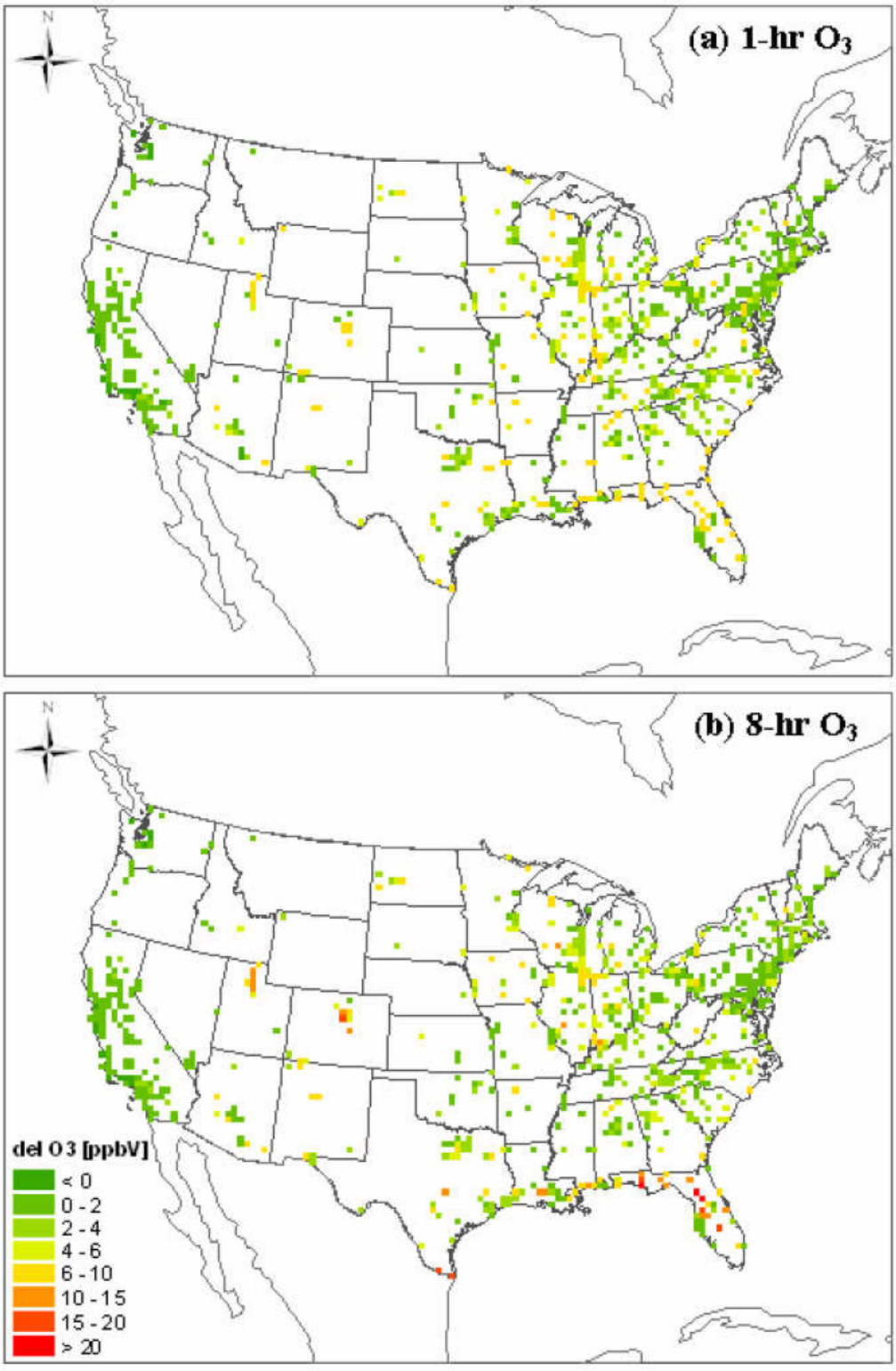

Figure 2.10. Differences in (a) 1-h and (b) 8-h maximum O_3 values for model grids with AIRS Ozone monitoring stations for July-August 2004 (Difference in maximum daily first highest values are selected for each grid)

without and with lightning NO_x emissions, respectively (Figure 2.11). The simulated difference, 1.7 ppbV, is statistically significant at the 95% confidence level. The slope of the line in Figure 2.11 suggests overall ozone production efficiency (OPE) of about 5.66 for the base case and 5.47 for the lightning case showing that addition of lightning NO_x resulted in a decrease in overall OPE's for ground level ozone. One alternative to this approach is to calculate the ozone production rates from the lightning, which can be derived from $\Delta O_3/\Delta NO_z$. This approach yields 1.2 ppbV increase in background ozone and a 5.56 for OPE. As discussed above, injection of NO_x in the late afternoon and night increases NO_z, but can decrease ozone due to direct titration and nighttime chemistry.

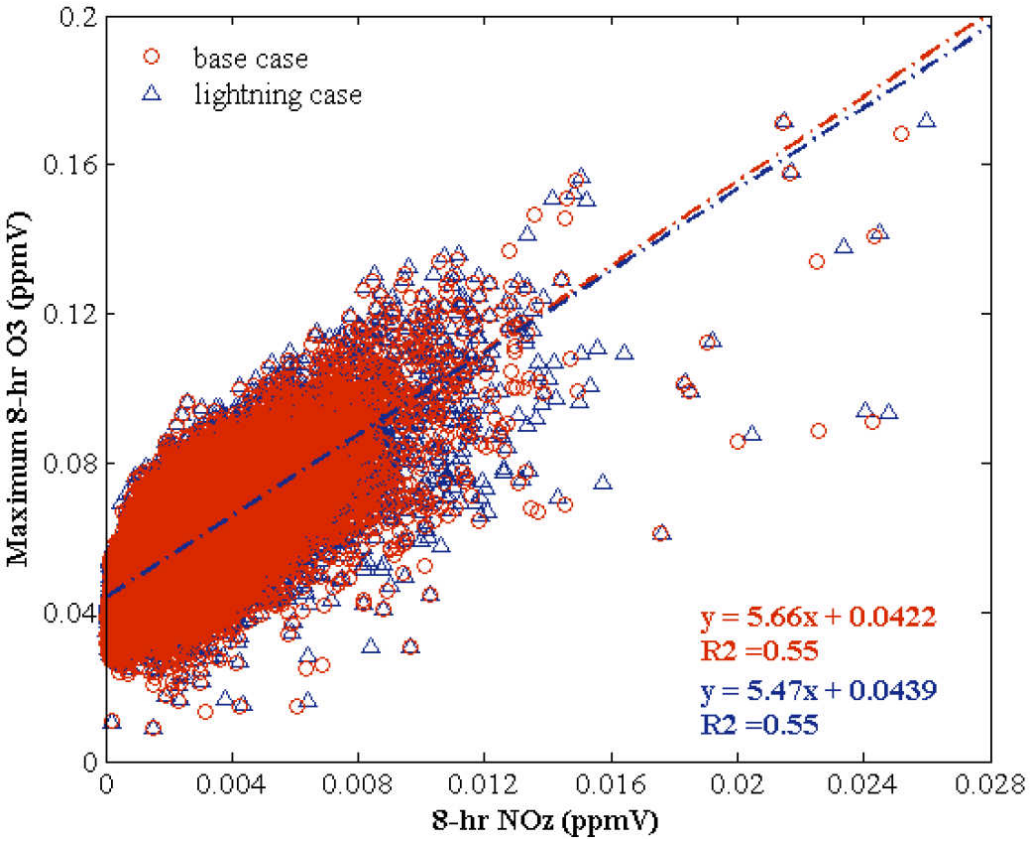

Figure 2.11. Daily 8-h maximum O_3 versus corresponding daily 8-h NO_z (NO_y-NO_x) for grids with AIRS Ozone monitoring stations for July-August 2004. Shown are results for the base case (no lightning emissions) and lightning case.

2.4. Conclusions

Lightning NO_x emissions estimated in this study account for 30% of the final total US emissions for July-August 2004 with the assumed NO_x production rate per flash and IC/CG ratio. Spatial distributions show emissions are significant in three main regions in the US: the Southeast, Texas and surrounding and the Midwest. Resulting differences in daily maximum 1-h and 8-h O_3 were typically small, with more than 77% and 71% of concentrations being within 2 ppbV, respectively. On average, the difference in the domain-wide peak was 1.1 ppbV and 1.7 ppbV for 1-h and 8-h O_3 values. While infrequent, there were a few days with significant increases in the domain-wide peaks (up to 6 ppbV in 1-h and 10 ppbV in 8-h levels). However, these did not occur on days of high maximum ozone.

In the 692 grids with ozone monitors, daily maximum 8-h O_3 with lightning emissions are usually, but not always, higher than the base case. Differences in the grids with monitors ranged from –16.7 to 41.5 ppbV for 1-h and–6.4 to 42.4 ppbV for 8-h O_3. For more than 43% of the cases, the differences were less than 2 ppbV, but there are a few cases of more than 20 ppbV increases for 1-h and 8-h O_3. The 1^{st} to 4^{th} highest values for these grids experienced a smaller simulated impact. The correlation between base case and lightning case ozone increased going from the 1^{st} to 4^{th} highest values showing the effect of lightning on the 4^{th} highest is less than on the highest. The maximum difference in the 4^{th} highest ozone in the domain is around 19 ppbV (36 ppbV for 1^{st} highest) for 8-h O_3. These results indicate lightning NO_x can cause significant increase of ozone in some extreme cases but its effect on ozone decreases if these extreme cases are excluded.

Allocating more NO_x to the near-surface atmosphere for August 2004 led to less O_3 on average. The destruction effect is more obvious for AIRS monitoring stations which focus on urban areas. Overall, the net additional exceedances from lightning with the older lightning NO_x distribution profile are either zero or negative for virtually all cases.

Even though the North American emissions of NO_x from lightning are significant, the impact on daily maximum 8-h O_3 for entire US and policy relevant background ozone is typically small. There was only a 1.7 ppbV increase in regional background ozone. On the other hand, spatial distribution of these emissions and some occasions of higher ozone suggest that these can lead to significant local impacts on a few occasions, especially in the southern US, and analyses of ozone exceedances should consider if lightning may be a contributing factor. Lightning elsewhere in the world may also contribute to background ozone over North America through long-range transport. Given the rather minor impacts of lightning NO_x on ground level ozone found here, reducing the assumed emissions would lead to a nearly linear reduction in the ozone impact calculated [*Cohan et al.*, 2005].

CHAPTER 3

COMPARISON OF WEEKLY CYCLE OF NO_2 SATELLITE RETRIEVALS AND NO_x EMISSION INVENTORIES FOR THE CONTINENTAL US*

Abstract

Spatially-resolved weekly NO_2 variations are obtained from 2003-2005 SCIAMACHY tropospheric NO_2 columns for 3 different types of regions: urban, rural and rural-point (rural with significant electricity generation unit (EGU) emissions). Regions are compared for magnitudes and weekly profiles. Rural regions do not show any weekly pattern, whereas urban areas show a distinct decrease on the weekends. Rural regions with EGU's show a slight decrease on Sundays. When compared with estimated mobile and stationary nitrogen oxides (NO_x) emissions from the year 2004 for 7 cities, the satellite data have greater variation during weekdays (Monday-Friday). Overall comparisons show that SCIAMACHY derived NO_2 correlate well with estimated NO_x emissions for "urban" and "rural" but less for "rural-point" regions.

3.1. Introduction

Nitrogen oxides (NO_x=NO+NO_2) play a key role in the chemistry of the troposphere and come mainly from fossil fuel combustion, biomass burning, soil release, oxidation of atmospheric ammonia, lightning, transport of NO_x from stratosphere and

---

* This chapter is published in the Journal of Geophysical Research - Atmosphere, Vol. 114, D05302, doi:10.1029/2008JD010714, 2009. Co-authors are Yongtao Hu, Randall V. Martin, Christopher E. Sioris, and Armistead G. Russell.

aircraft emissions. NO_x emission impacts include increasing tropospheric ozone, particulate matter, acid deposition and nutrient enrichment.

United States (US) anthropogenic NO_x emissions mainly come from transportation (55%), fuel combustion for electricity generation (22%) and industrial activities (14%) (http://www.epa.gov/ttn/chief/trends/). Recent control programs, including the 1998 NO_x State Implementation Plan (SIP) Call and the Clean Air Interstate Rule (CAIR) target power industry NO_x emissions to reduce ozone formation [*EPA*, 2005a] and estimated 2004 point source emissions in the US decreased to 55% of 1990 levels even though total electricity production is increased [*EPA*, 2005b]. Kim et al. [2006] recently showed that space-based instruments also observed these declining regional NO_x levels between 1999 and 2005.

The relationship between NO_x emissions and tropospheric NO_2 columns, which are closely related because of the short lifetime of NO_x, were investigated by several researchers. Most of the earlier studies have used models for this relationship [*Jaegle et al.*, 2005; *Kim et al.*, 2006; *Leue et al.*, 2001; *Martin et al.*, 2003; *Müller and Stavrakou*, 2005]. Toenges-Schuller et al. [2006] showed high correlations between tropospheric NO_2 columns and anthropogenic NO_x emissions. Observations from different satellite platforms were also compared (late morning -SCIAMACHY and early afternoon-OMI) to have more insight on the diurnal variation in different NO_x sources [*Boersma et al.*, 2008].

In a previous study of the weekly cycle of NO_2 using a remote sensing instrument, Beirle et al. [2003] used the Global Ozone Monitoring Experiment (GOME) instrument and observed a distinct Sunday minimum for all countries with a Christian tradition.

That study mainly focused the eastern US and Los Angeles. The spatial resolution of GOME is 320×40 km^2, which is approximately 7 times larger than SCIAMACHY's spatial resolution.

The aim of this study is to distinguish the relative effects of the urban NO_x sources which are dominantly mobile source-related (both on-road and off-road) and exhibit weekly variation from other sources like fuel combustion for electricity generation using satellite data and to compare these observed weekly and spatial variations with estimated emissions. Such comparison can help to assess the accuracy and consistency of current estimates. Comparing estimated emissions from relatively well-characterized areas with tropospheric columns obtained from satellites can also provide a better understanding of how to use satellite data in regions where emission estimates are unavailable or highly uncertain.

3.2. Methods

3.2.1. NO_2 Satellite Retrievals

The Scanning Imaging Absorption Spectrometer for Atmospheric Chartography (SCIAMACHY) instrument onboard the ENVISAT satellite measures atmospheric NO_2 columns through observation of global backscatter [*Bovensmann et al.*, 1999]. ENVISAT was launched in March 2002 into a sun-synchronous orbit with an equator crossing time of 10:00 am, and a typical US observation time of 10:30 am. The SCIAMACHY instrument has a typical spatial resolution of 30 km along track by 60 km across track in the nadir view with a global coverage over 6 days. Algorithms used for retrieval of tropospheric NO_2 columns from SCIAMACHY data, along with uncertainty estimates used in this study (2003-2005), are obtained from Martin et al. [2002; 2003; 2006].

Satellite retrievals depend on normalized *a priori* NO_2 profiles which are usually obtained from chemical transport models. Several studies compared these profiles with aircraft measurements [*Bucsela et al.*, 2008; *Martin et al.*, 2004; *Martin et al.*, 2006] and found minor differences.

Three different region types ("urban", "rural" and "rural-point", i.e. rural areas with a large-scale electricity generating unit (EGU)) are selected (Figure 3.1) in order to investigate how weekly patterns in NO_2 levels vary in different areas, and how they compare to emission estimates in urban and rural areas. Seven major cities in the US ("urban") are investigated (Atlanta, Chicago, Houston, Los Angeles, New York, Phoenix and Seattle). These cities are selected because of their large populations and related NO_x emissions. They also represent different topographical and meteorological conditions, both of which will affect ambient NO_2 concentrations and, possibly, satellite retrievals. All these cities, except Seattle, are in non-attainment of the 2008 US EPA 8-hr ozone standard of 0.075 ppmV. Eleven rural areas ("rural") are selected close to these 7 cities where there are neither significant point NO_x sources nor urbanized land (Figure 3.1). Additional rural areas ("rural-point") were identified that contain no urbanized land but do contain one or more large EGU's emitting more than 0.1% of total NO_x emissions from all listed facilities. Urbanized area definitions used are from Census2000 (http://www.census.gov/geo/www/cob/ua2000.html) and NO_x emission information for major EGU's are obtained from Environmental Protection Agency (EPA) (http://www.epa.gov/air/data).

SCIAMACHY pixels that intersect the selected areas at times with a cloud radiance fraction less than 0.5 are used for calculating the averaged weekly profiles of

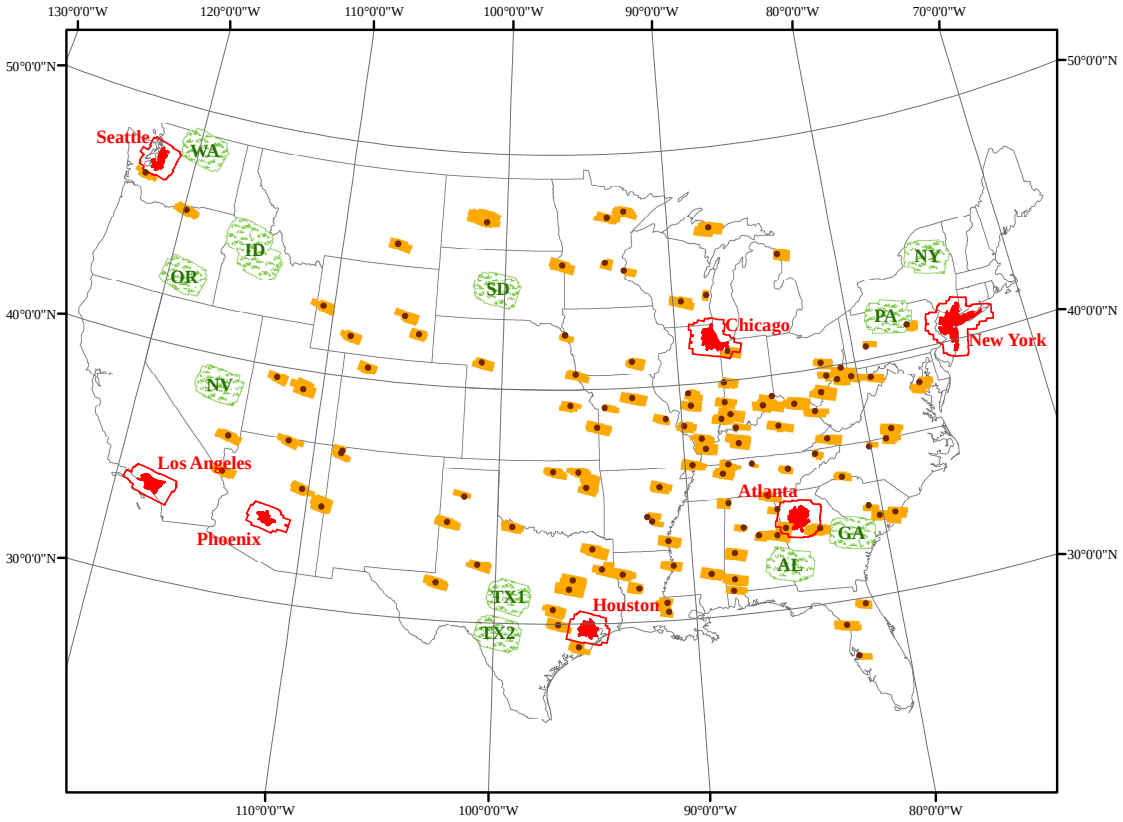

Figure 3.1. “Urban”, “rural” and “rural-point” areas selected

selected areas (Figure 3.1). SCIAMACHY maps the US in the late mornings; therefore averaged pixels actually represent morning averages. Weekly profiles of these regions are obtained by averaging the pixels by day of the week. The averages are also normalized seasonally for areas in order to eliminate the effect of seasonal variation of NO_2 lifetime on weekly profiles. Normalization is performed by averaging intersected pixels for each season for each location and then dividing them with the seasonal average for that location, over all days of the week. Individual pixel uncertainties are propagated to calculate overall uncertainty.

The SCIAMACHY nadir footprint is approximately 30×60 km^2, so when a pixel intersects an urban area, the pixel includes less urbanized land as well. However, as evidenced by emission estimates, urban emissions dominate over the extended region.

One complication that could rise is the case where there is a large-scale EGU near an urban area, which could obscure the urban analyses. This is the case in Atlanta, and is further investigated in the results and discussion part.

3.2.2. NO_x Emissions

The 2004 emission inventory (12 months) used in this study is estimated by applying growth and control factors to a 2002 base inventory (VISTAS) [*MACTEC*, 2005]. Growth factors are calculated using the Economic Growth Analysis System (EGAS) Version 4.0 and the control factors are obtained from EPA for the existing federal control strategies which were in place in 2004. In addition, hourly actual NO_x emissions in 2004 are obtained from the continuous emissions monitoring (CEM) database [*EPA*, 2008]. Mobile emissions here are the sum of on-road and non-road emissions; stationary emissions are the sum of area and point source emissions and total emissions are the sum of mobile, stationary and biogenic emissions. Gridded hourly emissions are prepared using the Sparse Matrix Operator Kernel for Emissions (SMOKE) [*Houyoux and Vukovich*, 1999].

NO_x emissions are summed using the intersected area ratios (urban area inside the grid divided by total area of the grid) for each grid cell -36km×36km- that is part of the 7 cities (“urban”) and the 11 rural areas (“rural”)). Daily totals for each city and rural area are averaged for each weekday to obtain weekly emission profiles for 2004. Emissions for grid cells that intersect with pixels for “rural-point” are also processed similarly.

Although about 90% of the NO_x emissions are emitted as NO, in the presence of O_3 or other oxidants, NO quickly oxidizes to NO_2 in the atmosphere. Measurements show that in the lower troposphere, most of the NO_x is in the form of NO_2 during the day

[*Bradshaw et al.*, 1999; *Martin et al.*, 2002], except near major NO_x sources, so NO_x emission estimates and SCIAMACHY NO_2 total tropospheric columns are comparable, recognizing that some NO_x will remain as NO, and a fraction will be oxidized to other products. Averaged NO_2 columns obtained from SCIAMACHY are multiplied by total pixel areas and converted to moles to obtain total NO_2 burden for each area to compare with NO_x emissions (moles/day). Total amounts calculated for each area by this method are directly related to the scanned urban area. The city with highest NO_2 columnar abundance is Los Angeles (molec/cm^2), while New York (moles) has the greatest total mass of NO_2 over the area investigated. This is consistent with the estimated total daily emissions.

3.3. Results and Discussion

Averaged satellite observations of the individual cities clearly show a weekend decrease, whereas the rural areas without EGU's show no significant change during the weekends (Table 3.1, Figure 3.2). The seasonally normalized weekly profiles for "urban" regions also show the Sunday minimum clearly (Figure 3.3). The minimum for "rural-point" is on Sunday as it is for cities, though the difference versus weekdays is small. New York has the highest and Seattle has the lowest net tropospheric NO_2 columns (area×NO_2 column density) among the seven cities (Figure 3.4). New York, Los Angeles, Chicago, Houston, Atlanta and Seattle show changes during the weekdays, whereas Phoenix does not show significant variation. All cities have minimums on Sunday. Atlanta, Chicago, Houston, Los Angeles, New York, Phoenix and Seattle, respectively show 28%, 47%, 42%, 46%, 37%, 56%, and 59% decreases on Sundays when compared with mean weekday values (Table 3.1). Rural regions with power plants show an average

Table 3.1. The average, standard deviation, uncertainty ($\times 10^{15}$ molecules/cm^2) and count of selected SCIAMACHY retrievals in each region for three years (2003-2005)

Region		Mon	Tue	Wed	Thu	Fri	Sat	Sun	Total	Weekend	Weekdays
Atlanta	Average	6.56	7.22	4.95	8.00	6.44	4.84	4.72	6.02	4.78	6.56
	Std Dev	4.01	5.51	3.24	5.89	4.06	3.04	3.73	4.39	3.42	4.64
	Uncertainty	0.36	0.34	0.24	0.47	0.25	0.23	0.22	0.11	0.16	0.14
	Count	74	113	98	71	157	103	118	734	221	513
Chicago	Average	10.65	7.58	12.80	10.45	11.41	6.64	5.77	9.64	6.22	10.80
	Std Dev	7.61	5.75	8.31	8.45	9.73	4.89	5.00	7.97	4.95	8.45
	Uncertainty	0.54	0.40	0.55	0.48	0.47	0.32	0.31	0.18	0.23	0.23
	Count	93	91	125	124	162	105	97	797	202	595
Houston	Average	6.29	5.86	7.70	7.77	5.23	4.62	3.91	6.11	4.16	6.76
	Std Dev	4.67	5.04	6.38	5.60	3.87	3.39	2.72	5.10	2.98	5.48
	Uncertainty	0.44	0.37	0.39	0.50	0.38	0.37	0.23	0.15	0.20	0.19
	Count	51	72	108	59	48	39	72	449	111	338
Los Angeles	Average	14.10	15.83	15.45	17.70	18.41	12.41	8.82	14.34	10.27	16.45
	Std Dev	10.63	11.17	10.24	12.39	12.23	7.79	6.69	10.70	7.36	11.53
	Uncertainty	0.73	0.64	0.79	0.75	0.81	0.54	0.33	0.24	0.29	0.33
	Count	93	147	87	132	118	120	178	875	298	577
New York	Average	10.14	8.55	9.91	13.02	11.26	7.64	6.61	9.48	7.11	10.47
	Std Dev	8.43	6.40	7.81	12.03	9.14	5.76	5.70	8.27	5.75	8.93
	Uncertainty	0.35	0.29	0.41	0.55	0.42	0.27	0.25	0.14	0.18	0.18
	Count	232	218	150	167	190	196	204	1357	400	957
Phoenix	Average	6.78	6.21	5.96	6.85	6.39	5.52	2.83	5.71	4.20	6.48
	Std Dev	6.39	3.93	4.20	5.74	4.74	4.07	2.16	4.80	3.53	5.17
	Uncertainty	0.36	0.29	0.41	0.43	0.45	0.28	0.15	0.13	0.16	0.17
	Count	106	105	50	71	50	99	96	577	195	382
Seattle	Average	3.15	3.32	4.05	3.82	4.26	3.35	1.51	3.31	2.37	3.71
	Std Dev	2.23	2.53	3.23	4.42	3.60	2.89	2.02	3.15	2.62	3.27
	Uncertainty	0.17	0.21	0.26	0.28	0.25	0.21	0.12	0.08	0.12	0.10
	Count	88	68	66	69	82	73	83	529	156	373
Urban	Average	8.76	8.60	9.23	10.94	10.03	7.01	5.56	8.52	6.23	9.49
	Std Dev	7.94	7.71	7.93	10.30	9.28	5.87	5.36	8.06	5.65	8.71
	Uncertainty	0.17	0.16	0.19	0.23	0.19	0.14	0.11	0.06	0.09	0.08
	Count	737	814	684	693	807	735	848	5318	1583	3735
Rural -Point	Average	3.14	3.35	3.36	3.79	3.57	3.24	2.76	3.30	2.99	3.43
	Std Dev	2.65	2.80	2.62	3.36	2.89	2.76	2.16	2.76	2.48	2.87
	Uncertainty	0.06	0.06	0.06	0.08	0.07	0.06	0.05	0.02	0.04	0.03
	Count	846	796	840	699	789	795	871	5636	1666	3970
Rural	Average	1.13	1.12	1.11	1.28	1.23	1.01	1.22	1.15	1.10	1.17
	Std Dev	1.42	1.54	1.74	1.83	1.84	1.64	1.85	1.70	1.74	1.69
	Uncertainty	0.02	0.02	0.03	0.03	0.03	0.02	0.03	0.01	0.02	0.01
	Count	1253	1274	1224	1294	1320	1376	1123	8864	2499	6365

NOTE: Std Dev is the standard deviation of the averaged pixels and is driven by seasonal variation and orbital changes in the location of the satellite footprint. Uncertainty is the uncertainty of the mean calculated from individual uncertainties $((\Sigma u_i^2)^{0.5}/ N)$. Random uncertainties are used here since major sources of systematic uncertainty, such as surface reflectivity and clouds, are unlikely to systematically affect day-of-week variation.

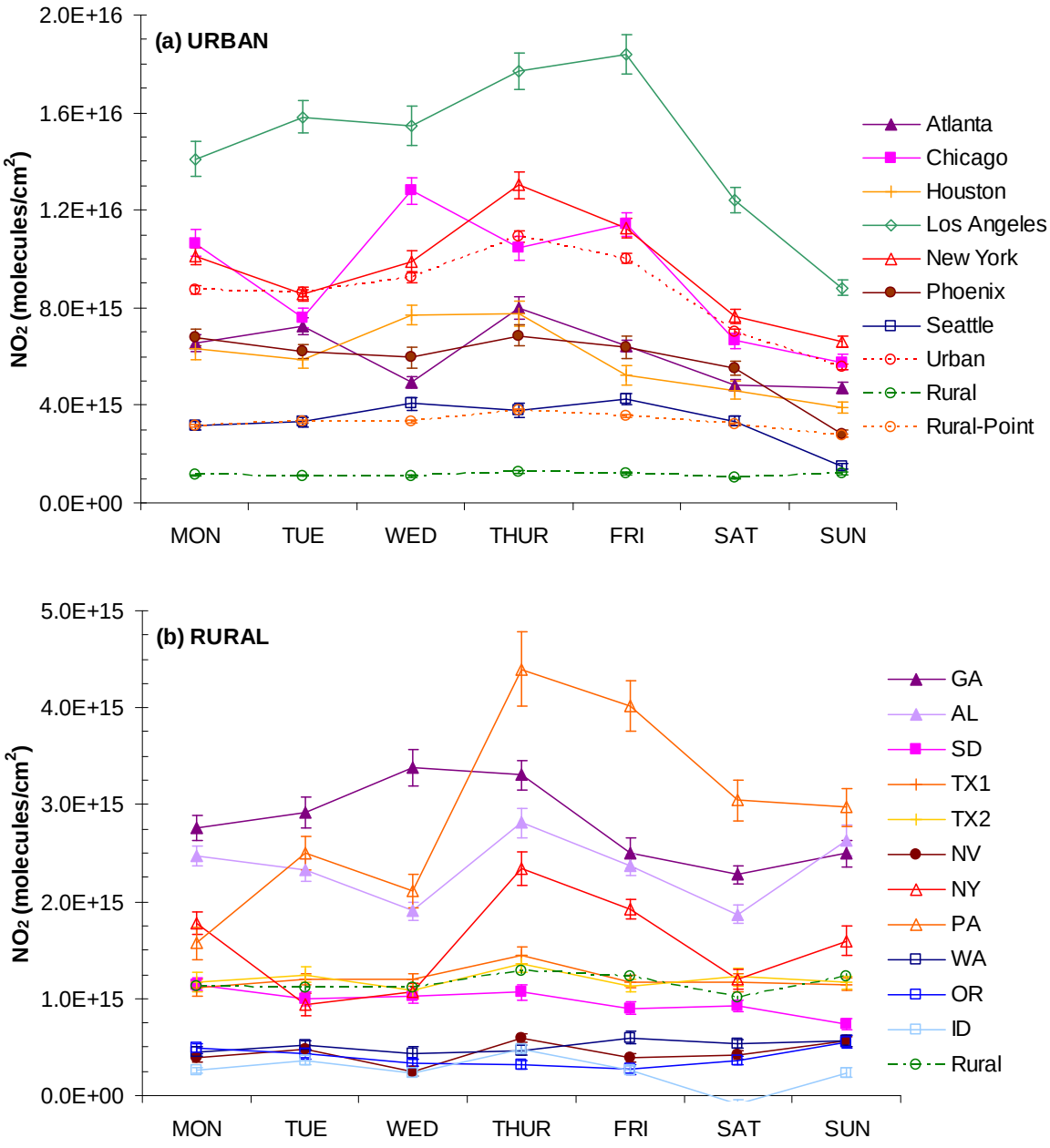

Figure 3.2. Averaged weekly profile of SCIAMACHY retrievals with uncertainties for (a) “urban” and (b) “rural” areas. Solid lines are the overall averages for indicated area types. (“Rural” areas are labeled by the abbreviation of the state they fall inside and color coded similarly with closest “urban” area for comparison)

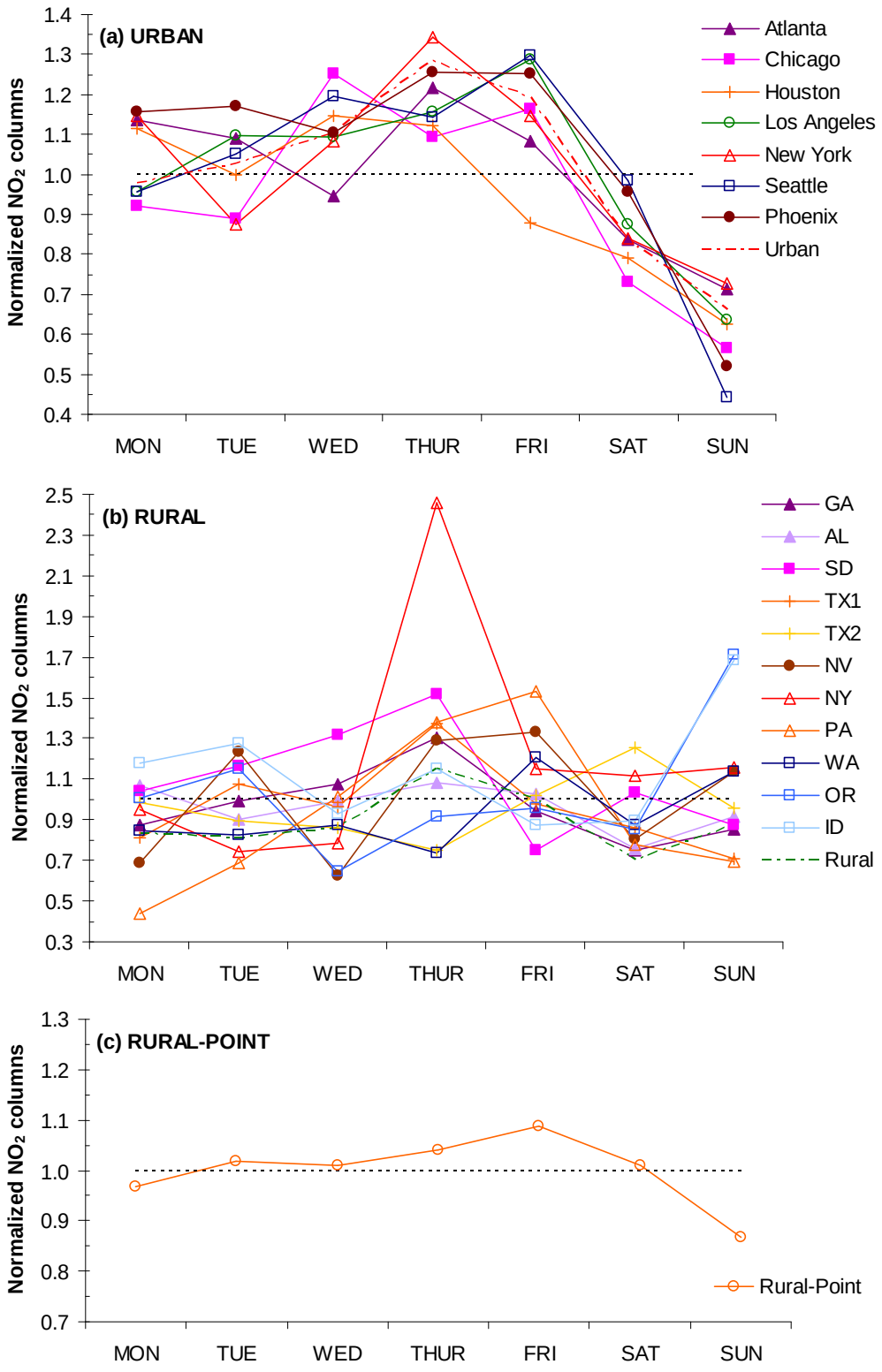

Figure 3.3. Seasonally normalized weekly profile of SCIAMACHY retrievals for (a) "urban", (b) "rural" and (c) "rural-point" areas. Dashed lines are the overall averages for all "urban" and "rural" areas. (High THUR value for rural area NY results from low number of scans with high columns available for fall season for that day)

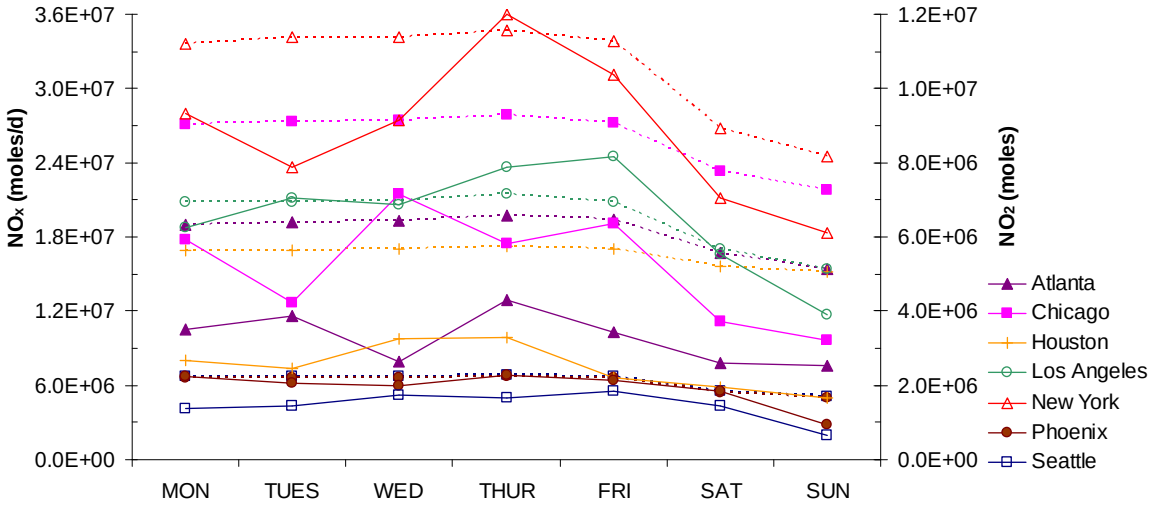

Figure 3.4. Comparison of SCIAMACHY derived NO_2 with total NO_x emissions for selected cities (dashed lines: emission derived NO_x, continuous lines: SCIAMACHY-derived NO_2 burden)

20% decrease on Sunday. Days with maximum and minimum NO_2 for Los Angeles (Friday-Sunday), Chicago (Wednesday-Sunday) and New York (Thursday-Sunday) are consistent with previous work of Beirle et al. [2003] using GOME NO_2 retrievals. Normalized weekly profiles for Los Angeles and Chicago are very similar to Beirle et al. [2003], but weekly profiles obtained by GOME from New York lacks the day-to-day variation that SCIAMACHY observes in our study. Lastly, Chicago has a significantly lower normalized Sunday column, but Los Angeles and New York have slightly higher normalized Sunday columns than compared to Beirle et al. [2003]. All cities except Seattle have significantly higher NO_2 columns than averaged "rural" and "rural-point" regions (Figure 3.2). All the "urban" regions have significantly higher tropospheric NO_2 columns than nearby "rural" regions, as expected.

Even though lightning emissions are prepared for this episode [*Kaynak et al.*, 2008], they are not included in total emissions for this comparison. Unlike anthropogenic

emissions which exist primarily as NO_2 in the lower troposphere, lightning NO_x in the free troposphere exists primarily as NO. Furthermore, lightning NO_x has a distinctive seasonal pattern with very intense activity in summer months. Including lightning emissions for one year may overestimate their effect on the emission inventory which would not be appropriate for comparison with 3-year averaged NO_2 retrievals. Further, lightning is associated with cloud cover, and one expects a decrease in the probability of capture its effects on clear days.

A number of factors impact comparing SCIAMACHY retrievals and emission estimates: (1) uncertainty in the SCIAMACHY retrievals; (2) seasonal variation of NO_x lifetime, (3) 12-month averaging of the emissions, and (4) limited conversion of NO to NO_2 (or significant conversion of NO_2 to other species). Even if individual pixel uncertainties are high, as the number of pixels averaged increases, the uncertainty of the mean decreases for weekly variation. Averaging of the pixels over a year decreases scatter, but seasonal variation of NO_2 lifetime and partitioning of NO_2 in NO_x emissions, particularly near sources in winter and transport or conversion of NO_2 to HNO_3 and PAN is a concern. As such, the available 3-year dataset is averaged to obtain statistically significant results for each area and normalized to remove seasonal variations. Emission inventories do not change significantly on a day-to-day basis (Table 3.2), except weekends and holidays, minimizing the need for long-term averaging.

Another important issue is that in the areas studied, SCIAMACHY total tropospheric NO_2 columns are morning averages but NO_x sources continue to emit during the day, and atmospheric chemistry will deplete NO_x. This, and the limited NO_x lifetimes, would suggest that the amount of NO_x emitted daily in each airshed is likely to be more

Table 3.2. The average and standard deviation of daily total NO_x emissions ($\times 10^6$ moles/day) averaged for the year of 2004

Region		Mon	Tue	Wed	Thu	Fri	Sat	Sun	Total
Atlanta	Average	19.01	19.22	19.30	19.73	19.42	16.70	15.37	18.40
	Std Dev	2.58	2.33	2.32	2.34	2.34	2.00	1.75	2.72
Chicago	Average	27.11	27.31	27.39	27.85	27.22	23.33	21.77	26.01
	Std Dev	2.34	1.44	1.23	1.71	1.82	1.58	1.48	2.79
Houston	Average	16.95	16.97	17.05	17.20	16.98	15.66	15.17	16.57
	Std Dev	0.76	0.69	0.30	0.54	0.81	0.25	0.48	0.94
Los Angeles	Average	20.77	20.86	20.92	21.47	20.84	17.00	15.36	19.61
	Std Dev	1.80	1.16	0.46	1.25	1.66	0.40	0.64	2.51
New York	Average	33.63	34.18	34.13	34.70	33.79	26.78	24.56	31.69
	Std Dev	3.91	2.67	2.47	3.10	3.30	2.89	2.62	4.89
Phoenix	Average	6.57	6.64	6.65	6.72	6.59	5.43	5.03	6.24
	Std Dev	0.63	0.55	0.47	0.59	0.68	0.39	0.42	0.84
Seattle	Average	6.68	6.71	6.73	6.87	6.71	5.54	5.13	6.34
	Std Dev	0.58	0.40	0.25	0.41	0.56	0.12	0.23	0.76
Urban	Average	18.67	18.84	18.88	19.22	18.79	15.78	14.63	17.84
	Std Dev	9.46	9.48	9.45	9.67	9.44	7.64	7.04	9.09

emissions in each city are always higher than column integrated NO_2 obtained from SCIAMACHY retrievals for "urban" areas (Figure 3.4). Observed NO_2 to estimated NO_x emissions ratios range between 0.11 (Houston-Sunday) to 0.39 (Los Angeles-Friday) for individual days and between 0.18 (Atlanta) to 0.33 (Los Angeles) on average. As discussed previously, a part of the reason for this can be due to transport out of the region used for comparison, conversion of NO_x to HNO_3 and PAN or a fraction of the emissions remaining as NO. Unlike SCIAMACHY retrievals, estimated total emissions for "urban" regions do not show significant differences between individual weekdays, but show decreases during the weekends (Table 3.2, Figure 3.4). The decrease in each city reflects the contribution of different NO_x sources.

Given the observed daily NO_2 variations, it is clear that the dominant emission category is not stationary sources as they lack the weekly variation observed or that there

is more variation in the stationary sources than is estimated. SCIAMACHY total NO_2 does not correlate to stationary emissions sources except Atlanta which has six EGU's inside its "urban" area. Additionally, all cities except Atlanta and New York have very low Sunday to mean weekday percentages in NO_2 retrievals which is not seen in NO_x emission estimates (Table 3.3, Figure 3.3).

Assuming weekly mobile emission profiles are representative, using Sunday to mean weekday percentages obtained from SCIAMACHY NO_2 retrievals and NO_x emission inventories (Table 3.3), one can approximate the contribution of mobile sources to total NO_x emissions for each city with the following formula;

$$R_{SCIAMACHY} = A_{STAT} \times R_{STAT} + A_{MOB} \times R_{MOB} + A_{NAT} \times 1.00 \quad \text{(Equation 3.1)}$$

where

$R_{SCIAMACHY}$ = ratio of Sunday to mean weekday (Monday-Friday) NO_2 total columns

A_{STAT} = fractional contribution to the mean weekday values by stationary NO_x emissions

R_{STAT} = ratio of Sunday to mean weekday stationary NO_x emissions

A_{MOB} = fractional contribution to the mean weekday values by mobile NO_x emissions

R_{MOB} = ratio of Sunday to mean weekday mobile NO_x emissions

A_{NAT} = fractional contribution to the mean weekday values by natural NO_x emissions

Estimated emissions suggest that natural emissions are negligible in urban areas, which then can be removed from equation (1). Further, this means $A_{STAT} = 1 - A_{MOB}$, so equation (1) can be solved for A_{MOB} using observed $R_{SCIAMACHY}$ and R_{MOB} and R_{STAT} from the inventory. This leads to all A_{MOB} values being greater than 100% which indicates current mobile emission contributions and weekly profiles can not explain the observed reductions on Sunday in SCIAMACHY NO_2 retrievals. Following are the

Table 3.3. Sunday to mean weekday percentage for total, stationary and mobile NO_x emissions with SCIAMACHY derived NO_2 columns

City	NO_x Emissions			NO_2 Retrievals
	(a) TOTAL	(b) STATIONARY	(c) MOBILE	SCIAMACHY
Atlanta	80 ± 4	90 ± 9	71 ± 3	72 ± 4
Chicago	80 ± 4	94 ± 5	69 ± 3	53 ± 3
Houston	89 ± 3	98 ± 3	82 ± 3	58 ± 4
Los Angeles	73 ± 4	94 ± 4	69 ± 4	54 ± 2
New York	72 ± 5	87 ± 8	64 ± 4	63 ± 3
Phoenix	76 ± 4	89 ± 4	65 ± 4	44 ± 3
Seattle	76 ± 4	98 ± 5	70 ± 4	41 ± 3

possible reasons: (1) Mobile emissions contribute more than shown in the current inventories, (2) diurnal profiles are different than assumed in the inventories; and (3) Day-to-day variation is not correctly represented in emission inventories. Harley et al., [2005] observed the timing of gasoline engine emissions is shifted with a single broad peak in the afternoon on weekends. SCIAMACHY's typical US observation time (10:30 am) combined with that shift may result in biased low satellite observations on Sundays compared to the rest of week. However, the Sunday to mean weekday ratios are significantly lower in satellite observations in all of the cities except New York and Atlanta. EGU NO_x data are actual hourly information. Mobile NO_x emissions, on the other hand, are ultimately based upon the Highway Performance Monitoring System (HPMS) traffic counts, though the data collected from HPMS is smoothed before being applied in estimating on-road emissions. The diurnal and daily changes (within a week) of mobile emissions in the inventory hence were obtained by averaging the sparse raw data first statewide and then across road types [*MACTEC*, 2005].

SCIAMACHY total NO_2 correlates reasonably well with estimated NO_x emissions for "urban" areas (Figure 3.5a). One interesting result is how New York

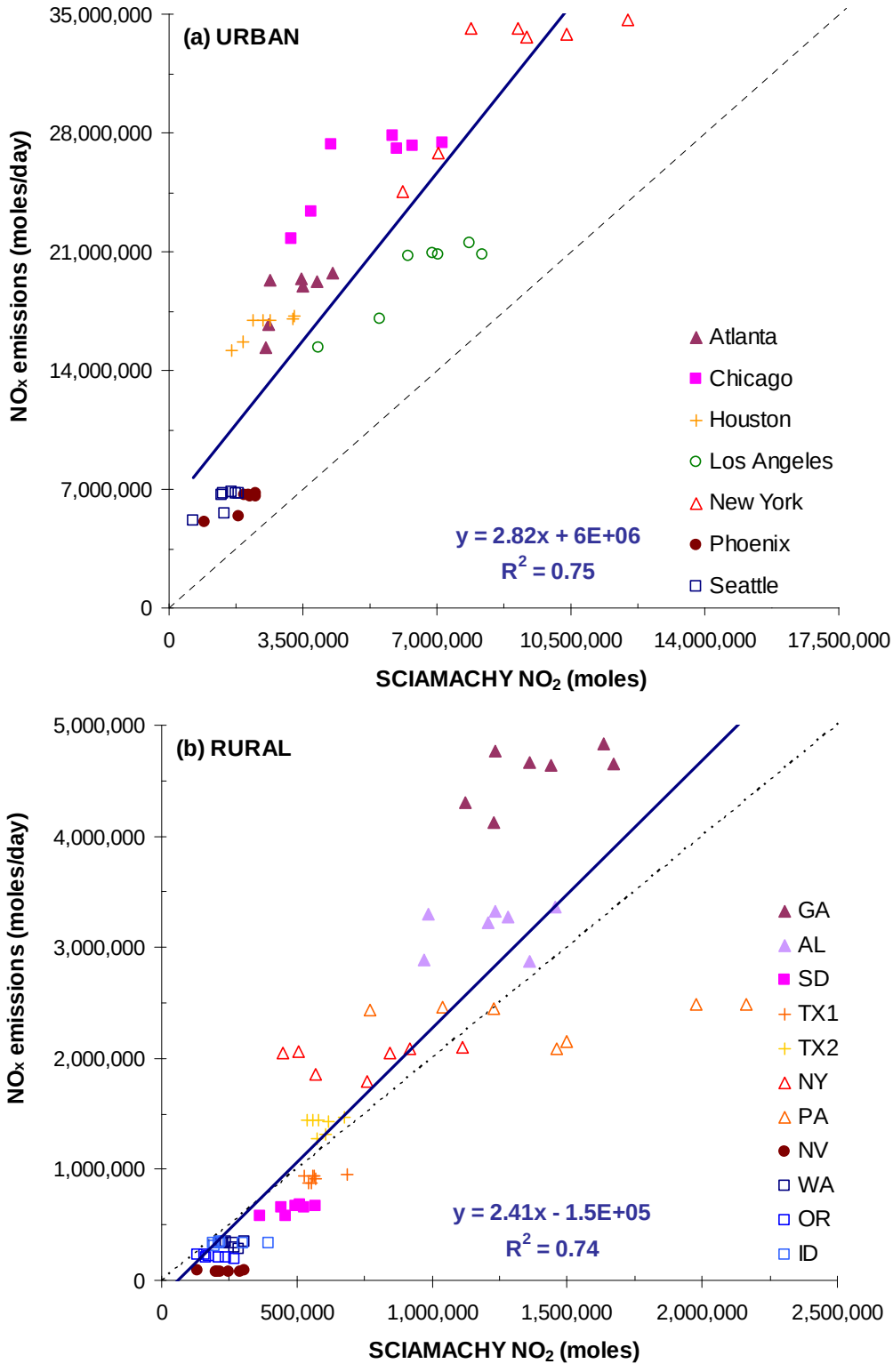

Figure 3.5. SCIAMACHY derived NO_2 versus of total NO_x emissions for (a) "urban" and (b) "rural" areas (each series contains 7 data points each one representing the average NO_2 for each day of the week, dashed line represents 2:1)

weekday (Monday-Friday) SCIAMACHY total NO_2 varies greatly while the estimated total or mobile emissions are almost constant. New York has the highest number of pixels available from SCIAMACHY (1357; Table 3.1), so representativeness should not be an issue in this case. This finding suggests that there is much more variation in New York NO_x emissions than captured in current emission inventories, though it is difficult to identify reasons. The lower value on Monday could be due to less NO_x carry-over from Sunday. However Tuesday is lower still. Nearby rural levels do not indicate regional transport is a reason. For all cities, the nearby rural pixels show much less NO_x.

Estimated NO_x emissions and SCIAMACHY derived total NO_2 for the eleven individual "rural" regions are also investigated and overall no significant decrease in the weekend is observed. ID and SD are the only rural areas showing around 30% decrease in total NO_2 on Sundays. Rural areas are usually dominated by natural emissions which do not have a weekly pattern, therefore it is expected that they could obscure any weekly cycle in anthropogenic emissions. Individual "rural" regions showed a similar correlation between total NO_2 and estimated NO_x emission as was found for "urban" regions (Figure 3.5b). Total observed NO_2 to total NO_x emissions ratios range between 0.30 (GA) to 2.87 (NV) on average. SCIAMACHY is actually seeing much more NO_2 compared to NO_x emissions in NV, WA and PA than in other "rural" regions (Figure 3.5b). Possible reasons could be (1) transport of NO_2 from another region (e.g. for PA, transport from the Ohio River Valley), (2) errors in retrieval of NO_2 and/or (3) missing emission sources in the inventory (e.g. for NV, underestimation of emissions coming from remote natural gas and oil pumps).

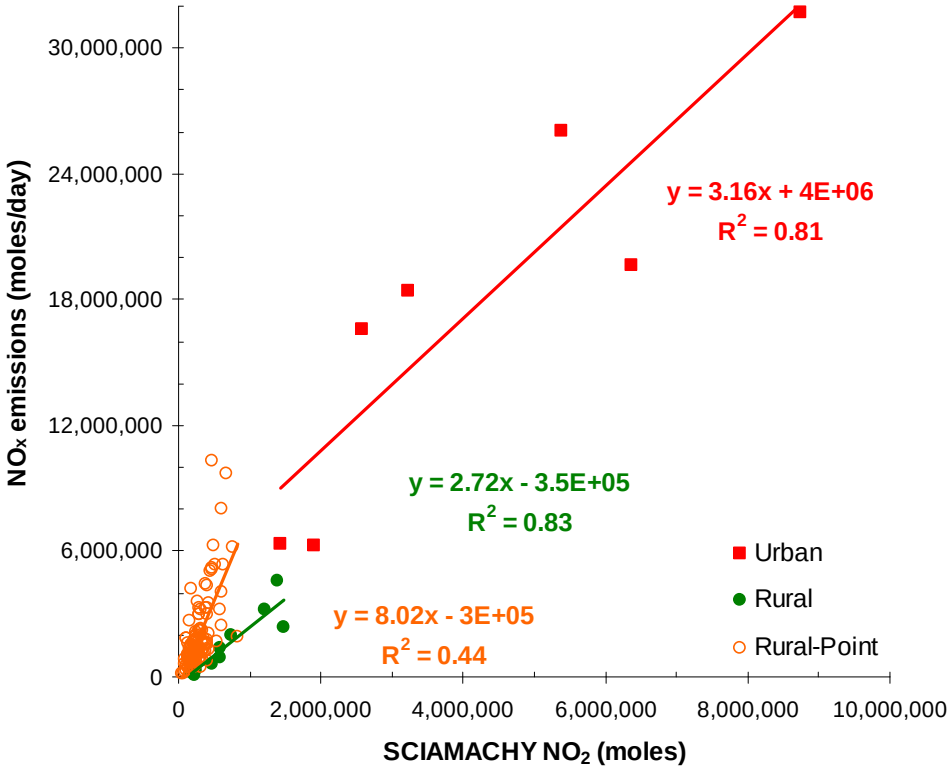

Figure 3.6. SCIAMACHY-derived NO_2 versus total NO_x emissions for individual "urban", "rural" and "rural-point" regions.

For the 117 EGU's in the "rural-point" areas, the observed total NO_2 from SCIAMACHY is, on average, 5 times smaller than the estimated total NO_x emissions and the correlation is worse than "urban" and "rural" regions (Figure 3.6). On the other hand, this is surprising because emissions from EGU's are directly measured, so their emissions are known best. Additionally, there are some cases where the estimated NO_x emissions and SCIAMACHY derived total NO_2 contradict each other (very high estimated NO_x emissions-very low SCIAMACHY total NO_2 column or vice versa). Given the large point source emissions, incomplete transformation of NO to NO_2 and transport of NO_x from the chosen areas could be possible reasons. Removing the "rural-point" regions having less than 10 scans available did not significantly alter the findings. The total

columns derived by a regional air quality model using these emissions resulted in a higher correlation ($R^2 = 0.54$), but still significantly lower than other region types (Figure 4.4). This brings in the question how well SCIAMACHY retrievals can be used to quantify emissions from large, single sources, or if it is necessary to use a model of the plume transformation to conduct the comparison.

3.4. Conclusions

NO_2 columns from SCIAMACHY during a 3-year period are analyzed for 3 different types of regions: urban, rural and rural-point. Total atmospheric burdens are compared to estimated NO_x emissions for the regions, both to identify how well the weekly variations agree as well as total mass. The existence of weekly patterns in urban areas (selected 7 cities) is obvious, whereas rural regions do not show any weekly pattern. Rural-point regions show a minor decrease on Sundays (20% compared to mean weekday). Phoenix weekly profile does not show much variation during the week, in contrast with other urban areas. All cities have minimums on Sunday. Estimated total NO_x emissions are lower on the weekends, but do not show the day-to-day variation for weekdays as SCIAMACHY NO_2. This is particularly true for New York. Further, for all cities, there is a greater reduction in observed NO_2 on weekends than found in the inventory.

Total NO_2 burden, which is the average NO_2 column multiplied by the area, over the cities derived from SCIAMACHY total tropospheric columns are always less than the total estimated NO_x emissions by a factor of 2.6 (Los Angeles) to 5.6 (Atlanta). A ratio greater than one is expected due to SCIAMACHY scanning over the areas in the morning before a majority of the NO_x is emitted for the day, and not all the NO_x will be NO_2 due

to chemical reactions. SCIAMACHY derived total NO_2 for "rural-point" is on average 5 times smaller than estimated total NO_x emissions and correlation is lower than individual "urban" and "rural" regions (Figure 3.6). This goes against expectations as major point sources are viewed as having their emissions well characterized due to the use of continuous emissions monitoring.

Using Sunday to mean weekday percentages obtained from SCIAMACHY NO_2 retrievals and NO_x emission inventories, the contribution of mobile sources to total NO_x emissions for each city are also calculated. Results suggest that the fractions of emissions from mobile sources are greater than current estimates or that day-to-day variability in mobile sources is underestimated.

This work suggests that current inventories lack day-to-day variability and satellites can provide information to improve the emission inventories. However it also highlights the need for a model to relate satellite observations to estimate emissions.

CHAPTER 4

COMPARISON OF NO_2 FROM A REGIONAL SCALE AIR QUALITY MODEL WITH SATELLITE RETRIEVALS OVER THE CONTINENTAL U.S.: EMISSION INVENTORY ASSESSMENT IMPLICATIONS

4.1. Introduction

Nitrogen oxides (NO_x: $NO+NO_2$) play a key role in tropospheric chemistry, including ozone (O_3), nitric acid and aerosol nitrate formation, and hydroxyl radical levels, which directly affects lifetime of many air pollutants. NO_x sources are mainly anthropogenic, particularly due to fossil fuel combustion, but they can also come from biogenic sources (e.g., biomass burning) to a lesser extent. For air quality policy purposes, it is important to have accurate emission inventories to develop strategies to effectively reduce air pollutant levels. Although estimated power plant NO_x emissions are viewed as relatively well quantified, emissions from area, on-road mobile, and off-road mobile sources have increasingly higher uncertainties [*Miller et al.*, 2006], approaching to a factor of two or more [*Hanna et al.*, 2001]. Current and future reductions in power plant emissions and on-road vehicles increase the importance of better quantifying emission rates from area and off-road mobile sources, which are relatively uncertain. This uncertainty could be reduced by using observations to estimate emissions, especially in remote regions. Compared to ground-based observations, satellite observations show

more promise with their global coverage and spatial availability over these remote regions.

NO_2 column densities are available from various satellite-borne instruments: Global Ozone Monitoring Experiment (GOME), Scanning Imaging Absorption Spectrometer for Atmospheric Chartography (SCIAMACHY), and Ozone Monitoring Instrument (OMI). GOME, SCIAMACHY and OMI have spatial resolutions of 320 × 40, 30 × 60 and 13 × 24-km^2 at nadir, respectively.

Several model comparisons to satellite retrieved tropospheric NO_2 columns have been conducted previously with GOME [*Jaegle et al.*, 2005; *Leue et al.*, 2001; *Martin et al.*, 2003; *Müller and Stavrakou*, 2005; *Toenges-Schuller et al.*, 2006; *Velders et al.*, 2001], SCIAMACHY [*Blond et al.*, 2007; *Martin et al.*, 2006; *Martin et al.*, 2007] and recently with OMI [*Zhang et al.*, 2008; *Zhao and Wang*, 2009]. While there is qualitative agreement in space, significant quantitative differences are found. Retrievals from different satellite platforms were also compared (late morning -SCIAMACHY and early afternoon-OMI) to better understand the diurnal variation in different NO_x sources [*Boersma et al.*, 2008]. Most of these studies aforementioned are on global scale. Regional scale studies have been conducted using the CHIMERE chemical transport model (CTM) over Europe with GOME [*Blond et al.*, 2007; *Konovalov et al.*, 2005; *Konovalov et al.*, 2006; *Konovalov et al.*, 2008] and SCIAMACHY [*Blond et al.*, 2007; *Konovalov et al.*, 2008], as well as Asia, using CMAQ with GOME NO_2 retrievals [*Han et al.*, 2009; *Kurokawa et al.*, 2009; *Uno et al.*, 2007]. However, more spatially and temporally detailed regional scale research is limited for North America [*Chune and*

Baoning, 2008; *Kim et al.*, 2006; *Kim et al.*, 2009; *Napelenok et al.*, 2008], particularly for comparison with detailed and up-to-date United States emission inventories.

In the previous chapter, we compared the day-of-week trends in urban NO_x levels, the sources of which are dominantly mobile (both on-road and off-road), and related 3-years of satellite NO_2 column data (2003-2005) obtained from SCIAMACHY. A greater reduction is observed in columnar NO_2 on weekends for most of the cities than found in the inventory. In other words, weekend-to-weekday NO_2 ratios from satellite retrievals are significantly lower than the ratios from the emission inventory. This result suggests that either the fractions of emissions from mobile sources are greater than what it is in current estimates or day-to-day variability in mobile sources is underestimated in current estimates [*Kaynak et al.*, 2009]. Therefore, satellites may provide information to improve the emission inventories; however the need for a model to relate satellite observations to estimate emissions is necessary.

Direct, one-to-one comparison of modeled and observed NO_2 column data helps to fill information gaps by accounting for chemistry and meteorology which can not be captured by comparing solely NO_x emissions with NO_2 satellite retrievals. One-to-one comparison can also help to identify reasons for discrepancies between retrievals and model predictions. In addition, this work provides information on the use of satellite retrievals in data assimilation for regional air quality models and their potential to further improve the emission inventories by assessing the accuracy and consistency of current estimates of NO_x for United States.

The objectives of the research reported in this chapter were to (a) compare modeled and observed NO_2 column data; and (b) identify and attempt to explain the

discrepancies between those two, (c) provide insight into the further use of satellite observations for inventory analysis and estimation.

4.2. Methods

4.2.1. Model Description

The Community Multi-scale Air Quality Model (CMAQ) [*Byun and Schere*, 2006] with a modeling domain covering the continental United States, Southern Canada and Northern Mexico (Figure 2.1) was used with 36km × 36km horizontal grid resolution and 13 vertical layers reaching up to approximately 15 km. The SAPRC99 Chemical Mechanism [*Carter*, 2000] was used for chemistry, the Fifth-Generation NCAR/Penn State Mesoscale Model (MM5) [*Seaman*, 2000] was used for meteorological simulations, and the Sparse Matrix Operator Kernel Emissions (SMOKE) [*Houyoux and Vukovich*, 1999] was used to prepare the emissions. Emissions were projected from the VISTAS 2002 emissions inventory [*MACTEC*, 2005] to the simulation year (2004) with growth factors obtained from the Economic Growth Analysis System (EGAS) Version 4.0, and control efficiency data obtained from EPA for the existing federal control strategies. Lastly, United States (US) power plant (i.e. electricity generating units, or EGUs) NO_x emissions obtained from the continuous emissions monitoring (CEM) database from EPA website [*E.P.A.*, 2008] were integrated into the emission inventory for 2004. Specific focus was on a two month period from the summer of 2004 (July-August) as aircraft measurements were also available during this period. Two simulations were performed: one with base case emissions and another with addition of lightning emissions, which are typically not included in regional inventories. Additional information on emissions, simulations, mechanisms and schemes selected can be found in Chapter 2.

4.2.2. NO_2 satellite retrievals and data comparison procedure

The SCIAMACHY instrument onboard the ENVISAT satellite measures atmospheric NO_2 columns and has an equator crossing time of 10:00 am, with a typical US observation time of 10:30 am. The typical spatial resolution of SCIAMACHY is 30 km along track by 60 km across track in the nadir view with a global coverage over 6 days. Algorithms used for retrieval of tropospheric NO_2 columns from SCIAMACHY data, along with uncertainty estimates used in this study were obtained from Martin et al. [*Martin et al.*, 2002; *Martin et al.*, 2003; *Martin et al.*, 2006]. The SCIAMACHY retrieval used here has been updated to include cloud fields from the FRESCO+ algorithm described by Wang et al. [2008].

Tropospheric NO_2 column densities from CMAQ were obtained by integrating concentrations from the surface to the top layer accounting for temperature, pressure and terrain height using the information from MM5. The areas corresponding to SCIAMACHY pixels that intersect the domain at times with a cloud radiance fraction less than 0.5 were used in the analysis. Pixel areas were intersected with CMAQ grid cells and matched with simulation-derived NO_2 columns at corresponding times and locations. Intersected pixel NO_2 columns were averaged using intersected areas as weighing factors according to the following equation.

$$C_i = \frac{\sum_{n=1}^{N} C_n \cdot A_{i,n}}{\sum_{n=1}^{N} A_{i,n}} \qquad \text{(Equation 4.1)}$$

In equation 4.1, C_i is the averaged NO_2 column for the i^{th} grid cell, C_n is the NO_2 column for the n^{th} scan, and $A_{i,N}$ is the intersected area between each grid cell *i* and individual scan *n*. Both simulation-derived and observed NO_2 columns were averaged for

two months (July, August 2004). Individual pixel uncertainties were also propagated with intersected areas as weighting factors to calculate overall uncertainty of the averages according to the following equation.

$$U_i = \sqrt{\frac{\sum_{n=1}^{N} U_n^{\,2} \cdot A_{i,n}}{N \cdot \sum_{n=1}^{N} A_{i,n}}} \qquad \text{(Equation 4.2)}$$

In equation 4.2, U_i is the mean uncertainty for the ith grid cell, U_n is the uncertainty for the nth scan reported with C_n, and $A_{i,N}$ is the intersected area between each grid cell *i* and individual scan *n*. It should be noted that this formula used for random errors. However, the SCIAMACHY NO_2 retrievals may have some systematic errors, so the uncertainty of the monthly averaged scans is also given as $U_i = 5\times10^{14} + 0.3C_i$ to account for those systematic errors [*Martin et al.*, 2006].

The retrieved tropospheric NO_2 columns were directly compared with the simulated vertically integrated amounts as explained above. However, the retrieved values depend on the *a priori* assumed shape of the vertical NO_2 profile which in this case comes from GEOS-Chem model. Differences in profile shapes simulated GEOS-Chem and CMAQ may therefore explain part of the biases in the NO_2 columns. The air mass factor uncertainties due to profile uncertainty are estimated as approximately 10%. [*Boersma et al.*, 2004]. We decided not to update the satellite retrievals by using CMAQ's vertical profile. The main reasoning was that the upper troposphere simulation of CMAQ was not evaluated in detail. In addition, our lightning emissions had high uncertainty and current NO_x emission inventory used in this study was missing aircraft emissions.

Three different region types (urban, rural and rural with a large-scale electricity generating unit (EGU)) that were selected and explained in detail in Chapter 3 (Figure 3.1) were also used here to investigate NO_2 levels in different areas, and how satellite derived NO_2 compare to simulations in urban versus rural areas. Seven major cities (Atlanta, Chicago, Houston, Los Angeles, New York, Phoenix and Seattle) in the US ("urban") were selected for their large population and related NO_x emissions. These cities also represent different topographical and meteorological conditions which possibly affect NO_2 tropospheric column densities and retrievals. Eleven rural areas ("rural") without any significant NO_x sources were selected close to these 7 cities. Additional rural areas ("rural-point") with no urbanized land but containing one or more large NO_x sources emitting more than 7,824 tons of NO_x annually (0.1% of total) from all listed facilities for 1999 were selected. Urbanized area definitions used were from Census2000 (http://www.census.gov/geo/www/cob/ua2000.html) and NO_x emission information for major EGU's were obtained from Environmental Protection Agency (EPA) (http://www.epa.gov/air/data).

4.3. Results and Discussion

Comparison of modeled and observed NO_2 columns indicated a low negative bias (-33.8% for base and -20.3% lightning case, Table 4.1) in simulated levels across the continent. Scans over US have a smaller bias (-15.4% for base and -0.1% lightning case) than the whole dataset (Table 4.1). On the other hand, scans over Canada, Mexico and Atlantic Ocean were higher than simulated (Figure 4.1).

Table 4.1. Statistics and correlation coefficients (R^2, slope and intercept) of CMAQ simulated versus SCIAMACHY retrieved tropospheric NO_2 columns for different regions

		Base case							Lightning case						
	N	**R^2**	**Slope**	**Inter (#/cm^2)**	**MBE (#/cm^2)**	**RMSE (#/cm^2)**	**MNB (%)**	**MNE (%)**	**R^2**	**Slope**	**Inter (#/cm^2)**	**MBE (#/cm^2)**	**RMSE (#/cm^2)**	**MNB (%)**	**MNE (%)**
Domain-wide	16251	0.60	0.92	-2.E+14	-2.5E+14	7.6E+14	-33.81	110.99	0.60	1.00	-1.E+14	-1.1E+14	7.9E+14	-20.29	111.63
U.S.	5980	0.58	0.96	-1.E+14	-1.5E+14	9.7E+14	-15.40	65.26	0.57	1.01	3.E+13	5.3E+13	1.0E+15	0.11	67.43
Western U.S.	2363	0.64	0.78	-8.E+13	-2.9E+14	8.3E+14	-37.00	102.83	0.65	0.80	4.E+12	-1.9E+14	7.9E+14	-26.75	100.09
Eastern U.S.	3617	0.52	1.07	-2.E+14	-6.5E+13	1.0E+15	-1.28	40.72	0.49	1.11	3.E+13	2.1E+14	1.2E+15	17.66	46.09
Ocean	5518	0.26	0.28	9.E+13	-3.7E+14	6.5E+14	-41.57	158.15	0.37	0.51	7.E+13	-2.4E+14	5.9E+14	-27.10	154.99
Canada	3463	0.58	0.84	-7.E+13	-1.4E+14	4.9E+14	-45.23	128.29	0.52	0.92	-6.E+13	-9.2E+13	5.7E+14	-39.94	133.69
Mexico	1085	0.26	0.79	-3.E+14	-4.8E+14	7.2E+14	-52.59	70.63	0.23	0.81	-2.E+14	-3.5E+14	6.7E+14	-27.23	66.52
California (CA)	316	0.75	0.83	-1.E+14	-4.5E+14	1.4E+15	-40.66	64.58	0.75	0.84	-1.E+14	-4.1E+14	1.4E+15	-38.97	64.03
Nevada (NV)	219	0.69	0.55	-1.E+14	-5.2E+14	6.7E+14	-58.60	66.42	0.69	0.57	-1.E+14	-4.8E+14	6.4E+14	-53.20	62.97
Washington (WA)	138	0.73	1.20	-3.E+14	-1.2E+14	7.0E+14	-12.39	75.94	0.73	1.19	-3.E+14	-1.0E+14	6.9E+14	-11.34	79.02
Georgia (GA)	119	0.72	1.45	-1.E+15	-1.4E+14	8.6E+14	-10.72	23.12	0.71	1.49	-8.E+14	3.3E+14	9.6E+14	12.60	21.66
Texas (TX)	536	0.46	1.34	-5.E+14	-2.8E+13	1.1E+15	-2.82	38.31	0.46	1.37	-3.E+14	2.5E+14	1.1E+15	17.98	37.74
Pennsylvania (PA)	89	0.63	0.96	-2.E+13	-1.3E+14	1.2E+15	4.76	38.81	0.61	0.94	2.E+14	4.8E+12	1.2E+15	12.47	40.53
Oregon (OR)	192	0.69	1.11	4.E+14	4.0E+14	6.2E+14	-3.05	434.88	0.69	1.11	4.E+14	4.2E+14	6.4E+14	-3.31	447.98
Idaho (ID)	166	0.37	0.66	2.E+14	8.4E+13	2.7E+14	-77.24	210.25	0.39	0.69	2.E+14	1.1E+14	2.8E+14	-82.48	230.67
Alabama (AL)	106	0.45	0.82	-2.E+14	-5.6E+14	8.0E+14	-27.07	31.36	0.44	0.81	1.E+14	-2.4E+14	6.4E+14	-10.77	19.71
New York (NY)	96	0.59	1.12	-4.E+14	-1.7E+14	9.9E+14	-5.37	34.20	0.65	1.17	-3.E+14	5.6E+13	9.2E+14	6.62	32.98
Arizona (AZ)	225	0.55	1.52	-1.E+15	-4.9E+14	9.5E+14	-47.36	55.86	0.60	1.59	-1.E+15	-2.5E+14	8.3E+14	-26.84	38.81
Illinois (IL)	111	0.49	1.62	-2.E+15	-3.2E+14	1.9E+15	-16.62	36.99	0.28	1.34	-6.E+14	2.8E+14	2.3E+15	12.81	53.98
South Dakota (SD)	152	0.04	0.16	6.E+14	-5.9E+12	3.1E+14	23.16	50.32	0.06	0.24	6.E+14	9.8E+13	3.4E+14	41.09	58.15
State averages	48	0.87	0.88	2.E+13	-2.0E+14	4.6E+14	-9.71	21.92	0.84	0.91	2.E+13	2.4E+13	4.6E+14	3.62	22.03
"Urban"	7	0.79	0.54	1.E+15	-9.3E+13	1.1E+15	6.65	19.75	0.76	0.53	2.E+15	8.2E+13	1.1E+15	12.78	24.18
"Rural"	11	0.88	0.90	1.E+13	-1.1E+14	2.5E+14	122.06	159.15	0.92	1.12	7.E+13	5.5E+13	2.3E+14	149.06	172.64
"Rural-Point"	117	0.58	1.05	2.E+14	-5.5E+13	7.4E+14	-3.30	25.99	0.54	1.10	1.E+13	2.3E+14	8.7E+14	11.12	28.84

Abbreviations: N, Number of observations; MBE, Mean bias error; RMSE, Root mean square error; MNB, Mean normalized bias; MNE, Mean normalized error.

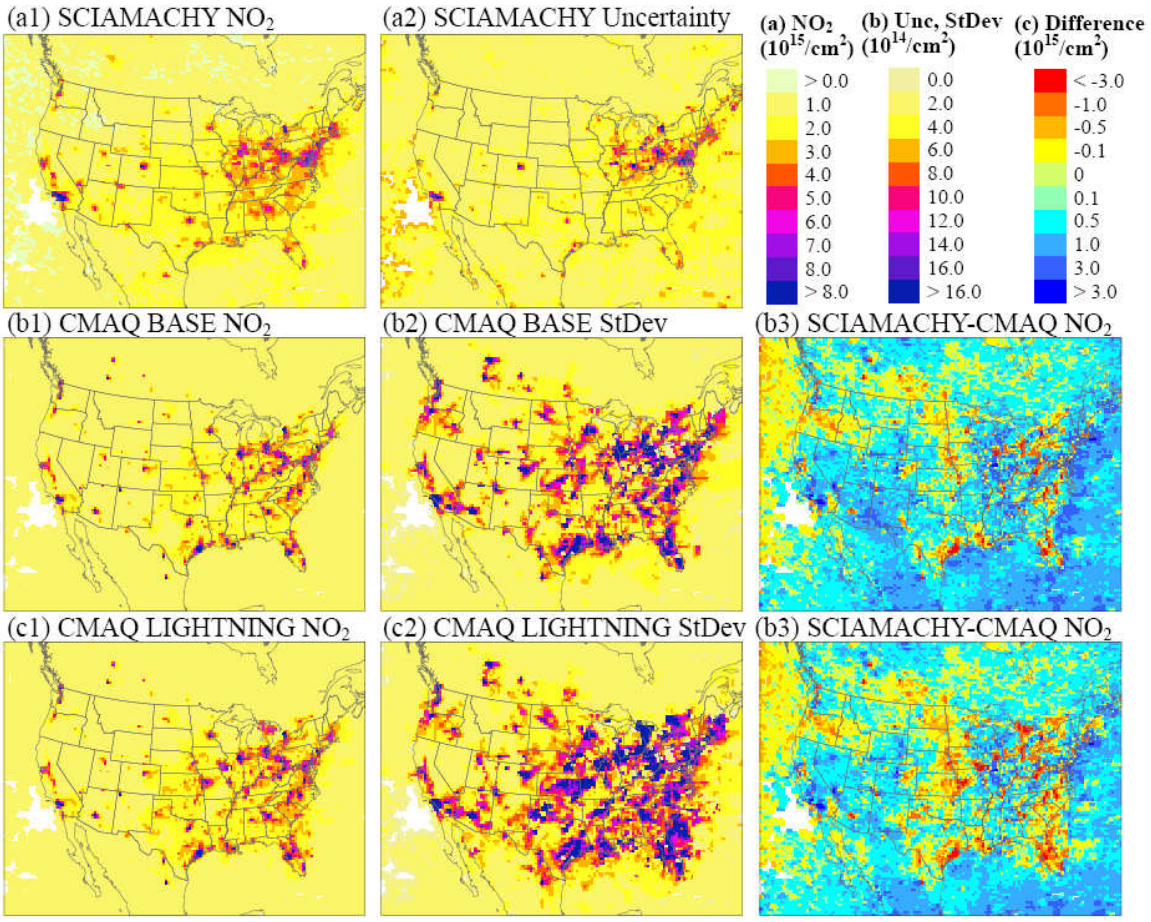

Figure 4.1. Spatial distribution of SCIAMACHY (a) and CMAQ (b,c) derived tropospheric monthly NO_2 column averages (1), SCIAMACHY mean uncertainties and CMAQ standard deviations, (2) and differences (3) for July-August 2004.

Adding lightning increased tropospheric NO_2 columns where high intensity lightning events occur, i.e. Florida, Texas, and the Midwest, and over the oceans, but the overall effect was minor (Figures 4.1, 4.2). Lightning emissions reduced the biases domain-wide, but effect on the error was minor. Both simulation cases –base and lightning– generally have lower NO_2 columns than the retrievals in rural areas across the domain. CMAQ usually has higher simulated levels than retrievals in city centers, but lower simulated levels in the surrounding areas of these centers. Possible reasons for this result are the pixel size of SCIAMACHY which has a smoothing effect, diagnostic biases in the

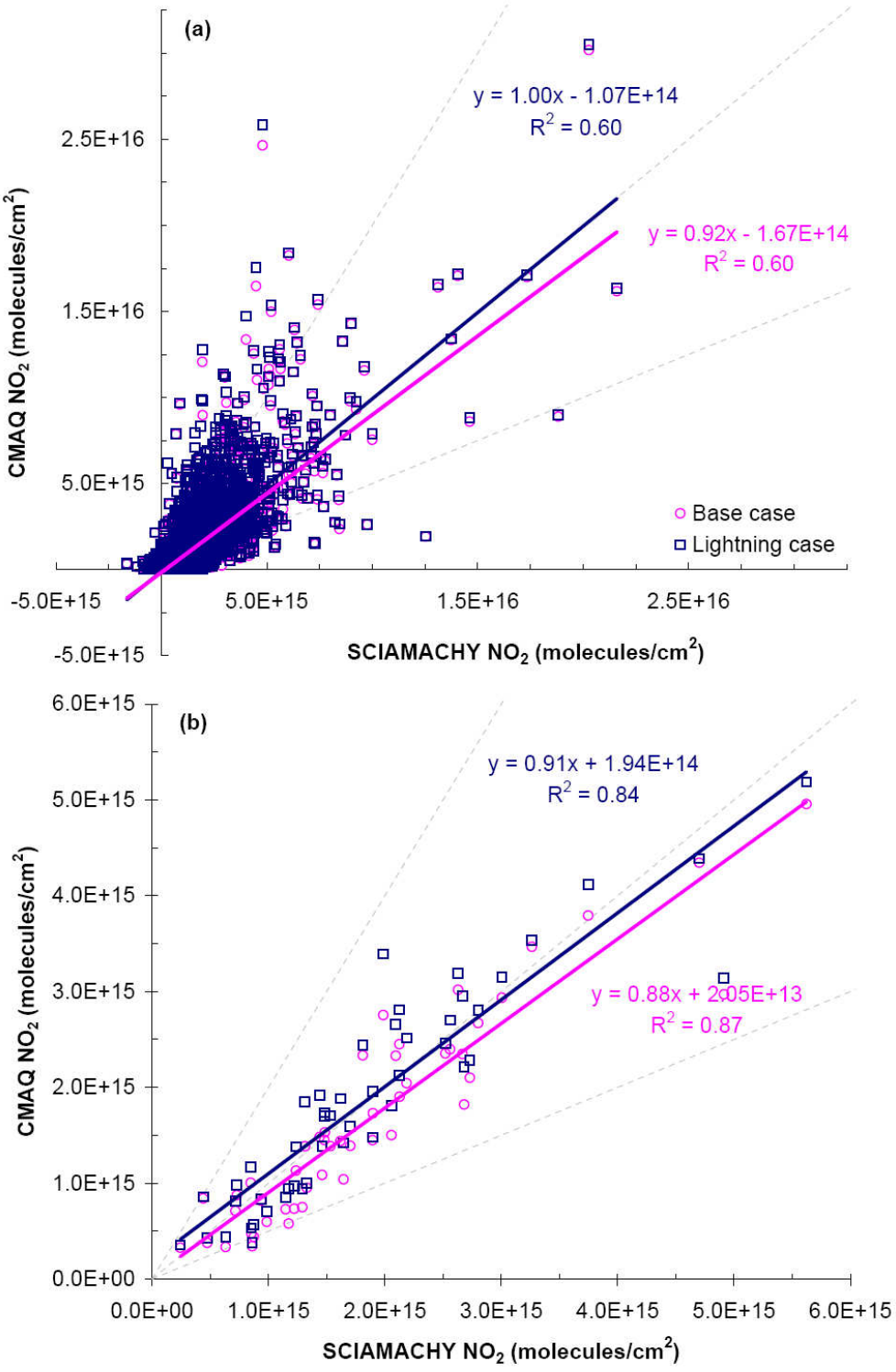

Figure 4.2. Correlation of SCIAMACHY and CMAQ derived tropospheric NO_2 column (a) averages for all grids for which observations are available and (b) State averages for July and August 2004.

SCIAMACHY retrieval analyses, biases in the emissions estimates, or chemistry and/or transport problems in the model (e.g., NO_2 being oxidized faster than actual). Over Los Angeles, California, SCIAMACHY consistently indicated more NO_2 than CMAQ. This area had very low lightning activity and low wind speeds which reduce the uncertainty in meteorological inputs being a major reason for the observed discrepancy. This underestimation of the model might be due to a problem with NO_x from diesel emissions [*CARB*, 2009]. Evaluation of the NO_2 simulations of the model with ground-based observations during daytime around Los Angeles were relatively unbiased overall, finding both lower and higher levels for different stations, unlike satellite observations being consistently higher. However if only the ground observations at 11:00 am local time are compared, there is a negative bias in the simulated results for Los Angeles as well as other cities like Seattle and Phoenix, similar to that was suggested by the satellite observations. The underestimations according to ground observations were not solely in Los Angeles, but also observed for other cities where the model successfully predicts NO_2 columns. Thus, the reason for ground-based underestimation possibly indicates the mixing layer should be shallower than currently modeled which is also supported by daytime underestimations over the domain. This issue should not affect the total columns observed from space.

High simulated levels of peroxy acetyl nitrate (PAN), when compared to aircraft observations (Chapter 5), indicated that not having PAN photolysis may lead to some of the high bias in the model results. Inclusion of PAN photolysis [*Carter,* 2008] led to minor improvements both in comparison to ICARTT PAN and NO_2 and SCIAMACHY NO_2 evaluations.

In the Western US (including 11 States: Washington (WA), Oregon (OR), California (CA), Arizona (AZ), Nevada (NV), Utah (UT), Idaho (ID), Montana (MT), Wyoming (WY), Colorado (CO) and New Mexico (NM)), CMAQ had lower NO_2 columns than observed, most obvious in July 2004, even though the correlation was significantly higher than in the East, whereas in Eastern US, CMAQ values were more comparable but the correlation between the model and satellite retrievals was low. NO_2 observations from aircraft observations, which covered the east to northeast parts of the United States, indicated a positive bias, but averaged vertical profile was very well matched with observations. Ground-based observations also showed similar comparisons with the satellite retrievals for the Western and the Eastern US. Both comparisons are discussed in more detail in the next chapter. Specifically, CA and WA had the highest correlations for both months (Table 4.1). Interestingly, results for PA showed a low correlation in July, but a high correlation in August. There was adequate number of observations in both months. This finding suggests that the sampling error should not be an explanation for this difference.

Given that each state is responsible for developing its own inventories, it is of interest if satellite observations suggest state-by-state biases. State averaged NO_2 columns results showed CMAQ levels in the western states (NV, WY, NM, UT, CO, AZ, CA) were lower than SCIAMACHY (Figure 4.3, Table 4.1), but one found underestimations in a few northeastern states as well (ME, DE, VT, NH, CT, WI). Some of the states had inconsistencies between two months' comparisons (OR, ID, MT, WA, SD). OR had an overestimation in July in CMAQ simulations, possibly due to an overestimation of the fire emissions for that month in 2004 as actual fire emissions are

variable from year-to-year and month-to-month, while inventories show less variability [*Tian et al.*, 2008].

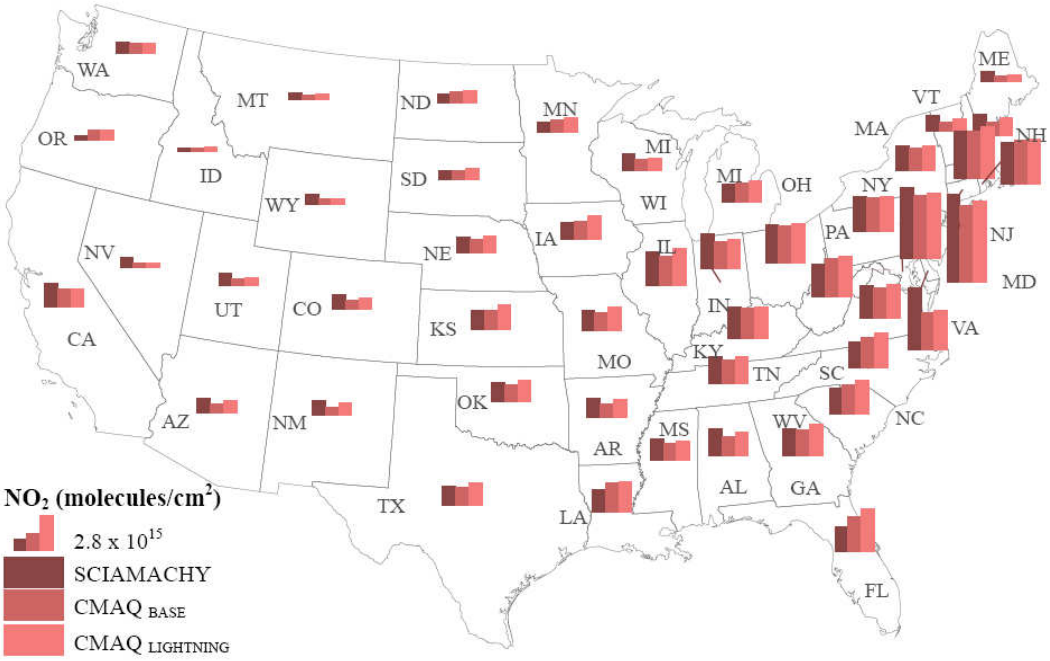

Figure 4.3. SCIAMACHY and CMAQ derived tropospheric NO_2 column state averages for July-August 2004 (2.8×10^{15} molecules/cm^2 is representing the height of the final bar for scaling purposes)

Comparisons according to land use for selected regions ("urban", "rural" and "rural-point") indicated that, except for Los Angeles, all urban regions show a strong temporal correlation between model and retrieval. On the other hand, Houston, Phoenix and Chicago had higher simulated NO_2 columns in comparison to SCIAMACHY observations (Figure 4.4). For rural regions in NV and WA, SCIAMACHY observations were much higher and in ID and OR, SCIAMACHY observations were much lower than simulated, but, overall, rural regions were highly correlated temporally (Figure 4.5).

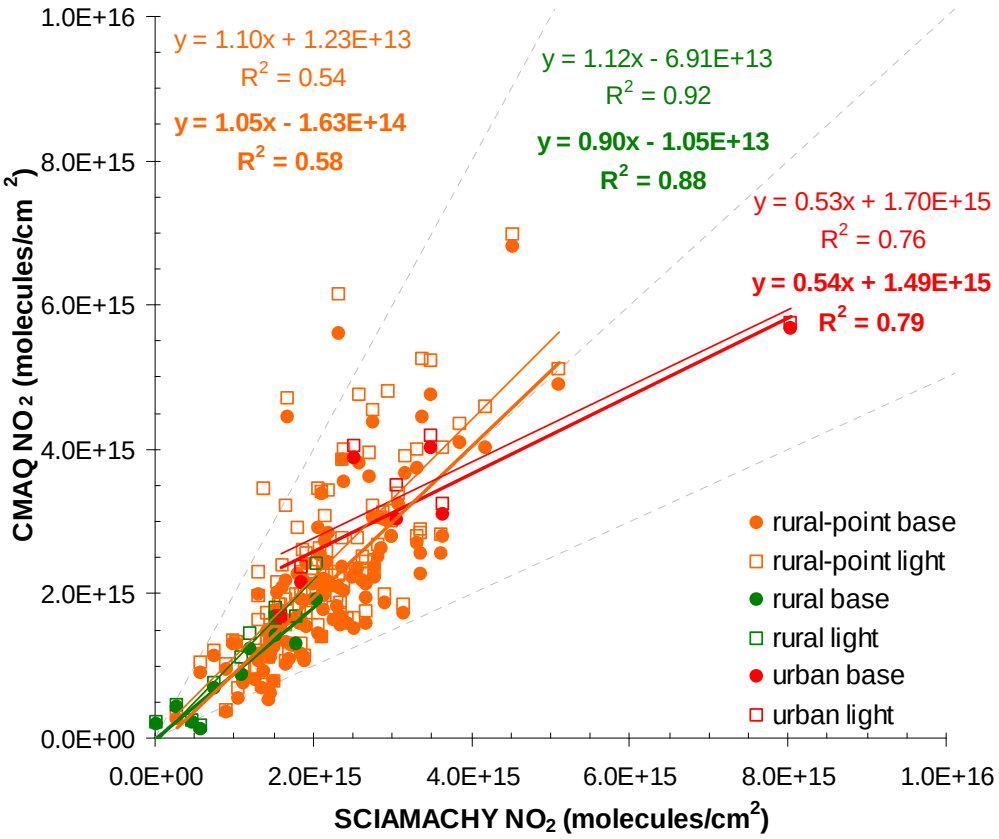

Figure 4.4. SCIAMACHY to CMAQ derived tropospheric NO_2 column correlations for "urban", "rural" and "rural-point" regions averaged for July-August 2004 (Bold fonts with thick lines and filled circles indicate base case and regular fonts with thin lines and void squares indicate lightning case).

For "rural-point" regions SCIAMACHY showed reasonable agreement, though with some outliers (four rural-point areas with emissions from two chemical plants, one in LA and one in TX, and two power plants) (Figures 4.4, 4.5). The correlation coefficient (R^2) increased from 0.54-0.58 to 0.62-0.67 if outliers mentioned are removed from the regression. Previous comparison of 3-year averaged SCIAMACHY tropospheric NO_2 columns versus 12 months of NO_x emissions showed better comparison for Los Angeles, and "urban" regions correspondingly (Chapter 3). The temporal correlation of the "rural" regions were similar, but the "rural-point" regions showed better correlation when

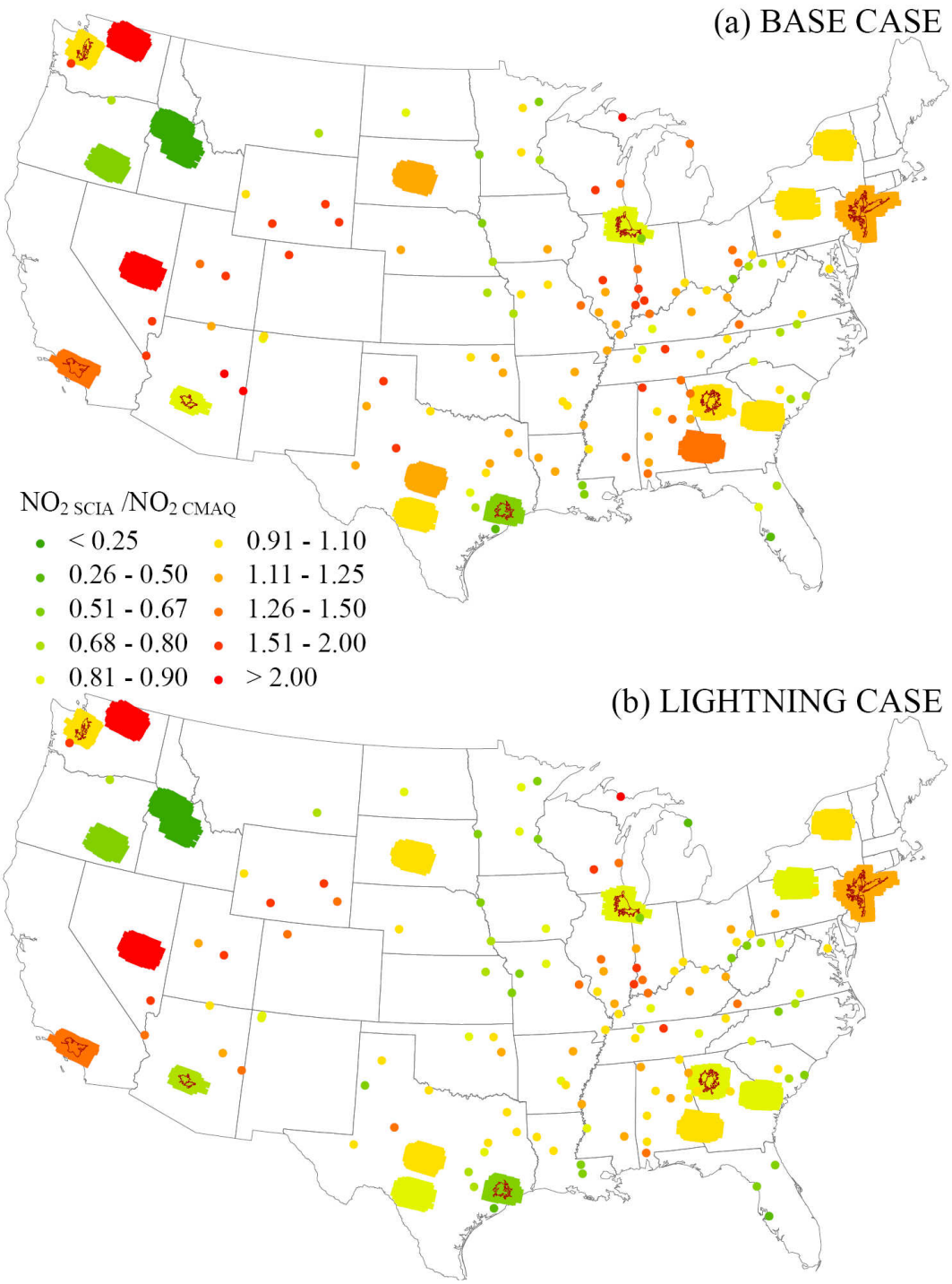

Figure 4.5. SCIAMACHY to CMAQ derived tropospheric NO_2 column ratios of (a) base and (b) lightning case simulations for the selected areas with different region types for July-August 2004. (Points represent “rural point”, areas represent “rural” and areas with city centers outlined in red represent “urban” regions)

compared with modeled concentrations instead of NO_x emissions. This is expected because NO_x emissions for individual point sources are subject to change within 3 years and more detailed transport and chemistry is important over the smaller scales.

Los Angeles, being the major outlier in "urban" regions, suggests there is a retrieval/analysis error, a bias in emission estimates specific to that region (or, conversely biases in the other regions), or modeling issues specific to that area. The low correlation for the "rural-point" regions is surprising as their emissions are viewed as relatively well known compared to other sources. The potential reasons for lower correlation of "rural-point" could be the transport of NO_2 out of the small scan area or insufficient time for conversion of NO to NO_2 in power point plumes. On the other hand, the high correlation of "rural" regions is promising for using the satellite retrievals to obtain emission estimates for area sources that are low in amounts but are sparse and are hard to capture otherwise. Results suggested that "rural" areas in NV, WA have higher and ID, OR have lower emissions than inventories show. Emission estimates from uncertain sources like fire may be improved using satellite NO_2 retrievals. Results also indicated that correlations increase if satellite retrievals are averaged over larger areas, which may be related to NO_2 lifetime.

There appears to be somewhat less temporal correlation between simulated and observed columns in areas containing sources that are viewed as having well known emissions ("rural-point"). In part, this can be a result of having somewhat fewer points for comparison at any one location because the selected areas were smaller than urban and rural. However, the slope of the regression is close to one, suggesting the overall bias is low. On the other hand, the good correlation found for other areas suggests that the

satellite retrievals can provide useful information for evaluating model performance and enhancing emission assessments as limitations in such retrievals are understood, and biases, errors and uncertainties quantified.

Overall comparisons are promising even though there are discrepancies. This suggests that using satellite retrievals can give insightful information for improving emission inventories. However, reasons for the model-to-satellite, ground and aircraft-based-to-model discrepancies should be resolved, and a detailed inter-comparison can identify biases, which will be the focus of the next chapter (Chapter 5).

4.4. Summary

NO_2 tropospheric columns simulated over the continental US were compared with those obtained by satellite for a two-month period from the summer of 2004 (July-August). Two model simulation cases were performed, one with and one without lightning emissions. Simulated NO_2 columns were usually lower than observed, though highly correlated (R^2=0.65-0.66) in the west, while in the eastern US, column amounts were comparable but had a lower correlation (R^2=0.49-0.52). Comparison of NO_2 columns by state improved the nation-wide correlation (R^2=0.84-0.87). State-by-state comparison revealed low simulated values in some Eastern states in addition to most Western states. Additional comparisons according to land use - “urban”, “rural” and “rural-point” - showed that NO_2 tropospheric columns derived from satellite correlate well with simulated NO_2 concentrations for “rural” regions but the correlation is lower for “urban” and “rural-point” regions. Simulated NO_2 columns in Los Angeles are significantly lower than satellite observations indicating either a retrieval/model error or a problem in emission estimates specific to that region. Higher biases and lower

correlations in “rural-point” regions is surprising with their emissions being viewed as relatively well known, potential reasons for this are 1) the transport of NO_2 out of the small scan area, 2) insufficient conversion of NO to NO_2 in power plant plumes and 3) potential issues with satellite retrievals. High correlations for “rural” regions is encouraging for using satellite observations to estimate NO_x emissions that are hard to capture otherwise such as area emissions that are sparse and poorly quantified, and prescribed fire or wildfire emissions.

CHAPTER 5

ANALYSIS OF NO, NO_2 AND O_3 BETWEEN MODEL SIMULATIONS AND GROUND-BASED, AIRCRAFT AND SATELLITE PLATFORMS

5.1. Introduction

Tropospheric ozone (O_3) is a serious air pollution problem in the United States (US), with approximately 60% of the population living in areas with levels above the standard. O_3 is generated through a series of photochemical reactions involving volatile organic compounds (VOC) and nitrogen oxides (NO_x: NO + NO_2).

Along with other pollutants, O_3 and its precursors are measured from different platforms such as ground-based networks, aircrafts and satellites for various different purposes. One of the purposes of these observations is model evaluation in order to assess model strengths and weaknesses. Traditional ground-based observations supply continuous and accurate monitoring. However, they have incomplete spatial coverage because of the limited number of stations and representativeness issues may arise because these are point measurements and may be significantly impacted by local influences. Further, they only provide information at the ground. Aircraft measurements, on the other hand, provide information on the vertical structure of the pollutant concentrations. They also typically include additional species which are not available from conventional ground-based observations. However, they are also very limited both temporally and spatially. Satellite retrievals, as an alternative, supply on-going global coverage, including remote areas where few other observations are available. Here, we aim to

extensively evaluate the air quality model with all available observations from different platforms in order to identify the commonalities and discrepancies. Previous detailed comparison of satellite NO_2 retrievals (Chapter 4) indicated possible issues with model and NO_2 retrievals which is be further investigated here. Overall, this work is an attempt to understand model and observation limitations and strengths with a detailed cross evaluation of the model.

Availability of these aforementioned measurements at the same time, during summer of 2004, provides us an opportunity to improve our scientific understanding of atmospheric processes by integrated analysis of satellite, aircraft, and ground-based observations with a regional air quality model.

From 1 July to 15 August 2004, the Intercontinental Chemical Transport Experiment-North America (INTEX-NA) field mission was conducted over North America (NA) and the Atlantic as part of the International Consortium for Atmospheric Research on Transport and Transformation (ICARTT). Some of the main goals of INTEX-NA which is relevant to our study were to characterize the composition of the troposphere over NA, validate satellite observations of tropospheric composition, and quantitatively relate atmospheric concentrations of gases with their sources and sinks [*Singh et al.*, 2006].

NO_2 satellite retrievals are relatively new observational platforms compared to other approaches for characterizing pollutant concentrations and are reported to have higher uncertainties due to several factors including measurement noise and spectral fitting, separation of stratospheric and tropospheric NO_2, and model parameters such as clouds, surface albedo, and *a priori* profile shape [*Boersma et al.*, 2004]. High

uncertainties in satellite retrievals lead to high uncertainties in the comparison between other observations and model results. Therefore, such inter-comparisons with other observations are essential in investigating the use of the satellite retrievals in data assimilation for regional air quality models and their potential to further improve the emission inventories by assessing the accuracy and consistency of current estimates of US. Such comparison can also help identify reasons for discrepancies between satellite retrievals and other measurements. Additionally, each observation covers different sides of the model that needs to be evaluated indicating where the model strengths and weaknesses lie.

Previously, Blond et al. [2007] compared satellite NO_2 retrievals from SCIAMACHY, ground-based observations and air quality modeling results over western Europe and concluded that their model is able to describe NO_2 surface concentrations and surface measurements correlate well with the satellite NO_2 tropospheric columns at rural sites. However, NO_2 concentrations for urban and suburban stations were systematically underestimated by their model which they attributed to the low spatial representativeness of the NO_2 surface measurements in areas with strong gradients of concentrations. They also showed that the model tends to systematically underestimate NO_2 tropospheric columns over large NO_x emission areas, and suggested that could be due to underestimations in the emissions and further commented that this could explain the model underestimations of surface NO_2 measurements at urban sites. Finally, they concluded that the model correctly represented the transport and chemistry of NO_2 and the spatial distribution of the NO_x emissions on a seasonal basis because of high

correlation coefficients obtained between modeled and observed NO_2 tropospheric columns.

Another study [*Yu et al.*, 2007] evaluated the Eta-CMAQ forecast model performance for ozone, and its related precursors over the eastern United States with the observations obtained by aircraft, ship, ozonesonde, and lidar and two surface networks during the ICARTT study. The model, in general reproduced O_3 vertical distributions on most of the days at low altitudes, but consistent overestimations above 6 km are evident. The model captured the vertical variation patterns of the observed values for other parameters (NO_2, and NO_y ($NO + NO_2 + HNO_3 + PANs$)) with some exceptions.

ICARTT NO_2 measurements were also used to evaluate the simulated NO_2 vertical profiles and to validate the retrieved NO_2 columns [*Martin et al.*, 2006]. Also, ICARTT O_3, CO and NO_y have been compared with GEOS-Chem simulations to improve and update estimates of North American influence on global tropospheric O_3. Results showed that the 50% decrease in US stationary NO_x sources since 1999 [*Hudman et al.*, 2009]. The spatial resolution of GEOS-Chem. is $2^o \times 2.5^o$, whereas CMAQ which was used in our study has a significantly higher resolution of 36×36km which has an advantage for better capturing the measurements through the flight tracks.

The objectives of the research reported in this chapter were to: (a) evaluate the air quality model used with available observations from different platforms for oxidized nitrogen species and ozone; (b) investigate the commonalities/discrepancies between different observations; (c) evaluate the satellite comparison and findings from the previous work (Chapter 4) and (d) attempt to understand model and observation limitations

5.2. Methods

5.2.1. Model Description

The Community Multi-scale Air Quality Model (CMAQ) [*Byun and Schere*, 2006] combined with the Fifth-Generation NCAR/Penn State Mesoscale Model (MM5) [*Seaman*, 2000] for meteorological simulations, and the Sparse Matrix Operator Kernel Emissions (SMOKE) [*Houyoux and Vukovich*, 1999] for the emissions is used in this study. Emissions are projected from the VISTAS 2002 emissions inventory [*MACTEC*, 2005] to the simulation year (2004) with growth factors obtained from the Economic Growth Analysis System (EGAS) Version 4.0, and control efficiency data obtained from EPA for the existing federal control strategies. In addition, emissions from large NO_x and SO_2 point sources in the US for 2004 were obtained from the continuous emissions monitoring (CEM) database [*E.P.A.*, 2008] are integrated into the emission inventory. Lightning NO_x emissions, which are typically not used in regional inventories are also prepared [*Kaynak et al.*, 2008] and included as a significant upper level NO_x source during the summer. The modeling domain includes the continental United States, Southern Canada and Northern Mexico (Figure 5.1). The horizontal grid resolution is 36km × 36km and vertical resolution includes 13 vertical layers (up to 15 km). The simulation episode is 1 July- 31 August 2004. Additional information on emissions, simulations, chemical mechanisms and schemes selected can be found in Chapter 2 [*Kaynak et al.*, 2008].

5.2.2. Satellite-based observations

Atmospheric NO_2 columns (molecules/cm^2) are available from The Scanning Imaging Absorption Spectrometer for Atmospheric Chartography (SCIAMACHY)

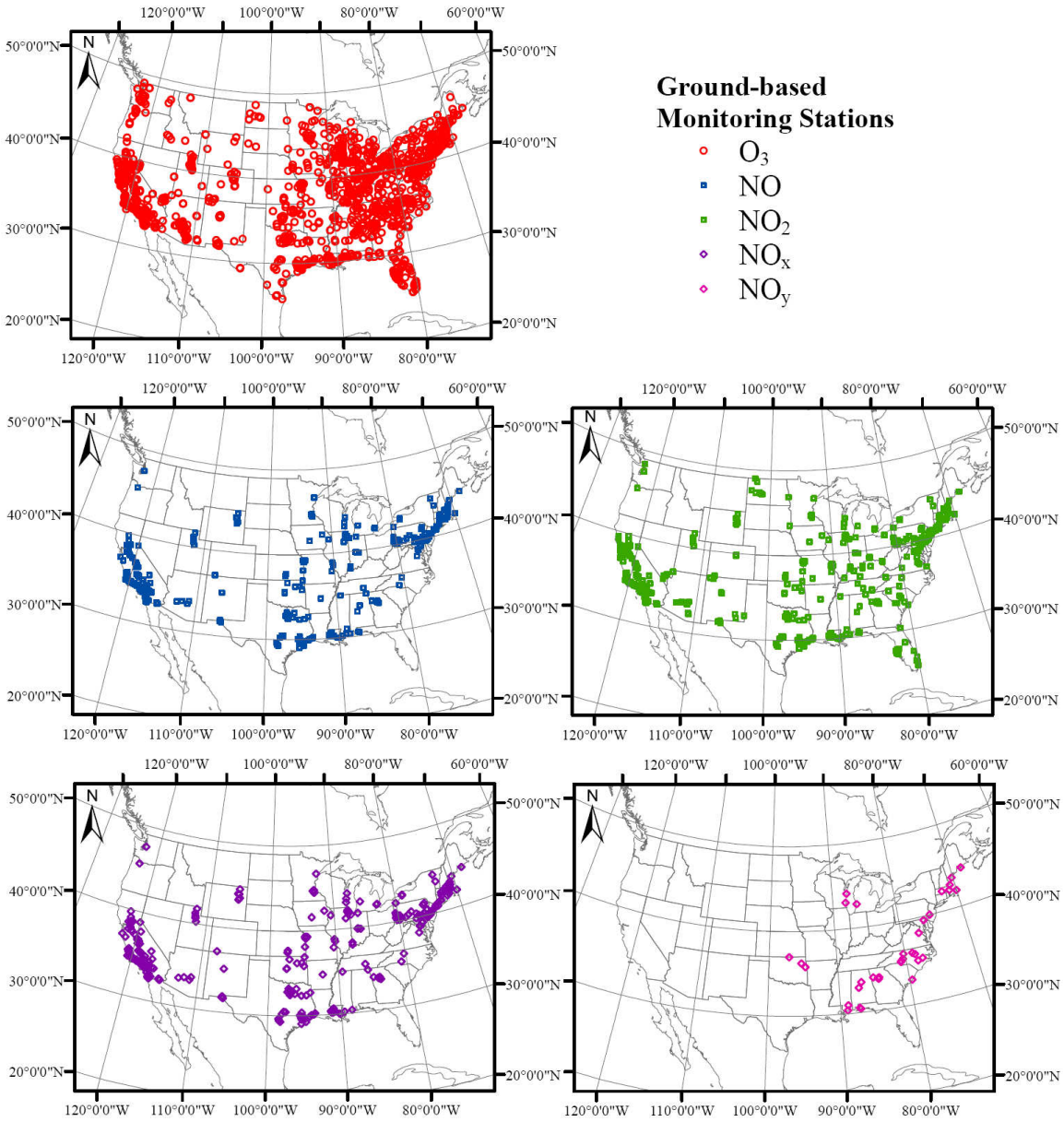

Figure 5.1. Locations of O_3, NO, NO_2, NO_x, and NO_y observation stations

instrument, SCIAMACHY passes over US around 10:30 am local time. The typical spatial resolution of SCIAMACHY is 30 km along track by 60 km across track in the nadir view. The global coverage is achieved over 6 days. Algorithms used for retrieval of tropospheric NO_2 columns from SCIAMACHY data, along with uncertainty estimates are obtained from Martin et al. [*Martin et al.*, 2002; *Martin et al.*, 2003; *Martin et al.*, 2004]. Tropospheric NO_2 column densities from CMAQ are obtained by integrating concentrations from the surface to the top layer accounting for temperature, pressure and terrain height using information from MM5 and then compared with satellite NO_2 retrievals. Additional information on the retrievals and data comparison procedure can be found in the previous chapter (Chapter 4, Section 4.2.2).

5.2.3. Aircraft-based observations

The International Consortium for Atmospheric Research on Transport and Transformation, Intercontinental Chemical Transport Experiment-North America, (ICARTT INTEX-NA P-3) Mission 2004 consisted of 18 flights (Figure 5.2) over the eastern US in July-August 2004 [*Singh et al.*, 2006]. Model simulations of NO, NO_2, NO_y sum, O_3 and peroxy acetyl nitrate (PAN) were compared with ICARTT measurements. Aircraft measurements within a model grid cell in a given hour were averaged to give one average measurement for one simulated concentration. Measurement techniques used, and their maximum resolution and lower detection limits are given in Table 5.1. Several other species were also compared with ICARTT measurements when available and additional information and comparisons are in Appendix A.

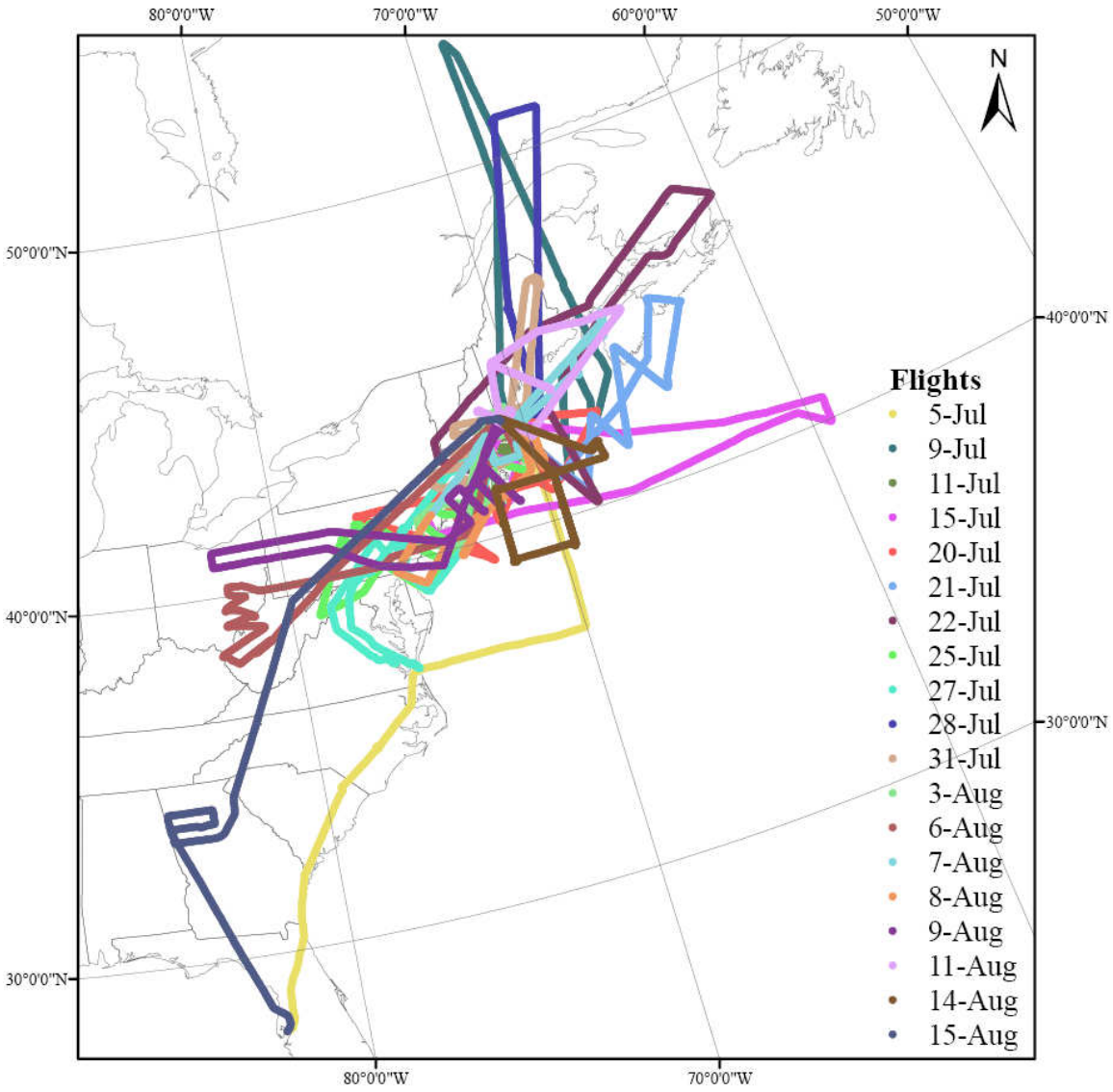

Figure 5.2. Routes of ICARTT P-3 flights

Table 5.1. Instrument detection approach, maximum resolution and lower detection limit information for NO, NO_2, NO_x, NO_y, and O_3 measurements available for comparison

Measurement Platform	Species (Units)	Detection approach	Maximum resolution	Detection limit
AIRS [1]	NO (ppbv)	chemiluminescence	1-min	5.0
	NO_2 (ppbv)	chemiluminescence	1-min	5.0
	NO_x (ppbv)	chemiluminescence	1-min	5.0
	NO_y (ppbv)	chemiluminescence	1-min	5.0
	O_3 (ppbv)	chemiluminescence, UV-absorption	1-min	2.0-5.0
SEARCH [2]	NO (ppbv)	chemiluminescence	1-min	0.05
	NO_2 (ppbv)	photolysis/ chemiluminescence	1-min	0.10
	NO_y (ppbv)	Mo reduction/ chemiluminescence	1-min	0.10
	O_3 (ppbv)	UV-absorption	1-min	1.0
CASTNET [3]	O_3 (ppbv)	UV-absorption	1-min	1.0
ICARTT [4]	NO (ppbv)	NO/O_3 chemiluminescence	1-sec	0.02
	NO_2 (ppbv)	photolysis/ chemiluminescence	1-sec	0.10
	O_3 (ppbv)	NO/O_3 chemiluminescence	1-sec	0.20
	PAN (pptv)	chemical ionization mass spectrometer (CIMS)	2-sec	1.0

[1] [*EPA*, 2009], [2] [*Hansen et al.*, 2003], [3] [*EPA*, 1995] [4] [*Fehsenfeld et al.*, 2006]

5.2.4. Ground-based observations

Several ground measurement networks are monitoring air pollutants over US. NO, NO_2, NO_x, NO_y and O_3 model simulations were compared with observations from the available ground measurement networks of (1) Aerometric Information Retrieval System (AIRS) database of the United States (US) Environmental Protection Agency (EPA) http://www.epa.gov/ttn/airs/airsaqs/) [*EPA*, 2008], (2) SouthEastern Aerosol Research and CHaracterization (SEARCH) (http://www.atmospheric-research.com/studies/SEARCH/index.html) [*Hansen et al.*, 2003], and (3) The Clean Air Status and Trends Network (CASTNet) (http://www.epa.gov/CASTNET/docs/) [*EPA*,

1995]. The locations of the monitoring stations used for evaluation of the focused two months are usually within more populated areas, though a number of stations are found in rural areas (Figure 5.1).

5.2.5. Cross-evaluation of the simulations

More detailed evaluations of the model would give additional information about the model simulations, where multiple observations are available at the same time and location. Ground observation stations that are within 20 km of the ICARTT flight paths were selected and model evaluations using both ground-based and aircraft observations were compared at the time of the flight passing. Second, the ground observation stations that are inside of a satellite scan are also selected and measurements at the time of the scans are compared. Third, the ICARTT flight paths collocated with SCIAMACHY scans were investigated. However, P-3 flights have only one collocation on July 31st, and this result indicates in situ measurements (ICARTT) showing more NO_2 than the satellite along with the comparison procedure [*Martin et al.*, 2006].

5.3. Results and Discussion

5.3.1. Simulations and satellite-based observations

Overall, the model captures the spatial distribution of the SCIAMACHY NO_2 columns well (Figure 5.3). Introduction of lightning NO_x emissions as an upper level source reduced the bias (Table 4.1), though not significantly. Simulated NO_2 columns were usually lower than observed, though highly correlated in the western US and were comparable, but had a lower spatial correlation, in the eastern US. Comparisons according to selected regions revealed the highest correlation for “rural” regions and

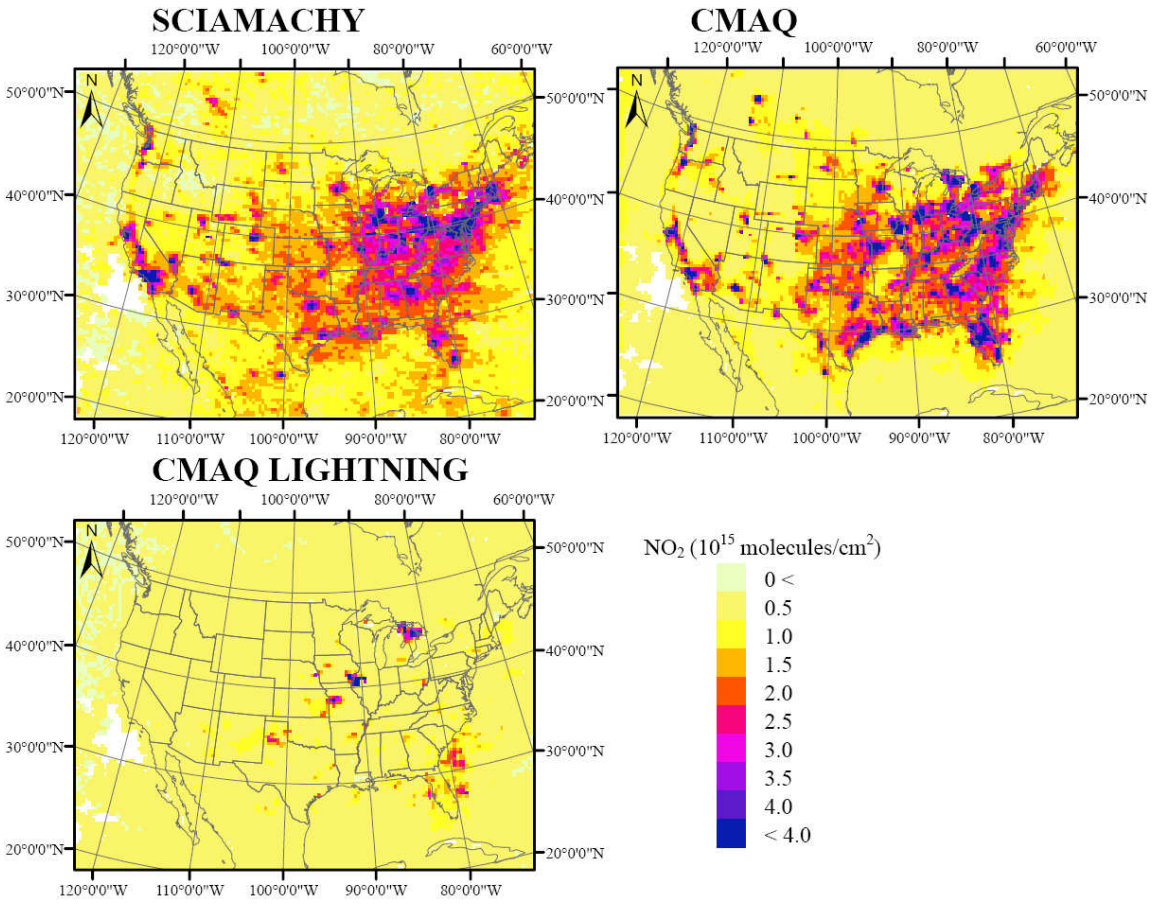

Figure 5.3. Spatial distribution of tropospheric NO_2 column averages from SCIAMACHY (upper left), CMAQ simulations (upper right) and NO_2 coming from lightning emissions (bottom) averaged for July-August 2004

lower correlation for "urban" and "rural-point" regions (Figure 4.4). Los Angeles was of specific interest because the simulated NO_2 columns are significantly lower than satellite observations indicating either a retrieval/model error or a problem in emission estimates specific to that region which was investigated previously (Chapter 4).

5.3.2. Simulations and aircraft-based observations

NO, NO_2, NO_y (NO + NO_2 + HNO_3 + all measured PANs), PAN and O_3 concentrations derived from model simulations were compared with upper level measurements obtained as part of the ICARTT campaign. Time series of O_3 matched for

altitude showed that the simulations capture most of the variation (Figure 5.4). O_3 showed the highest spatial correlation when compared with other species investigated (Figure 5.5), which is expected because of the secondary nature of O_3. Evaluation showed a mean normalized bias (MNB) of 8% and a mean normalized error (MNE) of 19% (Table 5.2). Lastly, the O_3 vertical profiles obtained by averaging all flights according to altitude revealed a positive bias for the model results at lower altitudes (0-2 km), and a negative bias above 3 km. However, all simulations except the highest level (6-6.5km) are within one standard deviation of the averaged observations (Figure 5.6).

Averaged vertical profiles of NO showed underestimations at lower altitudes (0-2km) and slight underestimations in the upper levels but all simulations were well within one standard deviation of the averaged observations (Figure 5.6). NO_2 simulations captured the observed vertical profile very well. Differences between the modeled and observed NO vertical profiles can be explained by model's limitation to simulate the power plant plumes (July 25th and August 6th), thunderstorms (July 27th) and nighttime chemistry (August 3rd and 11th) during these flights.

There is a consistent positive in the model simulations of PAN. The model captured the spatial variation (Figure 5.4) and the shape of the vertical profile but the simulations were approximately two times higher than the observations (Figure 5.6). Other PAN species like PAN2 (peroxy propionyl nitrate (PPN) and other higher alkyl PAN analogues), MPAN (peroxy methacryloyl nitrate) and PBzN (peroxy benzoyl nitrate) had the same consistent overestimation (Appendix A., Figures A.) even though their concentrations are lower. Photolysis, which might be a significant sink for PAN in

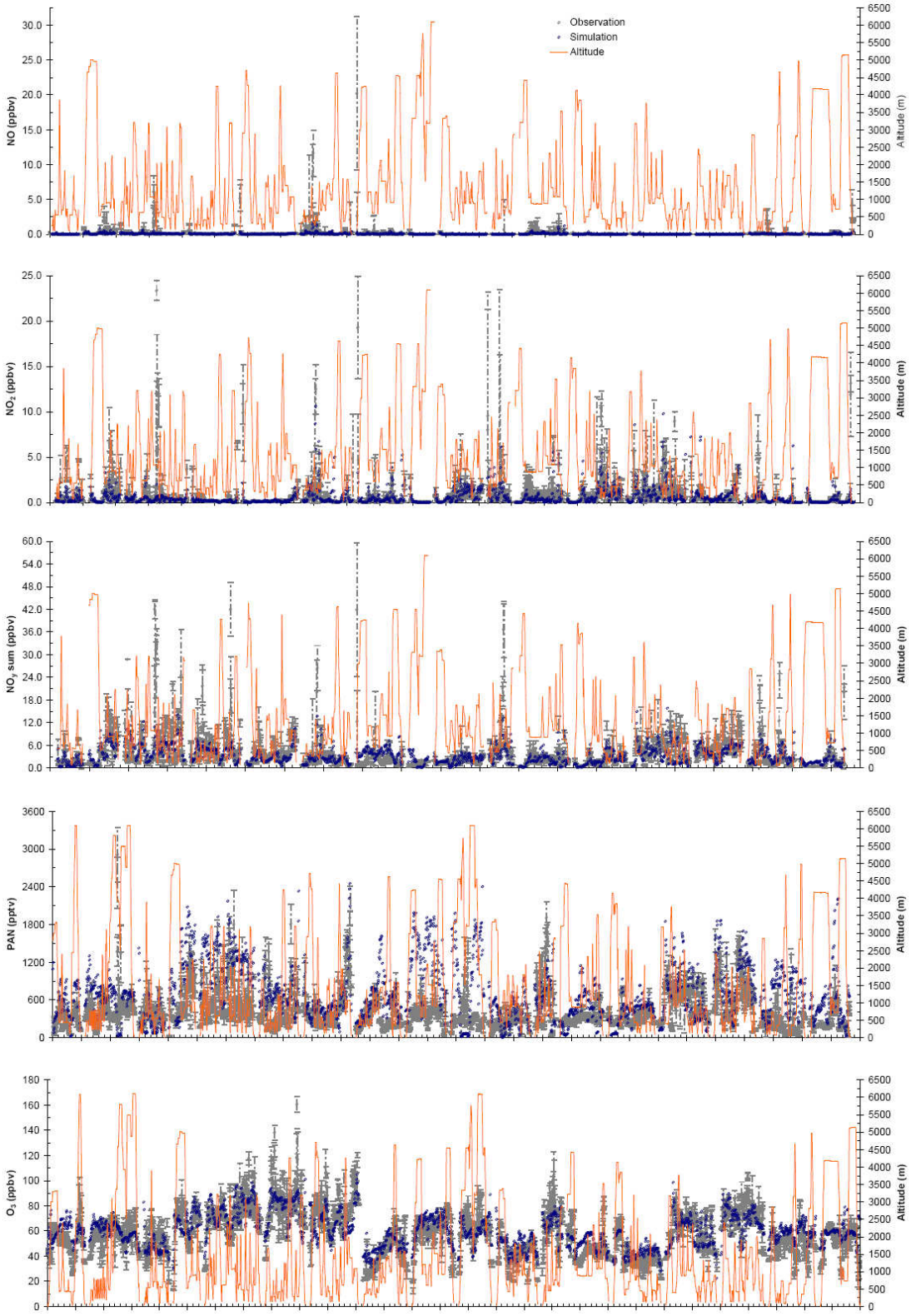

Figure 5.4. Time series of NO, NO_2, NO_y, PAN and O_3 altitude for the model simulations and aircraft observations for all flights combined (Error bars represent ± one standard deviation for the aircraft observations)

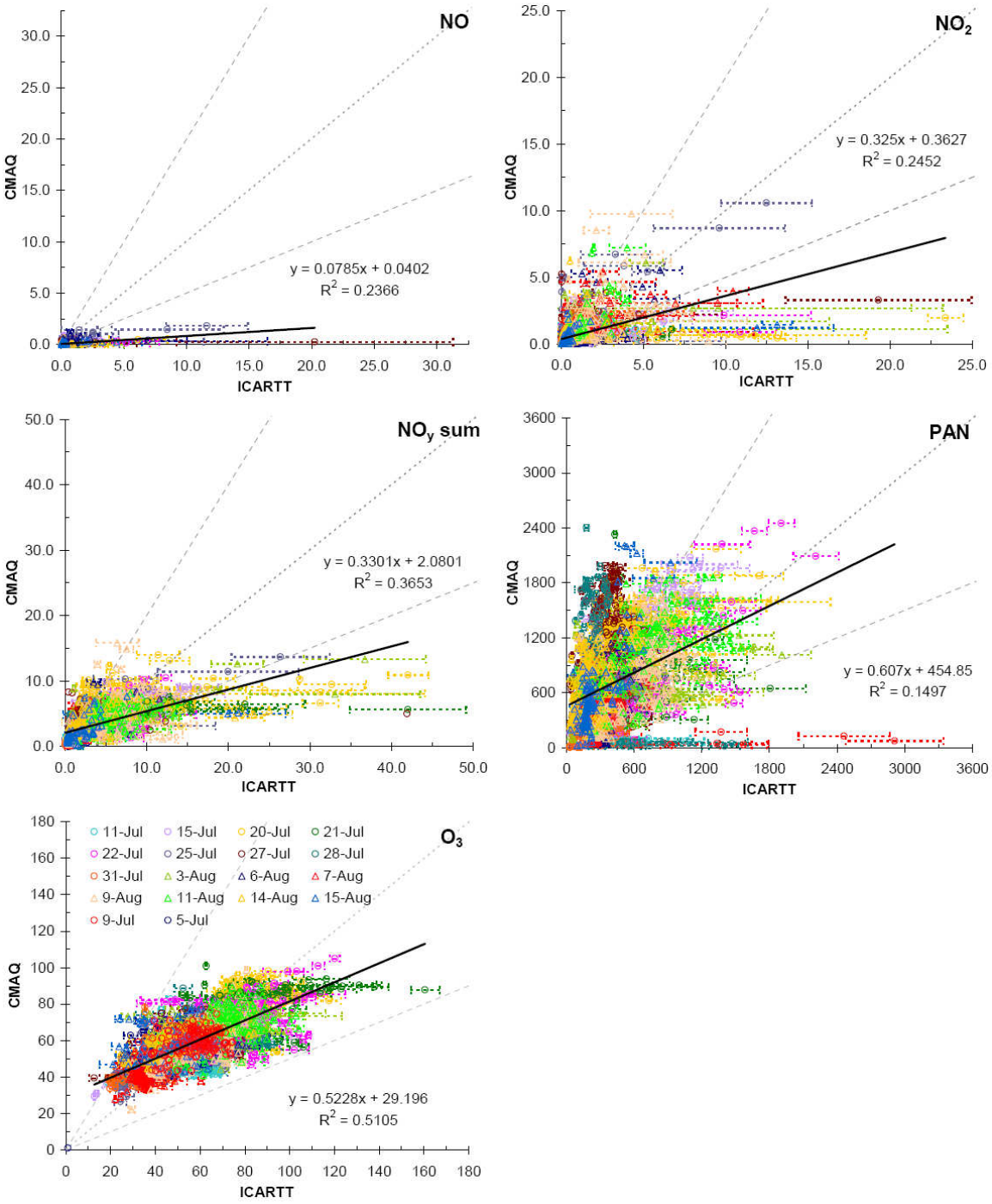

Figure 5.5. Comparison of NO, NO_2, NO_y, O_3, and PAN simulations with the aircraft observations (Error bars represent ± one standard deviation for the aircraft observations and dashed lines indicate slopes of 0.5, 1.0 and 1.5)

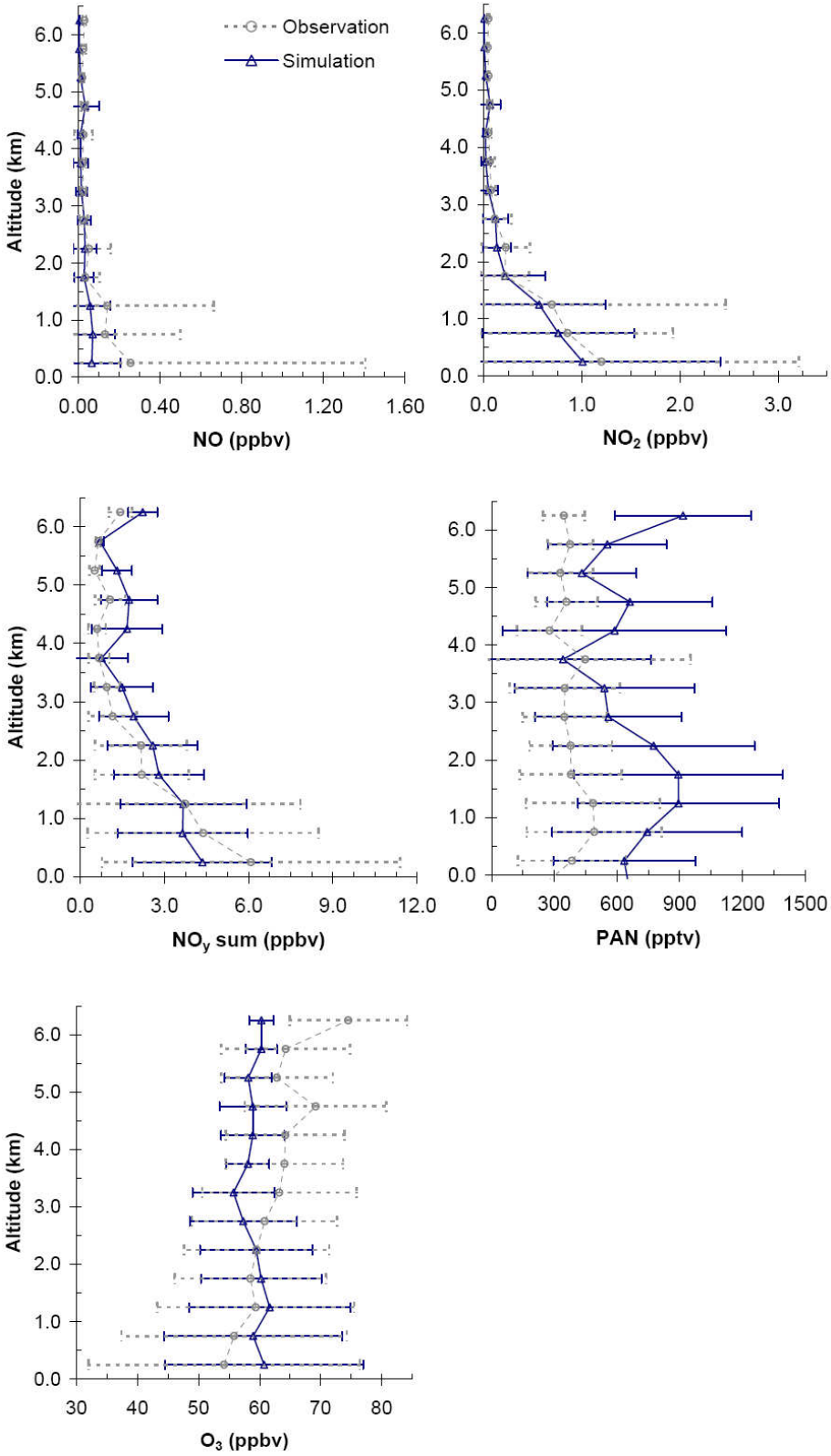

Figure 5.6. Comparison of average vertical profiles for NO, NO_2 (upper), NO_y, PAN, (middle) and O_3 (lower) for the model simulations and aircraft observations (Error bars represent ± one standard deviation)

the upper levels of the atmosphere where temperatures are lower, was added to the model by inclusion of the following reaction [*Carter*, 2008]:

$$PAN + h\nu \rightarrow 0.6\left(CCO - O_2 + NO_2\right) + 0.4\left(C - O_2 + NO_3 + CO_2\right) \quad \text{(Equation 5.1)}$$

Where CCO-O_2 is the acetyl peroxy radical and C-O_2 is the methyl peroxy radical. This addition resulted in minor improvement (reduction up to 5% MNE and MNB for individual flights) in the comparison and the vertical profile remained similar.

Lastly, NO_y simulations were compared with the observations, and the correlation was better and the bias was smaller than for NO, NO_2 and PAN (Table 5.2), indicating the model simulates the total nitrogen mass better than each individual species. This can be related to the issues of the model's chemistry of reactive nitrogen species in the upper levels of troposphere, because better capturing of the total mass strengths the magnitude of the emissions. The vertical profile was captured but NO_y showed a negative bias at lower altitudes (0-2km) (Figure 5.6).

5.3.3. Simulations and ground-based observations

Spatial distributions of the monthly averaged observations overlaid on monthly averaged simulations of O_3, NO, NO_2, NO_x and NO_y for the month of July (representative of the two-months) indicate a positive bias in O_3, negative bias in NO, and small biases in NO_2 and NO_x simulations (Figure 5.7). When the stations were separated into two regions, western and eastern US, NO_2 and NO_x showed different patterns. Simulated NO_2 and NO_x had a negative bias in the West and a positive bias in the East, which was also suggested by previous satellite NO_2 retrieval comparisons (Table 5.2). On the other hand, O_3 had a reduced positive bias and NO had an increased negative bias in the West.

Table 5.2. Statistics and correlation coefficients (R^2, slope and intercept) of CMAQ simulated pollutants versus observations from available observation platforms for the episode (July-August 2004)

Platform	Species (units)	Region	N	R^2	Slope	Inter (unit)	MBE (unit)	RMSE (unit)	MNB (%)	MNE (%)
AIRS & SEARCH & CASTNET	NO (ppbV)	West US	110	0.04	0.28	1.000	-2.662	7.773	-47.27	111.88
		East US	192	0.04	0.19	1.200	-2.517	5.684	-37.22	99.33
		All	302	0.04	0.23	1.130	-2.570	6.523	-40.88	103.90
	NO_2 (ppbV)	West US	151	0.27	0.65	1.800	-2.045	8.468	-3.31	66.51
		East US	273	0.28	0.66	3.400	0.283	6.536	30.46	75.02
		All	424	0.27	0.64	3.006	-0.546	7.283	18.44	71.99
	NO_x (ppbV)	West US	110	0.17	0.52	3.000	-4.674	15.690	-19.88	69.10
		East US	185	0.17	0.47	5.900	-1.175	11.178	27.31	86.05
		All	295	0.17	0.48	4.929	-2.480	13.044	9.72	79.73
	NO_y (ppbV)	All (East US)	34	0.13	0.39	6.137	0.337	9.563	43.20	71.21
	O_3 (ppbV)	West US	349	0.34	0.28	32.000	5.808	10.993	24.99	31.53
		East US	918	0.06	0.28	31.900	10.478	12.604	38.49	39.61
		All	1267	0.15	0.28	31.912	9.191	12.181	34.77	37.38
ICARTT	NO (ppbV)		2505	0.24	0.08	0.040	-0.077	0.597	6.40	99.30
	NO_2 (ppbV)		2142	0.24	0.32	0.372	-0.105	1.269	68.84	125.63
	NO_y (ppbV)		1791	0.37	0.33	2.080	-0.426	3.392	39.13	74.50
	PAN (pptV)		2512	0.15	0.61	454.853	291.183	517.028	122.26	140.48
	O_3 (ppbV)		2646	0.51	0.52	29.196	1.422	12.488	7.92	18.97
SCIAMACHY	NO_2 (molecules/cm^2)	West US	2363	0.65	0.80	4.E+12	-1.9E+14	7.9E+14	-26.75	100.09
		East US	3617	0.49	1.11	3.E+13	2.1E+14	1.2E+15	17.66	46.09
		US	5980	0.57	1.01	3.E+13	5.3E+13	1.0E+15	0.11	67.43
		All	16251	0.60	1.00	-1.E+14	-1.E+14	7.9E+14	-20.29	111.63

Abbreviations: N, Number of observations; MBE, Mean bias error; RMSE, Root mean square error; MNB, Mean normalized bias; MNE, Mean normalized error.

All NO_y observation sites are located in the eastern US (Figure 5.1), so comparison between regions was not possible. NO_y simulations usually captured the observations well, though had a positive bias (Figure 5.7, Table 5.2) and two major outliers. These two outliers were both rural stations, one of which is an AIRS station in Norfolk County, MA and another one is a SEARCH station in Paulding County, GA (Yorkville) where the model had a large positive bias in NO_y concentrations. The MNB and MNE were reduced to 11% and 41%, respectively and the correlation coefficient (R^2) was increased to 0.56 if those two stations were removed from the comparison. Reasons for these two outliers were likely due to artificial dilution of NO_y from the nearby urban areas.

When NO_2 from the model was compared with the three platforms, less than 20% bias was observed both with ground and satellite-based observations over the US. Additionally, ground and satellite-based observations indicate similar comparisons for western and eastern US as well. Aircraft based observations, on the other hand, indicated a worse performance of the model, but it is hard to capture the specific events such as power plant plumes and thunderstorms which may require smaller spatial resolution. The focus area of the flights were eastern US (Figure 5.2), where other observations indicated a positive bias too, though on smaller magnitudes. Satellite-based observations had the highest correlation spatially (R^2=0.60), resulting probably from the similar spatial scaling with the model simulations unlike other observations. Simulated NO was negatively biased as compared to ground observations. A similar bias was found in the comparison of the vertical profile obtained from aircraft observations, though the overall bias was small. NO_y from ground and NO_y from the aircraft both were lower than simulated and errors were similar (Table 5.2). This positive bias in the model is

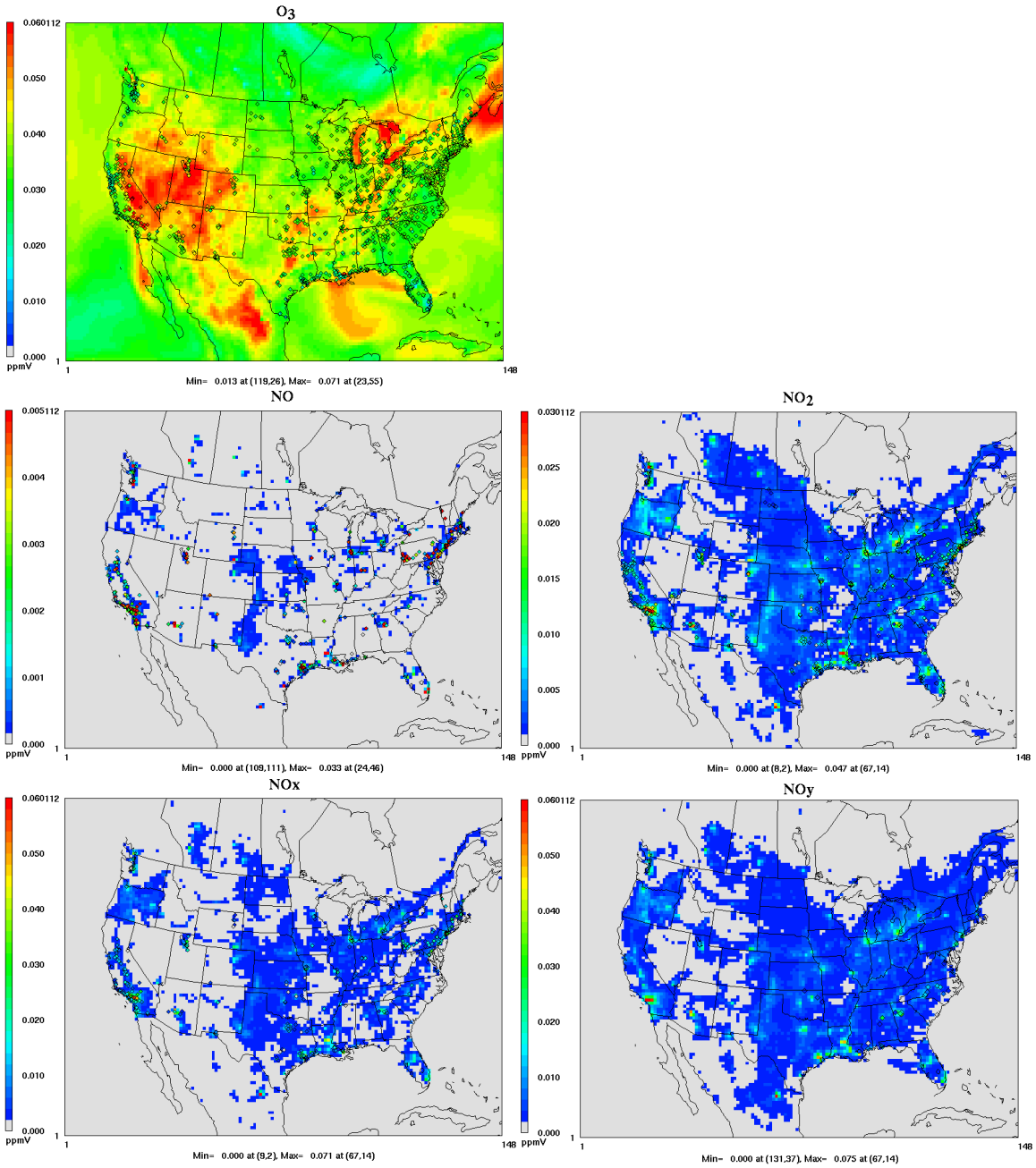

Figure 5.7. Spatial distribution of monthly averaged O_3 (upper), NO, NO_2 (middle), and NO_x, NO_y (bottom) from model simulations with overlaid available ground-based observation stations (diamonds) for July 2004

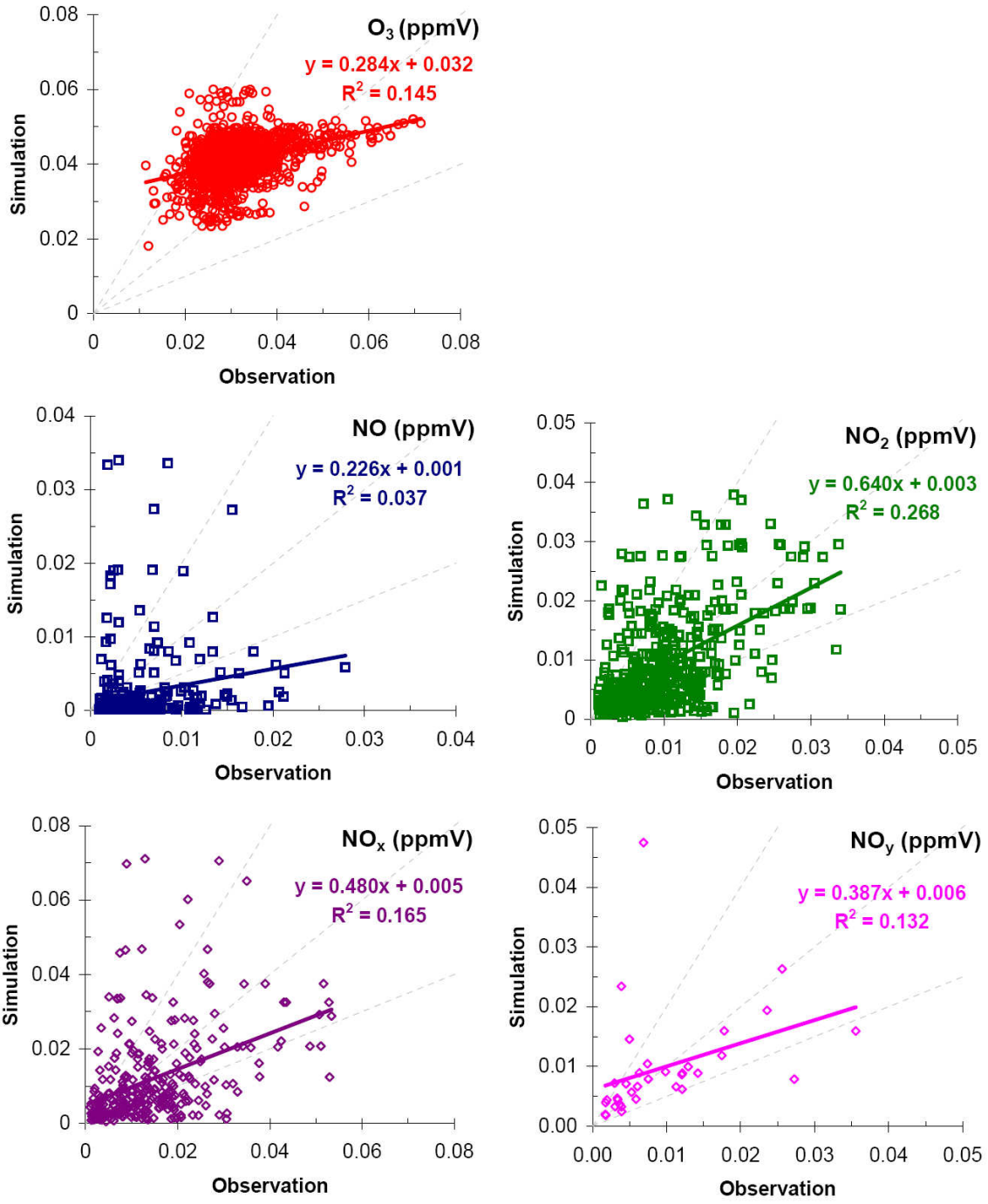

Figure 5.8. Comparison of monthly averaged O_3 (upper), NO, NO_2 (middle), and NO_x, NO_y (bottom) model simulations with ground-based observation stations for July-August 2004

consistent with the positive bias in the PANs. Simulated O_3 had smaller biases and errors and a higher correlation with aircraft-based observations than ground, though both suggest a positive bias in the model simulations. Vertical profiles of O_3 also indicate a positive bias near the surface. One reason of aircraft observations better performance may be the sensitivity of O_3 being higher to NO_x and VOC sources on the surface, but lower in the upper levels, which then results in better predicting the upper level concentrations.

5.3.4. Cross-comparisons with different observations

5.3.4.1. Satellite-based and ground-based observations

NO_2 ground stations that are within the satellite scans at the crossing times – approximately 11:00 am local time – were selected for further investigation. Time series show consistency, in that high and low concentrations were captured, but correlation of ground observations with satellite retrievals were very low (Figure 5.9). Satellite observations indicated a positive bias of the model, resulting from high simulations around urban areas or high lightning activity regions (order of 10^{16} molecules/cm^2). On the other hand, ground observations had a very low bias and indicated underestimation of the model around urban areas where model overestimated according to satellite retrievals. Both datasets had errors on the order of 100% (Table 5.3). The overall NO, NO_2 and NO_x performance of the model finds a negative bias in comparison to ground observations for 11:00 am local time. This may be related to the simulation of the increasing mixing layer depth through the mornings.

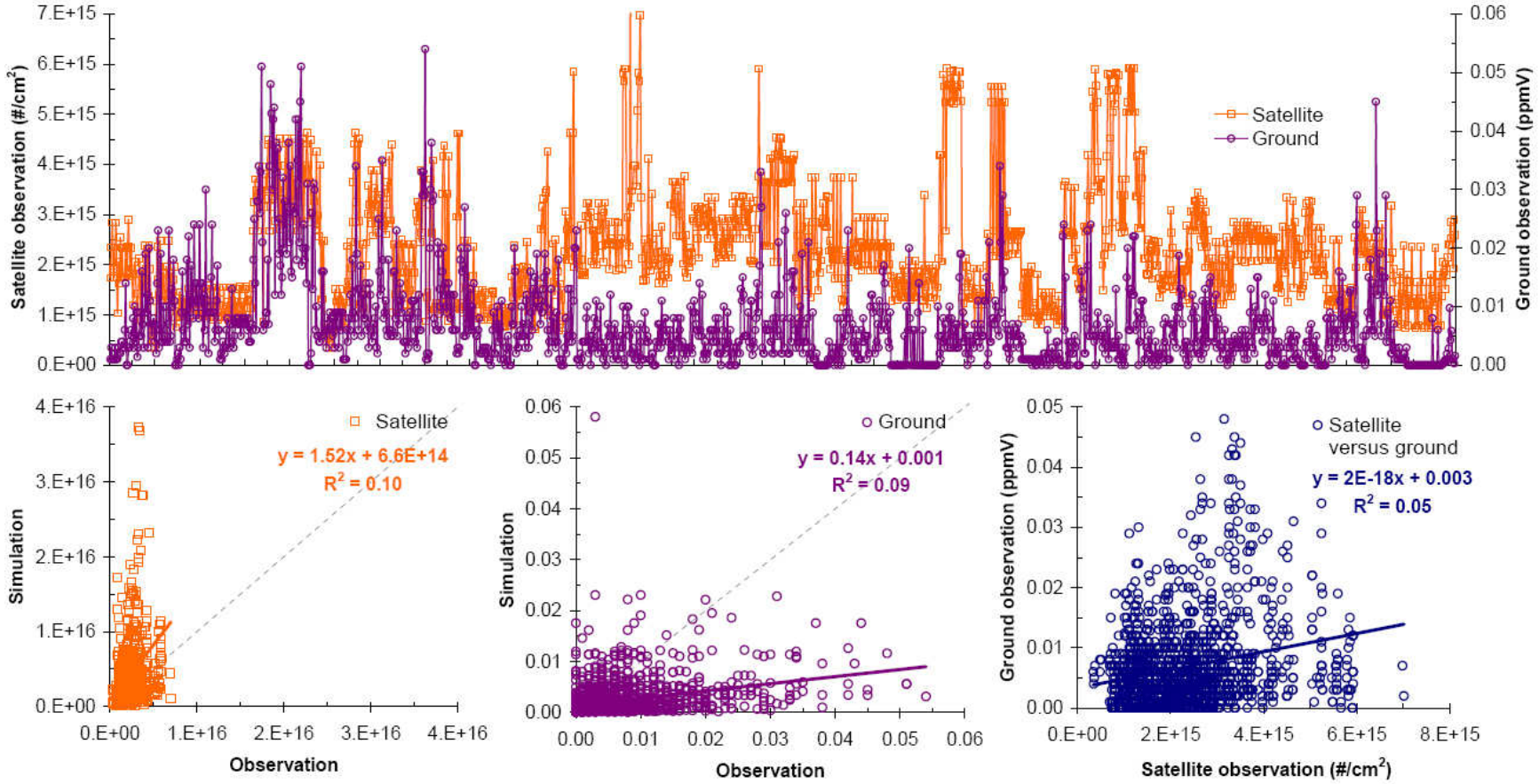

Figure 5.9. Comparison of selected satellite-based (lower, left) and corresponding ground-based (lower, middle) NO_2 observations with model simulations and with each other (lower, right) for July-August 2004

Table 5.3. Statistics and correlation coefficients (R^2, slope and intercept) of selected satellite-based and corresponding ground-based NO_2 observations with model simulations during the episode

Platform, Species	**N**	**R^2**	**Slope**	**Inter (unit)**	**MBE (unit)**	**RMSE (unit)**	**MNB (%)**	**MNE (%)**
AIRS & SEARCH & CASTNET NO_2, ppbV	1328	0.09	0.14	1.447	-3.978	8.913	5.63	128.46
SCIAMACHY NO_2, 10^{15} molec/cm^2	1496	0.10	1.52	0.66	1.85	5.52	79.90	117.93

5.3.4.2. Aircraft-based and ground-based observations

Ground-based NO, NO_2, NO_x, NO_y and O_3 observations within 20 km of the flight routes at the times aircraft were passing were selected for further investigation. For NO, both ground and aircraft observations indicated the model results were negatively biased. Aircraft observations were highly correlated with simulations, whereas ground observations had little correlation (Table 5.4). Simulated NO_2 and NO_x had similar biases and errors for both sources (Table 5.4) and ground observations were significantly higher than aircraft observations (Figure 5.10) probably because of their close proximity to NO_x sources. NO_y ground stations showed significant overestimation, whereas aircraft NO_y had a very good correlation and lower bias. Lastly, simulated O_3 had a small bias compared to both datasets, and better correlation. Evaluations with aircraft observations showed a better performance (Figure 5.11) and were higher than ground observations. The largest outliers when comparing simulated O_3 to ground observations were at night where observed O_3 mixing ratios drop to almost zero, but not the corresponding model simulations. Overall simulated NO_2 and O_3 were positively biased compared with ground observations at night. A stricter selection criterion i.e. shorter distance showed

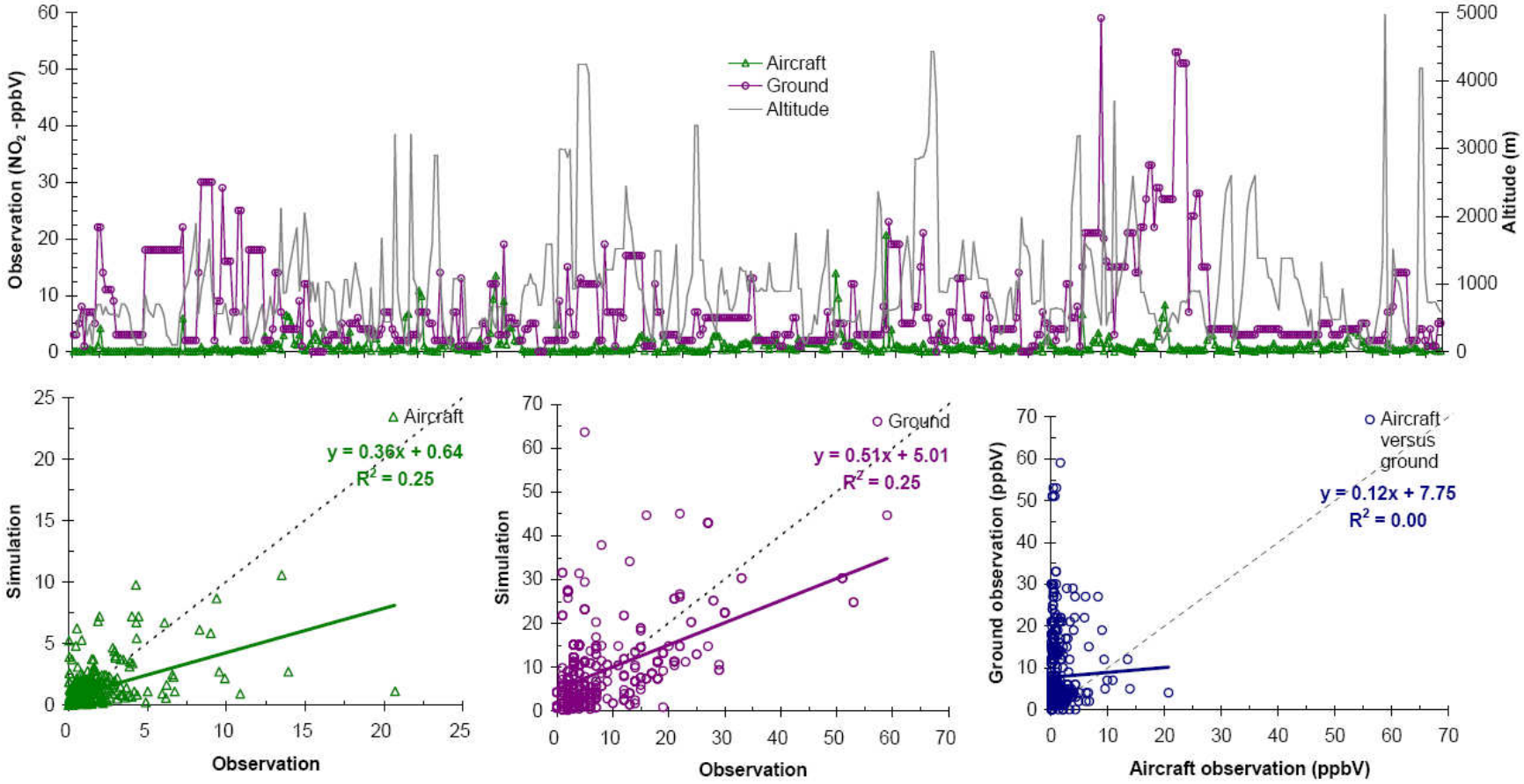

Figure 5.10. Comparison of selected aircraft-based (lower, left) and corresponding ground-based (lower, middle) NO_2 observations with model simulations and with each other (lower, right) for July-August 2004

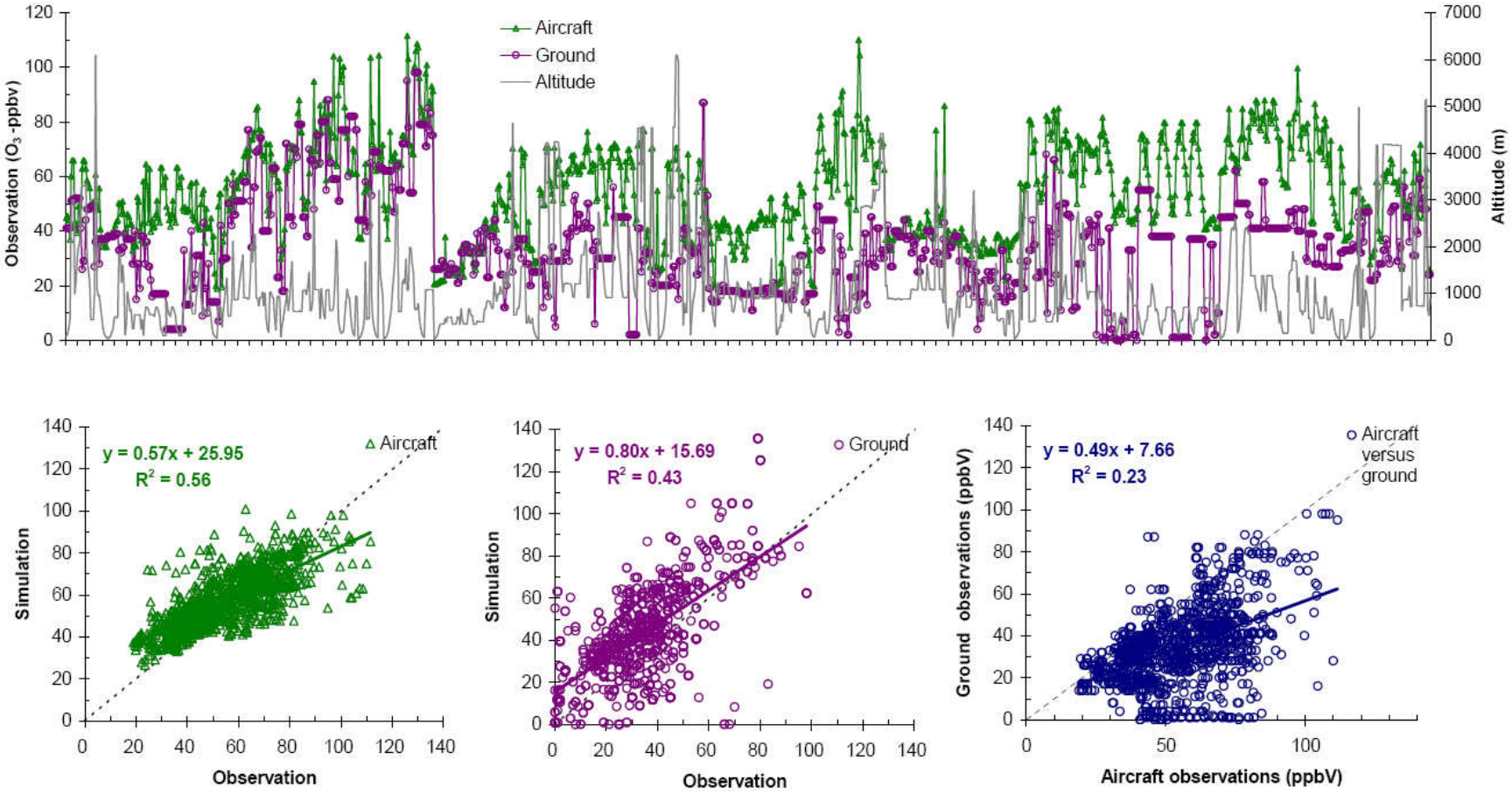

Figure 5.11. Comparison of selected aircraft-based (lower, left) and corresponding ground-based (lower, middle) O_3 observations with model simulations and with each other (lower, right) for July-August 2004

Table 5.4. Statistics and correlation coefficients (R^2, slope and intercept) of selected aircraft-based and corresponding ground-based NO, NO_2, NO_x, NO_y, and O_3 observations with model simulations during the episode

Platform	Species (ppbV)	N	R^2	Slope	Inter (ppbV)	MBE (ppbV)	RMSE (ppbV)	MNB (%)	MNE (%)
AIRS & SEARCH & CASTNET	NO	329	0.01	0.02	0.430	-3.494	9.083	-56.52	102.71
	NO_2	394	0.25	0.51	5.010	-0.009	8.592	44.91	97.72
	NO_x	384	0.26	0.36	5.544	-2.404	13.286	35.61	95.06
	NO_y	48	0.13	1.70	3.599	7.037	16.519	159.21	162.96
	O_3	363	0.43	0.80	15.688	5.457	20.856	10.49	29.93
ICARTT	NO	434	0.61	0.16	0.037	-0.165	0.768	13.93	130.19
	NO_2	464	0.25	0.36	0.643	-0.135	1.736	46.32	94.45
	NO_x	415	0.32	0.33	0.658	-0.324	2.119	36.16	86.27
	NO_y	49	0.62	0.90	0.487	0.242	1.214	17.31	53.20
	O_3	862	0.56	0.57	25.946	0.007	11.496	2.44	14.46

improvements only for O_3 comparisons. This implies the effect of meteorological parameters (wind speed and direction) and the difference between the surface and aloft concentrations were significant.

5.4. Summary

Inter-comparison of CMAQ with available satellite, ground and aircraft-based observations of NO, NO_2, NO_x, NO_y, PAN and O_3 for a two-month period from the summer of 2004 (July-August) found general agreement, but important differences as well.

NO_2 showed low biases between simulated levels and both ground and satellite-based observations over the US. Regional results were similar. Aircraft-based observations, on the other hand, indicated a higher positive bias and error resulting from specific events which are hard to simulate with a grid model than previous two measurements. The average vertical profiles for the various species were captured very well [*Yu et al.*, 2007]. Satellite-based NO_2 observations had the highest correlation

indicating the effect of similar spatial resolution between the model and satellite retrievals.

NO was underestimated in comparison with the ground observations and aircraft observations, especially near the surface. NO_y from ground and aircraft indicated both positive biases in the model and errors were on the same order of magnitude. This overestimation was possibly resulting from the consistent overestimations of PANs. Simulated O_3 compared better with aircraft-based observations than ground, though both found a positive bias in the model simulations. Vertical profiles of O_3 also indicate a positive bias near the surface, though a negative bias at the upper levels unlike *Yu et al.* [2007] who found consistent overestimations above 6 km.

Inter-comparison of ground observations with satellite observations indicate a positive bias in simulated NO_2 columns, but a negative bias in surface mixing ratios with low correlations for both. Here, the representativeness of the ground observations for the scan area becomes important. This result supports previous finding that the model overestimates the total NO_2 column and underestimates the surface observations of NO_2 over urban areas. This suggests that either the ground-based observations have somewhat limited utility for model evaluation and assessment of emission estimates, or that there may be biases in the satellite retrievals that need to be identified and corrected if such measurements are going to be used for emissions and model assessments.

Secondly, comparing ground observations with aircraft measurements result in a limited dataset and indicate the representativeness of the ground stations as indicators of concentrations aloft. However, only O_3 resulted in improvements in the correlations if a stricter selection criterion i.e. shorter distance was applied. This comparison could be

improved if additional investigation performed including meteorological parameters (wind speed and direction) combined with a time shift in the observations for correlation. However, neither of the comparison contradicted the findings from separate evaluations of the model.

CHAPTER 6

INVERSE MODELING WITH FOUR DIMENSIONAL DATA ASSIMILATION (FDDA) USING SATELLITE AND GROUND-BASED OBSERVATIONS

6.1. Introduction

Air quality modeling is a useful tool for predicting the future concentrations of pollutants emitted from different sources and for meteorology scenarios, understanding atmospheric dynamics, effects of pollutants on different ecosystems, etc. and simulating concentrations where measurements are not available. Simulations give insight to the relationship between the emissions and ambient concentrations of pollutants especially when this relationship is not linear. It is important to be able to simulate not only the ambient concentrations of the pollutants correctly, but also the contribution of each source. Determining the contributions of different sources is essential especially in policy development where reductions in ambient concentrations of harmful pollutants are required. Relative contribution of each source on ambient concentrations of pollutants can be calculated by various methods such as brute force (BF) and decoupled direct method (DDM). DDM is a method to directly and efficiently calculate the sensitivity of model outputs to model inputs and has been a widely used sensitivity analysis technique in three dimensional (3-D) air quality models [*Cohan et al.,* 2005; *Yang et al.,* 1997].

Emission inventories are usually prepared by a bottom-up approach and are based on the current knowledge of emission factors and process activities, including factory process rates and vehicle-miles traveled. This information is subject to uncertainties.

Using the emission inventories in air quality model simulations result in uncertainties in the simulated pollutant concentrations. The minimization of uncertainties in simulations via the optimal combination of observational data with relatively low uncertainties and *a priori* emissions is a common method called inverse modeling [*Tarantola*, 2005]. Inverse modeling can be used to incorporate the information from observations to AQMs to identify biases and errors coming from model inputs e.g. emissions, boundary conditions, model process and descriptions and such approaches have been used to improve the bottom-up emission inventories for 3-D air quality models (AQMs) both on global and regional scales [*Elbern and Schmidt*, 1999; *Jaegle et al.*, 2005].

Inverse modeling with satellite retrievals on a global scale has been investigated by several researchers for various pollutant species such as CO [*Arellano et al.*, 2006; *Müller and Stavrakou*, 2005], NO_2 [*Martin et al.*, 2003; *Martin et al.*, 2006; *Müller and Stavrakou*, 2005; *Stavrakou et al.*, 2008; *Wang et al.*, 2007] and isoprene [*Dufour et al.*, 2009; *Shim et al.*, 2005]. On regional scales, GOME and SCIAMACHY NO_2 retrievals were used to improve the European Monitoring and Evaluation Programme (EMEP) emission inventory in Europe [*Konovalov et al.*, 2006], GOME NO_2 retrievals were used to optimize NO_x emissions from Regional Emission Inventory in Asia over eastern China [*Kurokawa et al.*, 2009], OMI NO_2 retrievals were used to constrain fossil fuel NO_x emissions over east Asia [*Zhao and Wang*, 2009] and SCIAMACHY NO_2 retrievals were used to assess the 1999 National Emissions Inventory (NEI) over the southeastern United States (US) [*Napelenok et al.*, 2008]. Ground observation networks were also used for inverse modeling to improve NO_x emissions over Europe [*Deguillaume et al.*, 2007;

Pison et al., 2007; *Quelo et al.*, 2005], China [*Wang et al.*, 2004] and the US [*Mendoza-Dominguez and Russell*, 2001a; b].

In this study, we used an inverse modeling technique [*Mendoza-Dominguez and Russell*, 2000] to identify potential biases in an up-to-date NO_x emission inventory by using two different observation datasets; satellite NO_2 retrievals and ground-based NO, NO_2, O_3 observations for the US. The two datasets lead to different bias estimates. The main reason for using the datasets separately is the combined effect of the high level of uncertainty in satellite retrievals with issues of ground observations representing a larger area both of which were discussed in the previous chapter (Chapter 5). In addition, the satellite scans through the globe at a specific time of day (10:30 am for SCIAMACHY) unlike ground-based observations where hourly data are available throughout the day. So, applying the two datasets separately could also give additional information on the daily variation of the emissions. Weighting factors selection for multiple platform-based observations which determines how much the solution depends on any set of observation requires great care, because the selection will determine the relative weights of different platforms (satellite and ground-based) on the solution (emission adjustments). Lastly, the case of contradicting observations from two datasets could result in results mathematically reducing the error but without any physical meaning. The result from this study can give insight on adapting relative weighting factors to multiple measurements from different platforms and using these measurements simultaneously.

The objectives of the research reported in this chapter are to (a) perform inverse modeling to identify potential biases in the emission inventories of NO_x using satellite NO_2 retrievals as well as using ground-based O_3, NO_2, and NO observations; (b) compare

the results from those two data sets; and (c) evaluate the results with an independent measurement.

6.2. Methods

6.2.1. Model Description

The Community Multi-scale Air Quality Model (CMAQ) [*Byun and Schere*, 2006] coupled with the Decoupled, Direct Method [*Dunker*, 1984; *Yang et al.*, 1997] in Three Dimensions (DDM-3D) [*Cohan et al.*, 2005] was used for this study. Modeling domain, chemical mechanisms and model specifications were explained in previous chapters in detail. Meteorological simulations were performed using the Fifth-Generation NCAR/Penn State Mesoscale Model (MM5) [*Seaman*, 2000] and emissions were prepared using the Sparse Matrix Operator Kernel Emissions (SMOKE) [*Houyoux and Vukovich*, 1999]. The emission inventory used was VISTAS 2002 [*MACTEC*, 2005] projected to the episode year (2004) with growth factors obtained from the Economic Growth Analysis System (EGAS) Version 4.0, and control efficiency data obtained from EPA for the existing federal control strategies. In addition, US emissions from large NO_x and SO_2 point sources for 2004 obtained from the continuous emissions monitoring (CEM) database [*EPA*, 2008] and lightning NO_x emissions derived from US National Lightning Detection Network (NLDN) lightning flashes data [*Kaynak et al.*, 2008] were integrated into the emission inventory.

Seven major categories of NO_x emissions were selected and sensitivities of pollutants to these categories were calculated with CMAQ-DDM-3D along with the concentrations. Selected categories of NO_x emissions were lightning (L), Canada (C), Mexico (M), eastern US stationary (ES), western US stationary (WS), eastern US mobile

(EM) and western US mobile (WM) NO_x emissions. Canada and Mexico categories include all nation-wide NO_x emissions, mobile categories include on-road and non-road NO_x emissions and stationary categories include all area sources combined with point NO_x sources. Spatial definitions of western and eastern US regions were described previously (Chapter 4). Sensitivities to biogenic and anthropogenic volatile organic compounds (VOCs) emissions were also calculated. Since model simulations resulted in low sensitivities to VOC emissions compared to NO_x emissions, especially sensitivities of NO_2 concentrations to VOC emissions, and VOC emissions also have higher uncertainty, VOC emissions were not included in the inverse calculations.

6.2.2. Four Dimensional Data Assimilation (FDDA)

The FDDA approach [*Mendoza-Dominguez and Russell*, 2000] aims to identify emissions inventory improvements by combining emission-based modeling and observations using an inverse modeling technique. The method suggests improvements in emission strengths, patterns, and compositions of various source categories simultaneously by minimizing the error between the observational data and simulations. Additional information about the observational data and the emissions such as uncertainties is incorporated into the approach by means of weighting.

In this approach, the ambient concentrations and the corresponding sensitivities of these concentrations to the selected emission categories were simulated using CMAQ with DDM-3D using the original emission inventory. Then, adjustments to the emissions were calculated by ridge regression to minimize the objective function, Γ which includes the square of the weighted error between the simulations and the observations (first part) and the square of the penalized emissions adjustments (second part):

$$\Gamma = e^T W_e e + m^T W_m m \qquad \text{(Equation 6.1)}$$

where e represents the simulation errors (difference between the simulation and the observation) with the adjusted emissions, m represents the adjustments to each emission category, W_e include weightings of the observations, and W_m include the penalties which depend on the uncertainty of the original emission estimates and constrains the adjustment factors. Thus, adjustment factors m minimizing Γ are:

$$m = (G^T W_e G + W_m)^{-1} G^T W_e d \qquad \text{(Equation 6.2)}$$

where G contains the sensitivity coefficients and d is the vector of current simulation errors with the unadjusted emissions.

The adjustments calculated for each iteration were used to update the emissions inventory (Figure 6.1). Simulations with the updated inventory were then performed to calculate the concentrations and the sensitivities until the change in the adjustment factors from the previous iteration become less than 2% (Figure 6.2). Details of the inverse method used are described elsewhere [*Mendoza-Dominguez and Russell*, 2000].

6.2.3. Observation Data

Two different sets of observations are used to identify potential biases in the NO_x emission inventories; (1) ground-based observations of NO, NO_2, O_3 and (2) satellite NO_2 retrievals. Additional information on the measurement locations, methods and initial evaluations of the model simulations with ground-based and satellite retrievals can be found in the previous chapter (Chapter 5, Section 5.2.2 for satellite and Section 5.2.4 for ground-based observations).

The uncertainties of the emission source categories were adapted from Mendoza et al., [2000] as the geometric standard deviation of the emissions for all NO_x emission

categories (1.22), except lightning NO_x emissions (5.00) which has significantly higher uncertainty than other sources. Uncertainties (1 σ) used for weighting ground-based observations were: NO; 2.6, NO_2; 4.5 and O_3; 8.9 ppbV. Uncertainties used for weighting the monthly-averaged satellite retrievals were 5×10^{15} molecules/cm^2 + 30% of the concentration retrieved [*Martin et al.*, 2006].

Aircraft observations were also available for the period but they were too spatially and temporally limited to be used for adjusting NO_x emission estimates for the whole episode. Aircraft observations were not used for inversions but they were used in the final evaluation of the improved emission estimates.

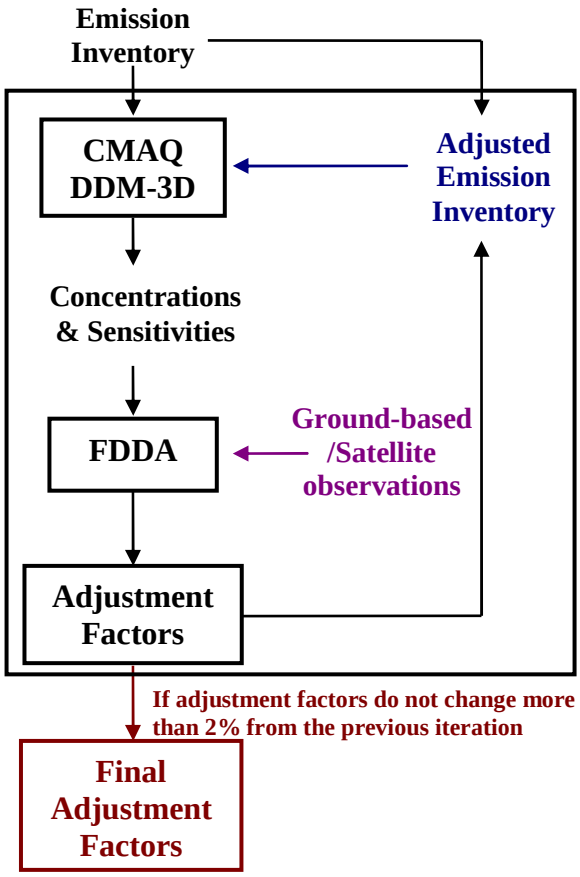

Figure 6.1. Schematic diagram of the FDDA method used for updating NO_x emissions

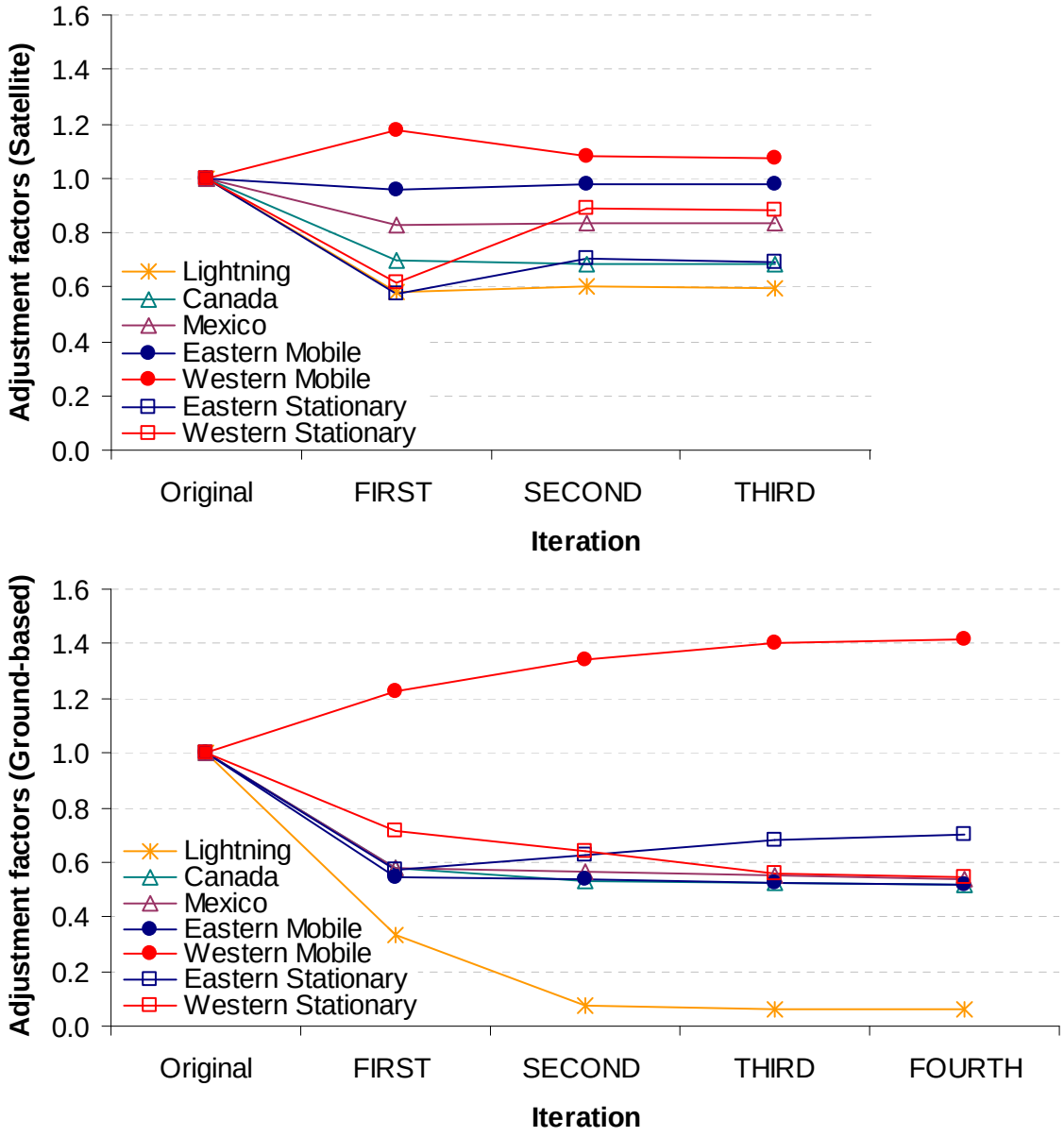

Figure 6.2. Adjustment factors for the emission categories obtained from using ground-based NO, NO_2, and O_3 observations (upper) and satellite NO_2 retrievals (lower) for each iteration

6.3. Results and Discussion

6.3.1. Adjustment factors obtained using satellite NO_2 retrievals

Initial comparison of modeled and observed NO_2 columns indicates a negative bias domain-wide (-32% mean normalized bias (MNB) and 52% mean normalized error (MNE)) (Table 6.1). After three iterations, the solution converged and root mean square error (RMSE) is reduced from 8.48 to 7.68×10^{14} molecules/cm^2 but MNB and MNE are not reduced. The spatial correlation improved and the number of outliers in the model simulation is reduced (Figures 6.3 and 6.4). The original dataset where pairs of simulations and observations are not averaged shows a higher improvement with the MNB reduced from 11 to -5% and MNE reduced from 246 to 219%. This indicates adjusted emissions improved model satellite comparison at specific times and locations but monthly averages did not improve significantly.

The adjustments suggested from assimilation of satellite NO_2 retrievals leads to reductions for all NO_x emission categories except western mobile emissions, which had a slight increase (8%) (Figure 6.5). The average daily NO_x emissions indicates significant amount of lightning NO_x produced (Table 6.2), this is common for the summer months, especially over south-eastern US and the Midwest. Satellite retrievals indicated a 40% reduction of lightning NO_x emissions. The high uncertainty in lightning emissions combined with significant positive biases over some regions due to lightning indicates that the production of NO_x from per flash of lightning should be reduced, or NO_x production should be estimated with additional information like flash length or energy dissipated as well as the number of flashes.

Table 6.1. Statistics for the iterations performed for inverse modeling with satellite observations for July-August 2004

Iteration	N	Observation		Simulation		R^2	Slope	Intercept	MBE	RMSE	MNB	MNE
		Aver	StDev	Aver	StDev			(#/cm^2)	(#/cm^2)	(#/cm^2)	(%)	(%)
Original	13398	1.11E+15	9.44E+14	8.51E+14	1.24E+15	0.58	1.00	-2.60E+14	-2.60E+14	8.48E+14	-31.98	52.08
1				6.48E+14	9.66E+14	0.62	0.81	-2.49E+14	-4.64E+14	7.76E+14	-47.42	55.72
2				6.90E+14	1.02E+15	0.62	0.85	-2.57E+14	-4.22E+14	7.71E+14	-44.56	54.63
3				6.92E+14	1.02E+15	0.62	0.85	-2.52E+14	-4.20E+14	7.68E+14	-44.28	54.31

Note: Statistics were calculated for pairs where satellite retrievals were higher than 2.5×10^{14} molecules/cm^2 which is taken as the detection limit for the monthly averaged NO_2 columns

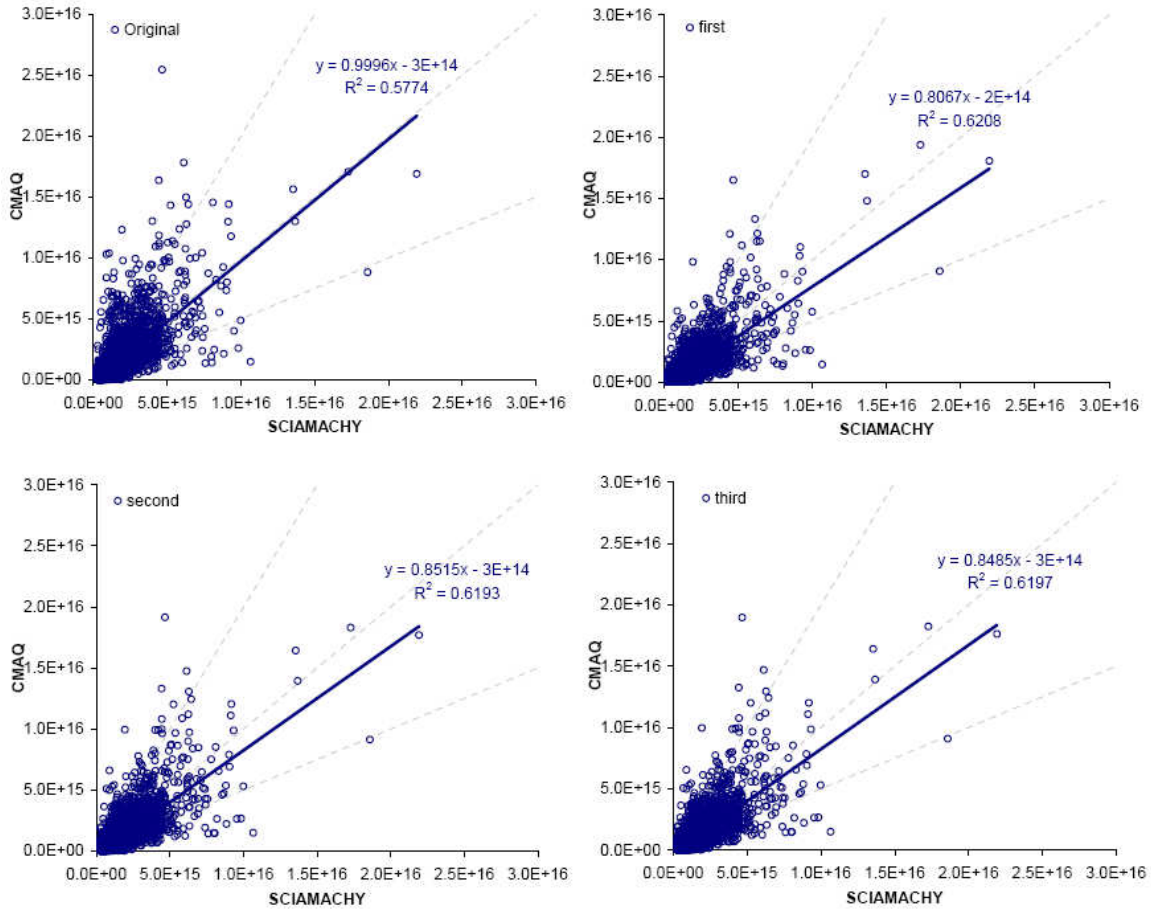

Figure 6.3. Comparison of simulated tropospheric NO_2 column averages with satellite retrievals from each iteration for columns greater than 2.5×10^{14} molecules/cm^2

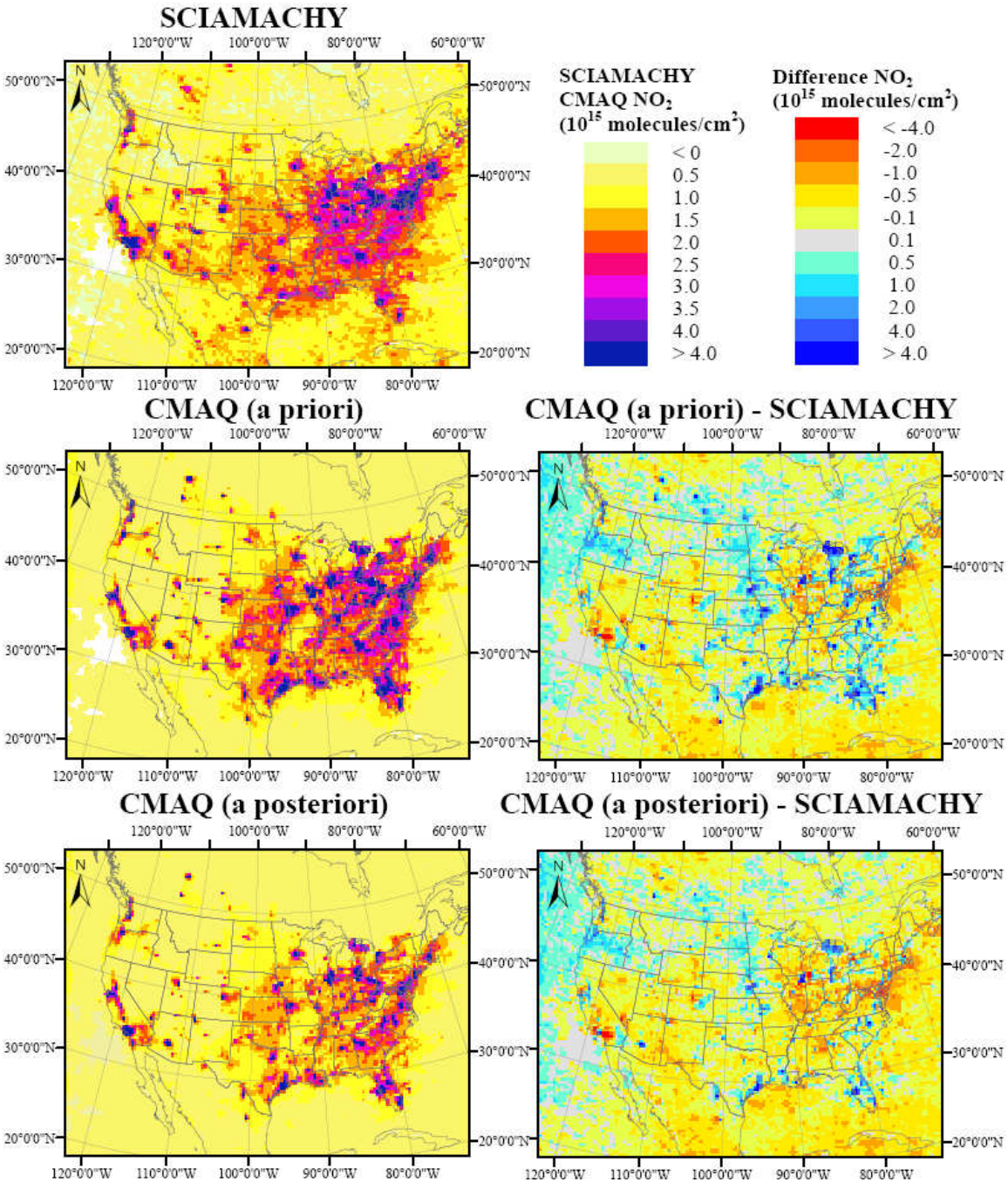

Figure 6.4. Spatial distribution of the tropospheric NO_2 column averages from SCIAMACHY (upper left), and model simulations with *a priori* (middle left) and *a posteriori* (lower left) emissions and the differences between the model simulations and SCIAMACHY (middle and lower right) for July-August 2004

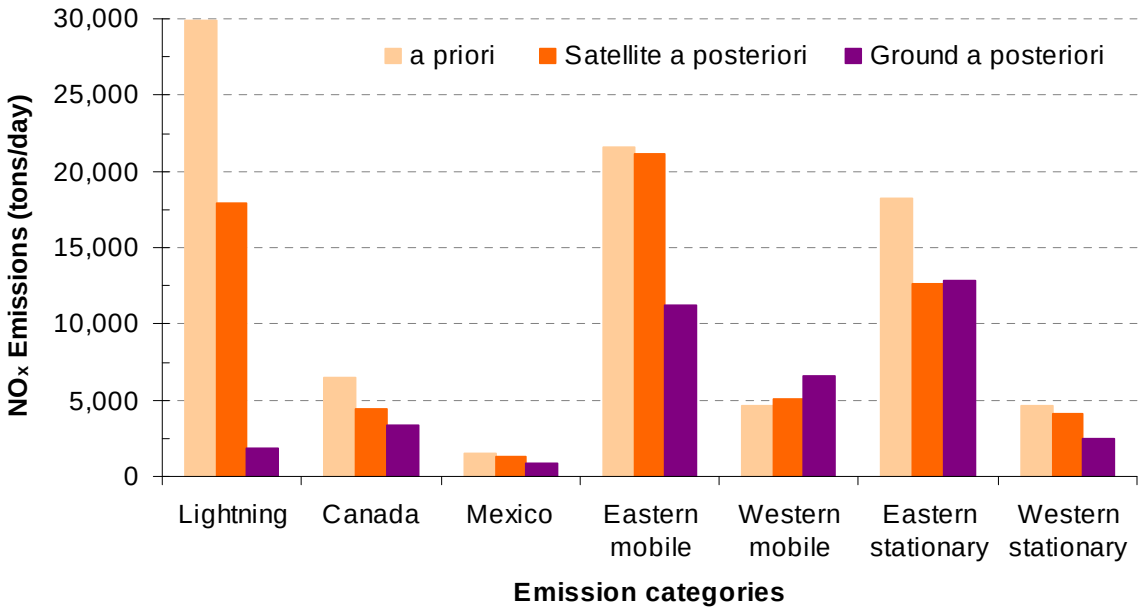

Figure 6.5. *A priori* and *a posteriori* daily averaged NO_x emissions for each category obtained from using satellite NO_2 retrievals and ground-based NO, NO_2, and O_3 observations for July-August 2004

Stationary source emissions are dominated by point sources and area sources in urban areas, but there are some facilities in remote areas as well. Final adjustment factors indicated decreases in these sources in both eastern and western US, though more significantly in the East (Table 6.2). The initial high positive biases over urban areas were the reason for this result.

Canada and Mexico emissions were suggested to be reduced by 32 and 16%, respectively. Mexico has a number of large cities with negative initial biases and rural areas that began with a positive bias, resulting in net reductions in total emissions. The spatial comparison of satellite retrievals with simulations (Figure 6.4) indicates more NO_2 in rural areas where the emission inventory could be underestimated.

Table 6.2. Final adjustment factors calculated using satellite and ground based observations and *a priori* and *a posteriori* average daily NO_x emissions from each source category

		Satellite		Ground-based	
Emission Categories	***a priori* (tons/day)**	**Adjustment Factors**	***a posteriori* (tons/day)**	**Adjustment Factors**	***a posteriori* (tons/day)**
Lightning	29,927	0.60	17,893	0.06	1,792
Canada	6,435	0.68	4,391	0.52	3,329
Mexico	1,528	0.84	1,276	0.54	821
Eastern mobile	21,628	0.98	21,187	0.52	11,189
Western mobile	4,663	1.08	5,020	1.42	6,619
Eastern stationary	18,247	0.69	12,656	0.70	12,803
Western stationary	4,593	0.88	4,047	0.54	2,499

6.3.2. Adjustment factors obtained using ground-based NO, NO_2 and O_3 observations

Observations from ground stations between 10:00 in the morning and 18:00 in the afternoon were selected for each day and averaged for the entire episode, resulting in one measurement to one simulation for each station. Because of the possible contamination of NO_2 measurements from other oxidized species of nitrogen, the model concentrations of NO_2, HNO_3 and PAN were summed up to match NO_2 observations. NO and O_3 concentrations are compared without adjustment. Initial comparison showed a negative bias for NO, positive biases for NO_2 and O_3 with an overall 14% mean normalized bias (MNB) and 49% mean normalized error (MNE) (Table 6.3, Figure 6.6). After four iterations, the solution converged and adjustment factors which are resulting in reduced overall MNB (-6%) and MNE (39%) are obtained. The correlation coefficients were improved for all species (Table 6.3). NO was the only species that has a higher MNB than the original simulation, but this result was not surprising considering the short lifetime of NO in daytime with photolysis and poor capture of the freshly emitted NO measured in the ground stations in the model grid cell scale. Previous comparisons also indicated significant negative bias and very low spatial correlations for NO (Chapter 5).

Table 6.3. Statistics* for the iterations performed for inverse modeling with ground observations for July-August 2004

Iteration	Species	N	Observation		Simulation		R^2	Slope	Intercept (ppbV)	MBE (ppbV)	RMSE (ppbV)	MNB (%)	MNE (%)
			Aver	StDev	Aver	StDev							
Original	NO_2	293	6.04	4.44	4.51	4.59	0.17	0.42	1.97	-1.59	5.14	21.30	88.70
	NO	215	2.03	2.43	0.72	2.83	0.03	0.20	0.32	-1.32	3.66	-31.14	94.83
	O_3	848	44.67	8.56	53.29	6.51	0.29	0.41	35.02	8.62	11.40	22.23	23.73
	All	1356								**4.84**	**9.44**	**13.57**	**49.05**
1	NO_2				3.43	3.84	0.23	0.41	0.93	-2.69	4.98	-13.09	75.10
	NO				0.43	1.26	0.09	0.16	0.11	-1.61	2.87	-54.08	90.83
	O_3				47.45	6.61	0.30	0.42	28.52	2.78	7.91	8.83	13.64
	All									0.90	6.77	-5.87	39.14
2	NO_2				3.45	4.02	0.23	0.44	0.81	-2.66	5.00	-14.10	74.98
	NO				0.46	1.34	0.11	0.18	0.09	-1.59	2.83	-52.67	91.36
	O_3				46.67	6.75	0.30	0.43	27.41	2.00	7.72	7.02	13.17
	All									0.42	6.63	-7.00	38.90
3	NO_2				3.51	4.10	0.24	0.45	0.80	-2.61	5.00	-12.97	74.93
	NO				0.47	1.36	0.12	0.20	0.07	-1.58	2.82	-52.17	91.30
	O_3				46.85	6.71	0.30	0.43	27.62	2.18	7.74	7.43	13.21
	All									0.55	6.64	-6.42	38.91
4	NO_2				3.54	4.13	0.24	0.45	0.81	-2.58	5.00	-12.14	75.05
	NO				0.46	1.34	0.13	0.20	0.06	-1.58	2.81	-52.58	91.08
	O_3				47.13	6.75	0.31	0.44	27.62	2.46	7.80	8.05	13.29
	All									**0.73**	**6.68**	**-5.92**	**38.95**

*MBE, RMSE, MNB, MNE were calculated for pairs where observations lower than 0.001 ppmV is assigned as 0.001 ppmV as the lower detection limit

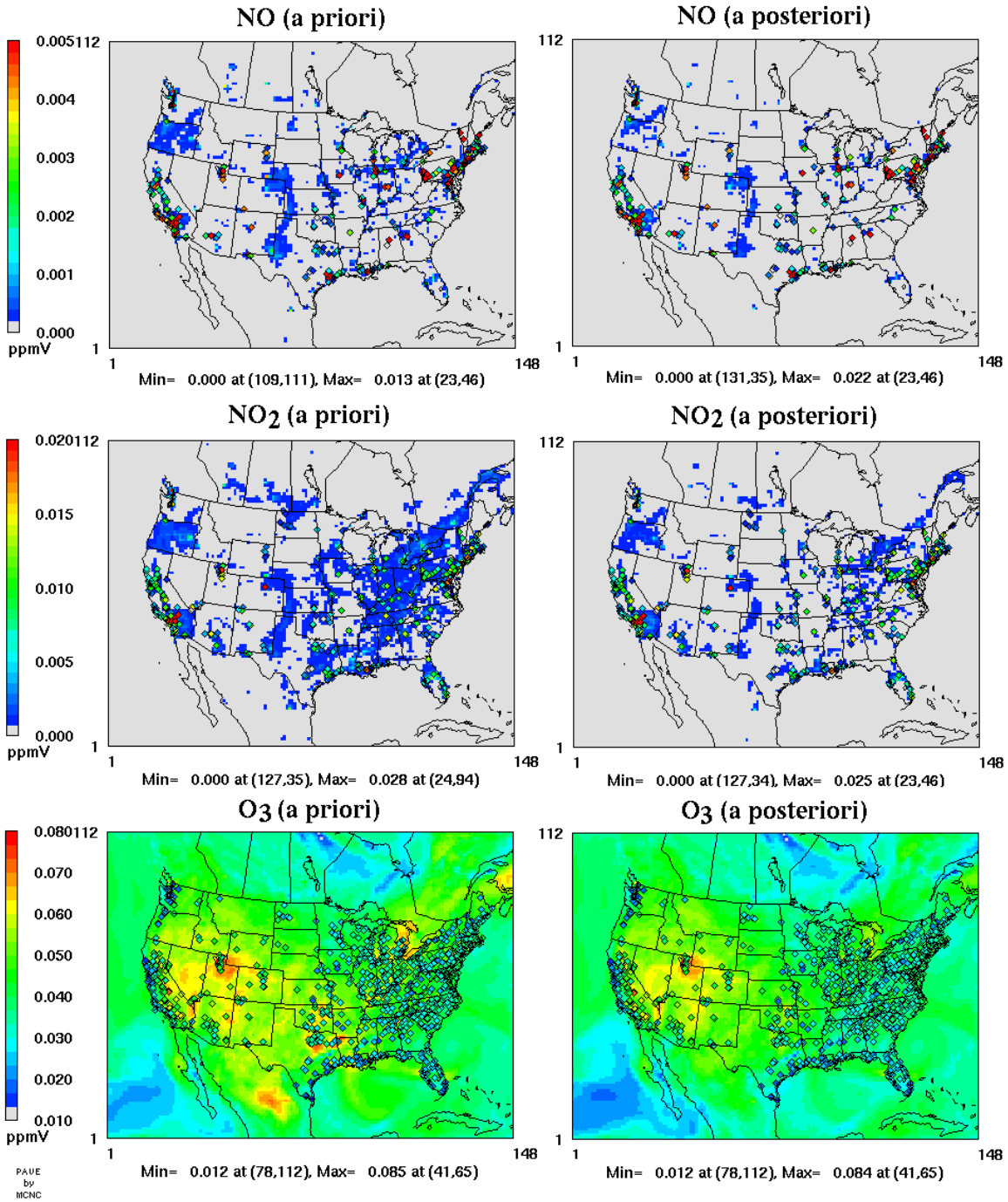

Figure 6.6. Spatial distribution of monthly averaged O_3 (upper), NO (middle), and NO_2 (lower) from model simulations with *a priori* (left) and *a posteriori* (right) emissions along with available ground-based observation stations (diamonds) overlaid for July 2004

The final adjustment factors obtained from assimilation of ground-based observations suggested reductions for all NO_x emission categories except western mobile emissions similar to that of satellite retrievals. Results suggest a larger increase (42%) in western mobile sources (Figure 6.3) than the satellite data assimilation. Ground-based observations indicated over 90% reductions for lightning NO_x emissions, but that is probably not realistic, and the sensitivity of NO_2 at the ground-based monitors is not very sensitive to lightning NO_x (Chapter 2).

Stationary source emissions are dominated by point sources and urban area sources and usually correlated with population, but also includes sparse emissions in remote areas. Final adjustment factors indicated reductions to be taken of these sources in both eastern and western US, though more significantly in the West (Table 6.1). Considering the locations of most of the stations were in urban areas, area sources probably should be reduced.

Canada and Mexico emissions were suggested to be reduced by 48 and 46%, respectively. Considering all the ground-based monitoring locations were in US, this result depends on the stations that are close to the border of these countries. After the results, it is clear that lightning, Canada and Mexico NO_x emissions could be removed from the emission categories used in the inverse modeling because their effect on US ground stations are minor.

6.3.3. Evaluation of the results with independent aircraft measurements

The model simulations obtained using the *a posteriori* emissions (according to adjustment factors) (Figure 6.5) were compared with available aircraft observations from ICARTT. These aircraft observations provide an independent evaluation of the new

emissions, because they were not used as an input in data assimilation. When simulated NO_2, O_3 and PAN with *a posteriori* emissions were compared with ICARTT measurements, all showed improvements compared to the simulations with the *a priori* emission profile. NO, on the other hand had reduced errors but not biases (Table 6.4). This finding strengthens the confidence in the adjustments suggested.

6.3.4. Comparison of the adjustment factors

When compared with each other, both datasets suggested increases in WM NO_x emissions and reductions in all other categories. The adjustments are larger when the ground-based observations used. The adjustments using both datasets for ES NO_x are very similar in magnitude, indicating a 30% reduction.

A posteriori emissions coming from anthropogenic sources (excluding lightning emissions) are 85% (48,578 tons/day) of the *a priori* emissions using the satellite retrievals and 65% (37,260 tons/day) of the *a priori* emissions using the ground-based observations. These ratios slightly increase for the US anthropogenic emissions to 87% and 67% using satellite and ground-based observations, respectively.

A priori and *a posteriori* emissions using satellite and ground-based observations were also compared with California Air Resources Board (ARB) emission inventory [*CARB*, 2009] for the summer of 2004. California (CA) has stricter air quality standards than nationwide air quality standards and uses a different model to estimate mobile emissions which are the major contributor to the NO_x emissions in CA. This comparison revealed that *a priori* mobile emissions are significantly lower than the ARB inventory and stationary emissions are higher than the ARB inventory. The adjustments on these sources from both datasets showed improved agreement with the ARB inventory. Out of

Table 6.4. Statistics for the evaluation of NO_2, NO, O_3, NO_y (NO + NO_2 + HNO_3 + PANs) and PAN simulations with *a priori* and *a posteriori* emissions derived using satellite and ground-based observations with available aircraft observations

		a priori				**Satellite *a posteriori***				**Ground *a posteriori***			
Species	**N**	**MBE (unit)**	**RMSE (unit)**	**MNB (%)**	**MNE (%)**	**MBE (unit)**	**RMSE (unit)**	**MNB (%)**	**MNE (%)**	**MBE (unit)**	**RMSE (unit)**	**MNB (%)**	**MNE (%)**
NO (ppbV)	2505	-0.08	0.60	6.40	99.30	-0.08	0.60	-8.50	91.83	-0.10	0.62	-36.78	81.48
NO_2 (ppbV)	2142	-0.10	1.27	68.84	125.63	-0.19	1.26	44.13	110.55	-0.36	1.31	-6.17	84.33
NO_y (ppbV)	1791	-0.43	3.39	39.13	74.50	-0.96	3.54	15.78	63.10	-1.94	4.09	-23.71	54.63
PAN (pptV)	2512	291.18	517.03	122.26	140.48	213.23	441.84	97.12	119.12	40.54	311.59	42.87	78.11
O_3 (ppbV)	2646	1.42	12.49	7.92	18.97	-1.66	12.51	2.58	17.78	-7.89	15.19	-8.00	19.52

the two datasets, *a posteriori* emissions using ground-based observations showed a better comparison (Table 6.5).

Evaluation of the *a posteriori* NO_x emissions using both datasets with aircraft measurements usually showed better agreements between simulations and observations than *a priori* NO_x emissions. Adjustment factors give lower errors and biases for NO_2, NO_y and PAN and O_3 showed improvements with satellite *a posteriori* emissions and NO showed increased negative biases even though the error is reduced especially with ground-based *a posteriori* emissions. For the specific flights of 25th, 27th of July and 14th August, all of which having high SO_2 concentrations indicating a plume, all species (NO, NO_2, NO_y, PAN and O_3) showed significant improvements in MNB and MNE. This finding strengthens the confidence in the stationary NO_x source adjustments, particularly for power plants.

Uncertainty in the adjustment factors estimated with FDDA method can be quantified with an approximation from estimating the variance-covariance matrix of the emission adjustment estimates [*Mendoza-Dominguez and Russell,* 2001a] which is valuable in determining how reliable are the emission adjustments. This uncertainty was shown to be small by Mendoza-Dominguez and Russell [2001a]. However, this uncertainty should not be viewed as the total uncertainty because other uncertainties such as uncertainty in meteorology, chemical mechanism parameters, numerical routines, etc. are not being taken into account. Another method can be used to estimate uncertainty is random sampling of ground observation stations and calculation of a set of adjustment factors from this sample to test the representativeness of the stations and estimate the

uncertainty coming from this sampling. Overall, a more extensive and detailed analysis is required to determine total uncertainty in adjustments quantitatively.

6.4. Summary

Inverse modeling (FDDA) was used to improve estimates of NO_x emission inventories for North America by combining the simulations and sensitivities from forward air quality modeling (CMAQ-DDM-3D) with satellite NO_2 retrievals and ground-based NO, NO_2 and O_3 observations. The method converged within 3-4 iterations and the adjustments did not change significantly after the first iteration. Simulations with *a posteriori* emissions obtained from ground-based observations showed improvements in MNB and MNE but simulations using *a posteriori* emissions obtained from satellite observations did not.

Table 6.5. Comparison of the daily *a priori* and *a posteriori* NO_x emissions for CA with California Air Resources Board (ARB) NO_x emission inventory for summer of 2004*

Emission Categories	***a priori* (tons/day)**	**Satellite *a posteriori* (tons/day)**	**Ground-based *a posteriori* (tons/day)**	**ARB (tons/day)**
On-road	995.50	1071.66	1412.99	1840.39
Non-road	734.28	790.46	1042.23	1280.48
Mobile	1729.78	1862.13	2455.22	3120.87
Stationary	743.49	655.04	404.40	476.07
Total	2826.04	2869.94	3212.39	3736.78

*The emissions for year 2004 are calculated by interpolation between the inventory from years 2000 and 2005.

Results from both sets of measurements indicated reductions for all emission categories except western mobile NO_x emissions, suggesting mobile emissions in western US are underestimated and other emissions are biased high. The previous investigation [*Kaynak et al.*, 2009] of weekend-to-weekday ratios of NO_x emissions and satellite NO_2 retrievals for selected cities indicated the ratio from satellite retrievals being significantly lower for the western cities of Seattle, Phoenix and Los Angeles. Adjustments using both datasets suggest a possible underestimation of the mobile emissions in west, ground observations indicating a greater increase being needed.

Lightning NO_x emissions were suggested to be reduced using both observational datasets. Ground observations suggested more than 90% decrease, highlighting the low sensitivity of the ground measurements to upper level lightning NO_x emissions. Uncertainty in estimated lightning emissions combined with significant positive biases in the model according to satellite retrievals over some regions due to lightning emissions suggest the production of NO_x from per flash of lightning should be either reduced, or NO_x production should be estimated with additional information like flash length or energy dissipated as well as the number of flashes.

The adjustments that are calculated are uncertain, so the magnitude changes in emissions should not be accepted as accurate. Both datasets suggest similarities in reductions or increases but differences in magnitudes. Availability of observations from multiple platforms and their consistency in adjustments actually strengthen the confidence in the findings. So the adjustment factors suggested here were not one value but a range between the adjustment factors derived from these two observation platforms. In addition, independent evaluation of the model with aircraft observations of NO_2, NO_y,

PAN and O_3 showed better overall performance with reduced bias and errors using the adjusted emission estimates. Comparison with California ARB NO_x emission inventory for the summer of 2004 showed the adjustments from both datasets showed improvements. *A posteriori* emissions using ground-based observations showed a better comparison with ARB NO_x emission inventory.

A posteriori emissions coming from anthropogenic sources (excluding lightning emissions) were 85% for satellite retrievals of the *a priori* emissions and 65% for ground-based emissions.

This analysis could benefit further emission category separation such as point and area sources in stationary, on-road and non-road sources in mobile and lastly urban and rural emissions for Mexico. Combining point sources (low uncertainty) with area sources with higher uncertainty and on-road sources (low uncertainty) with non-road sources with higher uncertainty reduced the power of using uncertainties to limit the adjustments. Additional information on emission uncertainty can be incorporated if the sources are further separated as suggested. In addition, observations available from Canada and Mexico monitoring networks could also be added to the US ground-based observations which are currently used.

CHAPTER 7

DETERMINING THE SOURCE STRENGTH OF AN UNKNOWN NO_x SOURCE FROM NO_2 SATELLITE RETRIEVALS AND RELATED UNCERTAINTIES: A CASE STUDY FOR POINT SOURCES

7.1. Introduction

Nitrogen oxides (NO_x: $NO+NO_2$) are important in tropospheric chemistry in ozone (O_3), nitric acid and aerosol nitrate formation, and ensuing deposition of the reactive nitrogen. NO_x sources are mainly anthropogenic (e.g. mobile sources, electricity generation), but they can also come from natural sources (e.g., biomass burning and lightning). Developing accurate NO_x emission estimates is an important step towards understanding the role of NO_x in leading to undesirable environmental effects and developing effective environmental strategies. Further, accurate inventories of NO_x emissions are essential to accurately simulate atmospheric pollutant dynamics using air quality models. NO_x emissions in United States (US) from point sources like power plants, even though they are decreasing, are still a significant part of the total NO_x emissions (34%) [*EPA*, 2009]. Emissions from these elevated point sources are relatively well known compared to area and mobile NO_x emissions. While the chemistry and transport of pollutants from area sources are well described in 3-D Eulerian gridded models, the dynamics of a power plant plume is significantly more concentrated which makes the simulation of transport and fate of NO_x emissions from elevated point sources

more challenging. The main problem is mixing of the stack emissions in the entire volume of the grid cell resulting in lower concentrations in the grid and incorrect chemical reaction rates due to the misrepresentation of the chemical concentrations [*Vijayaraghavan et al.*, 2009].

NO_2 column densities are available from various satellite-borne instruments: Global Ozone Monitoring Experiment (GOME), Scanning Imaging Absorption Spectrometer for Atmospheric Chartography (SCIAMACHY), and Ozone Monitoring Instrument (OMI). NO_2 satellite columns were used to constrain NO_x emissions by scaling the *a priori* emissions with the ratio of observed and simulated tropospheric NO_2 column for China with OMI [*Zhao and Wang*, 2009] and global scale with GOME [*Martin et al.*, 2003] and SCIAMACHY [*Martin et al.*, 2006]. Similar to gridded models, satellite retrievals of NO_2 give average amounts for the scan area. So, similar issues of plume representation in gridded modeling might be a problem in satellite retrieval scans where the scan sizes are similar in size as the grids of air quality models.

It is shown that satellites can capture the hotspots of NO_2 which include large-scale power plants with significant NO_x emissions [*Ghude et al.*, 2008]. The reductions in power plant NO_x emissions in eastern US can also be seen from space. [*Kim et al.*, 2006]. The NO_2 columns simulated using WRF-Chem were compared with SCIAMACHY and OMI NO_2 retrievals for selected western US power plants and found high correlations between simulated and satellite NO_2 columns [*Kim et al.*, 2009], we investigated power plants for the entire US and found fair correlations between SCIAMACHY NO_2 retrievals and CMAQ simulations (Chapter 4). These studies evaluated the NO_x emissions with satellite NO_2 retrievals with the help of an air quality model and update an

already known NO_x emission source. However, the discrepancies between the simulations and satellite retrievals observed could also come from the misrepresentation of the power plant plume in addition to model inputs (emissions, meteorology) or biases in satellite retrievals. In order to evaluate the capability of the satellite retrievals to determine point source emissions, the model use should be minimized. However, determining the strength/magnitude of a specific point source using satellite retrievals without model simulations has not been performed.

Previously, we focused on improving the total domain-wide NO_x emission inventory by using satellite retrievals with an iterative inverse method (Chapter 5). Apparent spatial biases in the satellite retrievals limited the improvements achieved in that study. Further reductions in bias and error could not be achieved. In addition, in another previous study (Chapter 3) our analysis comparing NO_x emission estimates with NO_2 retrievals indicated lower correlations in rural-point regions as compared to urban and rural regions. Here, we investigate the potential of using satellite retrievals to determine quantitatively an unknown point NO_x source emission rate and estimate the uncertainty related to that emission estimation.

The objectives of the research reported in this chapter are to (a) estimate the NO_x emissions from a significant point source using satellite NO_2 retrievals; (b) assess the uncertainty related to this estimation; and (c) investigate the potential use of satellite retrievals for determination of an unknown NO_x point source.

7.2. Methods

7.2.1. Satellite NO_2 retrievals

Atmospheric NO_2 columns retrieved by The Scanning Imaging Absorption Spectrometer for Atmospheric Chartography (SCIAMACHY) instrument are used in this study. SCIAMACHY scans over the US around 10:30 am with a global coverage over 6 days and has a spatial resolution of approximately 30 km×60 km in the nadir view. Additional information on NO_2 retrievals, uncertainty estimates and initial evaluations of the model simulations with satellite retrievals can be found in the previous chapters (Chapters 4-5).

7.2.2. Selected point NO_x sources

The satellite scans within the two month summer period (July-August 2004) were investigated in detail previously. Power plants with significant NO_x emissions so that their NO_x signal are larger than the uncertainty of the satellite retrievals in magnitude are the focus of this study to assess how well satellite measurements can be used to estimate emissions from large point sources. Here, we selected scans over power plants that are significantly farther away from other NO_x sources in order be confident that almost all of the emissions in the scan are coming from the point source. Also, one likelihood of upper level emissions from lightning emissions are minimized by choosing locations with lower occurrence of lightning causing storm clouds. This criterion resulted in selection of power plants from the western US. Another criterion is the location of the power plant in the scan, selecting cases where the source is not near the edge of the scan. This minimized the immediate transport of the emissions from the area of the scan such that

the resident time of NO_x emissions in the scan is sufficient. Scans over six power plants selected that satisfy the criteria are Four Corners, Colstrip, Jim Bridger, Big Stone, Huntington and Laramie River (Figure 7.1) and the retrievals from these scans over these power plants indicated significant amount of NO_2 (on the order of 10^{15} molecules/cm^2) (Table 7.1).

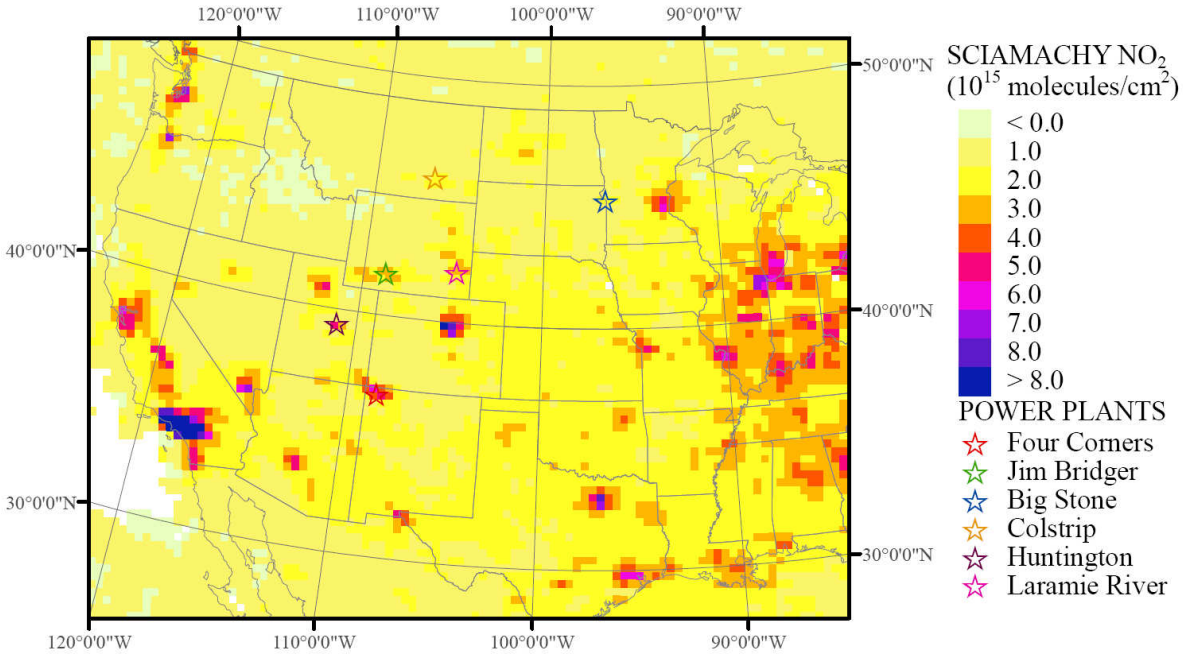

Figure 7.1. Power plant locations

7.2.3. Method Description

For determination of the NO_x emitted from the selected power plants, a mass balance for the scan is performed. A simple box model approximation for a mass balance for the concentration c_i of the species i is given as follows [*Seinfeld and Pandis*, 1997]:

$$\frac{dc_i}{dt} = \frac{q_i}{H} + R_i - S_i + \frac{u}{\Delta x}(c_i^0 - c_i) \qquad \text{(Equation 7.1)}$$

where H is the height of the box, q_i and S_i are the emission and removal rates of i per unit area (g/cm^3/s), R_i is the chemical production/loss rate (g/cm^3/s), u is the wind speed

(cm/s) and c_i^0 is the background concentration. Over an area of the size of a typical scan, the removal rate due to deposition compared to advection and chemical loss rate is minor so S_i is assumed as zero. The background concentration that is coming in the scan from the boundary is also neglected because it is significantly lower than the concentrations in the scan resulting from the very high emissions, so they are taken as zero though this will lead to a small bias. The advection term can be separated into u and v as components in x- and y-direction and the vertical advection in z-direction is assumed minor for practical purposes. If one assumes that the emission and chemical destruction rates are much larger than the rate of change of NO_2 in a box, then a pseudo-steady state approximation can be applied leaving the previous equation as:

$$0 = \frac{q_i}{H} + R_i - (\frac{u}{\Delta x} + \frac{v}{\Delta y})c_i \qquad \text{(Equation 7.2)}$$

Table 7.1. The NO_2 retrievals and uncertainty of the scans including selected power plants and physical dimensions of the scans (Each power plant have 1-3 scans available)

	CMAQ	**SCIAMACHY**		**Scan**			
	NO_2 col. (molec/cm^2)	**NO_2 col. (molec/cm^2)**	**NO_2 unc. (molec/cm^2)**	**Area (km^2)**	**X (km)**	**Y (km)**	**Angle (º)**
Four Corners	7.27E+15	2.65E+15	1.46E+15	1932.21	69.05	27.98	22.99
Colstrip	1.94E+15	1.11E+15	9.51E+14	1445.32	56.51	25.58	14.90
	7.19E+15	1.07E+15	9.60E+14	1335.13	53.63	24.90	19.33
Jim Bridger	1.87E+15	1.98E+15	7.28E+14	1344.77	53.92	24.94	20.94
	1.91E+15	1.44E+15	9.81E+14	1734.31	64.12	27.05	22.81
	3.65E+15	1.05E+15	4.26E+15	1397.57	55.42	25.22	21.71
Big Stone	8.51E+14	1.45E+15	4.64E+14	1486.99	57.73	25.76	14.90
	2.08E+15	1.94E+15	6.94E+14	1357.06	54.21	25.03	13.87
	1.36E+15	1.92E+15	5.49E+14	1332.71	53.61	24.86	13.62
Huntington	2.26E+15	9.65E+14	2.16E+15	1315.19	60.26	21.82	21.69
Laramie River	1.95E+15	1.50E+15	6.93E+14	1399.74	55.46	25.24	19.46
	6.45E+15	9.25E+14	1.17E+15	1399.53	55.43	25.25	19.06
	3.30E+15	2.29E+15	1.25E+15	1342.25	53.90	24.90	18.60

Here, we solve this equation to find q_i by integrating level-by-level information derived by CMAQ. This equation can be applied to each layer of the atmosphere. The velocity fields simulated using the meteorological model MM5 for the scan time and location are extracted and the appropriate velocity vectors are calculated by shifting the coordinates to account for the angle of the scan. Further, Δx and Δy are the distances between the power plant and corresponding boundary of the scan from which the mass will be transported to according to wind direction is found. Additional information about temperature, pressure, layer height and air density are also extracted from meteorological simulations. The mass of NO_2 retrieved from satellite is allocated to each layer according to vertical profile of NO_2 obtained from CMAQ. Hydroxyl (OH) radical and nitric oxide (NO) vertical mixing ratios are also obtained from the model (Figure 7.2).

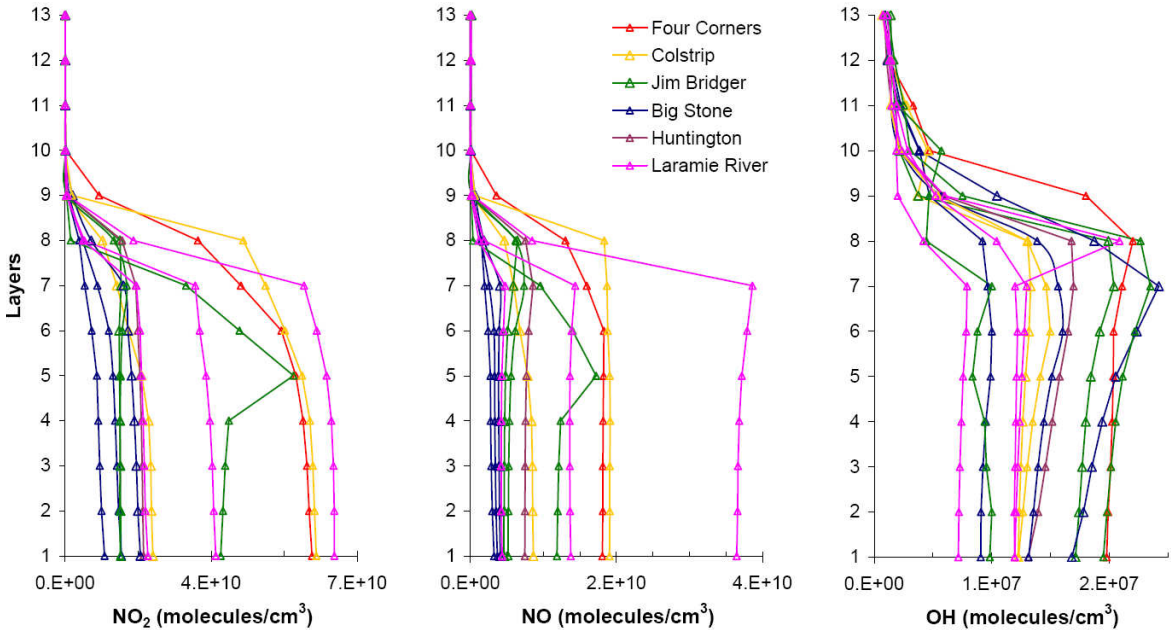

Figure 7.2. Vertical profiles of NO_2, NO and OH derived from CMAQ model

At 10:30 am, the time of the satellite scans, the loss of NO_x from the isolated power plant plumes is mainly by hydroxyl (OH) radical oxidation:

$$OH + NO_2 + M \xrightarrow{k} HNO_3 + M \qquad \text{(Equation 7.3)}$$

So in Equation 7.2 $R_i = -k[NO_2][OH][M]$.

NO quickly oxidizes to NO_2 in the troposphere. However, the ratio of NO/NO_2 is higher than the background atmosphere in the power plant plume, because of the plume chemistry. The NO to NO_2 ratio varies from 0.22-0.57 at the ground level to 0.29-0.56 for layer 9 (~2.8 km altitude) for the selected power plants. To account for the NO_x that is still NO, q_i calculated can be updated by the calculated NO_x/NO_2 ratio for every layer before summed for the column. Currently this is not performed, so the emissions estimated can be seen as the lower limit and would be higher than estimated here if this correction is performed.

The final equation used to estimate the NO_x emissions from a significant point source using satellite NO_2 retrievals with aforementioned information and assumptions is as follows:

$$q_i = \sum_{l=1}^{L} \Delta H_l \left[k(T_l, z_l)[NO_2]_l[OH]_l + \left(\frac{u_l}{\Delta x} + \frac{v_l}{\Delta y}\right)[NO_2]_l \right] \qquad \text{(Equation 7.4)}$$

where l is the model layer and $[C_i]_l$ is the concentration of species i (molecules/cm^3) for the layer k. The rate constant of Equation 7.2 depends on temperature (T) and altitude (z) and is given as follows [*DeMore et al.*, 1997]:

$$k(T,z) = \left\{ \frac{k_0(T)[M]}{1 + (k_0(T)[M]/k_\infty(T))} \right\} 0.6^{(1+[\log_{10}(k_0(T)[M]/k_\infty(T))]^2)^{-1}} \qquad \text{(Equation 7.5)}$$

$$k_0(T) = (2.5 \pm 0.1) \times 10^{-30} (T/300)^{-(4.4 \pm 0.3)} \, cm^6 / molecules^2 / s \qquad \text{(Equation 7.6a)}$$

$$k_\infty(T) = (1.6 \pm 0.2) \times 10^{-11} (T/300)^{-(1.7 \pm 0.2)} \, cm^3 / molecules / s \qquad \text{(Equation 7.6b)}$$

Along with the estimate of the NO_x emissions one should quantify the uncertainty of that emission estimate by propagating the uncertainties coming from each term in Equation 7.4. The wind speeds *u* and *v*, NO_2, OH concentrations, *k* and temperature, pressure are the terms with uncertainties on the right hand side. The uncertainties coming from temperature and pressure are significantly smaller than other terms and also do not have a direct effect in the formula but indirectly affect the concentrations of OH, NO_2 and the rate constant *k*. Given that they are considerably smaller than the others, the uncertainties coming from temperature and pressure are ignored. According to propagation of uncertainty through mathematical operations [*Taylor*, 1997], the uncertainty in the estimation of q_i is given as follows:

$$\delta q_i = \left[\left(\frac{\delta k(T_k, z_k)}{k(T_k, z_k)} + \frac{\delta [OH]_k}{[OH]_k} \right) + \frac{\delta u_k}{\Delta x} + \frac{\delta v_k}{\Delta y} \right] + \frac{\delta [NO_2]_k}{[NO_2]_k} \qquad \text{(Equation 7.7)}$$

The uncertainty in the rate constant *k* given by DeMore et al. [*DeMore et al.*, 1997; *IUPAC*, 2009] and resulted in ± 10% changes in the magnitude of *k*. The OH evaluations of CMAQ model are limited [*Zhang et al.*, 2006a; *Zhang et al.*, 2006b]. A combined uncertainty of 32% is assumed for *k(T,z)*[OH] terms together which is suggested by *Ren et al.*, [2006] for a zero-dimensional chemical model using a complete Regional Atmospheric Chemical Mechanism (RACM) because of the lack of uncertainty information of OH simulations from CMAQ. This uncertainty estimate is based on the combined uncertainties of the kinetic rate coefficients, the measured chemical concentrations, and the calculated photolysis frequencies, as estimated with a Monte

Carlo approach [*Ren et al.,* 2006]. The gross error ($\sum$ |Simulation-Observation|) for wind speeds for the 2-month episode is 1.32m/s and this error decreases as the altitude increases down to 0.5m/s at 840pa (layer 8) [*Hu et al.,* 2003]. The uncertainty for the wind velocity is taken as 1.32 m/s on the ground and interpolated with altitude to reach to 0.5m/s at layer 8. Above layer 8 the uncertainty is assumed as zero for practical purposes as the NO_2 concentration also becomes very small. The uncertainty coming from wind direction is not taken into consideration for this calculation for simplification. The uncertainty in NO_2 scans are given with the retrievals [*Martin et al.,* 2006] and generally dominate other terms. The overall uncertainties are given with the NO_x emission estimates calculated from satellite observations and Equation 7.4. (Table 7.2).

Table 7.2. NO_x emission rates estimated from box model approximation and given in gridded emission inventory (Each power plant have 1-3 scans available)

	NO_x (moles/s)		
	Inventory	**SCIAMACHY derived**	
Four Corners	26.51	24.00 ±	20.67
Colstrip	16.13	13.65 ±	14.46
	16.09	6.94 ±	8.79
Jim Bridger	16.19	15.45 ±	10.11
	22.28	16.80 ±	15.88
	18.02	9.22 ±	40.04
Big Stone	12.11	49.87 ±	19.96
	12.11	24.64 ±	16.50
	11.00	75.42 ±	28.24
Huntington	17.54	12.07 ±	29.56
Laramie River	14.49	19.85 ±	12.82
	13.34	4.75 ±	8.75
	14.32	24.99 ±	20.69

7.3. Results and Discussion

The NO_x emission rates estimated using Equation 7.4 are compared with the gridded NO_x emission rates (Table 7.2). The NO_x emission rate estimates are scattered in a wider range (4.75-75.42 moles/s) when compared with CEM derived emission rates (11.0-26.50 moles/s). The scans over the same power plants showed significant variation (e.g. Big Stone and Laramie River) and this variation in emissions is unlikely in reality.

NO_x emissions estimated from satellite retrievals showed comparable amounts to the inventory for selected time and location except for the scans over the Big Stone (Table 7.2, Figure 7.3). For all other power plants, the NO_x emissions from the inventory usually fall within the estimated range calculated from the satellite-based observations. Further investigation of the results for Big Stone found high wind speeds (10 m/s) for that area for two of the scans which can lead to rapid advection. However, it is not apparent how this would lead to the bias found. Estimates closest to the measured rates were from Four Corners, Jim Bridger and Huntington, though with significant uncertainties.

Uncertainties in those estimates are large (Table 7.2); they range between 0.38-4.33 times of the emission estimates. Three main sources of the uncertainties are advection, OH reaction and retrieval of the NO_2 column. Because these are individual scans, the uncertainties from NO_2 retrievals are large, sometimes even larger than the NO_2 retrievals (e.g. Huntington, Laramie River). Thus, most of the uncertainty is usually coming from satellite-based observations. The uncertainties for Big Stone where significant discrepancies were observed between estimations and inventory were usually driven by the advection term which combines the uncertainties coming from the satellite NO_2 retrievals and wind velocities.

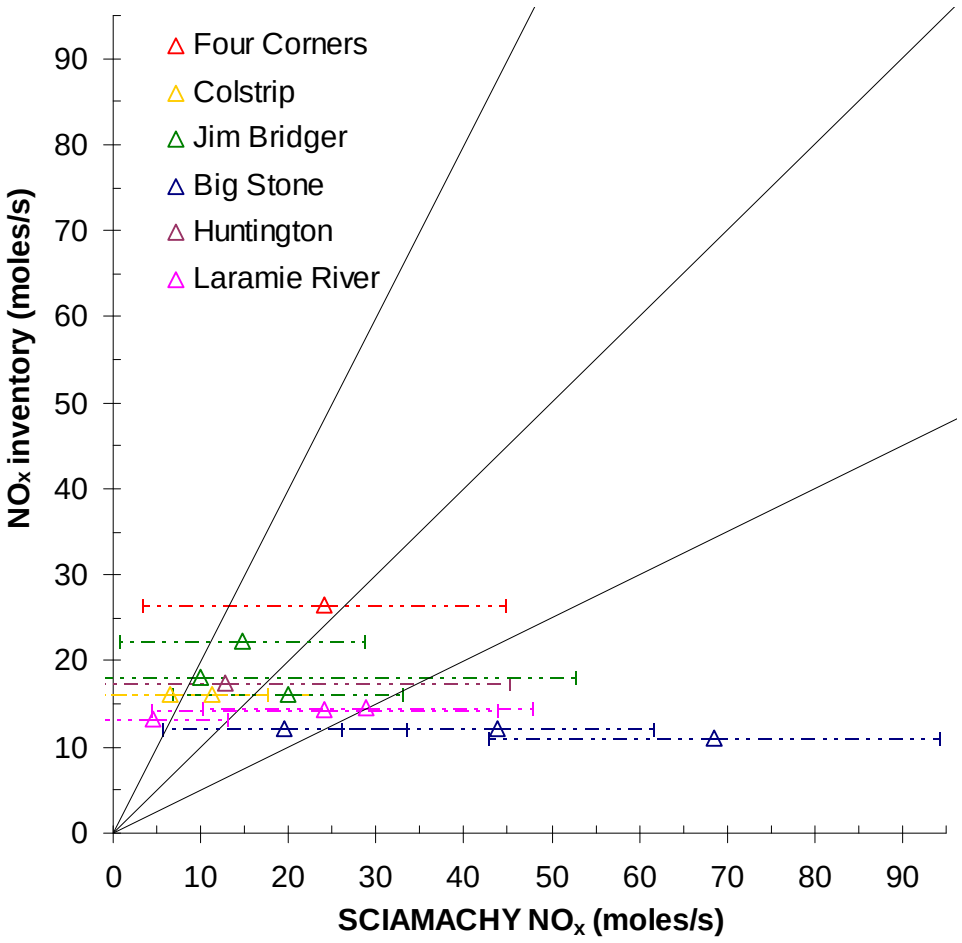

Figure 7.3. Comparison of NO_x emission rates estimated from box model approximation using satellite retrievals and given in gridded emission inventory (dashed lines indicate the uncertainties and black lines indicate 1:1, 1:1.5 and 1:0.5)

The lifetime of NO_x in the scans depends on the reaction with OH and the advection from the scan area. In the lower levels, these two terms are on the same order and compete with each other. In the upper layers where wind speeds are higher and OH concentrations are lower (Figure 7.2), the advection term dominates.

Calculations indicated very short NO_2 lifetimes, particularly in the lower levels down to about 2-h near the surface. Further investigation showed that OH concentrations simulated by the model are also higher than what has been suggested as typical for daytime summer levels (5-10×10^6 molecules/cm^3) [*Seinfeld and Pandis*, 1997]. In

addition, previous evaluation comparing the OH concentrations simulated here with aircraft measurements indicated the OH levels simulated by the model are positively biased (MNB 348%, MNE 366%) using data from six flights during ICARTT (Appendix A, Table A.3). Another studies also indicated OH overestimates from CMAQ [*Zhang et al.*, 2006a; *Zhang et al.*, 2006b]. OH concentration and the tropospheric oxidizing efficiency were shown to be strongly sensitive to the global lightning NO_x source magnitude [*Labrador et al.*, 2004]. Thus, some part of the discrepancy in our OH simulations can be explained by introduction of lightning NO_x emissions, considering the positive bias was lower when lightning NO_x emissions were not included in simulations (MNB 306%, MNE 330%). However the model still predicts OH high even without lightning NO_x emissions. Also, the lightning activity is usually minor in areas where the power plants were selected. Overall, this bias in OH would result in shorter lifetimes of NO_2 in the model and would lead to higher calculated emission rates.

Previous comparisons of simulated NO_2 columns with SCIAMACHY NO_2 columns over a set of power plants (N=118) which included the selected five here resulted in a mean normalized bias (MNB) of 11% and mean normalized error (MNE) of 29% (Chapter 4), with a fair correlation (R^2=0.54). The slight positive bias found is similar with another study where Kim et al. [2009] found a tendency for higher model results than the satellite for 2005 with another air quality model (WRF-Chem), but their correlation coefficient is significantly higher than our study (R^2=0.93). They focused on the western US, where the correlation in our study increases to (R^2=0.85) if only power plants in western region (N=17) are selected. This finding suggests the satellite capability

to capture point sources is significantly higher where the chance of another source existing is very low.

7.4. Summary

NO_x emissions from six elevated point sources were estimated with a simple approximation using SCIAMACHY NO_2 retrievals during the summer of 2004. The resulting emission estimates are compared with NO_x emissions from continuous emission monitoring (CEM). Out of these six sources, only the scans over Big Stone had estimated emissions significantly different than these from the inventory.

Overall, the satellite allowed calculation of NO_x emissions from a point source, but the high uncertainty limits the utility and ability to determine the exact amount emitted. Averaging the results from couple of scans would reduce the effect of meteorological conditions on the estimation and reduce the uncertainty. However, quantification of the NO_x emissions with low uncertainty is not possible due to the low frequency of the satellite scans.

This work also indicated the OH concentrations simulated by the model may be higher than the current estimates, for example those from aircraft measurements. This issue should be investigated further because this could result in shorter lifetimes of various trace species in the model, and indicate that some chemical processing may be missing or misinterpreted in the model.

CHAPTER 8

CONCLUSIONS AND RECOMMENDATIONS

8.1. Conclusions

This thesis examined how satellite observations could be used in conjunction with other observations and models by conducting an extensive comparison of observations from multiple platforms and model simulations followed by assimilation of the observations in the model by an iterative, inverse method in order to reduce model bias and uncertainties. The potential use of satellite NO_2 retrievals in estimation of large point sources was also investigated. In particular, this work made use of the satellite-based observations from SCIAMACHY, routine observations, observations from aircraft-based observations during ICARTT and the Community Multi-scale Air Quality Model (CMAQ).

A lightning NO_x emission inventory which was prepared for July-August 2004 was found to account for 30% of the total NO_x emissions. The simulations were performed with EPA's Models-3 system (MM5-SMOKE-CMAQ) over the continental US with and without lightning NO_x emissions. Including this upper level NO_x emission source led to sometimes modest, but infrequently significant increases in simulated surface ozone. Results from simulations with lightning NO_x suggest that while North American lightning production of NO_x can lead to significant local impacts on few occasions, they will have a relatively small impact on typical maximum levels and determination of Policy Relevant Background levels.

The NO_x emissions prepared for 2004 which were the input to the model simulations were compared with satellite NO_2 retrievals from SCIAMACHY in order to determine how well the satellite NO_2 retrievals represent NO_x emission location and magnitudes. Spatially-resolved weekly NO_2 satellite observations over 3 different region types: urban, rural and rural-point are compared with NO_x emissions for magnitudes and weekly profiles. Satellite retrievals indicated no weekly pattern for rural regions, a distinct decrease on the weekends for urban regions and a slight decrease on Sundays for rural-point regions. Overall comparisons showed that satellite derived NO_2 correlate well with estimated NO_x emissions for urban and rural but less for rural-point regions. When NO_2 satellite retrievals were compared with estimated mobile and stationary NO_x emissions for urban regions (7 cities), the satellite retrievals showed greater variation during weekdays (Monday-Friday) than NO_x emissions. Sunday to mean weekday ratios obtained from satellite NO_2 retrievals compared to NO_x emission inventories indicated that for urban regions either the contribution of mobile sources to total NO_x emissions for each city were underestimated or day-to-day variability in mobile sources were underestimated. This work suggested that current inventories lack the likely day-to-day variability actually present and satellites can provide information to improve the emission inventories.

With previous work highlighting the need for a model to relate satellite NO_2 retrievals to estimate NO_x emissions, NO_2 tropospheric columns were simulated with EPA's Models-3 system (MM5-SMOKE-CMAQ) over the continental US for a two-month period of the summer of 2004 (July-August). Two model simulation cases were performed, one with and one without lightning NO_x emissions. Lightning NO_x emissions

resulted in improvements specific to locations with high lightning intensity but resulted in minor overall performance improvements. Comparisons revealed high correlation with lower simulated NO_2 columns in the western US and lower correlation with similar NO_2 columns on average with the satellite retrievals in the eastern US. Additional comparisons according to land use - urban, rural and rural-point - which was also used in NO_x emission comparisons showed that NO_2 tropospheric columns derived from SCIAMACHY correlate well with simulated NO_2 concentrations for rural regions but the correlation is lower for urban and rural-point regions. State of California, particularly Los Angeles and surrounding area showed significantly lower simulated NO_2 than satellite observations. Higher biases and lower correlations in rural-point regions was surprising with their emissions being viewed as relatively well known, potential reasons for lower correlation were the transport of NO_2 out of the small scan area, insufficient conversion of NO to NO_2 in power plant plumes and potential issues with satellite retrievals in representing an upper level point source. High correlations for rural regions is encouraging for using satellite observations to estimate NO_x emissions that are hard to capture otherwise such as area emissions that are sparse, located in remote regions and poorly quantified, and prescribed fire or wildfire emissions.

Simulations of NO_2 and other species (NO, NO_x, NO_y, PAN and O_3) were compared with ground and aircraft-based observations in addition to satellite retrievals. Evaluations showed general agreement, but important differences as well. NO_2 showed low biases between simulated levels with both ground and satellite-based observations over the US. Aircraft-based observations, on the other hand, indicated a higher positive bias and error resulting from specific events which are hard to simulate with a grid model

than previous two measurements. The average vertical profiles obtained from aircraft observations for the various species were captured by the model very well. Satellite-based NO_2 observations had the highest correlation indicating the effect of similar spatial resolution between the model and satellite retrievals. The model underestimated NO when compared with the ground observations and aircraft observations, especially near the surface. NO_y from ground and aircraft indicated both positive biases in the model and errors were on the same order of magnitude. This overestimation was possibly resulting from the consistent overestimations of PANs. Simulated O_3 compared better with aircraft-based observations than ground-based observations, though both comparisons had a positive bias. Vertical profiles of O_3 also indicate a positive bias near the surface, though a negative bias at the upper levels. Inter-comparison of ground-based observations with satellite observations indicate a positive bias in simulated NO_2 columns, but a negative bias in surface mixing ratios with low correlations for both. Here, the representativeness of the ground observations for the scan area becomes important. This result supports previous finding that the model overestimates the total NO_2 column and underestimates the surface concentrations of NO_2 over urban areas. This suggests that either the ground-based observations have somewhat limited utility for model evaluation and assessment of emission estimates, or that there may be biases in the satellite retrievals that need to be identified and corrected if such measurements are going to be used for emissions and model assessments.

Four dimensional data assimilation (FDDA) was used to improve estimates of NO_x emission inventories for North America by combining the simulations and sensitivities from forward air quality modeling (CMAQ-DDM-3D) with satellite NO_2

retrievals and ground-based NO, NO_2 and O_3 observations. Simulations with *a posteriori* emissions obtained from ground-based observations showed improvements in MNB and MNE but simulations using *a posteriori* emissions obtained from satellite observations did not. Results from both measurements indicated reductions for all emission categories except western mobile NO_x emissions, suggesting that mobile emissions in western US are underestimated and other emissions are biased high. Adjustments using both datasets suggest a possible underestimation of the mobile emissions in west, ground observations indicating a greater increase being needed. Significant reductions found for lightning NO_x emissions indicating the production of NO_x from per flash of lightning should be either reduced, or NO_x production should be estimated with additional information like flash length or energy dissipated as well as the number of flashes. The adjustments suggested by both observations are quite uncertain, so the magnitude of changes in emissions should be used to suggest areas for further analysis. Both datasets suggests similar in reductions or increases but differ in magnitude, so the consistency strengthens the confidence in the findings. Emission adjustment factors found here provide a range of values. In addition, independent evaluation of the model with aircraft observations of NO_2, NO_y, PAN and O_3 showed better overall performance with reduced bias and errors using the adjusted emission estimates. *A posteriori* emissions compared better with California Air Resources Board (CARB) NO_x emission inventory for the summer of 2004 with ground-based observations find a better comparison. *A posteriori* anthropogenic NO_x emissions were 85% for satellite retrievals and 65% for ground-based emissions of the *a priori* emissions.

Lastly, in order to investigate the ability of satellite NO_2 retrievals to determine NO_x emissions from elevated point sources without using the model, six power plants were selected for detailed analysis. For each of these power plants, day and time specific emissions were found from CEM database. Next, the NO_x emissions were estimated with satellite NO_2 retrievals and a simple multilayer model approximation. The resulting emission estimations are compared with CEM-based NO_x emission inventory. Overall, the CEM-based NO_x emissions typically fell within range calculated the satellite-based estimate, but the high uncertainty of the scans made it harder to determine the amount emitted with significant accuracy. This approach was strongly affected by meteorological conditions and assumed hydroxyl (OH) radical mixing ratios, suggesting using multiple scans instead of one could reduce the effect of meteorology and reduce the uncertainty in the estimation. This work also indicated the OH concentrations simulated by the model being are higher than current estimates and aircraft measurements. This is a possible reason for shorter lifetime of NO_2 and could explain the model's low NO_2 simulations surrounding of the urban areas. OH also affects lifetimes of other trace species in the model.

This research contributes to a better understanding of the further use of satellite NO_2 retrievals in air quality modeling, and improvements in the NO_x emission inventories by correcting some of the inconsistencies that were found in the inventories. Therefore, it may provide groups that develop emissions estimates guidance on areas for improvement. In addition, this research indicates the weaknesses and the strengths of the satellite NO_2 retrievals and offers suggestions to improve the quality of the retrievals for further use in the tropospheric air pollution research.

8.2. Recommendations for Future Work

The satellite NO_2 retrievals were directly compared with the simulated vertically integrated amounts from CMAQ. However, the retrieved values depend on the *a priori* assumed shape of the vertical NO_2 profile which in this case comes from GEOS-Chem model. The air mass factor uncertainties due to profile uncertainty could explain some of the bias in our comparison. The main reasoning for not updating the vertical profile was that the upper troposphere simulation of CMAQ was not evaluated in detail. In addition, our lightning emissions had high uncertainty and current NO_x emission inventory used in this study was missing aircraft emissions. After improvements are performed; i.e. more evaluations for the upper level chemistry of the CMAQ model, investigation of PAN overestimations, the NO_2 retrievals could use vertical profiling from CMAQ model which has a higher spatial resolution than GEOS-Chem model.

Inverse modeling was performed for two datasets (ground-based and satellite) separately. The reasons for this selection were explained in detail in Chapter 6. A preliminary calculation was performed for a combined dataset for the first iteration. Next step could be using a combined dataset for the data assimilation, and have a sensitivity analysis on weighting factors and investigate relative uncertainties of these two datasets in order to decide the weighting functions between them.

Inverse analysis could also benefit from further emission category separation such as point and area sources in stationary, on-road and non-road sources in mobile and lastly urban and rural emissions for Mexico. Combining point sources (lower uncertainty) with area sources (higher uncertainty) and on-road sources (lower uncertainty) with non-road sources (higher uncertainty) reduced the power of using uncertainties to limit the

adjustments. But one should be careful with emission category separation because it may raise issues of colinearity and need to be supported by physical definition of the sources. In addition, observations available from Canada and Mexico monitoring networks could also be added to the US ground-based observations which are currently used for data assimilation.

Inverse modeling and comparison with CARB NO_x emission inventories both indicated significantly higher emissions from mobile sources than our emission inventory for California which could drive the western mobile NO_x category with its significant magnitude compared to other western US cities. A further set of simulations with CARB NO_x emission inventories could be helpful to improve model performances and find errors/biases in other NO_x sources in the west.

Cross comparisons performed between different observations, but because they represent different regions in the atmosphere (ground, upper levels and total columns) and have different weaknesses and strengths, and drawing conclusions from these evaluations were difficult to interpret. Conversion of one measurement to another such as getting vertical profiles from aircraft measurements and calculating the total NO_2 columns from that information might give additional information.

This work could benefit from additional comparisons with other satellite NO_2 retrievals like OMI or other retrieval products of SCIAMACHY, unfortunately OMI was not available for our episode which focused on summer of 2004 because of available aircraft measurements. Evaluation of the model with both SCIAMACHY and OMI NO_2 retrievals could be helpful for model evaluation for a more recent episode where data from both satellites are available.

APPENDIX A

SUPPLEMENTAL INFORMATION FOR CHAPTER 5:

DETAILED EVALUATION OF SPECIES MEASURED IN ICARTT INTEX-NA WITH REGIONAL SCALE AIR QUALITY MODEL SIMULATIONS

Table A.1. ICARTT INTEX-NA P-3 flight dates, times and definitions

Flight Definition	Date	Time (UTC)
Transit to NH	July 5, 2004	16:10-22:11
Canadian Fires	July 9, 2004	15:29-23:01
Boston at night: RHB Overflight	July 11, 2004	22:55-03:51
Balloon Intercept	July 15, 2004	13:10-21:13
NYC Part 1	July 20, 2004	14:11-22:13
NYC Part 2	July 21, 2004	14:02-20:29
NYC Part 3	July 22, 2004	13:58-21:34
Montour Power Plant et al	July 25, 2004	14:15-22:07
WCB Part 1: Thunderstorm	July 27, 2004	15:03-22:27
WCB Part 2: Fires	July 28, 2004	13:54-20:33
NYC at night: DC-8 Comparison	July 31, 2004	21:24-05:16
New England at dawn: Early arrival	August 3, 2004	01:53-08:23
Ohio Valley Power Plants	August 6, 2004	14:00-22:27
NYC, Boston at night: DC-8 Comparison RHB Overflight	August 7, 2004	20:08-04:36
Ohio Valley, NYC at night	August 9, 2004	22:57-07:29
NYC Plume night into day	August 11, 2004	03:00-10:51
Clouds	August 14, 2004	13:55-22:10
Transit to Florida via Atlanta	August 15, 2004	14:34-21:29

Table A.2. Species measured in ICARTT INTEX-NA flights (total of 44) and the corresponding species in CMAQ used for comparison

ICARTT Species measured	**Units**	**CMAQ Species summed**
AMS_Org	μg/m^3	AORGAJ + AORGAI + AORGPAJ + AORGPAI + AORGBJ + AORGBI
AMS_SO4	μg/m^3	ASO4J + ASO4I
AMS_NH4	μg/m^3	ANH4J + ANH4I
AMS_NO3	μg/m^3	ANO3J + ANO3I
CO_ppbv	ppbV	CO
oh_nd	molec/cm^3	HO
ho2ro2_nd	molec/cm^3	HO2 + RO2_R + R2O$_2$ + RO2_N
sulf_nd	molec/cm^3	SULF
H2CO_ppbv	ppbV	HCHO
HCOOH_ppbv	ppbV	HCOOH
hno3_ppbv	ppbV	HNO3
NH3_ppbv	ppbV	NH3
NO3_pptv	pptV	NO3
N2O5_pptv	pptV	N2O5
NO_ppbv	ppbV	NO
NO2_ppbv	ppbV	NO2
Sum_NOy_ppbv	ppbV	NO + NO2 + HNO3 + PAN + PAN2 + MA_PAN
PBN + PPN + APAN + MoPAN	pptV	PAN2
O3_ppbv	ppbV	O3
PAN	pptV	PAN
PBzN	pptV	PBZN
MPAN	pptV	MA_PAN
Ammonium	μg/m^3	ANH4J + ANH4I
Nitrate	μg/m^3	ANO3J + ANO3I
Sulfate	μg/m^3	ASO4J + ASO4I
WSOC_ugC_m_3	μg C/m^3	AORGAJ + AORGAI + AORGBJ + AORGBI
SO2_ppbv	ppbV	SO2
Methanol	pptV	MEOH
Acetaldehyde	pptV	CCHO
Acetone	pptV	ACET
Acetic_acid	pptV	CCO_OH
Isoprene	pptV	ISOPRENE
MVK_MACR	pptV	MVK + METHACRO
MEK	pptV	MEK
Monoterpenes	pptV	TRP1
a_pinene + b_pinene + d_limonene	pptV	TRP1

Table A.2. Continued

ICARTT Species measured	Units	CMAQ Species summed
ETHANE	pptV	ALK1
ETHENE	pptV	ETHENE
ISOPRENE	pptV	ISOPRENE
Methacrolein	pptV	METHACRO
METHYLVINYL_KETONE	pptV	MVK
ARO_PTPMS Benzene + Toluene + C8_aromatics + C9_aromatics	pptV	ARO1 + ARO2
ARO_WAS BENZENE + TOLUENE + Ethyl_benzene + m_p_xylene + o_xylene + iso_propyl_benzene + X2_ethyl_toluene + X3_ethyl_toluene + X4_ethyl_toluene + X1_3_5_trimethyl_benzene + X1_2_4_trimethyl_benzene + X1_2_3_trimethyl_benzene	pptV	ARO1 + ARO2
ALK ETHANE + PROPANE_MSD + I_BUTANE + N_BUTANE + I_PENTANE + N_PENTANE	pptV	ALK1 + ALK2 + ALK3 + ALK4 + ALK5

Table A.3. Statistics and correlation coefficients (R^2, slope and intercept) of CMAQ simulated pollutants versus aircraft observations

Species, Units	**UNIT**	**FLIGHT**	**MBE (unit)**	**RMSE (unit)**	**MNB (%)**	**MNE (%)**	**R^2**	**SLOPE**	**INT (unit)**	**AVE_{OBS} (unit)**	**AVE_{MOD} (unit)**	**N (#)**
Acetaldehyde	pptV	20040705	142.95	283.55	28.94	51.83	0.76	1.71	-120.55	370.55	513.50	111
		20040709	-74.54	160.66	-18.12	27.33	0.32	0.62	74.18	391.29	316.75	159
		20040711	-19.40	104.20	-4.83	19.75	0.43	1.04	-37.93	419.65	400.25	71
		20040715	28.94	148.84	9.80	26.20	0.57	0.82	116.19	485.18	514.12	75
		20040720	5.19	277.06	5.17	21.95	0.18	0.33	532.39	791.61	796.81	166
		20040721	-223.18	330.10	-30.05	39.54	0.10	0.27	264.31	668.53	445.35	122
		20040722	-11.68	227.86	-4.32	33.04	0.50	1.28	-179.43	592.33	580.65	147
		20040725	148.11	273.59	35.26	43.64	0.15	0.60	338.97	481.08	629.19	137
		20040727	404.48	482.68	95.29	96.70	0.32	1.20	310.13	463.45	867.93	129
		20040728	197.95	306.75	62.45	80.12	0.03	0.50	373.59	349.21	547.15	98
		20040731	104.83	277.22	30.35	60.96	0.09	0.57	281.03	410.74	515.57	128
		20040803	85.44	287.23	28.53	46.53	0.37	0.52	420.14	703.39	788.83	59
		20040806	-19.75	129.95	-5.01	29.95	0.18	0.83	35.68	329.38	309.63	139
		20040807	51.14	166.08	17.21	46.23	0.22	1.15	5.42	301.35	352.48	149
		20040809	494.46	577.35	98.14	98.14	0.52	1.93	24.54	503.37	997.83	158
		20040811	535.03	558.86	112.72	112.72	0.31	0.77	656.28	524.24	1059.27	125
		20040814	289.94	372.48	112.41	121.00	0.16	0.67	396.89	321.62	611.56	139
		20040815	132.80	262.96	50.78	67.94	0.52	1.32	43.41	282.86	415.66	113
Acetic_acid	pptV	20040705	-19.37	481.82	35.43	64.33	0.28	0.26	585.70	822.36	803.00	111
		20040709	197.00	497.05	124.39	144.55	0.17	-0.25	645.07	359.78	556.77	159
		20040711	-487.13	526.06	-55.60	55.90	0.01	-0.02	356.71	830.73	343.59	71
		20040715	-39.85	370.55	35.71	80.90	0.20	-0.29	627.46	517.34	477.49	75
		20040720	270.12	549.46	69.78	82.79	0.01	-0.06	1090.12	775.70	1045.82	166
		20040721	409.98	597.62	83.77	90.51	0.00	0.03	1228.94	841.27	1251.25	122
		20040722	98.98	707.45	54.85	79.34	0.02	0.04	1175.43	1123.16	1222.15	147
		20040725	-116.14	481.83	5.53	70.64	0.12	-0.47	867.73	668.25	552.11	137
		20040727	804.20	1034.15	173.87	176.61	0.01	0.10	1529.82	806.84	1611.04	129
		20040728	771.74	1287.06	277.51	296.65	0.04	-0.25	1461.74	551.42	1323.16	97
		20040731	-188.04	554.77	-6.77	70.01	0.12	-0.41	769.69	676.93	488.89	128

Table A.3. Continued

Species, Units	UNIT	FLIGHT	MBE (unit)	RMSE (unit)	MNB (%)	MNE (%)	R^2	SLOPE	INT (unit)	AVE_{OBS} (unit)	AVE_{MOD} (unit)	N (#)
Acetic_acid	pptV	20040803	-675.22	988.79	-27.68	50.46	0.00	-0.01	682.05	1347.65	672.43	59
		20040806	-366.51	396.89	-67.38	70.57	0.04	0.09	108.04	520.87	154.36	139
		20040807	-318.39	381.41	-60.12	63.92	0.06	0.24	72.85	517.26	198.87	149
		20040809	-392.78	575.48	-22.24	43.28	0.01	0.07	741.25	1214.63	821.85	158
		20040811	-229.98	475.55	-7.58	27.49	0.00	0.00	1190.89	1415.25	1185.27	125
		20040814	345.42	539.26	105.31	117.20	0.09	-0.55	1106.77	491.55	836.97	139
		20040815	19.60	468.29	86.17	111.92	0.13	0.13	469.33	517.71	537.31	113
Acetone	pptV	20040705	-1327.79	1420.26	-81.28	81.28	0.38	0.13	75.61	1619.32	291.53	111
		20040709	-1324.22	1386.36	-74.46	74.46	0.04	0.10	266.41	1761.95	437.74	159
		20040711	-1677.74	1683.76	-91.00	91.00	0.16	0.23	-260.66	1845.60	167.86	71
		20040715	-1302.90	1328.55	-69.31	69.31	0.73	0.62	-566.08	1931.60	628.70	75
		20040720	-1700.45	1761.65	-66.50	66.50	0.29	0.33	26.31	2561.28	860.83	166
		20040721	-1878.03	1967.13	-71.09	71.09	0.40	0.24	119.21	2642.76	764.73	122
		20040722	-2187.69	2273.51	-77.99	77.99	0.46	0.22	6.53	2806.88	619.19	147
		20040725	-1224.08	1255.37	-72.02	72.02	0.32	0.38	-165.04	1706.22	482.14	137
		20040727	-1401.26	1521.77	-61.68	61.68	0.24	0.13	523.65	2203.09	801.84	129
		20040728	-1076.56	1171.36	-67.44	67.44	0.01	-0.13	693.23	1571.37	494.81	98
		20040731	-949.50	968.93	-83.55	83.55	0.06	0.14	24.83	1137.45	187.95	128
		20040803	-1898.58	2026.78	-76.15	76.15	0.26	0.15	182.09	2454.25	555.66	59
		20040806	-1262.42	1274.71	-90.56	90.56	0.00	0.03	94.87	1392.68	130.26	139
		20040807	-1214.03	1226.33	-87.01	87.01	0.01	0.07	85.63	1393.78	179.75	149
		20040809	-1750.58	1781.47	-81.17	81.17	0.32	0.33	-301.50	2168.62	418.04	158
		20040811	-1887.07	1920.56	-75.28	75.28	0.23	0.18	164.16	2500.97	613.90	125
		20040814	-951.93	1021.93	-62.35	62.35	0.39	0.28	128.02	1498.18	546.25	139
		20040815	-996.78	1063.60	-77.63	77.63	0.65	0.31	-100.87	1297.04	300.26	113
ALK	pptV	20040715	-262.09	429.80	-19.21	28.82	0.15	0.20	587.85	1061.61	799.52	12
		20040720	-852.43	1474.48	-25.13	42.13	0.04	0.12	1370.79	2527.56	1675.14	64
		20040721	-3665.72	3858.07	-78.52	78.52	0.03	0.06	688.93	4609.72	944.00	54
		20040722	-5337.94	5553.74	-81.25	81.25	0.00	0.02	1060.21	6518.26	1180.32	53

Table A.3. Continued

Species, Units	UNIT	FLIGHT	MBE (unit)	RMSE (unit)	MNB (%)	MNE (%)	R^2	SLOPE	INT (unit)	AVE_{OBS} (unit)	AVE_{MOD} (unit)	N (#)
ALK	pptV	20040725	-5709.85	5956.11	-70.09	70.09	0.19	0.47	-1395.14	8162.79	2452.94	55
		20040727	-8004.26	8157.10	-82.85	82.85	0.07	0.08	889.63	9636.53	1632.28	62
		20040728	-10093.40	10306.50	-90.57	90.57	0.43	-0.16	2707.45	11074.14	980.79	57
		20040731	-10718.80	11053.30	-86.95	92.15	0.02	-0.04	1450.00	11742.61	1023.85	63
		20040803	-590.77	982.97	-17.53	34.86	0.53	0.60	408.54	2487.58	1896.81	27
		20040806	-1687.08	2025.82	-65.37	65.37	0.24	0.13	456.50	2449.96	762.88	57
		20040807	-2839.76	3104.59	-69.70	69.70	0.29	0.31	12.62	4155.96	1316.20	70
		20040809	-5128.35	5821.20	-69.98	70.20	0.01	0.03	1657.09	7021.01	1892.66	68
		20040811	-7747.13	8263.04	-76.11	76.11	0.00	0.00	2280.63	9983.75	2236.62	65
		20040814	-9982.70	10277.60	-85.98	85.98	0.34	0.19	-581.12	11667.93	1685.22	72
		20040815	-11851.10	12230.40	-92.39	92.39	0.18	0.13	-666.02	12877.98	1026.93	65
Ammonium	$\mu g/m^3$	20040709	-0.74	0.86	-62.76	62.76	0.08	0.21	0.18	1.15	0.41	58
		20040715	-0.54	0.63	-61.98	64.72	0.48	0.53	-0.11	0.92	0.38	71
		20040720	-1.16	1.43	-54.09	54.61	0.47	0.29	0.28	2.01	0.85	117
		20040721	-1.40	1.64	-59.86	60.66	0.48	0.24	0.25	2.18	0.78	81
		20040725	-0.11	0.42	3.92	53.67	0.14	0.32	0.33	0.65	0.54	94
		20040727	-0.49	0.83	-24.20	49.99	0.51	0.24	0.24	0.96	0.46	80
		20040728	-0.79	1.06	-81.21	82.49	0.08	-0.02	0.11	0.87	0.09	20
		20040731	-0.41	0.49	-50.43	54.59	0.20	0.33	0.12	0.79	0.38	85
		20040803	-0.89	1.15	-43.45	44.26	0.60	0.30	0.31	1.72	0.83	41
		20040806	-0.04	0.24	-1.88	43.49	0.11	0.45	0.23	0.50	0.46	86
		20040807	0.20	0.32	61.61	74.61	0.04	0.31	0.49	0.42	0.62	81
		20040809	-0.85	1.27	-32.80	46.16	0.33	0.21	0.56	1.79	0.95	112
		20040811	-1.63	1.79	-56.03	56.03	0.44	0.33	0.27	2.86	1.23	99
		20040814	-0.25	0.53	-19.14	47.48	0.25	0.29	0.26	0.72	0.46	96
		20040815	-0.38	0.65	-20.61	56.02	0.57	0.50	0.20	1.16	0.78	33
AMS_NH4	$\mu g/m^3$	20040705	-0.23	0.64	-1.33	96.82	0.00	0.07	0.37	0.64	0.41	113
		20040709	-0.18	0.39	-17.80	85.63	0.09	0.27	0.15	0.44	0.27	152
		20040711	-0.19	0.28	-44.36	53.75	0.05	0.14	0.13	0.37	0.18	54

Table A.3. Continued

Species, Units	UNIT	FLIGHT	MBE (unit)	RMSE (unit)	MNB (%)	MNE (%)	R^2	SLOPE	INT (unit)	AVE_{OBS} (unit)	AVE_{MOD} (unit)	N (#)
AMS_NH4	µg/m^3	20040715	-0.03	0.31	-2.61	68.01	0.25	0.90	0.02	0.42	0.39	79
		20040720	0.19	0.66	106.86	135.51	0.03	0.18	0.81	0.75	0.94	158
		20040721	0.02	0.51	57.38	94.64	0.06	0.21	0.65	0.79	0.81	118
		20040722	-0.23	0.60	4.51	72.49	0.11	0.23	0.40	0.82	0.59	145
		20040725	0.02	0.36	23.57	65.78	0.04	0.30	0.35	0.46	0.49	129
		20040727	-0.03	0.30	12.94	60.57	0.21	0.49	0.21	0.46	0.43	119
		20040728	-0.22	0.27	-63.37	66.31	0.00	-0.03	0.10	0.31	0.09	97
		20040731	-0.09	0.27	3.56	66.39	0.04	0.20	0.27	0.44	0.35	122
		20040803	0.17	0.41	53.27	79.55	0.15	0.53	0.45	0.61	0.78	62
		20040806	0.00	0.32	28.46	82.79	0.00	-0.07	0.41	0.38	0.38	137
		20040807	0.15	0.41	78.81	118.77	0.01	0.12	0.46	0.35	0.50	135
		20040809	0.17	0.47	51.95	75.70	0.29	0.57	0.48	0.71	0.88	165
		20040811	0.29	0.64	68.83	85.15	0.06	0.32	0.93	0.94	1.23	137
		20040814	-0.05	0.32	5.08	57.47	0.06	0.32	0.27	0.48	0.43	136
		20040815	0.02	0.37	12.37	76.28	0.28	1.09	-0.02	0.41	0.43	117
AMS_NO3	µg/m^3	20040705	-0.08	0.14	-42.90	129.91	0.01	-0.12	0.04	0.11	0.03	108
		20040709	-0.07	0.14	-66.55	105.78	0.02	0.20	0.02	0.10	0.04	160
		20040711	-0.12	0.14	-99.54	99.54	0.00	0.00	0.00	0.12	0.00	62
		20040715	-0.03	0.18	-18.96	151.27	0.06	0.78	-0.01	0.09	0.06	82
		20040720	-0.08	0.49	-46.39	138.33	0.00	-0.10	0.07	0.14	0.06	168
		20040721	-0.06	0.30	15.03	192.05	0.03	0.52	0.00	0.12	0.06	124
		20040722	-0.16	0.23	-97.59	97.59	0.01	0.02	0.00	0.16	0.00	138
		20040725	0.00	0.30	84.77	241.97	0.02	-0.58	0.17	0.11	0.11	143
		20040727	0.03	0.26	183.33	317.84	0.00	-0.23	0.14	0.09	0.12	132
		20040728	-0.04	0.22	9.09	183.18	0.00	-0.09	0.06	0.09	0.05	107
		20040731	-0.08	0.09	-98.80	99.04	0.00	0.00	0.00	0.09	0.00	126
		20040803	-0.11	0.14	-76.58	112.19	0.07	-0.25	0.04	0.12	0.01	62
		20040806	-0.02	0.34	-39.41	141.20	0.02	1.19	-0.04	0.09	0.06	137
		20040807	-0.07	0.09	-86.78	90.01	0.01	0.04	0.01	0.08	0.01	152

Table A.3. Continued

Species, Units	UNIT	FLIGHT	MBE (unit)	RMSE (unit)	MNB (%)	MNE (%)	R^2	SLOPE	INT (unit)	AVE_{OBS} (unit)	AVE_{MOD} (unit)	N (#)
AMS_NO3	µg/m^3	20040809	-0.12	0.15	-91.04	98.23	0.01	0.04	0.00	0.13	0.01	165
		20040811	-0.12	0.26	-79.38	106.78	0.01	0.24	-0.01	0.16	0.03	132
		20040814	-0.06	0.10	-69.00	106.31	0.01	0.14	0.01	0.08	0.02	136
		20040815	-0.04	0.12	-47.72	131.88	0.00	0.00	0.02	0.06	0.02	115
AMS_Org	µg/m^3	20040705	-0.90	1.08	-70.77	78.06	0.00	-0.01	0.23	1.12	0.22	110
		20040709	-0.93	1.32	-64.98	73.63	0.01	0.02	0.23	1.18	0.25	159
		20040711	-1.58	1.80	-76.67	79.09	0.00	0.00	0.31	1.90	0.31	65
		20040715	-0.58	0.71	-52.72	57.74	0.46	0.38	0.04	1.00	0.42	82
		20040720	-0.89	1.42	-35.22	62.67	0.00	0.04	0.76	1.72	0.83	175
		20040721	-1.21	1.89	-45.76	73.84	0.02	0.13	0.51	1.98	0.77	128
		20040722	-1.91	2.36	-65.94	72.07	0.27	0.14	0.30	2.58	0.67	146
		20040725	-0.39	0.72	-14.04	51.79	0.10	0.21	0.58	1.24	0.85	144
		20040727	-0.42	1.20	-3.26	92.92	0.00	0.10	0.56	1.09	0.68	133
		20040728	-0.71	1.40	-45.77	60.11	0.20	0.10	0.25	1.06	0.35	105
		20040731	-0.57	0.71	-51.28	68.01	0.00	-0.01	0.31	0.86	0.30	133
		20040803	-1.08	1.41	-55.83	64.46	0.03	0.14	0.46	1.78	0.71	64
		20040806	-0.45	0.73	-34.38	58.36	0.02	0.12	0.41	0.98	0.53	139
		20040807	-0.25	0.60	-15.70	58.00	0.12	0.38	0.31	0.91	0.66	156
		20040809	-1.26	1.55	-45.92	69.70	0.06	0.19	0.46	2.12	0.86	168
		20040811	-1.18	1.44	-42.04	49.80	0.02	0.10	1.05	2.47	1.29	137
		20040814	-0.50	0.64	-51.41	69.92	0.06	0.16	0.17	0.80	0.30	139
		20040815	-0.39	0.61	-35.23	62.27	0.31	0.33	0.12	0.76	0.38	118
AMS_SO4	µg/m^3	20040705	2.47	3.30	838.00	840.30	0.01	0.45	2.78	0.56	3.03	119
		20040709	1.80	3.25	446.66	456.62	0.16	0.75	2.08	1.09	2.89	160
		20040711	0.89	0.96	1208.93	1208.93	0.00	-0.11	1.08	0.17	1.06	63
		20040715	2.44	3.12	730.13	732.12	0.46	2.19	1.60	0.71	3.14	86
		20040720	7.61	8.95	702.89	702.89	0.40	1.51	6.35	2.46	10.07	180
		20040721	7.52	8.86	471.09	471.29	0.51	1.78	5.21	2.99	10.51	130
		20040722	3.10	4.40	357.73	361.66	0.15	0.50	4.27	2.32	5.42	148

Table A.3. Continued

Species, Units	UNIT	FLIGHT	MBE (unit)	RMSE (unit)	MNB (%)	MNE (%)	R^2	SLOPE	INT (unit)	AVE_{OBS} (unit)	AVE_{MOD} (unit)	N (#)
AMS_SO4	$\mu g/m^3$	20040725	1.84	2.81	711.52	715.00	0.08	0.64	2.10	0.72	2.56	144
		20040727	3.50	4.44	982.96	985.34	0.06	0.60	3.86	0.91	4.41	135
		20040728	1.21	1.74	1376.33	1378.22	0.00	0.49	1.29	0.15	1.36	106
		20040731	2.12	2.72	652.52	657.00	0.17	1.06	2.07	0.83	2.95	138
		20040803	2.71	3.74	333.37	338.38	0.27	0.85	3.02	2.12	4.82	64
		20040806	2.31	3.05	524.85	526.14	0.54	2.11	1.42	0.80	3.11	143
		20040807	1.60	1.85	1098.00	1098.00	0.06	1.25	1.54	0.25	1.85	156
		20040809	2.55	3.39	389.82	393.47	0.63	1.11	2.26	2.51	5.05	169
		20040811	9.54	10.99	333.58	334.74	0.01	0.32	12.12	3.77	13.31	137
		20040814	3.35	4.03	1226.00	1227.10	0.20	1.77	2.82	0.69	4.04	146
		20040815	2.44	4.30	1363.60	1370.59	0.46	3.05	1.36	0.52	2.96	120
ARO_PTPMS	pptV	20040705	-176.04	192.46	-83.55	83.55	0.22	0.21	-8.47	212.72	36.68	61
		20040709	-123.67	215.93	-58.81	60.52	0.00	0.02	55.56	183.17	59.49	45
		20040711	-110.75	163.84	-53.18	66.62	0.28	0.85	-77.32	230.12	119.37	49
		20040715	-44.55	148.96	-10.51	48.13	0.22	0.53	76.67	260.43	215.88	40
		20040720	-102.05	244.08	-21.62	71.99	0.07	0.16	115.43	257.99	155.94	96
		20040721	-176.41	197.55	-86.62	86.81	0.01	0.05	14.54	201.76	25.35	69
		20040722	-167.33	188.01	-77.24	79.01	0.47	0.65	-84.03	236.15	68.83	92
		20040725	268.81	483.93	149.39	164.08	0.55	2.21	-0.24	222.82	491.62	91
		20040727	-46.27	106.36	-7.78	60.45	0.02	0.15	75.64	142.91	96.64	74
		20040728	-138.62	181.88	-76.85	77.36	0.36	-0.11	33.22	155.43	16.81	30
		20040731	82.92	164.59	40.13	71.52	0.42	1.29	24.59	198.83	281.74	77
		20040803	-129.29	225.21	-29.23	48.27	0.47	0.51	59.59	389.02	259.73	41
		20040806	-23.63	122.51	-21.28	44.45	0.51	1.34	-77.78	159.51	135.89	89
		20040807	110.30	251.94	42.67	77.35	0.36	1.77	-52.82	212.28	322.58	102
		20040809	47.34	296.69	5.73	66.43	0.42	2.36	-244.72	215.35	262.69	131
		20040811	51.06	195.66	21.83	55.45	0.30	1.04	41.09	237.16	288.21	104
		20040814	20.45	133.54	25.99	89.53	0.21	0.63	69.56	132.17	152.62	80
		20040815	32.93	274.27	2.14	53.58	0.40	2.30	-291.64	249.86	282.80	24

Table A.3. Continued

Species, Units	UNIT	FLIGHT	MBE (unit)	RMSE (unit)	MNB (%)	MNE (%)	R^2	SLOPE	INT (unit)	AVE_{OBS} (unit)	AVE_{MOD} (unit)	N (#)
ARO_WAS	pptV	20040715	-13.58	18.76	-46.81	52.80	0.47	1.35	-24.20	30.60	17.02	7
		20040720	-58.37	257.02	21.87	97.12	0.03	0.08	101.59	173.00	114.63	63
		20040721	-218.39	244.81	-89.39	89.39	0.01	0.02	17.75	240.47	22.07	55
		20040722	-326.33	402.20	-83.00	85.27	0.01	0.06	46.84	395.42	69.10	44
		20040725	-150.95	468.89	-31.23	63.08	0.27	1.23	-273.67	533.34	382.39	56
		20040727	-527.74	601.06	-83.09	83.09	0.00	0.00	90.02	619.35	91.62	59
		20040728	-702.53	783.78	-95.32	95.32	0.04	-0.02	39.67	727.37	24.85	46
		20040731	-661.05	763.78	-68.11	84.39	0.00	0.01	162.55	833.69	172.64	63
		20040803	-23.17	186.22	13.57	63.92	0.54	0.60	88.66	282.24	259.08	26
		20040806	-22.67	69.79	-15.30	36.91	0.22	0.28	50.93	101.57	78.91	55
		20040807	10.07	232.05	-5.09	72.51	0.23	1.04	-1.70	263.29	273.37	70
		20040809	-192.86	310.18	-45.29	64.53	0.13	0.57	-12.60	419.91	227.05	72
		20040811	-307.97	381.23	-51.35	54.78	0.09	0.29	102.44	576.23	268.26	68
		20040814	-518.03	563.14	-77.02	77.02	0.05	0.14	57.01	670.13	152.11	68
		20040815	-579.53	650.40	-81.62	84.95	0.12	0.42	-154.28	733.94	154.41	48
CO_ppbv	ppbV	20040705	-32.93	38.85	-28.24	30.87	0.09	0.16	57.97	108.14	75.21	126
		20040709	-52.05	70.89	-36.82	37.47	0.00	0.02	77.68	131.86	79.82	179
		20040711	-99.09	104.85	-53.35	53.35	0.11	0.27	34.10	183.63	84.54	84
		20040715	-40.02	44.59	-29.34	30.03	0.70	0.91	-27.26	141.30	101.28	91
		20040720	-67.23	82.20	-34.52	36.43	0.07	0.22	77.99	186.34	119.11	194
		20040721	-89.80	98.65	-46.19	46.19	0.10	0.14	71.96	187.50	97.70	139
		20040722	-96.38	103.58	-49.81	49.93	0.36	0.37	23.02	189.60	93.21	173
		20040725	-38.27	49.43	-27.08	30.17	0.27	0.82	-13.49	141.10	102.83	156
		20040727	-27.81	43.22	-17.49	23.69	0.10	0.21	76.00	131.17	103.35	153
		20040728	-41.42	72.99	-24.23	27.16	0.24	-0.20	109.67	125.77	84.35	123
		20040731	3.65	19.72	3.56	13.25	0.37	1.07	-3.09	97.80	101.46	146
		20040803	-66.65	81.82	-34.27	39.28	0.30	0.31	51.04	169.60	102.95	72
		20040806	-44.03	46.96	-36.03	36.75	0.32	0.88	-29.15	122.99	78.96	152
		20040807	-48.08	52.52	-36.30	37.24	0.48	1.30	-88.82	135.43	87.35	169

Table A.3. Continued

Species, Units	UNIT	FLIGHT	MBE (unit)	RMSE (unit)	MNB (%)	MNE (%)	R^2	SLOPE	INT (unit)	AVE_{OBS} (unit)	AVE_{MOD} (unit)	N (#)
CO_ppbv	ppbV	20040809	-52.89	65.09	-33.99	37.16	0.31	0.87	-32.79	158.36	105.47	178
		20040811	-49.09	55.79	-29.09	30.61	0.25	0.64	11.86	168.47	119.38	147
		20040814	-20.22	31.91	-15.27	18.71	0.45	0.50	38.16	116.42	96.20	167
		20040815	-27.00	33.22	-25.06	27.21	0.57	0.64	9.94	103.92	76.92	129
ETHANE	pptV	20040715	-718.56	746.40	-86.45	86.45	0.36	0.07	53.96	827.67	109.11	12
		20040720	-1474.79	1576.13	-87.50	87.50	0.00	0.01	177.06	1664.48	189.69	64
		20040721	-1330.41	1406.31	-89.48	89.48	0.13	0.03	97.54	1477.03	146.62	55
		20040722	-1172.07	1217.86	-89.16	89.16	0.42	0.11	-4.51	1315.48	143.41	54
		20040725	-869.00	882.68	-82.36	82.36	0.44	0.29	-119.54	1059.27	190.27	57
		20040727	-832.74	849.71	-81.87	81.87	0.15	0.08	97.69	1013.77	181.03	62
		20040728	-839.59	897.45	-85.95	85.95	0.15	-0.08	198.32	960.84	121.26	59
		20040731	-461.81	494.29	-79.10	79.10	0.18	0.08	69.76	578.64	116.84	65
		20040803	-1213.93	1292.90	-85.33	85.33	0.40	0.09	66.24	1406.80	192.87	27
		20040806	-1548.93	1685.69	-94.38	94.38	0.48	0.03	33.68	1637.43	88.49	58
		20040807	-785.78	791.67	-87.89	87.89	0.22	0.28	-136.14	896.39	110.60	70
		20040809	-1593.25	2097.90	-88.28	88.28	0.12	0.02	131.88	1764.49	171.24	70
		20040811	-1627.45	1691.25	-89.17	89.17	0.32	0.06	81.50	1819.05	191.60	67
		20040814	-827.93	906.79	-81.96	81.96	0.33	0.09	77.15	992.67	164.74	73
		20040815	-768.55	862.64	-87.72	87.72	0.44	0.10	16.38	873.43	104.88	67
		20040715	-6.87	11.16	-37.54	64.71	0.65	0.85	-4.36	17.00	10.13	12
		20040720	-35.47	164.07	35.23	108.40	0.05	0.09	47.74	90.98	55.52	63
		20040721	-35.91	47.76	-82.04	82.04	0.16	0.13	1.88	43.35	7.44	54
		20040722	-29.49	51.52	-54.76	67.84	0.56	0.47	-0.12	55.37	25.88	54
		20040725	57.78	228.08	261.76	295.35	0.42	1.53	-11.15	130.21	187.99	55
		20040727	-13.17	65.63	87.70	133.67	0.13	0.20	31.81	56.40	43.23	59
		20040728	-40.84	106.64	80.72	167.15	0.08	-0.05	14.39	52.78	11.94	54
		20040731	8.46	76.96	20.09	70.13	0.53	0.86	22.52	99.20	107.66	63
		20040803	-26.06	95.69	10.59	72.59	0.63	0.76	12.41	159.45	133.39	27
		20040806	-2.91	27.75	35.96	74.23	0.59	0.74	12.56	60.09	57.18	57

Table A.3. Continued

Species, Units	UNIT	FLIGHT	MBE (unit)	RMSE (unit)	MNB (%)	MNE (%)	R^2	SLOPE	INT (unit)	AVE_{OBS} (unit)	AVE_{MOD} (unit)	N (#)
ETHENE	pptV	20040807	23.54	125.83	18.64	70.09	0.34	1.06	16.48	120.79	144.32	59
		20040809	21.67	138.69	45.00	93.07	0.22	1.04	17.55	105.81	127.48	69
		20040811	17.84	102.75	60.90	85.49	0.36	0.50	74.66	113.79	131.63	67
		20040814	17.12	89.03	163.46	201.50	0.11	0.35	52.65	54.48	71.60	69
		20040815	-4.44	44.11	94.32	148.14	0.56	0.78	7.65	53.84	49.40	46
H2CO_ppbv	ppbV	20040705	-0.63	1.25	-30.82	42.33	0.27	0.28	0.54	1.63	1.00	92
		20040709	-0.03	0.49	18.99	53.30	0.55	0.52	0.30	0.68	0.65	152
		20040711	-0.86	1.27	-42.74	51.38	0.13	0.25	0.46	1.76	0.90	86
		20040731	-0.75	1.42	12.01	78.69	0.22	0.27	0.84	2.20	1.44	107
		20040803	-1.68	2.45	-23.67	56.57	0.32	0.21	1.09	3.52	1.84	46
		20040807	-0.52	0.77	-27.79	47.09	0.31	0.32	0.39	1.32	0.81	121
		20040809	-0.58	1.01	-9.24	44.50	0.35	0.54	0.51	2.38	1.80	129
		20040811	-0.44	0.88	-5.76	34.33	0.35	0.31	1.06	2.19	1.75	105
		20040814	-0.79	1.44	-19.82	47.74	0.04	0.09	1.08	2.06	1.27	105
		20040815	-0.20	0.61	-0.61	48.25	0.67	0.69	0.12	1.02	0.82	100
HCOOH_ppbv	ppbV	20040705	-1.38	1.75	-94.62	94.62	0.00	0.00	0.05	1.44	0.06	92
		20040709	-0.71	1.15	-87.80	87.80	0.04	-0.01	0.05	0.75	0.05	139
		20040711	-3.13	3.72	-97.57	97.57	0.01	0.00	0.05	3.18	0.05	86
		20040731	-2.47	3.03	-96.32	96.32	0.00	0.00	0.05	2.52	0.05	102
		20040803	-1.31	1.75	-87.19	87.19	0.06	0.01	0.11	1.43	0.12	48
		20040807	-0.41	0.48	-87.05	88.49	0.09	0.05	0.03	0.46	0.05	116
		20040809	-0.85	0.96	-75.14	77.23	0.02	0.03	0.17	1.05	0.20	127
		20040811	-2.13	2.30	-86.38	88.33	0.04	0.01	0.21	2.37	0.24	105
		20040814	-1.03	1.40	-83.48	83.67	0.00	0.00	0.08	1.11	0.08	90
		20040815	-0.76	1.00	-86.11	86.11	0.07	0.02	0.05	0.83	0.07	89
hno3_ppbv	ppbV	20040705	0.40	1.51	73.47	113.76	0.10	1.21	0.23	0.81	1.22	72
		20040709	-0.33	0.89	6.00	65.98	0.35	0.52	0.33	1.39	1.05	105
		20040711	-0.20	0.53	-23.48	64.98	0.14	0.42	0.18	0.65	0.45	87
		20040715	-1.04	2.02	0.66	70.18	0.62	0.41	0.55	2.66	1.63	84

Table A.3. Continued

Species, Units	UNIT	FLIGHT	MBE (unit)	RMSE (unit)	MNB (%)	MNE (%)	R^2	SLOPE	INT (unit)	AVE_{OBS} (unit)	AVE_{MOD} (unit)	N (#)
hno3_ppbv	ppbV	20040720	-1.69	4.09	47.65	106.72	0.31	0.26	1.75	4.65	2.96	177
		20040721	-2.06	4.44	-24.09	43.08	0.40	0.20	1.64	4.62	2.55	144
		20040722	-1.67	2.44	-40.97	49.69	0.43	0.30	0.52	3.14	1.47	142
		20040725	-0.49	0.74	-37.16	48.03	0.42	0.33	0.22	1.05	0.56	136
		20040727	-0.19	0.90	66.47	117.12	0.01	0.05	0.97	1.23	1.04	140
		20040728	0.02	0.61	52.52	110.83	0.07	0.28	0.38	0.51	0.53	104
		20040731	-0.15	0.37	-10.84	44.35	0.13	0.32	0.30	0.66	0.51	142
		20040803	-2.64	5.52	-12.63	70.70	0.42	0.16	1.10	4.48	1.84	64
		20040806	-0.12	0.59	-9.51	46.39	0.31	0.53	0.25	0.77	0.66	138
		20040807	-0.13	0.38	-0.54	53.30	0.36	0.51	0.15	0.58	0.45	144
		20040809	-1.54	2.22	-38.85	59.15	0.40	0.37	0.31	2.92	1.38	170
		20040811	-2.06	3.09	-34.35	50.99	0.08	0.10	1.68	4.17	2.11	137
		20040814	-1.15	2.86	-4.15	54.53	0.38	0.22	0.84	2.54	1.39	150
		20040815	-0.25	0.83	75.25	132.66	0.38	0.34	0.30	0.84	0.59	125
ho2ro2_nd	molec/cm^3	20040715	4.73E+08	4.93E+08	258.67	258.67	0.04	0.27	6.45E+08	2.34E+08	7.07E+08	19
		20040720	6.38E+08	6.70E+08	888.77	888.77	0.03	0.27	7.75E+08	1.87E+08	8.26E+08	68
		20040809	1.98E+08	4.16E+08	651.22	651.22	0.02	3.09	1.22E+08	3.64E+07	2.34E+08	143
		20040811	7.71E+07	3.07E+08	73.01	108.60	0.13	2.15	-5.72E+07	1.17E+08	1.94E+08	113
ISOPRENE	pptV	20040715	-0.40	0.41	-97.72	97.72	0.18	0.07	-0.02	0.41	0.01	12
		20040720	-35.47	157.81	1126.50	1259.42	0.26	0.14	12.76	56.16	20.70	64
		20040721	-2.45	84.23	1112.26	1294.89	0.05	0.19	10.27	15.72	13.26	55
		20040722	-55.88	163.91	903.92	1019.63	0.55	0.43	17.89	129.53	73.64	54
		20040725	16.51	161.94	2053.78	2111.95	0.25	0.32	98.24	120.85	137.36	58
		20040727	10.78	98.06	1345.73	1409.92	0.66	0.99	11.54	53.88	64.67	65
		20040728	28.35	85.84	3288.83	3398.60	0.53	55.73	-12.74	0.75	29.10	62
		20040731	17.46	78.00	902.61	942.56	0.19	0.44	40.05	40.17	57.62	66
		20040803	-17.55	128.52	1112.45	1199.86	0.05	0.06	15.35	34.81	17.27	27
		20040806	-24.35	59.77	9.01	84.75	0.18	0.17	15.44	47.84	23.49	60
		20040807	-13.93	87.41	72.58	153.58	0.26	0.33	19.47	50.05	36.12	72

Table A.3. Continued

Species, Units	UNIT	FLIGHT	MBE (unit)	RMSE (unit)	MNB (%)	MNE (%)	R^2	SLOPE	INT (unit)	AVE_{OBS} (unit)	AVE_{MOD} (unit)	N (#)
ISOPRENE	pptV	20040809	22.87	103.52	1890.52	1935.70	0.11	0.47	40.27	32.94	55.81	72
		20040811	5.55	16.45	637.50	730.58	0.02	0.91	5.71	1.76	7.31	68
		20040814	0.85	9.37	188.74	365.42	0.00	-0.10	1.72	0.79	1.64	74
		20040815	7.73	131.76	1566.49	1674.40	0.34	0.52	39.16	65.82	73.55	68
Isoprene	pptV	20040705	-155.93	242.22	-91.92	91.92	0.78	0.37	-25.78	205.67	49.74	110
		20040709	-24.72	35.90	-91.59	100.87	0.21	0.13	-1.80	26.45	1.74	153
		20040711	-70.03	120.64	-60.81	99.29	0.16	0.11	5.15	84.75	14.72	71
		20040715	-52.38	93.16	-87.36	87.87	0.39	0.15	2.04	64.37	11.99	74
		20040720	-86.57	183.03	-64.33	111.36	0.51	0.17	-0.99	102.85	16.28	163
		20040721	-37.41	129.08	-82.78	108.82	0.37	0.28	0.71	53.16	15.75	102
		20040722	-115.32	204.76	-24.49	106.17	0.56	0.39	8.70	204.17	88.84	116
		20040725	-34.92	193.70	189.60	258.41	0.24	0.31	94.44	186.88	151.96	121
		20040727	-6.68	127.69	123.09	213.82	0.30	0.62	20.46	70.51	63.84	110
		20040728	17.21	79.70	125.44	276.84	0.69	1.22	12.05	23.38	40.58	70
		20040731	-2.16	73.41	37.46	118.73	0.31	0.62	23.48	68.27	66.11	125
		20040803	-78.27	175.92	-9.59	145.76	0.05	0.05	12.93	96.34	18.07	56
		20040806	-49.38	75.87	-64.16	76.35	0.21	0.18	9.37	71.63	22.25	131
		20040807	-29.45	69.26	-9.08	109.56	0.40	0.50	5.43	69.20	39.74	138
		20040809	-6.68	72.56	33.00	133.77	0.22	0.70	9.60	54.07	47.40	147
		20040811	-13.10	23.73	-28.57	120.14	0.00	-0.08	8.67	20.07	6.98	113
		20040814	-12.23	17.66	-65.71	125.36	0.01	-0.09	3.07	13.99	1.75	123
		20040815	-28.99	138.37	-22.58	113.33	0.42	0.50	27.10	112.54	83.55	75
MEK	pptV	20040705	419.04	517.27	169.83	172.46	0.60	1.97	139.53	289.62	708.66	111
		20040709	385.31	403.47	237.61	237.98	0.17	0.70	441.03	188.42	573.73	159
		20040711	340.09	350.18	186.30	186.30	0.31	0.81	379.09	205.21	545.30	71
		20040715	532.58	569.67	253.30	253.30	0.47	1.65	379.13	237.57	770.15	75
		20040720	729.45	752.19	276.42	276.42	0.21	0.71	820.34	309.37	1038.82	166
		20040721	478.46	516.14	186.87	187.03	0.23	0.84	527.72	298.95	777.41	122
		20040722	469.07	513.00	166.12	166.12	0.67	1.67	256.55	318.54	787.61	147

Table A.3. Continued

Species, Units	UNIT	FLIGHT	MBE (unit)	RMSE (unit)	MNB (%)	MNE (%)	R^2	SLOPE	INT (unit)	AVE_{OBS} (unit)	AVE_{MOD} (unit)	N (#)
MEK	pptV	20040725	572.73	608.54	315.65	315.65	0.07	0.81	612.33	203.97	776.70	137
		20040727	940.63	1014.40	459.94	459.94	0.10	1.31	868.09	234.78	1175.41	129
		20040728	705.75	790.64	558.90	558.90	0.00	-0.43	901.00	136.51	842.26	98
		20040731	403.31	448.08	285.09	285.09	0.08	0.69	458.46	180.81	584.12	128
		20040803	447.68	484.81	193.62	193.62	0.39	0.74	545.86	373.58	821.26	59
		20040806	377.34	390.97	287.84	287.84	0.25	1.32	332.05	142.32	519.66	139
		20040807	328.90	347.33	241.42	241.42	0.41	1.71	225.24	146.64	475.54	149
		20040809	713.26	751.14	272.54	272.54	0.46	2.17	372.84	292.11	1005.37	158
		20040811	884.65	898.61	305.92	305.92	0.41	1.22	811.85	325.08	1209.73	125
		20040814	626.58	678.45	486.39	486.39	0.05	0.84	652.64	165.55	792.13	139
		20040815	454.27	538.18	424.84	424.93	0.43	2.02	295.86	155.30	609.57	113
Methacrolein	pptV	20040715	-5.03	5.56	-65.80	65.80	0.37	0.38	-0.22	7.75	2.72	12
		20040720	-52.88	122.74	-60.64	88.36	0.44	0.18	6.54	72.81	19.93	64
		20040721	-20.94	80.93	-56.05	119.79	0.02	0.08	8.27	31.83	10.89	55
		20040722	-58.80	134.74	38.99	153.90	0.34	0.28	21.70	112.22	53.42	54
		20040725	-10.67	100.92	148.26	213.99	0.20	0.25	70.31	107.35	96.68	58
		20040727	-4.84	54.79	119.80	176.27	0.70	0.64	16.67	59.79	54.95	65
		20040728	22.17	66.27	67.71	163.41	0.40	2.84	-3.82	14.10	36.27	62
		20040731	-15.46	82.47	2.03	77.62	0.24	0.49	29.90	89.09	73.64	66
		20040803	-108.86	199.21	15.95	112.93	0.56	0.31	29.60	200.83	91.97	27
		20040806	-25.34	35.21	-47.82	54.95	0.33	0.38	5.17	49.09	23.75	60
		20040807	-31.64	55.44	-24.75	84.70	0.41	0.37	11.82	69.47	37.83	72
		20040809	22.21	113.88	77.24	118.14	0.02	0.21	101.09	100.35	122.56	72
		20040811	7.85	60.37	48.84	99.22	0.18	0.53	38.16	64.17	72.02	68
		20040814	-8.27	19.92	-55.45	78.50	0.04	0.20	3.69	14.93	6.66	74
		20040815	-9.63	58.45	1.16	107.56	0.59	0.69	9.70	61.47	51.84	67
Methanol	pptV	20040705	-2064.14	2584.68	-88.85	88.85	0.33	-0.01	175.42	2207.40	143.26	111
		20040709	-2099.64	2310.81	-93.96	93.96	0.34	-0.02	147.80	2202.32	102.68	159
		20040711	-3367.84	3394.12	-97.85	97.85	0.01	0.00	66.82	3440.61	72.78	71

Table A.3. Continued

Species, Units	UNIT	FLIGHT	MBE (unit)	RMSE (unit)	MNB (%)	MNE (%)	R^2	SLOPE	INT (unit)	AVE_{OBS} (unit)	AVE_{MOD} (unit)	N (#)
Methanol	pptV	20040715	-2642.97	2716.14	-96.70	96.70	0.12	-0.01	106.67	2725.09	82.13	75
		20040720	-2879.82	2957.01	-95.79	95.79	0.27	-0.02	167.62	2997.25	117.43	166
		20040721	-2541.82	2631.31	-94.71	94.71	0.05	-0.01	146.45	2672.04	130.21	122
		20040722	-3184.68	3489.42	-94.51	94.51	0.19	-0.01	170.16	3327.39	142.71	147
		20040725	-2185.03	2323.48	-94.50	94.50	0.34	-0.04	190.34	2280.66	95.63	137
		20040727	-1976.08	2187.17	-88.22	88.22	0.05	-0.01	228.09	2187.38	211.29	129
		20040728	-1664.75	2101.76	-86.61	86.61	0.30	-0.04	246.64	1840.49	175.75	98
		20040731	-1312.28	1379.07	-82.53	82.53	0.07	-0.02	285.20	1561.51	249.23	128
		20040803	-2935.28	3195.51	-93.36	93.36	0.51	-0.02	183.41	3047.06	111.78	59
		20040806	-1931.19	1943.12	-98.21	98.21	0.05	0.02	4.20	1966.19	34.99	139
		20040807	-1872.27	1900.04	-95.37	95.37	0.00	0.00	91.02	1960.58	88.31	149
		20040809	-3658.61	3742.78	-97.52	97.52	0.00	0.00	89.52	3743.75	85.14	158
		20040811	-3325.48	3394.02	-96.51	96.51	0.06	0.00	102.66	3440.32	114.83	125
		20040814	-1058.04	1130.77	-85.51	85.51	0.23	-0.05	210.19	1211.16	153.12	139
		20040815	-1089.58	1277.91	-88.88	88.88	0.03	0.01	96.73	1196.76	107.18	113
METHYLVINYL _KETONE	pptV	20040720	-149.83	335.06	-51.66	85.02	0.52	0.15	15.42	193.61	43.79	64
		20040721	-200.92	408.28	-76.35	104.53	0.08	0.05	9.54	222.32	21.39	55
		20040722	-495.26	650.35	-78.99	89.68	0.39	0.16	8.21	595.96	100.71	54
		20040725	-676.84	876.06	-70.54	74.86	0.12	0.06	112.86	842.67	165.84	58
		20040727	-974.36	1180.22	-87.34	87.34	0.29	0.09	4.64	1081.56	107.20	65
		20040728	-1075.76	1260.51	-94.85	94.85	0.06	0.04	13.32	1131.37	55.62	62
		20040731	-1376.04	1619.16	-86.83	87.85	0.00	0.00	128.74	1511.57	135.53	66
		20040803	-327.99	540.85	-16.27	95.69	0.60	0.20	52.91	474.69	146.70	27
		20040806	-68.01	92.84	-39.79	58.36	0.33	0.28	18.10	118.96	50.95	60
		20040807	-231.69	277.29	-79.08	81.22	0.42	0.19	7.13	293.76	62.08	72
		20040809	-357.53	465.15	-52.79	68.11	0.01	0.04	175.85	555.28	197.76	72
		20040811	-633.92	711.34	-84.34	84.34	0.17	0.09	39.41	738.89	104.98	68
		20040814	-814.30	876.81	-97.41	97.41	0.00	0.00	17.11	833.34	19.04	74
		20040815	-900.22	977.17	-92.22	92.22	0.50	0.22	-118.37	999.53	99.30	67

Table A.3. Continued

Species, Units	UNIT	FLIGHT	MBE (unit)	RMSE (unit)	MNB (%)	MNE (%)	R^2	SLOPE	INT (unit)	AVE_{OBS} (unit)	AVE_{MOD} (unit)	N (#)
Monoterpenes	pptV	20040705	-41.77	58.56	-95.06	95.06	0.47	0.13	-1.79	45.95	4.18	97
		20040709	-13.75	17.86	-98.09	98.09	0.10	0.02	-0.01	14.00	0.25	145
		20040711	-19.23	21.81	-96.80	96.80	0.02	0.02	0.20	19.76	0.52	70
		20040715	-14.06	16.44	-96.81	96.81	0.33	0.06	-0.29	14.63	0.57	74
		20040720	-16.02	18.76	-96.29	96.29	0.21	0.08	-0.63	16.78	0.76	139
		20040721	-18.50	43.70	-94.09	100.88	0.36	0.11	-0.43	20.30	1.80	107
		20040722	-26.17	42.25	-63.86	94.11	0.44	0.19	2.16	35.11	8.94	126
		20040725	-20.26	27.61	-70.41	75.33	0.38	0.17	2.11	27.11	6.84	127
		20040727	-10.53	15.56	-82.80	84.34	0.25	0.18	-0.11	12.73	2.20	115
		20040728	-10.11	24.31	-79.34	101.38	0.67	0.35	-1.25	13.72	3.60	84
		20040731	-9.66	15.10	-60.29	88.86	0.10	0.27	0.12	13.39	3.73	118
		20040803	-16.99	21.20	-99.20	99.20	0.01	0.00	0.03	17.03	0.05	58
		20040806	-10.16	11.80	-84.84	85.10	0.04	0.04	0.83	11.49	1.33	131
		20040807	-9.10	11.80	-67.38	98.55	0.13	0.25	-0.46	11.54	2.43	141
		20040809	-11.54	14.25	-96.29	96.29	0.26	0.10	-0.68	12.07	0.53	143
		20040811	-7.86	15.96	-70.26	115.56	0.00	-0.04	2.90	10.34	2.47	113
		20040814	-7.41	8.89	-98.32	98.32	0.00	0.01	0.05	7.50	0.09	121
		20040815	-7.26	11.54	-67.23	92.80	0.40	0.63	-2.76	12.16	4.90	96
MPAN	pptV	20040705	29.95	66.14	274.52	318.26	0.29	0.91	34.47	53.17	83.12	96
		20040709	27.57	44.78	334.76	352.89	0.03	0.23	52.00	31.60	59.17	172
		20040711	-13.86	59.88	-22.15	67.31	0.06	0.70	3.80	58.63	44.77	90
		20040715	67.41	79.80	742.54	742.54	0.31	0.81	75.35	41.23	108.64	88
		20040720	42.32	63.48	152.41	162.68	0.20	0.65	60.14	50.69	93.01	189
		20040721	-4.61	73.85	34.94	121.00	0.02	0.32	29.66	50.09	45.48	132
		20040722	15.86	43.58	90.65	118.01	0.50	0.91	20.30	49.89	65.75	167
		20040725	75.87	96.70	548.65	548.65	0.07	0.84	81.02	31.31	107.17	157
		20040727	132.44	151.94	895.25	897.01	0.03	0.53	145.90	28.83	161.27	141
		20040728	79.05	103.35	1831.67	1841.28	0.22	-2.56	119.61	11.40	90.45	117
		20040731	51.37	73.17	283.46	297.43	0.09	0.91	54.05	28.43	79.80	145

Table A.3. Continued

Species, Units	UNIT	FLIGHT	MBE (unit)	RMSE (unit)	MNB (%)	MNE (%)	R^2	SLOPE	INT (unit)	AVE_{OBS} (unit)	AVE_{MOD} (unit)	N (#)
MPAN	pptV	20040803	35.96	66.01	150.27	162.74	0.28	0.65	59.14	65.83	101.79	72
		20040806	39.47	48.45	175.24	176.56	0.39	1.54	24.99	27.06	66.53	151
		20040807	37.17	43.88	189.89	190.21	0.46	1.17	32.34	28.54	65.72	164
		20040809	62.49	79.86	229.29	231.31	0.20	1.03	61.07	51.40	113.89	171
		20040811	93.04	117.63	289.96	298.26	0.27	1.92	57.14	38.93	131.97	148
		20040814	60.03	81.51	768.03	770.04	0.04	0.85	62.43	15.68	75.71	157
		20040815	83.06	110.62	1606.52	1612.49	0.61	3.29	49.83	14.52	97.58	139
MVK_MACR	pptV	20040705	-179.86	391.75	-48.16	96.80	0.87	0.45	4.99	339.11	159.24	110
		20040709	-40.16	89.79	-64.51	86.41	0.30	0.12	3.14	49.48	9.31	158
		20040711	-262.79	390.06	-48.33	77.01	0.42	0.18	20.29	345.49	82.70	70
		20040715	-159.38	262.16	-47.39	70.26	0.63	0.23	11.38	221.83	62.45	72
		20040720	-171.06	345.11	-54.90	84.89	0.53	0.20	14.21	230.24	59.17	164
		20040721	-37.23	90.42	-80.17	95.18	0.47	0.67	-15.57	65.55	28.32	119
		20040722	-260.38	526.22	10.50	127.90	0.36	0.20	71.55	416.19	155.81	144
		20040725	-120.25	364.92	387.26	462.17	0.23	0.22	191.65	397.94	277.69	133
		20040727	-70.44	254.38	290.11	350.27	0.59	0.40	65.59	227.36	156.92	128
		20040728	47.10	127.28	217.95	280.62	0.65	1.53	27.86	36.60	83.69	92
		20040731	-130.75	296.47	20.07	89.86	0.24	0.31	109.61	348.17	217.43	128
		20040803	-412.98	640.86	55.06	161.06	0.61	0.25	63.21	636.58	223.61	57
		20040806	-106.73	146.81	-41.11	63.64	0.36	0.28	20.79	178.35	71.62	138
		20040807	-152.64	224.45	-48.36	73.13	0.49	0.28	30.94	253.74	101.11	149
		20040809	-84.78	283.57	50.66	107.36	0.09	0.27	194.04	382.96	298.18	156
		20040811	-47.69	156.67	17.50	76.26	0.36	0.44	65.33	203.20	155.51	125
		20040814	0.44	66.21	57.99	148.08	0.01	0.21	24.15	29.94	30.38	134
		20040815	-56.52	186.35	160.19	203.60	0.82	0.54	32.18	191.69	135.16	101
N2O5_pptv	pptV	20040709	-1.63	1.75	-87.13	106.15	0.02	-0.05	0.14	1.68	0.05	159
		20040711	-14.15	74.68	231.16	345.07	0.32	0.17	8.01	26.66	12.51	89
		20040715	-1.71	2.00	-90.23	91.72	0.07	0.06	0.05	1.87	0.17	87
		20040720	-1.91	2.10	-96.23	96.23	0.01	0.02	0.03	1.98	0.07	186

Table A.3. Continued

Species, Units	UNIT	FLIGHT	MBE (unit)	RMSE (unit)	MNB (%)	MNE (%)	R^2	SLOPE	INT (unit)	AVE_{OBS} (unit)	AVE_{MOD} (unit)	N (#)
N2O5_pptv	pptV	20040721	-1.25	1.34	-98.15	98.15	0.02	0.02	0.00	1.27	0.02	136
		20040722	-0.95	1.03	-85.23	103.79	0.03	-0.12	0.18	1.01	0.06	73
		20040727	-0.45	1.72	-48.75	118.40	0.00	0.38	0.08	0.85	0.40	141
		20040728	-0.54	0.76	-78.76	101.83	0.00	0.18	0.02	0.68	0.15	113
		20040731	6.13	12.43	410.56	485.42	0.14	0.54	8.04	4.19	10.32	110
		20040803	3.43	114.15	736.36	774.24	0.35	0.46	37.88	64.29	67.71	70
		20040806	-0.84	1.26	-87.03	93.73	0.11	0.35	-0.15	1.07	0.22	145
		20040807	-11.35	56.61	32.98	161.90	0.45	0.40	9.37	34.39	23.04	174
		20040809	-69.81	242.88	14.41	132.01	0.22	0.16	20.47	107.92	38.11	183
		20040811	15.30	67.07	139.13	170.75	0.28	1.56	5.33	17.68	32.98	147
		20040814	-0.54	0.62	-85.73	87.47	0.00	0.03	0.07	0.63	0.09	153
		20040815	-0.63	0.79	-83.65	100.16	0.04	0.29	-0.10	0.75	0.13	128
NH3_ppbv	ppbV	20040709	-0.45	0.79	-95.38	95.38	0.19	0.11	-0.01	0.50	0.05	69
		20040711	-0.72	0.86	-99.07	99.07	0.17	0.01	0.00	0.73	0.01	74
		20040720	-0.30	0.44	-97.50	98.21	0.03	0.01	0.00	0.31	0.00	130
		20040722	-0.58	0.88	-99.70	99.70	0.05	0.00	0.00	0.58	0.00	121
		20040725	-0.09	0.15	-56.13	90.99	0.50	0.79	-0.06	0.16	0.07	102
		20040728	-0.61	0.69	-99.80	99.80	0.00	0.00	0.00	0.61	0.00	14
		20040731	-0.55	0.66	-97.93	97.93	0.29	0.01	0.00	0.56	0.01	61
		20040803	-0.54	0.60	-97.99	97.99	0.10	0.02	0.00	0.55	0.01	39
		20040806	-0.23	0.30	-95.16	95.16	0.43	0.21	-0.03	0.25	0.02	94
		20040807	-0.43	0.53	-80.15	83.27	0.09	0.14	0.02	0.52	0.09	103
		20040809	-0.25	0.44	-44.79	136.39	0.00	0.03	0.05	0.31	0.06	131
		20040811	-0.16	0.23	-98.47	98.47	0.45	0.03	0.00	0.16	0.00	105
		20040814	-0.22	0.26	-98.06	98.06	0.13	0.10	-0.02	0.22	0.01	102
		20040815	-0.18	0.27	-73.02	92.64	0.15	0.97	-0.17	0.27	0.09	28
Nitrate	$\mu g/m^3$	20040709	-0.23	0.36	-32.91	121.86	0.05	0.11	0.05	0.31	0.08	18
		20040715	-0.25	0.39	-62.86	114.92	0.06	-0.10	0.07	0.28	0.04	9
		20040720	-0.33	0.72	-96.77	96.77	0.01	0.00	0.00	0.34	0.00	26

Table A.3. Continued

Species, Units	UNIT	FLIGHT	MBE (unit)	RMSE (unit)	MNB (%)	MNE (%)	R^2	SLOPE	INT (unit)	AVE_{OBS} (unit)	AVE_{MOD} (unit)	N (#)
Nitrate	µg/m^3	20040721	-0.60	1.14	-71.34	104.62	0.02	-0.03	0.07	0.65	0.05	12
		20040722	-0.06	0.07	-93.19	95.70	0.06	0.31	-0.01	0.07	0.01	18
		20040725	-0.14	0.23	-56.15	86.01	0.12	0.28	0.03	0.23	0.09	16
		20040727	-0.65	1.30	-83.58	97.78	0.03	-0.01	0.02	0.66	0.02	15
		20040728	-0.52	0.92	-93.06	93.65	0.00	0.00	0.01	0.54	0.02	31
		20040731	-0.13	0.21	-100.00	100.00	0.00	0.00	0.00	0.13	0.00	23
		20040803	-0.04	0.12	-38.87	144.47	0.04	-0.54	0.07	0.07	0.03	12
		20040806	-0.10	0.21	-58.11	103.38	0.15	0.49	-0.02	0.17	0.07	33
		20040807	-0.07	0.09	-77.73	77.73	0.02	0.09	0.01	0.09	0.02	18
		20040809	-0.36	0.60	-99.94	99.94	0.37	0.00	0.00	0.36	0.00	14
		20040811	-0.30	0.64	-40.88	115.30	0.03	-0.03	0.04	0.33	0.04	14
		20040814	-0.07	0.16	-21.56	96.11	0.13	-0.28	0.10	0.13	0.06	12
		20040815	-0.07	0.29	5.58	163.49	0.03	-0.30	0.12	0.15	0.08	15
NO_ppbv	ppbV	20040705	-0.11	0.81	29.06	88.03	0.44	0.05	0.04	0.16	0.05	124
		20040709	-0.04	0.20	-24.38	74.14	0.33	0.16	0.02	0.08	0.03	176
		20040711	0.01	0.03	36.48	169.58	0.46	2.61	-0.01	0.01	0.01	82
		20040715	-0.20	0.50	4.44	108.16	0.18	0.11	0.09	0.33	0.13	95
		20040720	-0.15	0.69	34.69	76.43	0.13	0.04	0.08	0.24	0.09	194
		20040721	-0.05	0.19	-15.46	41.51	0.45	0.08	0.03	0.09	0.04	139
		20040722	-0.06	0.50	-1.17	40.16	0.38	0.04	0.03	0.10	0.04	169
		20040725	-0.23	1.04	129.79	192.57	0.64	0.17	0.09	0.38	0.15	155
		20040727	-0.18	1.68	94.19	153.91	0.09	0.01	0.06	0.23	0.06	144
		20040728	-0.02	0.08	-53.03	78.50	0.14	0.09	0.01	0.03	0.01	78
		20040731	0.00	0.02	-19.26	102.76	0.78	0.94	0.00	0.02	0.02	143
		20040803	-0.02	0.08	-99.77	99.77	0.00	0.00	0.00	0.02	0.00	69
		20040806	-0.14	0.32	-34.67	63.60	0.33	0.29	0.05	0.26	0.12	146
		20040807	-0.01	0.04	-21.47	100.94	0.12	0.37	0.01	0.02	0.01	165
		20040809	-0.01	0.02	-47.30	114.61	0.09	0.65	0.00	0.01	0.01	178
		20040811	-0.01	0.02	-97.39	97.39	0.59	0.20	0.00	0.01	0.00	147

Table A.3. Continued

Species, Units	UNIT	FLIGHT	MBE (unit)	RMSE (unit)	MNB (%)	MNE (%)	R^2	SLOPE	INT (unit)	AVE_{OBS} (unit)	AVE_{MOD} (unit)	N (#)
NO_ppbv	ppbV	20040814	-0.04	0.27	109.56	144.06	0.03	0.03	0.05	0.09	0.05	164
		20040815	-0.10	0.51	17.49	67.27	0.30	0.08	0.04	0.14	0.05	137
NO2_ppbv	ppbV	20040711	-0.01	0.86	90.13	137.02	0.17	0.21	0.37	0.48	0.47	82
		20040715	-0.58	1.32	-6.28	88.32	0.40	0.26	0.26	1.14	0.55	91
		20040720	-0.53	2.44	2.91	56.60	0.15	0.05	0.34	0.93	0.39	187
		20040721	-0.18	0.76	-11.05	47.49	0.56	0.13	0.13	0.36	0.18	138
		20040722	-0.12	1.00	10.33	54.13	0.37	0.17	0.16	0.34	0.22	168
		20040725	0.19	1.02	276.49	316.44	0.62	0.82	0.32	0.71	0.90	151
		20040727	0.02	1.56	421.24	464.76	0.16	0.20	0.43	0.51	0.53	143
		20040728	-0.02	0.21	-31.22	95.27	0.78	0.66	0.03	0.13	0.12	62
		20040731	0.10	0.56	58.87	89.29	0.54	0.65	0.37	0.76	0.86	143
		20040803	-0.09	1.54	77.76	110.82	0.27	0.33	0.75	1.25	1.16	69
		20040806	-0.37	0.84	-49.94	65.45	0.45	0.59	-0.03	0.84	0.47	143
		20040807	-0.21	1.19	4.67	76.92	0.43	0.43	0.40	1.08	0.87	166
		20040809	-0.08	1.37	13.15	73.24	0.24	0.56	0.46	1.22	1.14	178
		20040811	0.26	0.82	72.50	88.45	0.56	1.07	0.21	0.63	0.89	146
		20040814	0.11	0.93	149.64	171.61	0.08	0.21	0.36	0.33	0.43	142
		20040815	-0.13	1.40	-13.18	79.60	0.19	0.12	0.19	0.36	0.23	133
NO3_pptv	pptV	20040709	-0.84	0.91	-94.49	94.49	0.01	-0.01	0.05	0.88	0.04	161
		20040711	1.71	12.10	178.71	266.58	0.13	0.43	5.12	5.97	7.67	89
		20040715	-0.40	0.43	-81.83	81.83	0.04	0.17	0.00	0.49	0.09	87
		20040720	-0.49	0.56	-81.28	82.51	0.00	0.01	0.09	0.58	0.09	185
		20040721	-0.51	0.54	-89.34	89.34	0.04	-0.05	0.08	0.57	0.05	132
		20040722	-0.36	0.40	-87.70	93.70	0.21	0.16	-0.02	0.40	0.04	71
		20040727	-0.36	0.47	-69.47	78.87	0.02	0.13	0.08	0.51	0.15	141
		20040728	-0.60	0.64	-91.73	92.72	0.01	0.11	-0.02	0.66	0.05	113
		20040731	3.98	7.42	247.63	314.21	0.36	0.89	4.40	3.70	7.67	110
		20040803	10.67	30.50	226.09	250.22	0.43	0.65	19.90	26.20	36.88	70
		20040806	-0.53	0.55	-92.83	92.83	0.04	0.11	-0.02	0.57	0.04	142

Table A.3. Continued

Species, Units	UNIT	FLIGHT	MBE (unit)	RMSE (unit)	MNB (%)	MNE (%)	R^2	SLOPE	INT (unit)	AVE_{OBS} (unit)	AVE_{MOD} (unit)	N (#)
NO3_pptv	pptV	20040807	-0.82	6.76	-35.62	73.56	0.63	0.67	1.54	7.24	6.42	170
		20040809	-20.66	51.95	-1.31	90.88	0.57	0.31	6.71	39.44	18.78	184
		20040811	7.27	15.52	101.20	120.02	0.35	0.76	11.00	15.87	23.13	147
		20040814	-0.26	0.32	-64.72	75.58	0.03	-0.21	0.19	0.37	0.12	156
		20040815	-0.40	0.47	-83.65	92.77	0.02	0.11	0.01	0.47	0.07	127
O3_ppbv	ppbV	20040705	7.53	14.17	19.65	26.10	0.06	0.15	51.57	52.05	59.58	134
		20040709	2.09	9.82	6.14	14.49	0.09	0.21	47.54	57.44	59.53	179
		20040711	-3.16	13.50	-0.73	20.83	0.00	0.02	45.66	50.07	46.91	91
		20040715	0.47	13.10	6.68	20.46	0.28	0.36	42.56	65.82	66.29	98
		20040720	0.69	10.91	2.90	12.29	0.42	0.54	34.09	73.35	74.04	199
		20040721	-3.64	17.33	-0.97	15.69	0.24	0.32	51.07	80.15	76.50	146
		20040722	-8.22	16.72	-8.44	17.80	0.14	0.31	43.90	75.34	67.12	175
		20040725	4.65	10.45	18.76	25.31	0.53	0.40	29.92	42.05	46.70	160
		20040727	4.78	11.92	13.52	20.32	0.32	0.41	39.56	59.21	63.98	150
		20040728	-3.13	14.41	-0.31	19.49	0.13	0.24	44.06	62.36	59.24	120
		20040731	6.48	11.09	21.12	25.12	0.30	0.42	31.02	41.98	48.46	150
		20040803	-3.57	16.04	0.42	20.80	0.08	0.15	54.89	69.02	65.46	73
		20040806	2.95	11.03	10.45	20.36	0.18	0.21	40.13	47.29	50.24	149
		20040807	4.68	8.05	14.95	18.41	0.56	0.56	22.11	39.60	44.28	172
		20040809	-2.81	9.45	-3.00	11.80	0.56	0.65	18.24	60.64	57.83	184
		20040811	-2.95	12.07	-2.19	13.30	0.22	0.37	41.70	71.23	68.28	154
		20040814	8.97	11.97	21.45	22.81	0.32	0.34	41.71	49.75	58.72	169
		20040815	6.10	13.31	18.30	23.56	0.03	0.11	52.42	52.07	58.17	143
oh_nd	molec/cm^3	20040709	5.50E+06	8.13E+06	171.92	184.32	0.00	0.09	1.12E+07	6.26E+06	1.18E+07	80
		20040715	6.73E+06	7.50E+06	231.28	231.76	0.09	0.27	1.01E+07	4.60E+06	1.13E+07	26
		20040720	8.50E+06	9.08E+06	883.31	884.69	0.02	0.39	9.44E+06	1.55E+06	1.00E+07	134
		20040725	1.10E+06	2.79E+06	107.26	136.09	0.00	-0.08	3.94E+06	2.64E+06	3.73E+06	126
		20040727	1.24E+06	5.79E+06	185.97	231.95	0.03	-0.29	6.31E+06	3.93E+06	5.17E+06	78
		20040809	-3.69E+04	2.87E+05	31.69	105.72	0.05	-0.29	3.24E+05	2.79E+05	2.42E+05	33

Table A.3. Continued

Species, Units	UNIT	FLIGHT	MBE (unit)	RMSE (unit)	MNB (%)	MNE (%)	R^2	SLOPE	INT (unit)	AVE_{OBS} (unit)	AVE_{MOD} (unit)	N (#)
PAN	pptV	20040705	267.01	341.06	125.64	132.02	0.35	1.11	234.93	282.12	549.12	96
		20040709	186.79	493.34	79.59	97.77	0.14	-0.30	792.70	467.82	654.60	172
		20040711	-104.58	305.89	-16.19	60.72	0.01	0.17	215.71	384.22	279.64	90
		20040715	466.73	587.17	101.23	111.64	0.63	1.41	228.20	583.47	1050.20	93
		20040720	628.00	724.11	144.09	146.66	0.10	0.32	1032.47	598.25	1226.25	189
		20040721	299.45	469.78	134.34	144.53	0.01	0.11	676.41	421.86	721.31	141
		20040722	88.43	280.16	43.93	61.10	0.57	0.75	211.60	495.67	584.10	167
		20040725	285.86	431.66	145.14	146.51	0.05	0.40	476.31	316.46	602.32	158
		20040727	818.25	942.39	292.39	294.82	0.04	0.66	947.30	374.58	1192.83	141
		20040728	558.54	970.90	294.81	344.00	0.20	-1.37	1337.02	328.65	887.19	117
		20040731	134.42	269.19	73.23	102.03	0.06	0.49	260.23	245.73	380.15	145
		20040803	31.78	429.33	107.21	137.17	0.17	0.29	483.10	633.22	664.99	72
		20040806	134.05	267.81	40.75	70.38	0.29	1.42	0.89	320.23	454.28	151
		20040807	76.50	180.12	29.41	56.30	0.26	0.76	152.24	320.25	396.75	164
		20040809	105.34	356.03	28.90	58.49	0.31	0.92	150.50	595.75	701.09	172
		20040811	336.18	466.73	91.54	100.24	0.42	0.72	522.64	654.55	990.73	148
		20040814	465.09	560.24	346.28	349.65	0.05	0.34	620.75	234.98	700.07	157
		20040815	307.00	436.32	137.08	143.54	0.59	2.08	36.79	250.64	557.64	139
PAN2	pptV	20040715	599.91	654.00	1063.90	1063.90	0.66	3.76	363.78	85.43	685.34	93
		20040720	748.72	772.64	1001.45	1001.45	0.05	0.62	787.48	102.27	851.00	189
		20040721	458.33	486.19	926.77	926.77	0.02	0.37	504.47	72.93	531.25	141
		20040722	376.68	425.27	690.49	690.59	0.57	3.23	217.49	71.43	448.11	167
		20040725	376.13	418.70	1300.87	1300.87	0.01	0.65	390.92	42.17	418.30	158
		20040727	852.99	924.70	2290.22	2290.22	0.01	-1.28	958.42	46.19	899.18	141
		20040728	653.78	851.17	2634.98	2660.58	0.22	-5.91	947.54	42.49	696.27	116
		20040731	223.31	278.95	812.59	816.22	0.00	-0.31	272.13	37.19	260.50	145
		20040803	348.97	396.99	800.79	800.79	0.09	0.67	383.51	104.17	453.14	72
		20040806	260.63	301.55	519.05	520.97	0.59	5.28	50.39	49.08	309.72	151
		20040807	212.01	232.66	440.99	440.99	0.48	2.99	110.49	51.11	263.12	164

Table A.3. Continued

Species, Units	UNIT	FLIGHT	MBE (unit)	RMSE (unit)	MNB (%)	MNE (%)	R^2	SLOPE	INT (unit)	AVE_{OBS} (unit)	AVE_{MOD} (unit)	N (#)
PAN2	pptV	20040809	379.78	442.67	491.43	491.43	0.26	2.38	230.70	107.99	487.77	172
		20040811	609.36	649.72	703.55	703.55	0.30	2.40	457.43	108.67	718.03	148
		20040814	458.81	499.06	1959.92	1959.92	0.01	0.32	488.84	44.46	503.27	155
		20040815	349.53	421.60	1517.57	1517.57	0.46	6.03	188.94	31.95	381.47	139
PBzN	pptV	20040705	0.83	1.63	152.80	176.57	0.04	0.99	0.83	0.66	1.49	96
		20040709	2.40	4.35	206.86	225.50	0.00	-0.07	4.31	1.78	4.18	173
		20040711	-0.87	3.01	-21.48	75.06	0.00	-0.04	2.21	2.95	2.08	90
		20040715	6.22	9.41	220.69	240.29	0.74	4.49	-2.05	2.37	8.59	93
		20040720	5.85	7.98	226.68	232.39	0.06	0.55	7.43	3.55	9.40	189
		20040721	1.04	3.52	79.57	101.28	0.02	0.29	2.56	2.13	3.17	142
		20040722	0.64	2.92	15.08	54.53	0.55	2.04	-1.38	1.94	2.58	167
		20040725	3.86	5.62	557.28	559.47	0.00	-0.15	5.05	1.03	4.89	157
		20040727	2.08	2.85	229.90	237.57	0.01	-0.20	3.99	1.60	3.67	141
		20040728	0.69	3.75	239.56	293.24	0.20	-0.41	3.18	1.77	2.46	117
		20040731	0.85	1.69	70.72	97.69	0.15	1.15	0.66	1.27	2.13	145
		20040803	2.15	4.45	179.89	204.47	0.20	0.71	3.06	3.21	5.36	72
		20040806	1.26	2.51	65.81	106.49	0.42	2.41	-1.03	1.62	2.88	151
		20040807	1.93	2.93	130.97	157.51	0.32	2.49	-0.19	1.43	3.36	164
		20040809	1.69	4.19	64.30	105.41	0.19	1.26	0.97	2.82	4.51	172
		20040811	2.96	3.95	129.85	135.81	0.39	1.39	1.90	2.71	5.67	148
		20040814	3.32	4.67	315.87	324.51	0.16	1.27	2.93	1.43	4.75	157
		20040815	2.11	3.66	203.74	227.24	0.57	3.50	-0.60	1.08	3.19	139
SO2_ppbv	ppbV	20040705	-0.15	0.65	-39.70	73.11	0.68	1.10	-0.23	0.74	0.59	136
		20040709	-0.20	0.61	-26.83	98.75	0.10	0.35	0.15	0.54	0.34	172
		20040711	0.32	1.48	129.73	185.98	0.06	0.32	0.85	0.78	1.10	83
		20040715	-0.50	1.16	-33.88	62.25	0.39	0.41	0.31	1.38	0.87	91
		20040720	-1.27	2.86	5.67	81.41	0.12	0.09	0.72	2.19	0.92	193
		20040721	-1.50	3.37	-48.42	79.34	0.03	0.03	0.27	1.82	0.32	139
		20040722	-0.83	1.71	-52.09	66.88	0.19	0.22	0.18	1.29	0.46	171

Table A.3. Continued

Species, Units	UNIT	FLIGHT	MBE (unit)	RMSE (unit)	MNB (%)	MNE (%)	R^2	SLOPE	INT (unit)	AVE_{OBS} (unit)	AVE_{MOD} (unit)	N (#)
SO2_ppbv	ppbV	20040725	-1.36	7.53	29.34	84.05	0.00	0.01	1.01	2.38	1.02	62
		20040727	-0.82	4.69	6.11	110.34	0.02	0.02	0.44	1.29	0.47	154
		20040728	-0.30	0.38	-83.59	83.59	0.47	0.19	-0.01	0.37	0.06	121
		20040731	-0.62	0.98	-45.07	63.18	0.16	0.19	0.22	1.04	0.42	148
		20040803	-0.83	4.28	25.97	100.39	0.18	0.23	1.14	2.55	1.72	71
		20040806	-0.42	3.40	39.07	94.14	0.21	0.26	1.58	2.71	2.30	135
		20040807	-0.61	2.55	-19.69	79.63	0.12	0.07	0.41	1.10	0.49	173
		20040809	-0.51	4.81	80.00	133.49	0.35	0.41	2.08	4.38	3.87	184
		20040811	-0.16	1.83	50.84	95.20	0.00	0.04	1.99	2.24	2.07	149
		20040814	-0.47	1.05	-17.42	78.24	0.28	0.19	0.22	0.86	0.39	164
		20040815	0.38	2.87	90.97	151.06	0.20	1.03	0.36	0.71	1.08	131
sulf_nd	molec/cm^3	20040705	1.58E+07	3.75E+07	245.30	296.48	0.16	0.71	2.03E+07	1.55E+07	3.13E+07	68
		20040709	1.58E+07	4.61E+07	163.36	217.93	0.18	0.64	2.58E+07	2.76E+07	4.34E+07	86
		20040715	7.43E+07	9.24E+07	495.27	497.91	0.08	1.00	7.44E+07	2.43E+07	9.86E+07	46
		20040720	2.79E+07	5.14E+07	196.21	225.12	0.05	0.88	3.01E+07	1.81E+07	4.60E+07	174
		20040721	-3.81E+06	3.36E+07	1.64	93.34	0.02	0.25	1.33E+07	2.28E+07	1.90E+07	125
		20040722	4.75E+05	2.56E+07	66.95	157.19	0.01	0.16	1.14E+07	1.30E+07	1.34E+07	61
		20040725	1.79E+07	3.91E+07	213.04	240.25	0.04	0.81	2.01E+07	1.22E+07	3.01E+07	148
		20040727	-1.39E+06	2.13E+07	-10.43	93.95	0.08	0.91	5.99E+04	1.61E+07	1.47E+07	99
		20040728	-7.68E+06	9.59E+06	-68.66	79.87	0.04	0.11	1.19E+06	9.91E+06	2.23E+06	45
		20040731	-1.99E+06	2.03E+06	-93.51	93.51	0.18	0.15	-1.81E+05	2.14E+06	1.48E+05	35
		20040803	-4.50E+05	1.42E+06	-34.68	84.21	0.12	0.43	3.41E+05	1.38E+06	9.30E+05	73
		20040806	9.97E+07	1.41E+08	386.89	401.63	0.40	2.65	5.02E+07	3.00E+07	1.30E+08	121
		20040807	5.02E+05	9.28E+06	223.89	271.48	0.00	0.00	4.45E+06	3.93E+06	4.43E+06	73
		20040809	8.07E+04	2.44E+06	14.87	90.04	0.00	0.13	1.30E+06	1.40E+06	1.49E+06	175
		20040811	-2.03E+06	4.59E+06	-87.56	87.56	0.01	0.00	2.37E+05	2.28E+06	2.45E+05	144
		20040814	1.94E+07	2.97E+07	3396.96	3416.65	0.03	-0.76	2.26E+07	1.81E+06	2.12E+07	86

Table A.3. Continued

Species, Units	UNIT	FLIGHT	MBE (unit)	RMSE (unit)	MNB (%)	MNE (%)	R^2	SLOPE	INT (unit)	AVE_{OBS} (unit)	AVE_{MOD} (unit)	N (#)
Sulfate	µg/m^3	20040709	1.85	4.08	149.30	171.40	0.00	-0.07	4.85	2.80	4.65	58
		20040715	1.61	2.35	213.26	233.22	0.53	1.54	0.87	1.37	2.98	72
		20040720	4.28	5.64	141.48	142.68	0.58	1.09	3.81	5.37	9.65	116
		20040721	2.69	4.58	87.96	94.15	0.65	0.90	3.49	7.97	10.66	81
		20040722	-0.78	4.51	36.51	70.84	0.14	0.22	4.42	6.72	5.93	74
		20040725	1.39	2.93	377.55	389.33	0.06	0.29	2.40	1.42	2.81	102
		20040727	2.57	3.95	538.31	545.31	0.08	0.37	3.81	1.97	4.54	104
		20040731	0.42	1.73	40.67	67.48	0.27	0.57	1.54	2.60	3.02	96
		20040803	-1.85	4.11	11.97	62.25	0.41	0.42	1.98	6.64	4.78	44
		20040806	1.39	2.14	157.37	160.99	0.58	1.23	1.03	1.58	2.97	111
		20040807	1.13	1.40	224.24	224.40	0.30	1.22	0.99	0.67	1.80	106
		20040809	-1.54	4.30	63.08	102.95	0.65	0.48	1.99	6.76	5.22	124
		20040811	2.47	6.17	30.18	53.04	0.07	0.39	9.39	11.26	13.74	98
		20040814	1.90	2.87	300.57	310.07	0.33	0.75	2.49	2.31	4.21	107
		20040815	1.42	3.28	872.74	891.21	0.41	0.85	1.66	1.61	3.02	95
Sum_NOy_ppbv	ppbV	20040711	-0.46	1.45	-13.57	54.58	0.31	0.41	0.67	1.90	1.44	65
		20040715	-0.83	2.93	29.89	65.61	0.64	0.47	1.86	5.13	4.30	76
		20040720	-1.10	6.19	36.95	67.35	0.23	0.18	4.57	6.93	5.83	155
		20040721	-1.68	4.85	1.85	46.04	0.31	0.18	3.11	5.80	4.13	128
		20040722	-1.31	2.44	-16.73	37.75	0.46	0.44	1.02	4.16	2.85	128
		20040725	0.01	1.82	29.02	49.58	0.70	0.54	1.22	2.66	2.66	124
		20040727	1.41	4.42	174.31	187.89	0.00	0.02	3.91	2.55	3.96	118
		20040728	0.85	1.87	128.52	181.73	0.01	-0.32	2.14	0.98	1.83	51
		20040731	0.31	0.97	46.34	65.59	0.32	0.50	1.20	1.78	2.09	126
		20040803	-1.90	5.63	20.70	68.12	0.47	0.27	2.52	6.09	4.19	62
		20040806	-0.09	1.54	2.62	44.52	0.34	0.59	0.82	2.21	2.12	126
		20040807	0.07	1.20	18.88	48.98	0.52	0.67	0.72	1.99	2.06	132
		20040809	-1.05	3.06	-4.88	50.00	0.25	0.50	1.54	5.15	4.10	147
		20040811	-1.15	2.71	-10.30	32.01	0.16	0.25	3.18	5.75	4.59	121

Table A.3. Continued

Species, Units	UNIT	FLIGHT	MBE (unit)	RMSE (unit)	MNB (%)	MNE (%)	R^2	SLOPE	INT (unit)	AVE_{OBS} (unit)	AVE_{MOD} (unit)	N (#)
Sum_NOy_ppbv	ppbV	20040814	0.11	3.83	103.61	122.16	0.27	0.22	2.60	3.19	3.30	119
		20040815	0.28	2.39	122.39	139.94	0.32	0.29	1.43	1.62	1.90	113
TRP1	pptV	20040715	-0.71	0.75	-99.98	99.98	0.12	0.00	0.00	0.71	0.00	8
		20040720	-2.06	4.47	-68.39	93.11	0.30	0.25	0.37	3.24	1.18	53
		20040721	-1.55	9.29	-46.46	140.07	0.00	0.09	1.74	3.62	2.07	42
		20040722	-0.17	10.44	3.35	82.11	0.34	0.61	3.84	10.17	10.00	37
		20040725	-13.28	20.03	-57.73	71.93	0.00	0.03	5.12	18.97	5.69	55
		20040727	-20.58	26.39	-91.10	91.10	0.24	0.08	-0.30	22.13	1.54	58
		20040728	-24.33	30.30	-88.00	88.00	0.16	0.22	-1.29	29.37	5.04	53
		20040731	-29.07	40.87	-49.25	107.06	0.00	-0.01	4.32	33.06	3.99	63
		20040803	-2.40	3.85	-96.93	96.93	0.01	0.00	0.04	2.43	0.03	27
		20040806	-0.19	1.75	6.38	58.15	0.01	0.08	1.69	2.04	1.84	47
		20040807	-2.85	6.09	-66.07	76.09	0.34	0.53	-0.14	5.73	2.89	58
		20040809	-7.99	10.83	-98.65	98.65	0.05	0.00	0.09	8.05	0.06	47
		20040811	-1.20	35.51	28.29	194.66	0.01	-0.40	16.85	12.92	11.73	34
		20040814	-13.44	16.68	-97.94	97.94	0.04	-0.01	0.29	13.60	0.16	57
		20040815	-6.07	18.46	-11.61	71.93	0.43	0.72	0.72	23.92	17.85	42
WSOC_ugC_m_3	µg C/m^3	20040709	-2.08	3.41	-91.16	91.16	0.00	0.00	0.10	2.18	0.10	85
		20040711	-2.84	3.12	-94.40	94.40	0.04	-0.01	0.17	2.97	0.13	65
		20040715	-1.38	1.51	-88.07	88.07	0.37	0.09	0.03	1.54	0.16	46
		20040720	-2.70	3.95	-86.99	86.99	0.00	0.00	0.27	2.97	0.27	123
		20040721	-3.04	4.39	-88.83	88.83	0.01	0.02	0.25	3.35	0.31	77
		20040722	-3.75	4.53	-88.11	89.87	0.21	0.03	0.16	4.04	0.29	113
		20040725	-0.87	1.06	-57.57	67.50	0.00	0.01	0.38	1.27	0.40	111
		20040727	-1.42	1.94	-72.27	74.03	0.00	-0.01	0.28	1.68	0.26	91
		20040728	-1.70	3.19	-75.22	76.22	0.27	0.04	0.14	1.91	0.21	59
		20040731	-0.73	0.81	-91.37	91.37	0.00	-0.01	0.07	0.79	0.05	83
		20040803	-1.78	2.27	-80.58	81.90	0.00	0.01	0.27	2.06	0.28	45
		20040806	-0.66	0.71	-71.49	71.49	0.30	0.36	-0.07	0.93	0.27	117

Table A.3. Continued

Species, Units	UNIT	FLIGHT	MBE (unit)	RMSE (unit)	MNB (%)	MNE (%)	R^2	SLOPE	INT (unit)	AVE_{OBS} (unit)	AVE_{MOD} (unit)	N (#)
WSOC_ugC_m_3	µg C/m^3	20040807	-0.46	0.59	-56.84	59.02	0.34	0.39	0.02	0.80	0.34	105
		20040809	-2.23	2.43	-84.67	86.28	0.00	-0.03	0.41	2.56	0.33	119
		20040811	-2.71	2.90	-81.30	81.30	0.00	0.01	0.49	3.25	0.54	111
		20040814	-0.77	0.95	-86.20	86.20	0.10	0.05	0.06	0.87	0.10	94
		20040815	-1.22	1.78	-67.28	68.72	0.04	0.03	0.18	1.44	0.22	47

REFERENCES

Allen, D. J., and K. E. Pickering (2002), Evaluation of lightning flash rate parameterizations for use in a global chemical transport model, *J. Geophys. Res.-Atmos.*, *107*(D23), 4711.

Altshuller, A. P., and A. S. Lefohn (1996), Background ozone in the planetary boundary layer over the United States, *J. Air Waste Manage. Assoc.*, *46*(2), 134-141.

Arellano, A. F., et al. (2006), Time-dependent inversion estimates of global biomass-burning CO emissions using Measurement of Pollution in the Troposphere (MOPITT) measurements, *J. Geophys. Res.-Atmos.*, *111*(D9).

Beirle, S., et al. (2003), Weekly cycle of NO_2 by GOME measurements: a signature of anthropogenic sources, *Atmos. Chem. Phys.*, *3*, 2225-2232.

Beirle, S., et al. (2006), Estimating the NO_x produced by lightning from GOME and NLDN data: a case study in the Gulf of Mexico, *Atmos. Chem. Phys.*, *6*, 1075-1089.

Biazar, A. P., and R. T. McNider (1995), Regional estimates of lightning production of nitrogen-oxides, *J. Geophys. Res.-Atmos.*, *100*(D11), 22861-22874.

Blond, N., et al. (2007), Intercomparison of SCIAMACHY nitrogen dioxide observations, in situ measurements and air quality modeling results over Western Europe, *J. Geophys. Res.-Atmos.*, *112*(D10).

Boccippio, D. J., et al. (2001), Combined satellite- and surface-based estimation of the intracloud-cloud-to-ground lightning ratio over the continental United States, *Monthly Weather Review*, *129*(1), 108-122.

Boersma, K. F., et al. (2004), Error analysis for tropospheric NO_2 retrieval from space, *J. Geophys. Res.-Atmos.*, *109*(D4).

Boersma, K. F., et al. (2005), Estimates of lightning NO_x production from GOME satellite observations, *Atmos. Chem. Phys.*, *5*, 2311-2331.

Boersma, K. F., et al. (2008), Intercomparison of SCIAMACHY and OMI tropospheric NO_2 columns: Observing the diurnal evolution of chemistry and emissions from space, *J. Geophys. Res.-Atmos.*, *113*(D16S26).

Bond, D. W., et al. (2001), NO_x production by lightning over the continental United States, *J. Geophys. Res.-Atmos.*, *106*(D21), 27701-27710.

Bovensmann, H., et al. (1999), SCIAMACHY: Mission objectives and measurement modes, *J. Atmos. Sci.*, *56*(2), 127-150.

Bradshaw, J., et al. (1999), Photofragmentation two-photon laser-induced fluorescence detection of NO_2 and NO: Comparison of measurements with model results based on airborne observations during PEM-Tropics A, *Geophys. Res. Lett.*, *26*(4), 471-474.

Bucsela, E. J., et al. (2008), Comparison of tropospheric NO_2 from in situ aircraft measurements with near-real-time and standard product data from OMI, *J. Geophys. Res.-Atmos.*, *113*(D16S31).

Byun, D. W., and C. J.K.S. (1999), Science algorithms of the EPA Models-3 Community Multi-scale Air Quality (CMAQ) Modeling System, Research Triangle Park, NC.

Byun, D., and K. L. Schere (2006), Review of the governing equations, computational algorithms, and other components of the Models-3 Community Multiscale Air Quality (CMAQ) Modeling System, *Appl. Mech. Rev.*, *59*(2), 51-77.

CARB (2009), The California almanac of emissions & air quality, 2009 Edition, California Air Resources Board, Sacramento, CA.

Carter, W. P. L. (2000), Implementation of the SAPRC-99 Chemical Mechanism into the Models-3 Framework, United States Environmental Protection Agency.

Carter, W. P. L. (2008), Personal communication.

Choi, Y., et al. (2005), Evidence of lightning NO_x and convective transport of pollutants in satellite observations over North America, *Geophys. Res. Lett.*, *32*(L02805).

Christian, H. J., et al. (2003), Global frequency and distribution of lightning as observed from space by the Optical Transient Detector, *J. Geophys. Res.-Atmos.*, *108*(D1), 4005.

Chune, S., and Z. Baoning (2008), Tropospheric NO_2 columns over Northeastern North America: Comparison of CMAQ model simulations with GOME satellite measurements, *Advances in Atmospheric Sciences*, *25*, 59-71.

Cohan, D. S., et al. (2005), Nonlinear response of ozone to emissions: Source apportionment and sensitivity analysis, *Environ. Sci. Technol.*, *39*(17), 6739-6748.

Cooper, O. R., et al. (2006), Large upper tropospheric ozone enhancements above midlatitude North America during summer: In situ evidence from the IONS and MOZAIC ozone measurement network, *J. Geophys. Res.-Atmos.*, *111*(D24S05).

DeCaria, A. J., et al. (2000), A cloud-scale model study of lightning-generated NO_x in an individual thunderstorm during STERAO-A, *J. Geophys. Res.-Atmos.*, *105*(D9), 11601-11616.

DeCaria, A. J., et al. (2005), Lightning-generated NO_x and its impact on tropospheric ozone production: A three-dimensional modeling study of a Stratosphere-Troposphere Experiment: Radiation, Aerosols and Ozone (STERAO-A) thunderstorm, *J. Geophys. Res.-Atmos.*, *110*(D14303).

Deguillaume, L., et al. (2007), Bayesian Monte Carlo analysis applied to regional- scale inverse emission modeling for reactive trace gases, *J. Geophys. Res.-Atmos.*, *112*(D2).

Delmas, R., et al. (1997), Global inventory of NO_x sources, *Nutr. Cycl. Agroecosys.*, *48*(1-2), 51-60.

DeMore, W. B., et al. (1997), Chemical kinetics and photochemical data for use in stratospheric modeling. Evaluation number 12, *JPL Publication 97-4*, 1 - 266.

Dudhia, J., et al. (2005), PSU/NCAR Mesoscale Modeling System tutorial class notes and Users' Guide (MM5 Modeling System Version 3), National Center for Atmospheric Research.

Dufour, G., et al. (2009), SCIAMACHY formaldehyde observations: constraint for isoprene emission estimates over Europe?, *Atmos. Chem. Phys.*, *9*(5), 1647-1664.

Dunker, A. M. (1984), The Decoupled Direct Method For Calculating Sensitivity Coefficients In Chemical-Kinetics, *Abstracts Of Papers Of The American Chemical Society*, *188*(AUG), 88-PHYS.

Egorova, T., et al. (1999), Lightning production of NO_x and ozone, *Phys. Chem. Earth Pt. C*, *24*(5), 473-479.

Elbern, H., and H. Schmidt (1999), A four-dimensional variational chemistry data assimilation scheme for Eulerian chemistry transport modeling, *J. Geophys. Res.-Atmos.*, *104*(D15), 18583-18598.

EPA (1995), CASTNet: National Dry Deposition Network 1990-1992 Status Report, U.S. Environmental Protection Agency, Research Triangle Park, NC.

EPA (2005), Guidance on the Use of Models and Other Analyses in Attainment Demonstrations for the 8-hour Ozone NAAQS, Research Triangle Park, NC.

EPA (2005a), Evaluating ozone control programs in the eastern United States: Focus on the NO_x budget trading program, Environmental Protection Agency (EPA), Washington, DC

EPA (2005b), Acid rain program, 2004 progress report, Environmental Protection Agency (EPA), Washington, DC

EPA (2006), Air Quality Criteria for Ozone and Related Photochemical Oxidants, Research Triangle Park, NC.

EPA (2008), Clean Air Markets, http://camddataandmaps.epa.gov/gdm, last access date: 8 January 2008

EPA (2008), Air Quality System (AQS), http://www.epa.gov/ttn/airs/airsaqs, last access date: 8 January 2008

EPA (2009), Air Quality System (AQS), Protocols with Sampling Methodologies, http://www.epa.gov/ttn/airs/airsaqs/manuals/codedescs.htm, last access date: 5 July 2009

EPA (2009), Clean Air Act (CAA), http://www.epa.gov/air/caa/, last access date: 3 August 2009

EPA (2009), National Emissions Inventory (NEI) Air Pollutant Emissions Trends Data, http://www.epa.gov/ttn/chief/trends/, last access date: 4 August 2009

Fehr, T., et al. (2004), Model study on production and transport of lightning-produced NO_x in a EULINOX supercell storm, *J. Geophys. Res.-Atmos.*, *109*(D09102).

Fehsenfeld, F. C., et al. (2006), International Consortium for Atmospheric Research on Transport and Transformation (ICARTT): North America to Europe - Overview of the 2004 summer field study, *J. Geophys. Res.-Atmos.*, *111*(D23).

Fiore, A., et al. (2003), Variability in surface ozone background over the United States: Implications for air quality policy, *J. Geophys. Res.-Atmos.*, *108*(D24).

Fiore, A. M., et al. (2002), Background ozone over the United States in summer: Origin, trend, and contribution to pollution episodes, *J. Geophys. Res.-Atmos.*, *107*(D15).

Ghude, S. D., et al. (2008), Detection of surface emission hot spots, trends, and seasonal cycle from satellite-retrieved NO_2 over India, *J. Geophys. Res.-Atmos.*, *113*(D20).

Grell, G. A., et al. (1995), A description of the fifth generation Penn State/NCAR Mesoscale Model (MM5), National Centre for Atmospheric Research, Boulder, Colorado, USA. .

Han, K. M., et al. (2009), Investigation of NO_x emissions and NO_x-related chemistry in East Asia using CMAQ-predicted and GOME-derived NO_2 columns, *Atmos. Chem. Phys.*, *9*(3), 1017-1036.

Hanna, S. R., et al. (2001), Uncertainties in predicted ozone concentrations due to input uncertainties for the UAM-V photochemical grid model applied to the July 1995 OTAG domain, *Atmos. Environ.*, *35*(5), 891-903.

Hansen, D. A., et al. (2003), The southeastern aerosol research and characterization study: Part 1-overview, *J. Air Waste Manage. Assoc.*, *53*(12), 1460-1471.

Harley, R. A., et al. (2005), Changes in motor vehicle emissions on diurnal to decadal time scales and effects on atmospheric composition, *Environ. Sci. Technol.*, *39*(14), 5356-5362.

Hirsch, A. I., et al. (1996), Seasonal variation of the ozone production efficiency per unit NO_x at Harvard Forest, Massachusetts, *J. Geophys. Res.-Atmos.*, *101*(D7), 12659-12666.

Houyoux, M. R., and J. M. Vukovich (1999), Updates to the Sparse Matrix Operator Kernel Emissions (SMOKE) Modeling System and Integration with Models-3, paper presented at The Emission Inventory: Regional Strategies for the Future, Air & Waste Management Association, Raleigh, NC, 26-28 October.

Hu, Y., et al. (2003), Final Report: Meteorological Modeling of the August 11-20, 2000 Episode for the Fall Line Air Quality Study, prepared by Georgia Institute of Technology, Georgia Department of Natural Resources, Atlanta, GA.

Hudman, R. C., et al. (2007), Surface and lightning sources of nitrogen oxides in the United States: magnitudes, chemical evolution, and outflow, *J. Geophys. Res.*, *112*(D12S05).

Hudman, R. C., et al. (2009), North American influence on tropospheric ozone and the effects of recent emission reductions: Constraints from ICARTT observations, *J. Geophys. Res.-Atmos.*, *114*.

IUPAC (2009), International Union of Pure and Applied Chemistry (IUPAC): Data sheets for gas phase reactions of NO_x species, http://www.iupac-kinetic.ch.cam.ac.uk/datasheets/pdf/NOx13_HO_NO2.pdf, last access date: 6 August 2009

Jaegle, L., et al. (2005), Global partitioning of NO_x sources using satellite observations: Relative roles of fossil fuel combustion, biomass burning and soil emissions, *Faraday Discuss.*, *130*, 407-423.

Kaynak, B., et al. (2008), The effect of lightning NO_x production on surface ozone in the continental United States, *Atmos. Chem. Phys.*, *8*(17), 5151-5159.

Kaynak, B., et al. (2009), Comparison of weekly cycle of NO_2 satellite retrievals and NO_x emission inventories for the continental U.S. , *J. Geophys. Res.-Atmos.*, *114*.

Kim, S. W., et al. (2006), Satellite-observed US power plant NO_x emission reductions and their impact on air quality, *Geophys. Res. Lett.*, *33*(L22812).

Kim, S. W., et al. (2009), NO_2 columns in the western United States observed from space and simulated by a regional chemistry model and their implications for NO_x emissions, *J. Geophys. Res.-Atmos.*, *114*.

Konovalov, I. B., et al. (2005), Comparison and evaluation of modelled and GOME measurement derived tropospheric NO_2 columns over Western and Eastern Europe, *Atmos. Chem. Phys.*, *5*, 169-190.

Konovalov, I. B., et al. (2006), Inverse modelling of the spatial distribution of NO_x emissions on a continental scale using satellite data, *Atmos. Chem. Phys.*, *6*, 1747-1770.

Konovalov, I. B., et al. (2008), Satellite measurement based estimates of decadal changes in European nitrogen oxides emissions, *Atmos. Chem. Phys.*, *8*(10), 2623-2641.

Kurokawa, J., et al. (2009), Adjoint inverse modeling of NO_x emissions over eastern China using satellite observations of NO_2 vertical column densities, *Atmos. Environ.*, *43*(11), 1878-1887.

Labrador, L. J., et al. (2004), Strong sensitivity of the global mean OH concentration and the tropospheric oxidizing efficiency to the source of NO_x from lightning, *Geophys. Res. Lett.*, *31*(6).

Labrador, L. J., et al. (2005), The effects of lightning-produced NO_x and its vertical distribution on atmospheric chemistry: sensitivity simulations with MATCH-MPIC, *Atmos. Chem. Phys.*, *5*, 1815-1834.

Lefohn, A. S., et al. (2001), Present-day variability of background ozone in the lower troposphere, *J. Geophys. Res.-Atmos.*, *106*(D9), 9945-9958.

Leue, C., et al. (2001), Quantitative analysis of NO_x emissions from Global Ozone Monitoring Experiment satellite image sequences, *J. Geophys. Res.-Atmos.*, *106*(D6), 5493-5505.

Liang, J. Y., et al. (1998), Seasonal budgets of reactive nitrogen species and ozone over the United States, and export fluxes to the global atmosphere, *J. Geophys. Res.-Atmos.*, *103*(D11), 13435-13450.

Lin, C. Y. C., et al. (2000), Increasing background ozone in surface air over the United States, *Geophys. Res. Lett.*, *27*(21), 3465-3468.

MACTEC (2005), Documentation of the Revised 2002 Base Year, Revised 2018, and Initial 2009 Emission Inventories for VISTAS, Visibility Improvement State and Tribal Association of the Southeast (VISTAS).

Martin, R. V., et al. (2002), An improved retrieval of tropospheric nitrogen dioxide from GOME, *J. Geophys. Res.-Atmos.*, *107*(D20).

Martin, R. V., et al. (2003), Global inventory of nitrogen oxide emissions constrained by space-based observations of NO_2 columns, *J. Geophys. Res.-Atmos.*, *108*(D17).

Martin, R. V., et al. (2004), Evaluation of GOME satellite measurements of tropospheric NO_2 and HCHO using regional data from aircraft campaigns in the southeastern United States, *J. Geophys. Res.-Atmos.*, *109*(D24307).

Martin, R. V., et al. (2006), Evaluation of space-based constraints on global nitrogen oxide emissions with regional aircraft measurements over and downwind of eastern North America, *J. Geophys. Res.-Atmos.*, *111*(D15308).

Martin, R. V., et al. (2007), Space-based constraints on the production of nitric oxide by lightning, *J. Geophys. Res.-Atmos.*, *112*(D09309).

Martin, R. V. (2008), Satellite remote sensing of surface air quality, *Atmos. Environ.*, *42*(34), 7823-7843.

Mendoza-Dominguez, A., and A. G. Russell (2000), Iterative inverse modeling and direct sensitivity analysis of a photochemical air duality model, *Environ. Sci. Technol.*, *34*(23), 4974-4981.

Mendoza-Dominguez, A., and A. G. Russell (2001a), Estimation of emission adjustments from the application of four-dimensional data assimilation to photochemical air quality modeling, *Atmos. Environ.*, *35*(16), 2879-2894.

Mendoza-Dominguez, A., and A. G. Russell (2001b), Emission strength validation using four-dimensional data assimilation: Application to primary aerosol and precursors to ozone and secondary aerosol, *J. Air Waste Manage. Assoc.*, *51*(11), 1538-1550.

Miller, C. A., et al. (2006), Air emission inventories in North America: A critical assessment, *J. Air Waste Manage. Assoc.*, *56*(8), 1115-1129.

Müller, J. F., and T. Stavrakou (2005), Inversion of CO and NO_x emissions using the adjoint of the IMAGES model, *Atmos. Chem. Phys.*, *5*, 1157-1186.

Napelenok, S. L., et al. (2008), A method for evaluating spatially-resolved NO_x emissions using Kalman filter inversion, direct sensitivities, and space-based NO_2 observations, *Atmos. Chem. Phys.*, *8*(18), 5603-5614.

Ott, L. E., et al. (2007), Effects of lightning NO_x production during the 21 July European Lightning Nitrogen Oxides Project storm studied with a three-dimensional cloud-scale chemical transport model, *J. Geophys. Res.-Atmos.*, *112*(D05307).

Pickering, K. E., et al. (1998), Vertical distributions of lightning NO_x for use in regional and global chemical transport models, *J. Geophys. Res.-Atmos.*, *103*(D23), 31203-31216.

Pickering, K. E. (2007), Personal communication.

Pison, I., et al. (2007), Inverse modeling of surface NO_x anthropogenic emission fluxes in the Paris area during the Air Pollution Over Paris Region (ESQUIF) campaign, *J. Geophys. Res.-Atmos.*, *112*(D24).

Pleim, J. E., and J. S. Chang (1992), A nonlocal closure-model for vertical mixing in the convective boundary-layer, *Atmos. Environ.*, *26*(6), 965-981.

Price, C., and D. Rind (1993), What determines the cloud-to-ground lightning fraction in thunderstorms, *Geophys. Res. Lett.*, *20*(6), 463-466.

Price, C., et al. (1997), NO_x from lightning .1. Global distribution based on lightning physics, *J. Geophys. Res.-Atmos.*, *102*(D5), 5929-5941.

Quelo, D., et al. (2005), Inverse modeling of NO_x emissions at regional scale over northern France: Preliminary investigation of the second-order sensitivity, *J. Geophys. Res.-Atmos.*, *110*(D24).

Ren, X. R., et al. (2006), OH, HO_2, and OH reactivity during the PMTACS-NY Whiteface Mountain 2002 campaign: Observations and model comparison, *J. Geophys. Res.-Atmos.*, *111*(D10).

Ridley, B. A., et al. (1996), On the production of active nitrogen by thunderstorms over New Mexico, *J. Geophys. Res.-Atmos.*, *101*(D15), 20985-21005.

Ridley, B. A., et al. (2005), Comments on the parameterization of lightning-produced NO in global chemistry-transport models, *Atmos. Environ.*, *39*(33), 6184-6187.

Russell, A. G., et al. (1986), On some aspects of nighttime atmospheric chemistry, *Environ. Sci. Technol.*, *20*(11), 1167-1172.

Russell, A. (1997), Regional photochemical air quality modeling: Model formulations, history, and state of the science, *Annu. Rev. Energ. Environ.*, *22*, 537-588.

Schumann, U., and H. Huntrieser (2007), The global lightning-induced nitrogen oxides source, *Atmos. Chem. Phys.*, *7*(14), 3823-3907.

Seaman, N. L. (2000), Meteorological modeling for air-quality assessments, *Atmos. Environ.*, *34*(12-14), 2231-2259.

Seinfeld, J. H., and S. N. Pandis (1997), *Atmospheric Chemistry and Physics: From Air Pollution to Climate Change*, First ed., Wiley-Interscience, New York.

Shim, C., et al. (2005), Constraining global isoprene emissions with Global Ozone Monitoring Experiment (GOME) formaldehyde column measurements, *J. Geophys. Res.-Atmos.*, *110*(D24).

Singh, H. B., et al. (2006), Overview of the summer 2004 intercontinental chemical transport experiment - North America (INTEX-A), *J. Geophys. Res.-Atmos.*, *111*(D24).

Stavrakou, T., et al. (2008), Assessing the distribution and growth rates of NO_x emission sources by inverting a 10-year record of NO_2 satellite columns, *Geophys. Res. Lett.*, *35*(10).

Stockwell, D. Z., et al. (1999), Modelling NO_x from lightning and its impact on global chemical fields, *Atmos. Environ.*, *33*(27), 4477-4493.

Tarantola, A. (2005), *Inverse Problem Theory and Methods for Model Parameter Estimation*, Society for Industrial and Applied Mathematics, Philadelphia.

Taylor, J. R. (1997), *An Introduction to Error Analysis: The study of uncertainties in physical measurements*, Second ed., Univercity Science Books, Sausalito, CA.

Tian, D., et al. (2008), Air quality impacts from prescribed forest fires under different management practices, *Environ. Sci. Technol.*, *42*(8), 2767-2772.

Tie, X. X., et al. (2002), Global NO_x production by lightning, *J. Atmos. Chem.*, *43*(1), 61-74.

Toenges-Schuller, N., et al. (2006), Global distribution pattern of anthropogenic nitrogen oxide emissions: Correlation analysis of satellite measurements and model calculations, *J. Geophys. Res.-Atmos.*, *111*(D05312).

Trainer, M., et al. (1993), Correlation of ozone with NO_y in photochemically aged air, *J. Geophys. Res.-Atmos.*, *98*(D2), 2917-2925.

Uno, I., et al. (2007), Systematic analysis of interannual and seasonal variations of model-simulated tropospheric NO_2 in Asia and comparison with GOME-satellite data, *Atmos. Chem. Phys.*, *7*(6), 1671-1681.

Velders, G. J. M., et al. (2001), Global tropospheric NO_2 column distributions: Comparing three-dimensional model calculations with GOME measurements, *J. Geophys. Res.-Atmos.*, *106*(D12), 12643-12660.

Vijayaraghavan, K., et al. (2009), Export of reactive nitrogen from coal-fired power plants in the U. S.: Estimates from a plume-in-grid modeling study, *J. Geophys. Res.-Atmos.*, *114*.

Wang, P., et al. (2008), FRESCO+: An improved O_2 A-band cloud retrieval algorithm for tropospheric trace gas retrievals, *Atmos. Chem. Phys.*, *8*(21), 6565-6576.

Wang, Y. X., et al. (2007), Seasonal variability of NO_x emissions over east China constrained by satellite observations: Implications for combustion and microbial sources, *J. Geophys. Res.-Atmos.*, *112*(D6).

Wang, Y. X. X., et al. (2004), Asian emissions of CO and NO_x: Constraints from aircraft and Chinese station data, *J. Geophys. Res.-Atmos.*, *109*(D24).

Xiu, A. J., and J. E. Pleim (2001), Development of a land surface model. Part I: Application in a mesoscale meteorological model, *J. Appl. Meteorol.*, *40*(2), 192-209.

Yang, Y. J., et al. (1997), Fast, direct sensitivity analysis of multidimensional photochemical models, *Environ. Sci. Technol.*, *31*(10), 2859-2868.

Yu, S. C., et al. (2007), A detailed evaluation of the Eta-CMAQ forecast model performance for O_3, its related precursors, and meteorological parameters during the 2004 ICARTT study, *J. Geophys. Res.-Atmos.*, *112*(D12).

Zhang, L., et al. (2008), Transpacific transport of ozone pollution and the effect of recent Asian emission increases on air quality in North America: an integrated analysis using satellite, aircraft, ozonesonde, and surface observations, *Atmos. Chem. Phys.*, *8*(20), 6117-6136.

Zhang, M. G., et al. (2006a), A three-dimensional simulation of HO_x concentrations over East Asia during TRACE-P, *J. Atmos. Chem.*, *54*(3), 233-254.

Zhang, M. G., et al. (2006b), Evaluation of the Models-3 Community Multi-scale Air Quality (CMAQ) modeling system with observations obtained during the TRACE-P experiment: Comparison of ozone and its related species, *Atmos. Environ.*, *40*(26), 4874-4882.

Zhang, R. Y., et al. (2000), Enhanced NO_x by lightning in the upper troposphere and lower stratosphere inferred from the UARS global NO_2 measurements, *Geophys. Res. Lett.*, *27*(5), 685-688.

Zhang, R. Y., et al. (2003), Impacts of anthropogenic and natural NO_x sources over the US on tropospheric chemistry, *Proc. Natl. Acad. Sci. USA*, *100*(4), 1505-1509.

Zhao, C., and Y. H. Wang (2009), Assimilated inversion of NO_x emissions over east Asia using OMI NO_2 column measurements, *Geophys. Res. Lett.*, *36*.

VITA

Burçak Kaynak was born in Ankara, Turkey on June 1, 1979. She received her bachelor's degree in 2001 and her master's degree in 2003 in Environmental Engineering from Middle East Technical University. She worked on the cleaner energy production potential of biomass combustion under supervision of Dr. Aysel Atimtay. After her Master's degree, she joined Dr. Russell's research group in the School of Civil and Environmental Engineering at the Georgia Institute of Technology in Atlanta, GA, USA in 2004. Her research includes integrated analysis of satellite, aircraft, and ground-based observations with regional scale models for NO_2 in particular. She received her Ph. D. degree in December 2009.